UNIVERSITY OF LJUBLJANA
FACULTY OF ELECTRICAL ENGINEERING

Gregor Taljan

THE USE OF HYDROGEN IN ELECTRIC POWER SYSTEMS

PhD thesis

Ljubljana, 2009

UNIVERSITY OF LJUBLJANA
FACULTY OF ELECTRICAL ENGINEERING

Gregor Taljan

THE USE OF HYDROGEN IN ELECTRIC POWER SYSTEMS

PhD thesis

Supervisor: As. Prof. Gregor Verbič

Ljubljana, 2009

UNIVERZA V LJUBLJANI
FAKULTETA ZA ELEKTROTEHNIKO

Gregor Taljan

UPORABA VODIKA V ELEKTROENERGETSKIH SISTEMIH

Doktorska disertacija

Mentor: doc. dr. Gregor Verbič

Ljubljana, 2009

AUTHOR'S STATEMENT

The author herewith declares that the thesis entitled "The use of hydrogen in power systems" is solely a product of his own research work under the supervision of As. Prof. Gregor Verbič and co-supervisor Prof. Dr. Claudio Cañizares. Contributions and help from other coworkers and colleagues are properly stated in the Acknowledgments.

IZJAVA AVTORJA

Izjavljam, da je doktorska disertacija z naslovom "Uporaba vodika v elektroenergetskih sistemih" izključno rezultat mojega lastnega raziskovalnega dela pod vodstvom mentorja doc. dr. Gregorja Verbiča in somentorja prof. dr. Claudia Cañizaresa. Izkazano pomoč drugih sodelavcev sem v celoti navedel v zahvali.

Gregor Taljan

Acknowledgements

Most of all, my thanks go to Assistant Professor Gregor Verbič for guiding me through the doctoral study, and for his optimistic and inspiring attitude. He has helped me in all aspects of the work, and has made a great effort to keep me active and focused on my research. In particular, I would like to thank Professors Claudio Canizares and Michael Fowler from the University of Waterloo, who were very helpful with excellent ideas and directions all along the work on this dissertation.

Special thanks also go to Assistant Professor Miloš Pantoš, who contributed a lot during my graduate research work. Our collaboration has been very useful and inspiring for me. My thanks also go to Assistant Professor Andrej Gubina from the Laboratory for Energy Policy for his advice and contributions, especially during the first part of the study. Especially, I would like to thank my brother Urban, who contributed a lot to the development of the economic model and to evaluating the assumptions. Endless debates with him are responsible for the realistic and exact economic assessment of the hydrogen system. Thanks also to Eva and Jerneja, who have shown a lot of patience while witnessing these discussions.

Many thanks also to all my colleagues and friends Matjaž, Matej, Andraž, Samo, Vito, Iztok and Borut from the Department of Power Systems who are acknowledged for their valuable support and cooperation throughout my doctoral study and for accepting offers to take academic lunches and coffee-breaks at any time. I would also like to thank my girlfriend, Eva, for her kindness and love, and for being supportive and understanding when I was struggling with the work.

Many thanks also to the Slovenian Research Agency for making this doctoral study possible and to the Ad-Futura foundation who facilitated my research visits to the University of Waterloo (UW) and to Graz University of Technology during my studies. The financial and logistical support provided by the Natural Sciences and Engineering Research Council of Canada (NSERC) and Mathematics of Information Technology and Complex Systems (MITACS) as well as the UW is also acknowledged; they provided funding as well as laboratory space and access to computers, library and other university facilities during my stay at the UW.

My parents, Ana and Drago, are also kindly acknowledged for their endless support, love and devotion. They must have been very patient and denied themselves a lot for me to come so far. Support from the Krevh family is also greatly appreciated. They have always been encouraging and helpful.

Gregor Taljan
Ljubljana, 2009

I CONTENTS

II ABSTRACT

A techno-economic evaluation of the various scenarios for the use of hydrogen in power systems with a mixed wind-nuclear power plant in the context of a "Hydrogen Economy" is presented in this thesis. The main motivation for applying hydrogen in this context is the unpredictability and intermittency of wind-nuclear power generation facilities, which are often found in areas with limited grid capacity. Moreover, energy storage in the form of hydrogen makes it possible to provide clean fuel for prospective hydrogen economy markets (e.g., transportation).

To assess the economics of different hydrogen applications in wind-nuclear energy production hubs, a novel methodology was developed in the thesis, taking into account all the relevant operational and economic parameters. The simulation of the operation of the combined nuclear-wind-hydrogen system is discussed first, where the selling and buying of electricity and the selling of excess hydrogen and oxygen are optimized to maximize profits. This simulation is made in two phases: In the pre-dispatch phase, the system operation is optimized according to stochastic wind and price forecasts to obtain optimal hydrogen charge levels for the operational horizon. In the second phase, a real-time dispatch is carried out on an hourly basis to optimize the operation of the system to maximize profits, and to follow the storage levels of the pre-dispatch phase. Based on the operation planning and dispatch results, an economic evaluation is performed to determine the feasibility of the proposed hydrogen-utilization scheme for investment purposes.

The proposed method was tested on a realistic system setup consisting of the Bruce nuclear power plant and the Ripley wind farm, both located in the Bruce region in Ontario, Canada, and connected to the main load center in the Greater Toronto area via the Bruce-Milton transmission line. The following hydrogen application scenarios were evaluated:

- Chapter 4.7: the scenario where hydrogen was used as electricity storage medium with an without the option of hydrogen sales;
- Chapter 4.8: the same as chapter 4.7, but with the utilization of oxygen and heat;
- Chapter 4.9: the use of a hydrogen system as an alternative to transmission-system upgrading, assuming that permanent transmission congestions prevent the transport of all the produced electricity to load centers;
- Chapter 4.10: the use of a hydrogen system if periodic congestions occur in the transmission system.

The results of the scenarios studied in this thesis demonstrate that the use hydrogen for the sole purpose of the storage of electricity is not economically feasible for the current state of hydrogen-technology development, even if the byproducts such as oxygen and heat are

utilized, the efficiencies are considerably improved, the investment costs reduced or if the transmission system is frequently congested.

On the other hand, hydrogen is shown to be a technically, environmentally and economically acceptable option if sold directly to a hydrogen market for other purposes, such as transportation, as in the case of a Hydrogen Economy. This scenario, however, can only be expected if the battery technology in the context of the so-called "electron economy" turns out to be technically and commercially inferior to the "hydrogen economy". Some sensitivity analyses show that the economics in this case is strongly correlated with the hydrogen prices. Other parameters, e.g., efficiencies, oxygen and heat prices and costs reduction, do not represent such a significant investment risk.

Another successful application of the hydrogen system is shown to be the use of hydrogen as an alternative to a transmission-system upgrade, especially in the regions where, due to environmental, location or other issues, the spatial planning prevents new transmission investments. The profits in this scenario, made from the utilization of surplus electricity that would otherwise be permanently shed, suffice for the hydrogen system to be utilized economically. Again, as shown in several sensitivity analyses, the strong dependence on hydrogen prices presents the greatest risk for a potential investor in this scenario.

In addition to the permanent-congestion scenario described in the previous paragraph, a scenario considering only temporal congestions is analyzed in the thesis. This scenario is probable, e.g., in the context of foreseen additional wind-capacity investments in the Bruce area. These intermittent congestions make the hydrogen system profitable only in the case when the hydrogen produced is sold to a hydrogen market and not if it is converted back to electricity in available transmission-capacity periods.

The main scientific contributions of this thesis are the following:

- a novel methodology for the modeling of coupled wind-nuclear-hydrogen systems with the bulk electric-power system;
- a novel methodology for a two-step stochastic optimization of the dispatch of hydrogen-electric systems;
- an assessment of the profitability of hydrogen as a storage medium in electric power systems;
- an assessment of the impacts of residual oxygen and heat utilization on the profitability of hydrogen as an energy carrier;
- an assessment of the profitability of hydrogen as a storage medium in electric power systems with a constrained network capacity, i.e., the possibility to utilize hydrogen as an energy carrier to substitute for transmission-system expansion or to alleviate line congestions.

Key words: wind power, nuclear power, hydrogen storage, Hydrogen Economy, power-generation planning, mixed-integer stochastic linear programming, dispatch optimization, investment evaluation, electricity markets.

III RAZŠIRJEN POVZETEK

V kontekstu globalnega boja proti podnebnim spremembam se kot okolju sprejemljivi energetski viri omenjajo obnovljivi viri energije, ki pa zaradi svojih obratovalnih lastnosti (npr. nestalnost proizvodnje električne energije iz vetrnih elektrarn) postavljajo nove tehnične izzive in tudi ekonomske priložnosti vsem stranem v dereguliranih elektroenergetskih sistemih. V disertaciji smo zato preučili tehnično-ekonomske možnosti vključevanja vodika v elektroenergetski sistem v kontekstu ekonomije vodika. Glavna motivacija pri tem je bila uporaba vodika kot shranjevalnika električne energije za blaženje neravnovesij med porabo in proizvodnjo električne energije, ki nastaja zaradi nepredvidljive proizvodnje električne energije iz nekaterih obnovljivih virov in omejenih prenosnih zmogljivosti zaradi neugodnih lokacij s primernim potencialom teh obnovljivih virov. V doktoratu smo poleg omenjenega upoštevali še možnost prodaje vodika kot energenta prihodnosti na potencialni trg z vodikom v okviru ekonomije vodika. Pri tem smo raziskali scenarije, v katerih bi se prihodki vodikovega sistema ustvarjali z naslednjimi poslovnimi priložnostmi:

- del proizvedene električne energije se lahko shrani v obliki vodika v obdobjih z nizkimi cenami električne energije in se pretvori nazaj v električno energijo ter proda na trgu z električno energijo v obdobjih z visokimi cenami;
- ob pomanjkanju prenosnih zmogljivosti se lahko presežek električne energije shrani kot vodik, ta pa se nato pretvori nazaj v električno energijo, ki se proda, ko so prenosne zmogljivosti na voljo;
- proizvedeni vodik se lahko proda direktno na trgu z vodikom, kadar je to iz finančnega vidika smiselno;
- možnost proizvodnje in shranjevanja vodika lahko uporabimo za blaženje stabilnostnih problemov in problemov zamašitev v prenosnem omrežju, ki so povezani s spremenljivo proizvodnjo električne energije iz vetrnih elektrarn;
- možnost prodaje kisika in toplotne energije kot stranskih produktov pri proizvodnji vodika.

Vse opisane scenarije smo v disertaciji raziskali s pomočjo ekonomskega modela, ki temelji na prihodkih izračunanih z modeli za stohastično optimizacijo obratovanja vodikovega sistema.

Razširjen povzetek doktorata obsega naslednja poglavja. V uvodu opisujemo ožje znanstveno področje, ki podaja tudi pregled obstoječe literature iz tega področja. V nadaljevanju okvirno predstavljamo model za ocenjevanje ekonomske primernosti posameznega scenarija uporabe vodika v elektroenergetskih sistemih. Temu sledi poglavje z opisom realističnega sistema, na katerem smo uporabili razvito metodologijo. Na koncu predstavljamo rezultate in izvirne prispevke k znanosti, ki potrjujejo namen doktorata.

III.I Opis simbolov

III.I.I ***Parametri***

c^H : prodajna cena vodika (CAD/kg)
c^{HEAT} : prodajna cena toplotne energije (CAD/MWh)
c^O : prodajna cena kisika (CAD/Nm^3)
μ_{ef} : izkoristek pretvorbe vodika v električno energijo v gorivnih celicah (kg/MWh)
μ_{hc} : izkoristek stiskanja vodika v kompresorju (kg/MWh)
μ_{he} : izkoristek pretvorbe električne energije v vodik v elektrolizatorju (kg/MWh)
μ_{hf} : izkoristek pretvorbe vodika v toplotno energijo v gorivnih celicah (kg/MWh)
μ_{oc} : izkoristek stiskanja kisika v kompresorju (Nm^3/MWh)
μ_{oe} : izkoristek pretvorbe električne energije v kisik v elektrolizatorju (Nm^3/MWh)
N_p : število scenarijev napovedi cen električne energije
N_w : število scenarijev napovedi hitrosti vetra
$P_{\max}^{CH}$: nazivna moč elektrolizatorja (MW)
$P_{\min}^{CH}$: minimalna moč elektrolizatorja (MW)
$P_{\max}^{DIS}$: nazivna moč gorivne celice (MW)
$P_{\min}^{DIS}$: minimalna moč gorivne celice (MW)
$P_{\max,i}^{NET}$: prenosna zmogljivost prenosnega sistema v uri i (MW)
$V_{\max}^{STG}$: kapaciteta shranjevalnika vodika (kg)
T : število časovnih korakov pri optimizaciji

III.I.II ***Spremenljivke***

$\alpha_{w,p,i}$: stanje vklopa/izklopa gorivne celice v vetrnem scenariju w in cenovnem scenariju p v uri i
$\hat{\alpha}_i$: dejansko stanje vklopa/izklopa gorivne celice v uri i
$\beta_{w,p,i}$: stanje vklopa/izklopa elektrolizatorjev za vetrni scenarij w in cenovni scenarij p v uri i
$\hat{\beta}_i$: dejansko stanje vklopa/izklopa elektrolizatorjev v uri i
P_C : poraba kompresorja (MW)
$P_{w,p,i}^{CH}$: poraba vodikovega sistema za vetrni scenarij w in cenovni scenarij p v uri i (MW)
$\hat{P}_i^{CH}$: dejanska poraba vodikovega sistema v uri i (MW)
$P_{w,p,i}^{DIS}$: proizvodnja električne moči vodikovega sistema za vetrni scenarij w in cenovni scenarij p v uri i (MW)
$\hat{P}_i^{DIS}$: dejanska proizvodnja električne moči vodikovega sistema v uri i (MW)
P_E : poraba elektrolizatorja (MW)
P_F : proizvodnja električne moči v vodikovem sistemu (MW)
P_G : skupna proizvodnja vetrnih elektrarn in jedrske elektrarne (MW)
$P_{w,p,i}^{G}$: porabljena moč proizvedena v jedrski in vetrnih elektrarnah za vetrni scenarij w v uri i (MW)
$\hat{P}_i^{G}$: dejansko porabljena moč proizvedena v jedrski in vetrnih elektrarnah v uri i (MW)

P_H : proizvodnja toplotne moči v vodikovem sistemu (MW)
$P_{w,p,i}^{HEAT}$: proizvodnja toplote za vetrni scenarij *w* in cenovni scenarij *p* v uri *i* (MW)
$\hat{P}_i^{HEAT}$: dejanska proizvodnja toplote v uri *i* (MW)
P_M : izmenjava s trgom za električno energijo (MW)
P_N : proizvodnja jedrske elektrarne (MW)
P_W : proizvodnja vetrnih elektrarn (MW)
V_E : proizvodnja vodika iz elektrolizatorjev (kg v eni uri)
V_F : poraba vodika v gorivnih celicah (kg v eni uri)
V_H : prodaja vodika na trg z vodikom (kg v eni uri)
$V_{w,p,i}^H$: prodaja vodika na trg z vodikom za vetrni scenarij *w* in časovni scenarij *p* v uri *i* (kg)
$\hat{V}_i^H$: dejanska prodaja vodika na trg z vodikom v uri *i* (kg v eni uri)
V_O : prodaja kisika na trg s kisikom (Nm^3 v eni uri)
$V_{w,p,i}^O$: prodaja kisika za vetrni scenarij *w* cenovni scenarij *p* v uri *i* (Nm^3)
$\hat{V}_i^O$: dejanska prodaja kisika v uri *i* (Nm^3 v eni uri)
V_i^{STG} : nivo vodikovega shranjevalnika v uri *i* (kg)
$\hat{V}_i^{STG}$: dejanski nivo vodikovega shranjevalnika v uri *i* (kg)
$\hat{V}_d^{STGEND}$: končni nivo shranjevalnika vodika v zadnji uri trenutnega dneva *d* (kg)

III.I.III ***Vhodni podatki***

$c_{p,i}^M$: napoved cene električne energije za cenovni scenarij *p* v uri *i* (CAD/MWh)
$\hat{c}_i^M$: dejanska cena električne energije v uri *i* (CAD/MWh)
$P_{w,i}^{GA}$: napoved proizvodnje vetrnih in jedrske elektrarne v scenariju *w* v uri *i* (MW)
$\hat{P}_i^{GA}$: dejanska proizvodnja vetrnih in jedrske elektrarne v uri *i* (MW)
p_p : verjetnost cenovnega scenarija *p*
p_w : verjetnost vetrnega scenarija *w*

III.II Uvod

V svetu obstaja vse večja potreba po zamenjavi pojemajočih zalog fosilnih goriv, ki onesnažujejo okolje, in njihovem nadomeščanju z okolju bolj prijaznimi energenti, še posebej v transportnem sektorju. V tem kontekstu je ena izmed trajnostnih rešitev zamenjava fosilnih primarnih goriv z jedrskimi in obnovljivimi viri energije, ki imajo zanemarljive emisije toplogrednih in ostalih okolju škodljivih plinov [3]. Jedrska energija je tehnološko zrela in uveljavljena tehnologija za pridobivanje električne energije v elektroenergetskih sistemih v državah po svetu [13]. Obnovljivi viri energije zaradi svoje okoljske prijaznosti in razpršenosti doživljajo množičen razvoj (še posebej veter) ter že predstavljajo pomemben del v proizvodnji električne energije. Tako je pričakovati, da se bo delež obnovljivih virov energije brez hidroenergije v proizvodnji električne energije povečal iz 2 % v letu 2006 na 7 % v letu 2030 [74].

Koncept ekonomije vodika trenutno doživlja močno podporo kot rešitev za zamenjavo fosilnih goriv, ki trenutno igrajo vlogo tako primarnega kot tudi prenosnega energenta. Ekonomija vodika je hipotetična ekonomija, kjer vodik uporabljamo kot energent za prenos energije in ga je možno pridobiti iz raznih primarnih virov, kot so na primer prej omenjeni jedrski in obnovljivi viri [1]. Predvideni so različni scenariji razvoja ekonomije vodika, ki predvidevajo uporabo vodika v različne namene, katerim je skupno, da se vodik uporablja kot gorivo v transportnem sektorju ali kot energent za proizvodnjo električne energije. Ekonomija vodika je ugodna tudi zaradi dobro razvitih tehnologij za proizvodnjo vodika iz CO_2 nevtralnih energentov, kot sta jedrska in obnovljiva energija, zaradi česar je v njen razvoj usmerjeno veliko raziskovalnega dela.

Nekaj tehničnih in ekonomskih raziskav s področja različne uporabe tehnologije vodika je bilo že opravljenih. Avtorji v [16] predstavljajo rezultate analize ekonomike pridobivanja vodika s pomočjo elektrolize v kontekstu trga z električno energijo v Alberti v Kanadi. Avtorji v članku rezultate primerjajo z najbolj pogostim postopkom pridobivanja vodika, reformacijo metana, in ugotavljajo, da je vodik možno pridobivati iz električne energije po primerljivih cenah. Primerjave v omenjenem delu pa temeljijo na nizkih privzetih investicijskih stroških vodikovega sistema in so brez podrobne obravnave optimalnega obratovanja sistema.

Sestavka [13] in [14] prikazujeta možno uporabo jedrskih elektrarn za izključno pridobivanje vodika na podlagi novega termo-kemičnega cikla in visokotemperaturne elektrolize. Rezultati kažejo, da te tehnologije omogočajo proizvodnjo vodika s 50–60 % namesto z manj kot 30 % izkoristkom, kar omogoča ekonomsko upravičeno proizvodnjo vodika.

Avtorji v [2] prikazujejo tehnično in ekonomsko analizo izvedljivosti uporabe vodika kot prenosnega energenta v izoliranem sistemu z obnovljivimi viri energije v Avstraliji. Rezultati kažejo, da je električna energija proizvedena z omenjenim sistemom dražja od električne energije za gospodinjske odjemalce priključene na distribucijsko omrežje. Vira [5] in [6] kažeta, da vodik trenutno ni konkurenčen skladiščenju električne energije z baterijami zaradi svojih nizkih izkoristkov in visokih investicijskih ter vzdrževalnih stroškov. Zadnji dve študiji sta omejeni samo na uporabo vodika za shranjevanje električne energije in ne vključujeta možnosti prodaje vodika na trg z vodikom.

Optimalno obratovanje vodika kot shranjevalnika električne energije z obnovljivimi viri energije z nestalno proizvodnjo (npr. veter) na Evropskih trgih z električno energijo opisujeta vira [7] in [8], ki nakazujeta, da lahko vodik občutno poveča prihodek proizvajalca in da lahko stranski produkti, kot sta kisik in toplota, dodatno izboljšajo ekonomičnost njegovega poslovanja. Vendar pa za boljšo oceno ekonomske upravičenosti manjka podrobnejša analiza

ekonomike, ki bi zajemala investicijske, vzdrževalne, obratovalne in ostale stroške takšnega sistema.

Nekateri strokovnjaki, npr. v [12], se ne strinjajo z ekonomijo vodika zaradi manjših celotnih izkoristkov v primerjavi z ekonomijo električne energije, kjer je kot glavni prenosni energent predvidena električna energija. Vendar pa v tem delu manjka analiza velikih potencialnih primarnih energentov, kot na primer namenskih jedrskih elektrarn za proizvodnjo vodika, ki bi lahko dosegale tudi 50–60 % izkoristek in s tem omogočale masovno proizvodnjo vodika po ugodnih cenah. Ti viri bi z ustreznimi prenosnimi zmogljivostmi (cevovodi ali transport po vodi) omogočili, da vodik postane učinkovit energent, ki bi v prihodnosti lahko nadomestil tekoča fosilna goriva. Zaradi omejenega dosega avtomobilov na električni pogon, ki se napajajo iz baterij z nizko energijsko gostoto, ima vodik prav v transportnem sektorju največji potencial [15]. Poleg tega baterije tudi ne dosegajo zadostne življenjske dobe in števila polnitev, kar sta dva osnovna kriterija za njihovo razširjeno uporabo v transportnem sektorju.

Vodik lahko uporabljamo tudi v elektroenergetskih sistemih, kar je lahko možna rešitev za povečanje instalirane moči nestalnih obnovljivih virov. Tak primer sta veter in sončna energija, ki lahko zaradi svoje nenapovedljivosti in nestalnosti povzročata probleme pri obratovanju omrežja, če je njuna penetracija v omrežju prevelika. Uporaba vodika lahko tako pomaga pri zmanjševanju izpustov toplogrednih in ostalih škodljivih plinov v okolje [4].

Preden postane ekonomija vodika realnost, moramo premagati več ovir. Hitra rast porabe in s tem povezana potreba po izgradnji infrastrukture sta velika izziva pri popolni implementaciji ekonomije vodika. Literatura v tem kontekstu večkrat omenja maloserijsko proizvodnjo vodika z elektrolizo električne energije iz elektroenergetskih sistemov v začetnih fazah razvoja ekonomije vodika [19]; temu scenariju pa manjka natančnejše ekonomsko vrednotenje.

Namen pričujoče disertacije je tako natančna tehnično-ekonomska analiza raznih vidikov uporabe vodika v elektroenergetskih sistemih oziroma sinergij med ekonomijama vodika in električne energije. V tem kontekstu so pričakovane prednosti ekonomija vodika predvsem s stališča njene relativno visoke energijske gostote in možnosti shranjevanja velikih količin energije, ekonomija električne energije pa zagotavlja boljše izkoristke energetskih pretvorb. Ta analiza bo vsebovala vse pomembne parametre za ovrednotenje optimalnega obratovanja vodikovega sistema s ciljem doseganja maksimalnih dobičkov, kakor tudi vse relevantne ekonomske podatke.

III.III Opis modela

V doktoratu predstavljamo novo metodologijo za analizo ekonomike sistema za proizvodnjo in shranjevanje vodika v mešanih vetrno-jedrsko-vodikovih proizvodnih enotah priključenih v

elektroenergetski sistem z upoštevanjem nekaterih stranskih produktov, kot sta na primer kisik in toplota. Vodikov sistem je tako sestavljen iz elektrolizatorja, kompresorja, shranjevalnika za vodik in gorivnih celic, kot to prikazuje Sl. 1.

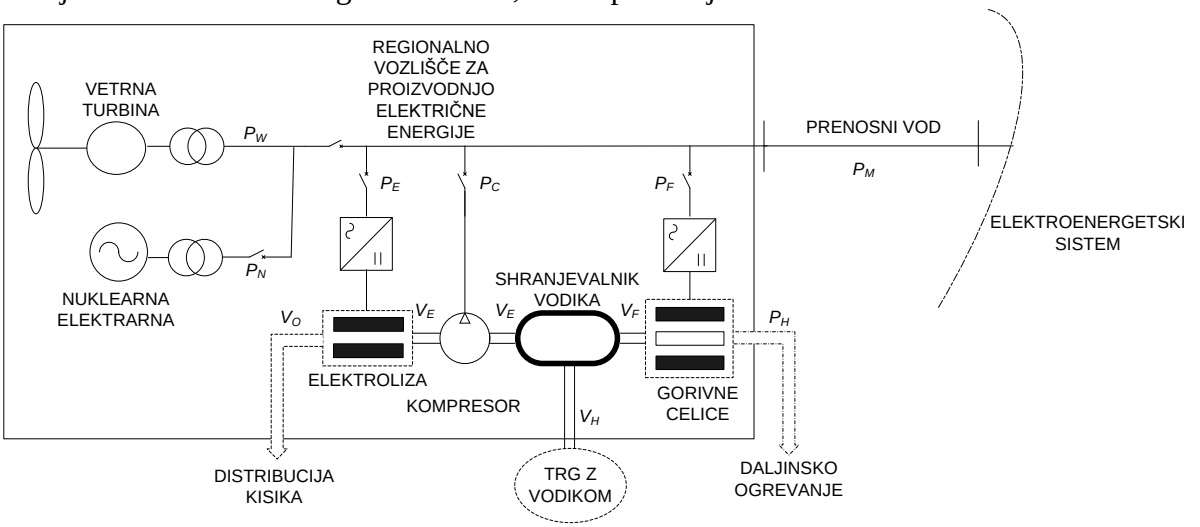

Sl. 1: Shema analiziranega vodikovega sistema z vetrnimi in nuklearno elektrarno.

V modelu, prikazanem na zgornji sliki, je P_W proizvodnja vetrnih elektrarn, P_N proizvodnja jedrske elektrarne, P_C poraba kompresorja, P_E poraba elektrolizatorja, P_F proizvodnja električne moči v vodikovem sistemu, P_H proizvodnja toplotne moči v vodikovem sistemu, P_M izmenjava s trgom za električno energijo, V_E proizvodnja vodika iz elektrolizatorjev, V_F poraba vodika v gorivnih celicah, V_O prodaja kisika na trg s kisikom in V_H prodaja vodika na trg z vodikom. Ta model je najbolj splošen in je v doktoratu prilagojen za ocenjevanje posameznih scenarijev uporabe vodikovega sistema.

Postopek za ocenjevanje ekonomike zgoraj prikazanega sistema je razdeljen na dva dela. V prvi fazi se izvede optimizacija obratovanja vodikovega sistema z izračunom pričakovanih letnih prihodkov. Ta optimizacija se izvede za vsak dan posebej in je razdeljena na dva dela zaradi doseganja višjih prihodkov pri obratovanju sistema s shranjevalnikom energije. V prvem se optimira obratovanje za en dan vnaprej na podlagi napovedi obratovalnih parametrov kot sta cena električne energije in hitrost vetra. V drugem delu se nato za vsako uro posebej optimira obratovanje vodikovega sistema v realnem času z upoštevanjem polnosti shranjevalnika vodika iz vnaprejšnje optimizacije. Pri obeh optimizacijah se zasleduje maksimalni dobiček iz obratovanja vodikovega sistema. Na koncu se v ekonomskem modelu izvede še ekonomsko vrednotenje vodikovega sistema v njegovi življenjski dobi na podlagi letnih prihodkov iz modela za optimizacijo obratovanja in ostalih ekonomskih parametrov. Metodologijo podrobneje prikazuje Sl. 2; podrobneje pa jo predstavljamo v sledečih poglavjih.

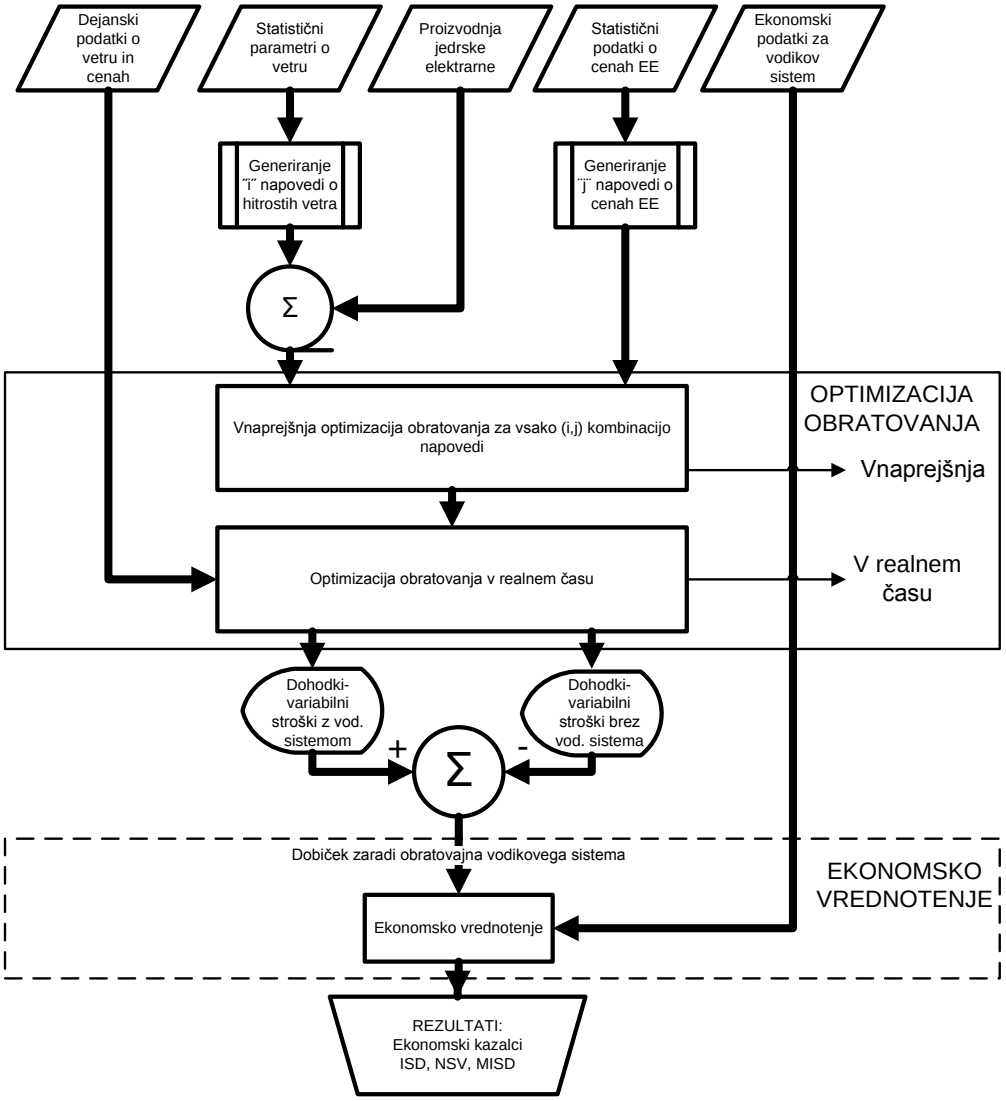

Sl. 2: Shema metodologije za ocenjevanje ekonomike vodikovega sistema.

III.III.I *Vnaprejšnja optimizacija obratovanja*

Vnaprejšnja optimizacija temelji na napovedih nekaterih parametrov, kot sta hitrost vetra in cena električne energije, ki sta po svoji naravi stohastična in jih bomo tako tudi obravnavali v modelu. Rezultat te optimizacije je "vozni red" obratovanja vseh komponent vodikovega sistema za določeno obdobje, t.j. za en dan vnaprej. Optimizacijski model je stohastičen, linearen in s celoštevilčnimi spremenljivkami ter temelji na modelih, razvitih v [8], [20], in [21]. Enačba (1) predstavlja ciljno funkcijo, ki maksimizira prihodke vodikovega sistema ob upoštevanju vseh možnih stohastičnih scenarijev cen na trgu z električno energijo in scenarijev hitrosti vetra:

$$\max \quad \sum_{w=1}^{Nw} p_w \cdot \sum_{p=1}^{Np} p_s \cdot \sum_{i=1}^{T} (c_{p,i}^{M}(P_{w,p,i}^{G} + P_{w,p,i}^{DIS} - P_{w,p,i}^{CH}) + c^{H} V_{w,p,i}^{H} + c^{O} V_{w,p,i}^{O} + c^{HEAT} P_{w,p,i}^{HEAT}) \qquad (1)$$

V zgornji enačbi je $P^{G}_{w,p,i}$ porabljena moč proizvedena v jedrski in vetrnih elektrarnah za vetrni scenarij *w* v uri *i*, $P^{CH}_{w,p,i}$ je poraba vodikovega sistema za vetrni scenarij *w* in cenovni scenarij *p* v uri *i*, $P^{DIS}_{w,p,i}$ je proizvodnja električne moči vodikovega sistema za vetrni scenarij *w* in cenovni scenarij *p* v uri *i*, $P^{HEAT}_{w,p,i}$ je proizvodnja toplote za vetrni scenarij *w* in cenovni scenarij *p* v uri *i*, $V^{H}_{w,p,i}$ je prodaja vodika na trg z vodikom za vetrni scenarij *w* in časovni scenarij *p* v uri *i*, $V^{O}_{w,p,i}$ je prodaja kisika za vetrni scenarij *w* cenovni scenarij *p* v uri *i*, p_w je verjetnost vetrnega scenarija *w*, p_p je verjetnost cenovnega scenarija *p*, N_w je število scenarijev napovedi hitrosti vetra, N_p je število scenarijev napovedi cen električne energije, $c^{M}_{p,i}$ napoved cene električne energije za cenovni scenarij *p* v uri *i*, c^{H} je prodajna cena vodika, c^{O} je prodajna cena kisika in c^{HEAT} je prodajna cena toplotne energije.

Enačba (2) zajema omejitve proizvodnje in porabe vodikovega sistema z zmogljivostjo prenosnega omrežja, ki povezuje proizvodno vozlišče s preostalim elektroenergetskim sistemom:

$$-P^{NET}_{\max,i} \le P^{G}_{w,p,i} + P^{DIS}_{w,p,i} - P^{CH}_{w,p,i} \le P^{NET}_{\max,i}, \tag{2}$$

kjer je $P^{NET}_{\max,i}$ prenosna zmogljivost prenosnega sistema v uri *i*. Enačba (3) omejuje proizvodnjo električne energije iz vetrne in nuklearne elektrarne na največjo možno proizvodnjo glede na hitrost vetra in obratovalno stanje nuklearke. Ta enačba je dodana za primere, ko bi se del proizvodnje zaradi omejitev v prenosnem sistemu ali premajhne zmogljivosti vodikovega sistema zavrgel.

$$0 \le P^{G}_{w,p,i} \le P^{GA}_{w,i} \tag{3}$$

V zgornji enačbi predstavlja $P^{GA}_{w,i}$ napoved proizvodnje vetrnih in jedrske elektrarne v scenariju *w* v uri *i* (MW). V enačbi (4) se izračuna nivo polnosti vodikovega shranjevalnika glede na prejšnje stanje in pritoke ter odtoke vodika v shranjevalnik, pri čemer začetno stanje shranjevalnika z vodikom podaja enačba (5).

$$V^{STG}_{i} = V^{STG}_{i-1} + \mu_{he} \cdot \frac{1}{\left(1 + \frac{\mu_{oe}}{\mu_{oc}} + \frac{\mu_{he}}{\mu_{hc}}\right)} \cdot P^{CH}_{w,p,i} - \mu_{ef} P^{DIS}_{w,p,i} - V^{H}_{w,p,i} \tag{4}$$

$$V^{STG}_{0} = \hat{V}^{STGEND}_{d-1} \tag{5}$$

V^{STG}_{i} je nivo vodikovega shranjevalnika v uri *i*, μ_{he} izkoristek pretvorbe električne energije v vodik v elektrolizatorju, μ_{oe} izkoristek pretvorbe električne energije v kisik v elektrolizatorju, μ_{hc} izkoristek stiskanja vodika v kompresorju, μ_{oc} izkoristek stiskanja kisika v kompresorju in $\hat{V}^{STGEND}_{d}$ končni nivo shranjevalnika vodika v zadnji uri trenutnega dneva *d*. Enačbi (6) in

(7) skrbita, da elektrolizatorji in gorivne celice obratujejo v skladu s svojimi obratovalnimi omejitvami:

$$\alpha_{w,p,i} \cdot P_{\min}^{DIS} \le P_{w,p,i}^{DIS} \le \alpha_{w,p,i} \cdot P_{\max}^{DIS}, \tag{6}$$

$$\beta_{w,p,i} \cdot \left(1+\frac{\mu_{oe}}{\mu_{oc}}+\frac{\mu_{he}}{\mu_{hc}}\right) \cdot P_{\min}^{CH} \le P_{w,p,i}^{CH} \le \beta_{w,p,i} \cdot \left(1+\frac{\mu_{oe}}{\mu_{oc}}+\frac{\mu_{he}}{\mu_{hc}}\right) \cdot P_{\max}^{CH}, \tag{7}$$

kjer je $\alpha_{w,p,i}$ stanje vklopa/izklopa gorivne celice v vetrnem scenariju *w* in cenovnem scenariju *p* v uri *i*, $\beta_{w,p,i}$ stanje vklopa/izklopa elektrolizatorjev za vetrni scenarij *w* in cenovni scenarij *p* v uri *i*, $P_{\max}^{CH}$ nazivna moč elektrolizatorja, $P_{\min}^{CH}$ minimalna moč elektrolizatorja, $P_{\max}^{DIS}$ nazivna moč gorivne celice in $P_{\min}^{DIS}$ minimalna moč gorivne celice. Enačba (8) omejuje polnost rezervoarja z vodikom na kapaciteto rezervoarja:

$$0 \le V_i^{STG} \le V_{\max}^{STG}, \tag{8}$$

kjer je $V_{\max}^{STG}$ kapaciteta shranjevalnika vodika. Na koncu uporabimo enačbi (9) in (10) za izračun proizvodnje kisika in toplote v odvisnosti od obratovalnih parametrov vodikovega sistema:

$$V_{w,p,i}^{O} = \mu_{oe} \cdot \frac{1}{\left(1+\frac{\mu_{oe}}{\mu_{oc}}+\frac{\mu_{he}}{\mu_{hc}}\right)} \cdot P_{w,p,i}^{CH}, \tag{9}$$

$$P_{w,p,i}^{HEAT} = \frac{\mu_{ef}}{\mu_{hf}} \cdot P_{w,p,i}^{DIS}, \tag{10}$$

pri čemer je μ_{ef} izkoristek pretvorbe vodika v električno energijo v gorivnih celicah, μ_{hf} pa je izkoristek pretvorbe vodika v toplotno energijo v gorivnih celicah. Zgoraj prikazan model je splošen in smo ga tekom doktorata prilagajali različnim scenarijem. Razvoji enačb, kakor tudi pomeni posameznih spremenljivk, so bolj natančno definirani v doktoratu. Model se rešuje za dan, t.j. 24 ur, vnaprej za vsak dan v obravnavanem letu in sledi polnosti rezervoarja z vodikom iz prejšnjega dneva.

III.III.II *Optimizacija obratovanja v realnem času*

Pri optimizaciji obratovanja v realnem času optimiramo sprotno obratovanje sistema glede na razpoložljive podatke v realnem času za vsako uro posebej s ciljem čim večjega dobička, upoštevajoč rezultate "voznega reda" vodikovega sistema iz vnaprejšnje optimizacije. Sistem optimiramo z enakimi omejitvami kot pri vnaprejšnji optimizaciji, vendar brez stohastičnih spremenljivk. Kriterijska funkcija ima naslednjo obliko:

$$\max \quad (\hat{c}_i^M (\hat{P}_i^G + \hat{P}_i^{DIS} - \hat{P}_i^{CH}) + c^H \hat{V}_i^H + c^O \hat{V}_i^O + c^{HEAT} \hat{P}_i^{HEAT}), \tag{11}$$

pri čemer je $\hat{P}_i^G$ dejansko porabljena moč proizvedena v jedrski in vetrnih elektrarnah v uri *i*, $\hat{P}_i^{CH}$ dejanska poraba vodikovega sistema v uri *i*, $\hat{P}_i^{DIS}$ dejanska proizvodnja električne moči vodikovega sistema v uri *i*, $\hat{P}_i^{HEAT}$ dejanska proizvodnja toplote v uri *i*, $\hat{V}_i^H$ dejanska prodaja vodika na trg z vodikom v uri *i*, $\hat{V}_i^O$ dejanska prodaja kisika v uri *i*, $\hat{c}_i^M$ pa dejanska cena električne energije v uri *i*. Omejitve prenosnega omrežja so predstavljene v naslednji enačbi:

$$-P_{\max,i}^{NET} \le \hat{P}_i^G + \hat{P}_w^{DIS} - \hat{P}_i^{CH} \le P_{\max,i}^{NET}. \tag{12}$$

Omejitve razpoložljive moči vetrne in jedrske elektrarne pa v naslednji enačbi:

$$0 \le \hat{P}_i^G \le \hat{P}_i^{GA} \tag{13}$$

kjer je $\hat{P}_i^{GA}$ dejanska proizvodnja vetrnih in jedrske elektrarne v uri *i*. Polnost rezervoarja z vodikom za dve zaporedni uri se izračuna po naslednji enačbi:

$$\hat{V}_i^{STG} = \hat{V}_{i-1}^{STG} + \mu_{he} \cdot \frac{1}{\left(1 + \frac{\mu_{oe}}{\mu_{oc}} + \frac{\mu_{he}}{\mu_{hc}}\right)} \cdot \hat{P}_i^{CH} - \mu_{ef} \hat{P}_w^{DIS} - \hat{V}_i^H \tag{14}$$

V zgornji enačbi $\hat{V}_i^{STG}$ predstavlja dejanski nivo vodikovega shranjevalnika v uri *i*. Enačba (15) omejuje polnost vodikovega rezervoarja v realnem času z optimalnimi nivoji, izračunanimi z vnaprejšnjim optimizacijskim algoritmom:

$$\hat{V}_1^{STG} = V_i^{STG} \tag{15}$$

Omejitve gorivnih celic in elektrolizatorjev predstavljata enačbi (16) in (17):

$$\hat{\alpha}_i \cdot P_{\min}^{DIS} \le \hat{P}_i^{DIS} \le \hat{\alpha}_i \cdot P_{\max}^{DIS}, \tag{16}$$

$$\hat{\beta}_i \cdot \left(1 + \frac{\mu_{oe}}{\mu_{oc}} + \frac{\mu_{he}}{\mu_{hc}}\right) \cdot P_{\min}^{CH} \le \hat{P}_i^{CH} \le \hat{\beta}_i \cdot \left(1 + \frac{\mu_{oe}}{\mu_{oc}} + \frac{\mu_{he}}{\mu_{hc}}\right) \cdot P_{\max}^{CH}, \tag{~~17~~}$$

pri čemer je $\hat{\alpha}_i$ dejansko stanje vklopa/izklopa gorivne celice v uri *i*, $\hat{\beta}_i$ pa dejansko stanje vklopa/izklopa elektrolizatorjev v uri *i*. Omejitve velikosti shranjevalnika vodika in njegovo končno stanje, ki se uporabi pri optimizaciji v naslednjem časovnem intervalu, podajata naslednji enačbi:

$$0 \le V_i^{STG} \le V_{\max}^{STG}, \tag{18}$$

$$\hat{V}_d^{STGEND} = \hat{V}_T^{STG} \tag{19}$$

Proizvodnja kisika in toplote se na koncu izračuna z naslednjima enačbama:

$$\hat{V}_i^O = \mu_{oe} \cdot \frac{1}{\left(1 + \frac{\mu_{oe}}{\mu_{oc}} + \frac{\mu_{he}}{\mu_{hc}}\right)} \cdot \hat{P}_i^{CH}, \tag{20}$$

$$\hat{P}_i^{HEAT} = \frac{\mu_{ef}}{\mu_{hf}} \hat{P}_i^{DIS}. \tag{21}$$

Tako kot model vnaprejšnje optimizacije smo tudi ta model prilagajali različnim scenarijem uporabe vodika. Omejitve so enake omejitvam v modelu za vnaprejšnjo optimizacijo, razen omejitve v enačbi (15), ki omejuje nivo v shranjevalniku vodika na nivo pridobljen v vnaprejšnji optimizaciji. Enačbe in posamezne spremenljivke so bolj natančno definirane v nadaljevanju doktorata. Model se rešuje posebej za vsako obratovalno uro in sicer za 24 ur. Temu ponovno sledi model za vnaprejšnjo optimizacijo obratovanja za naslednji dan.

III.III.III *Ekonomsko vrednotenje projektov*

Pri ekonomskem vrednotenju projektov analiziramo donos v obliki premoženja, zmanjšanja stroškov ali družbene dobrobiti glede na trenutne odhodke premoženja ali ostalih sredstev [45]–[49]. Investicija se izplača, če vse prihodnje koristi v zadostni meri odtehtajo poprejšnje izdatke, ki so potrebni za dosego teh koristi. Disertacija predvideva, da bo ekonomsko vrednotenje temeljilo na rezultatih optimizacije obratovanja in na ostalih ekonomskih postavkah relevantnih za ekonomsko vrednotenje. Ekonomsko vrednotenje bo podano v obliki ekonomskih indeksov, ki bodo nosili informacijo o donosnosti preučevanih scenarijev.

Ti indeksi se izračunavajo na podlagi denarnih tokov, ki upoštevajo več postavk prihodkov in odhodkov. Zato, da se ovrednotijo davki na dobiček na letnem nivoju, se najprej, v okviru izkaza poslovnega izida, izračuna dobiček pred obdavčitvijo, ki zajema naslednje postavke:

- dohodke iz poslovanja vodikovega sistema (rezultata optimizacije obratovanja),
- investicijske stroške,
- variabilne stroške,
- stroške financiranja,
- amortizacijo,
- preostalo vrednost,
- stroške obratovanja in vzdrževanja naprav.

Nato se izračunajo projekcije denarnih tokov, ki poleg davkov, upoštevajo še naslednje postavke:

- dohodke iz poslovanja vodikovega sistema,
- investicijske stroške,

- variabilne stroške,
- preostalo vrednost,
- anuiteto za odplačevanje kreditnih obveznosti,
- stroške obratovanja in vzdrževanja naprav.

Na podlagi denarnih tokov se nato izračunajo naslednji ekonomski kazalci. **Neto sedanja vrednost** (NSV) je indeks pogosto uporabljen pri ekonomskem vrednotenju; predstavlja trenutno vrednost vseh pričakovanih bodočih prihodkov in odhodkov v življenjski dobi projekta. V splošnem je investicija sprejemljiva, če je NSV, ki se izračuna iz denarnega toka, pozitiven. V nasprotnem primeru projekt za investitorja ni sprejemljiv. Glavna pomanjkljivost tega indeksa je, da ne zagotavlja informacije o stopnji donosnosti, kar je pomemben podatek za investitorja, da ta lažje razlikuje med različnimi projekti različnih vrednosti. **Interna stopnja donosnosti** (ISD) je prav tako indeks, ki se pogosto uporablja, in daje informacijo o stopnji donosnosti vloženega kapitala [45]. ISD je diskontna stopnja, ki enači pozitivni in negativni del denarnega toka, oziroma je diskontna stopnja, pri kateri je neto sedanja vrednost enaka nič. Če je ISD enak ali večji od stroškov izgubljenih priložnosti kapitala (diskontne stopnje) v zasebnih projektih ali socialne diskontne stopnje v državnih projektih, se v projekt izplača investirati. V disertaciji bomo uporabili tudi **modificirano interno stopnjo donosnosti** (MISD), ki se od ISD razlikuje predvsem v tem, da upošteva vnaprej določeno stopnjo reinvestiranja za pozitivni denarni tok in privzema prav tako vnaprej določeno stopnjo diskontiranja negativnega denarnega toka na sedanjo vrednost. S tem bolj natančno ponazarja dejansko dogajanje z denarnim tokom pri projektih [47], [48]. Zato MISD rešuje tudi problem pri izračunu ISD, kjer lahko dobimo več rezultatov zaradi večkratnih sprememb predznaka v denarnem toku tekom življenjske dobe projekta.

Podrobnejši opis ekonomskega modela s pripadajočimi enačbami za izračun denarnih tokov in posameznih ekonomskih indeksov je podan v disertaciji.

III.III.IV *Opis testnega sistema*

Metodologijo opisano v zgornjem poglavju, smo uporabili na realnem sistemu, ki trenutno obratuje v Ontariu, Kanada. Ta je sestavljen iz jedrske elektrarne Bruce Power in polja vetrnih elektrarn Ripley, povezanih z glavnim centrom porabe v Torontu preko dvosistemskega 500 kV daljnovoda in 230 kV voda, ki povezuje elektrarno z jugom Ontaria. V vseh scenarijih v doktoratu smo nato privzeli, da bo vodikov sistem z vsemi komponentami vključen v to obstoječe proizvodno vozlišče (angl. »electricity production hub«).

I.I.I.I Vodikov sistem

Predpostavili smo, da vodikov sistem vsebuje vse najpomembnejše komponente potrebne za njegovo delovanje, kot to opisujejo [7], [26] in [27]. Vodik se proizvaja iz električne energije s pomočjo elektrolize vode v elektrolizatorju, nato se s kompresorjem stisne na ustrezen tlak,

shrani v posebnih namenskih rezervoarjih za vodik in se v končni fazi proda na trg z vodikom ali pretvori nazaj v električno energijo s pomočjo gorivnih celic ter proda na trg z električno energijo. Parametre komponent vodikovega sistema podaja tabela 1, pri čemer je podroben opis vodikovega sistema opisan v doktoratu in se spreminja glede na scenarije njegove uporabe. Obratovanje vseh komponent vodikovega sistema smo optimirali z namenom doseganja čim višjih dohodkov.

Tabela 1: Parametri komponent vodikovega sistema.

PARAMETER	ELEKTROLIZATORJI	KOMPRESORJA (Za vodik in kisik)	SHRAJNEVALNIKI (Za vodik in kisik)	GORIVNE CELICE
Število	264	2	28	322
Cena (CAD na modul)	413985	2560121	881353	65000
Življenjska doba (leta)	10	20	20	20
Max. moč	0,288 (MW/modul)	1661 (kg/h vodika na modul) 9250 (Nm^3/h kisika na modul)	1240 (kg/modul na 410 bar)	0,065 (MW/modul)
Min. moč (MW/module)	0,072	—	—	0,065
Izkoristek pretvorbe v vodik (kg/MWh)	18,73	449	—	68,10
Izkoristek pretvorbe v kisik (Nm^3/MWh)	104,16	2500	—	—
Izkoristek pretvorbe v toploto (kg/MWh)	—	—	—	76,92

I.I.I.I Polje vetrnih elektrarn

Vetrna energija kot primarni energent ne emitira škodljivih toplogrednih plinov in je lokalnega značaja, kar pomeni, da manjša odvisnost držav od uvoza energentov. Zato se raziskuje in uporablja povsod po svetu, disertacija pa jo predvideva kot primarni energent za proizvodnjo vodika [39], [40]. Pri analizi smo upoštevali polje vetrnih elektrarn Ripley z instalirano močjo 76 MW, za katerega smo dobili letni profil hitrosti vetra in s pomočjo tehničnih podatkov proizvajalca turbin izračunali proizvodnjo električne energije tega polja na letni ravni.

I.I.I.II Jedrska energija

Jedrska energija je uveljavljena že od petdesetih let prejšnjega stoletja, do sedaj pa je bil razvit že širok spekter tehnologij za izrabo energije jeder atomov [41]. Skupno tem tehnologijam je, da proizvajajo toplotno energijo, ki se pretvori v mehansko energijo in na koncu v električno energijo brez omembe vrednih emisij toplogrednih ali drugih okolju škodljivih plinov po sprejemljivih cenah. Avtorji v [13] predlagajo jedrsko energijo kot glavni vir primarne energije v ekonomiji vodika z visokim izkoristkom pretvorbe v vodik (50 %− 60 %); te izkoristke se lahko dosega s sodobnimi termo-kemičnimi postopki in visokotemperaturno elektrolizo. Jedrska energija lahko tudi učinkovito dopolnjuje vetrno energijo, ki je po naravi nestalna, in s tem povečuje uporabo vodikovega sistema, kar predpostavlja tudi pričujoča disertacija. Sistem, na katerem smo uporabili metodologijo, poleg ostalih objektov sestavlja tudi jedrska elektrarna Bruce Power, ki ima instalirano moč 4820 MW in je v letu 2004 obratovala s 7446 ekvivalentnimi obratovalnimi urami polne moči [71], kar pomeni, da je proizvajala v povprečju 3952,4 MW moči.

I.I.I.I Trg z električno energijo v Ontariu

Ker predpostavljamo, da je predlagani sistem postavljen v provinci Ontario v Kanadi, temelji model za optimizacijo proizvodnje na pravilih trga z električno energijo v Ontariu [58], [59] in [60]. Privzeli smo, da sodelovanje opisanega testnega vodikovega sistema ne vpliva na cene na tem trgu zaradi relativno majhne proizvodnje vodikovega sistema. Vpliv jedrske elektrarne Bruce na cene na tem trgu je pri tem že upoštevan v uporabljenih cenah električne energije. Za obratovanje v realnem času smo vetrne elektrarne obravnavali kot nestalnega proizvajalca v skladu s pravili [59], po katerih je vsak nestalni proizvajalec obvezan zagotavljati sistemskemu operaterju napoved proizvodnje, ni pa zavezan dejansko proizvesti napovedane energije in tudi ni zavezan slediti obratovalnim navodilom sistemskega operaterja o proizvodnji električne energije. V doktoratu so privzete cene električne energije za leto 2006, pridobljene iz spletne strani sistemskega operaterja prenosnega omrežja v Kanadi [62]. Napovedi cen so oblikovane na podlagi rezultatov modelov predstavljenih v [58] in so podrobneje opisane v doktoratu.

I.I.I.I Cene vodika, kisika in toplote

Cene vodika, kisika in toplote so bile oblikovene na podlagi razpoložljive literature in so podrobneje pojasnjene in utemeljene v doktoratu. Tipično so pogodbene cene fiksne za čas trajanja pogodbe. Tako je privzeta cena vodika v višini 4,35 CAD/kg, ki pa je zelo odvisna od dogajanj na trgu z vodikom v okviru potencialnega razvoja ekonomije vodika. Cena kisika je bila ovrednotena na 0,15 CAD/Nm^3, cena toplote pa na 33,24 CAD/MWh. Ker so te cene zelo nepredvidljive, smo v okviru doktorata opravili številne občutljivostne analize, pri katerih smo opazovali vpliv sprememb teh cen na ekonomiko vodikovega sistema.

III.IV Rezultati

Pričujoče poglavje prikazuje rezultate metodologije uporabljene na zgoraj opisanem sistemu za različne scenarije uporabe vodika. Scenariji so opisani sproti v vsakem posameznem podpoglavju. Zaradi omejene dolžine razširjenega povzetka opisujemo le glavne rezultate brez vseh pripadajočih analiz občutljivosti.

III.IV.I ***Osnovni scenarij***

Namen tega poglavja je analizirati ekonomičnost vodikovega sistema z uporabo za shranjevanje električne energije in izkoriščanja cenovnih razlik na sprotnem trgu z električno energijo v Kanadi. Scenarij ne upošteva morebitnih omejitev v prenosnem sistemu, kakor tudi možnosti prodaje stranskih produktov, kisika in toplote, ki nastajata pri obratovanju vodikovega sistema. Poglavje je razdeljeno na naslednji podpoglavji:

- podpoglavje v katerem je vodikov sistem uporabljen zgolj kot shranjevalnik električne energije;
- podpoglavje, ki omogoča tudi prodajo vodika na trg z vodikom.

Podrobnejši opis modela in rezultatov prikazuje doktorat.

III.IV.I.I Scenarij brez možnosti prodaje vodika

Rezultate scenarija brez možnosti prodaje vodika direktno na trg z vodikom prikazuje tabela 2. Ti so ločeno prikazani z napako napovedovanja cen električne energije (Z NN) in brez napake napovedovanja te veličine (Brez NN). Rezultati kažejo, da so letni prihodki premajhni, da bi skozi življenjsko dobo projekta pokrili celo samo obratovalne stroške. Za nizke prihodke je kriva premajhna uporaba vodikovega sistema zaradi neugodnih izkoristkov in cenovnih razmerij na trgu z električno energijo. Zaradi vsega omenjenega sta tako NSV kot tudi MISD celotnega projekta negativni tudi ob neupoštevanju napake pri napovedovanju cen.

Tabela 2: Rezultati osnovnega scenarija brez možnosti prodaje vodika.

FAKTOR	Z NN	Brez NN
Prihodek [CAD/leto]	160744	162153
Investicijski stroški [CAD]	145121103	145121103
Obratovalni in vzdrževalni stroški [CAD/leto]	2902422	2902422
Faktor uporabe gorivnih celic [%]	2,9	2,8
Faktor uporabe elektrolizatorjev [%]	2,9	2,8
NSV [CAD]	-214845944	-214817468
MISD [%]	Neg.	Neg.

V doktoratu je bilo opravljenih več analiz občutljivosti, v katerih smo opazovali spremembe ekonomskih kazalcev glede na spremembe različnih vrednosti ključnih ekonomskih parametrov vodikovega sistema. Tako smo preučili vplive možnih izboljšav v izkoristkih elektrolizatorjev in gorivnih celic, zmanjšanje investicijskih stroškov vodikovega sistema in cenovnih profilov na različnih trgih z električno energijo v različnih časovnih obdobjih. Rezultati teh analiz, v katerih smo zgoraj omenjene parametre spreminjali znotraj realnih vrednosti, so podrobneje prikazane v doktoratu samem in so pokazali, da se ekonomika vodikovega sistema ne izboljša do sprejemljive mere niti ob najbolj optimistično postavljenih vrednostih omenjenih parametrov.

III.IV.I.II Scenarij z možnostjo prodaje vodika

Rezultati zgodnjega scenarija, ki predvidevajo tudi prodajo vodika direktno na trg z vodikom in so zajeti v tabeli 3, kažejo, da bi se ob primerno visokih cenah vodika (4,35 CAD/kg) investicija v vodikov sistem izplačala. To omogočajo zadosti visoki prihodki, ki zaradi zadosti visoke uporabe vodikovega sistema pokrivajo tako obratovalne stroške kot tudi investicijske stroške. Iz rezultatov lahko tudi razberemo, da se uporabljajo predvsem elektrolizatorji za proizvodnjo vodika, ki se nato prodaja direktno na trg z vodikom; gorivne celice zaradi premajhnih cenovnih razlik na sprotnem trgu z električno energijo in zaradi premajhnih izkoristkov skorajda ne obratujejo. Zato smo posebej analizirali scenarij z gorivnimi celicami (Z GC) in scenarij brez gorivnih celic (Brez GC), pri čemer se izkaže, da je slednji iz ekonomskega vidika veliko ugodnejši, saj ne predvideva dodatnih stroškov za gorivne celice, ki ne prinašajo skorajda nikakršnega prihodka.

Tabela 3: Rezultati osnovnega scenarija z možnostjo prodaje vodika.

FAKTOR	Z GC/Z NN	Brez GC/Z NN	Z GC/Brez NN	Brez GV/Brez NN
Prihodek [CAD/leto]	23337511	23322516	23337546	23322516
Investicijski stroški [CAD]	0,03	/	0,05	/
Obratovalni in vzdrževalni stroški [CAD/leto]	92,18	92,18	92,19	92,18
Faktor uporabe gorivnih celic [%]	145121103	124191103	145121103	124191103
Faktor uporabe elektrolizatorjev [%]	2902422	2483822	2902422	2483822
NSV [CAD]	5848016	26411385	5848303	26411385
MISD [%]	8,62	10,67	8,62	10,67

V tem scenariju smo analizirali občutljivost na vse faktorje, naštete v analizi občutljivosti prejšnjega scenarija, in dodatno še na cene vodika na trgu z vodikom. Rezultati kažejo, da je ekonomika močno korelirana le s cenami vodika, ki določijo, ali bo vodikov sistem ekonomsko sprejemljiv ali ne. To odvisnost prikazuje Sl. 3, iz katere je moč razbrati, da morajo biti cene vodika višje od 3–4 CAD/kg, da bo vodikov sistem ekonomsko upravičen pri različnih obravnavanih investicijskih stroških in ob upoštevanju privzetih ekonomskih in tehničnih parametrih vodikovega sistema.

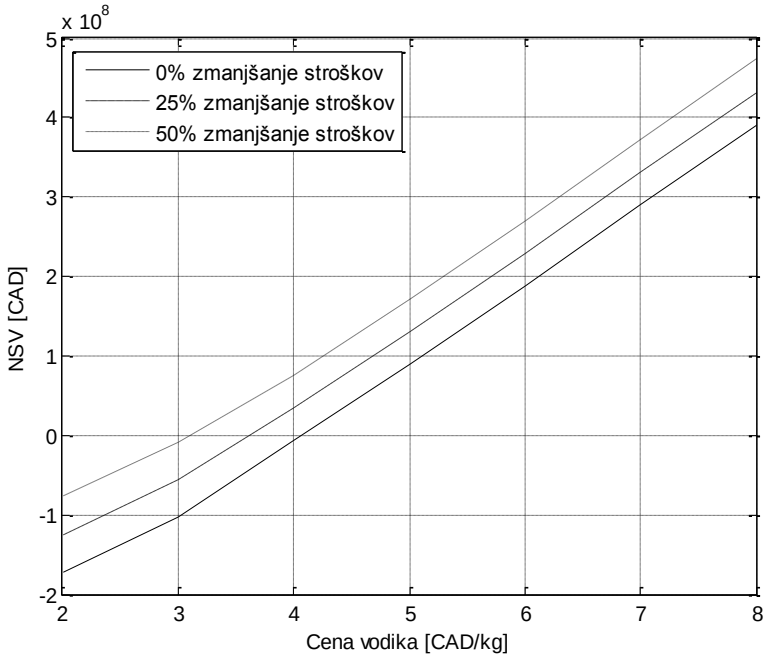

Sl. 3: NSV brez gorivnih celic v odvisnosti od prodajnih cen vodika.

III.IV.II ***Scenarij z možnostjo prodaje stranskih produktov kisika in toplote***

V tem scenariju privzamemo možnost prodaje stranskih produktov obratovanja vodikovega sistema, t.j. kisika in toplote. Zaradi dodatnih prihodkov iz prodaje teh dveh produktov pričakujemo bistveno izboljšanje ekonomike vodikovega sistema. Tudi ta scenarij ne predvideva omejitev v prenosnem omrežju.

III.IV.II.I Brez možnosti prodaje vodika

Rezultate scenarija brez možnosti prodaje vodika prikazuje tabela 4. Le ti ponovno kažejo nezadostno uporabo elementov, da bi zagotovili rentabilnost celotnega vodikovega sistema. Čeprav so prihodki gleda na scenarij brez prodaje kisika in toplote več kot desetkrat višji, ti še vedno ne pokrijejo niti obratovalnih ter vzdrževalnih stroškov. Investicijski stroški so v tem scenariju nekoliko višji, saj sama investicija, ki vpliva tudi na obratovalne in vzdrževalne stroške, predvideva tudi kompresorje za stiskanje kisika in ustrezne rezervoarje za začasno shranjevanje kisika. Glede na prejšnji scenarij je moč opaziti izrazito povečanje faktorja uporabe vodikovega sistema in ponovno zanemarljiv vpliv napovedovanja cen električne energije.

Tabela 4: Rezultati scenarija s koriščenjem kisika in toplote brez možnosti prodaje vodika.

FAKTOR	Z NN	Brez NN
Prihodek [CAD/leto]	1919194	1958731
Investicijski stroški [CAD]	160020166	160020166
Obratovalni in vzdrževalni stroški [CAD/leto]	3200403	3200403
Faktor uporabe gorivnih celic [%]	25,24	26,80
Faktor uporabe elektrolizatorjev [%]	25,22	26,82
NSV [CAD]	-214682774	-214294598
MISD [%]	Neg.	Neg.

III.IV.II.II Scenarij z možnostjo prodaje vodika

Če pri obratovanju vodikovega sistema poleg kisika in toplote upoštevamo še možnost prodaje vodika direktno na trg z vodikom, se ekonomičnost ponovno drastično izboljša, kar kažejo rezultati v tabeli 5. Ti ponovno kažejo, da se izplača zgolj uporaba vodikovega sistema za proizvodnjo vodika ne pa tudi za shranjevanje električne energije, saj so stopnje donosnosti v tem primeru dosti nižje. Dodatni prihodki zaradi trženja kisika in toplote izboljšajo donosnost naložbe za približno 4 %, pri čemer ima trženje toplote, zaradi majhnega faktorja uporabe gorivnih celic, zanemarljiv delež.

Tabela 5: Rezultati scenarija s koriščenjem kisika in toplote z možnostjo prodaje vodika.

FAKTOR	Z GC/Z NN	Brez GC/Z NN	Z GC/Brez NN	Brez GV/Brez NN
Prihodek [CAD/leto]	32013388	31994948	32013389	31994948
Investicijski stroški [CAD]	0,057	/	0,057	/
Obratovalni in vzdrževalni stroški [CAD/leto]	95,40	95,40	95,40	95,40
Faktor uporabe gorivnih celic [%]	160020166	139090166	160020166	139090166
Faktor uporabe elektrolizatorjev [%]	3200403	2781803	3200403	2781803
NSV [CAD]	62248598	82783723	62248607	82783723
MISD [%]	12,48	13,91	12,48	13,91

Sl. 4 prikazuje rezultate analize občutljivosti na enake parametre kot v poglavju III.IV.I.II z dodatnim pregledom občutljivosti na ceno kisika in ponovno kaže na močno korelacijo ekonomike vodikovega sistema le s cenami na trgu z vodikom. Vendar pa so lahko cene vodika v tem scenariju nižje, in sicer med 2,5 CAD/kg in 3,5 CAD/kg za različne cene komponent vodikovega sistema, zaradi dodatnih prihodkov iz prodaje kisika in toplote.

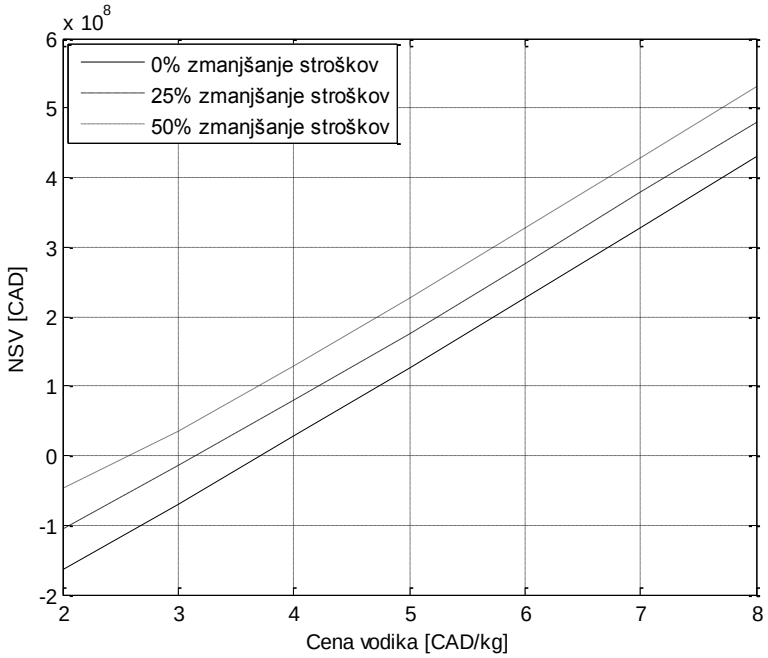

Sl. 4: NSV v odvisnosti od prodajnih cen vodika ob upoštevanju prodaje kisika in toplote.

III.IV.III ***Alternativa gradnji prenosnih zmogljivosti***

Ta scenarij obravnava ekonomiko vodikovega sistema v situacijah, ko iz obstoječih proizvodnih enot, zaradi trajno nezadostnih prenosnih zmogljivosti, električne energije ni možno dobavljati porabnikom. Ta scenarij je verjeten v okraju Bruce v Ontariu v Kanadi, kjer se obnavlja reaktor Bruce A, lokalne iniciative pa zavirajo gradnjo dodatnega voda, ki bi imel zadostne zmogljivosti za prenos dodatno proizvedene električne energije [55]. Zato predvidevamo, da bi višek proizvedene električne moči (207 MW) spremenili v vodik, katerega bi po obstoječih transportnih povezavah dobavljali na trg z vodikom. Rezultati takšnega scenarija so prikazani v tabeli 6 in kažejo visoke donose na investicijo zaradi opisanih razmer privzetih v tem scenariju.

Tabela 6: Rezultati scenarija uporabe vodika kot alternative nadgradnji prenosnega sistema.

FAKTOR	Z NN
Prihodek [CAD/leto]	202565891
Investicijski stroški [CAD]	99,14
Obratovalni in vzdrževalni stroški [CAD/leto]	/
Faktor uporabe gorivnih celic [%]	475455009
Faktor uporabe elektrolizatorjev [%]	9509100
NSV [CAD]	1046296770
MISD [%]	20,40

Zaradi omejenih prenosnih zmogljivosti v scenariju niso upoštevane gorivne celice ampak le direktna prodaja vodika na trg z vodikom. Zaradi tega tudi ni potrebno napovedovanje cen na trgu z električno energijo. Visoka odvisnost ekonomike vodikovega sistema od cene vodika je prisotna tudi v tem scenariju, kar prikazuje Sl. 5. Kljub temu pa je NSV vodikovega sistema v

celotnem območju pozitiven, kar pomeni, da je vodikov sistem ekonomičen tudi ob zelo nizkih cenah vodika.

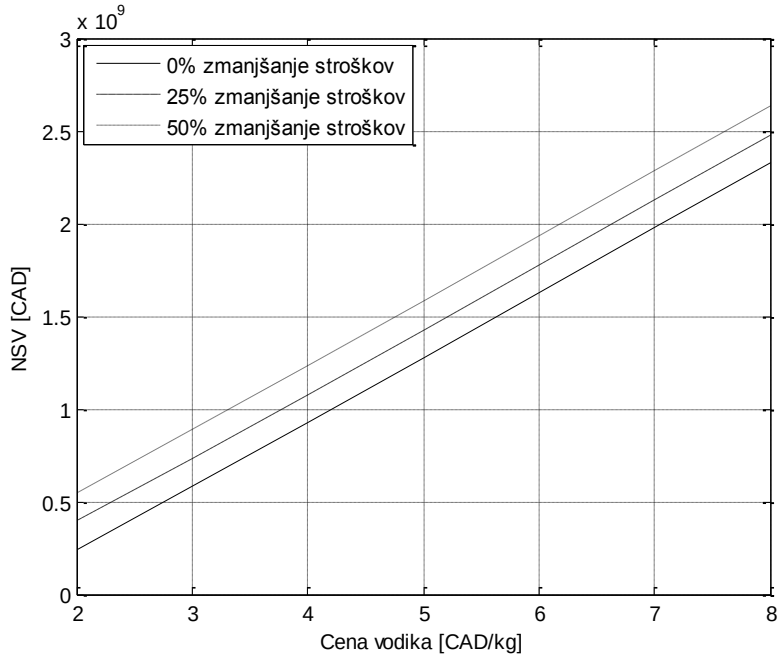

Sl. 5: NSV v odvisnosti od prodajnih cen vodika v scenariju s trajno omejenimi prenosnimi zmogljivostmi.

III.IV.IV ***Scenarij z občasnimi zamašitvami v prenosnem omrežju***

Poleg obnovitve bloka A nuklearne elektrarne Bruce Power, so na tem področju predvidene tudi številne nove investicije v vetrne elektrarne [55]. Te zaradi svojega nestalnega režima proizvodnje električne energije ne bi povzročale stalnih zamašitev v sistemu, ampak le začasne. Razlike med urnimi vrednostmi prenosnih zmogljivosti in pripadajočih vrednosti proizvodnje na tem območju prikazuje Sl. 6.

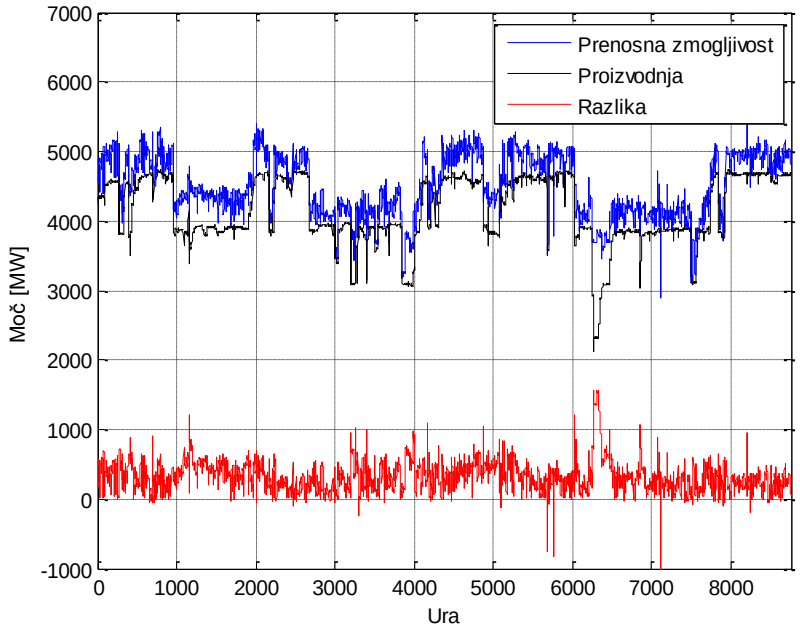

Sl. 6: Razpoložljive prenosne zmogljivosti iz območja Bruce, vsota proizvodenj vetrnih in jedrskih elektrarn in razlika teh veličin.

III.IV.IV.I Scenarij brez možnosti prodaje vodika

Rezultate scenarija z opisanimi omejitvami v prenosnem sistemu podaja tabela 7; le ti jasno kažejo, da brez prodaje vodika scenarij z občasnimi omejitvami v prenosnem omrežju ni ekonomičen, kljub trženju kisika in toplote. Ekonomika je v teh poglavjih nekoliko boljša kot v scenarijih brez omejitev v omrežju, opisanih v poglavjih III.IV.I.I in III.IV.II.I. Napake v napovedovanju imajo na rezultate zanemarljiv vpliv.

Tabela 7: Rezultati scenarija s koriščenjem kisika in toplote brez možnosti prodaje vodika.

FAKTOR	Z NN	Brez NN
Prihodek [CAD/leto]	1998013	2046656
Investicijski stroški [CAD]	160020166	160020166
Obratovalni in vzdrževalni stroški [CAD/leto]	3200403	3200403
Faktor uporabe gorivnih celic [%]	25,,26	26,95
Faktor uporabe elektrolizatorjev [%]	25,28	26,98
NSV [CAD]	-213908923	-213431339
MISD [%]	Neg.	Neg.

Analize občutljivosti so ponovno pokazale, da spremembe nobenega izmed parametrov ne vplivajo na dohodke v zadostni meri, da bi vodikov sistem lahko postal ekonomsko spremenljiv. Izsledki so enaki tudi ob spremembah instaliranih moči vetrnih elektrarn med 76 MW in 760 MW ob upoštevanju konstantnega proizvodnega profila.

III.IV.IV.II Scenarij z možnostjo prodaje vodika

Možnost prodaje vodika na trg z vodikom tudi v tem scenariju pripelje do ekonomsko ugodnih kazalcev vodikovega sistema kot to prikazuje tabela 8. Ti so zaradi trženja kisika,

vodika, toplote in elektrike ob začasno omejenih prenosnih zmogljivostih boljši od tistih iz primerljivih scenarijev, a brez omejitev v prenosnih sistemih.

Tabela 8: Rezultati scenarija s koriščenjem kisika in toplote z možnostjo prodaje vodika.

FAKTOR	Z GC/Z NN	Brez GC/Z NN	Z GC/Brez NN	Brez GV/Brez NN
Prihodek [CAD/leto]	32150372	32131931	32150372	32131931
Investicijski stroški [CAD]	0,057	/	0,057	/
Obratovalni in vzdrževalni stroški [CAD/leto]	95,42	95,42	95,42	95,42
Faktor uporabe gorivnih celic [%]	160020166	139090166	160020166	139090166
Faktor uporabe elektrolizatorjev [%]	3200403	2781803	3200403	2781803
NSV [CAD]	63371611	83906727	63371611	83906727
MISD [%]	12,54	13,96	12,54	13,96

Rezultati analize občutljivosti, ki jih prikazuje Sl. 7, kažejo, da bi v tem scenariju cene vodika morale presegati 2,5 CAD/kg do 3,5 CAD/kg, kar je skorajda enako kot v rezultatih scenarija brez omejitev prikazanih v poglavju III.IV.II.II. Ta zaključek kaže, da se ekonomika zaradi občasno omejenih prenosnih zmogljivosti le zanemarljivo izboljša. Izboljšave so večje le ob večjih proizvodnih zmogljivosti vetrnih elektrarn, ki povzročajo pogostejše zamašitve in s tem pogostejšo dobavo električne energije za proizvodnjo vodika.

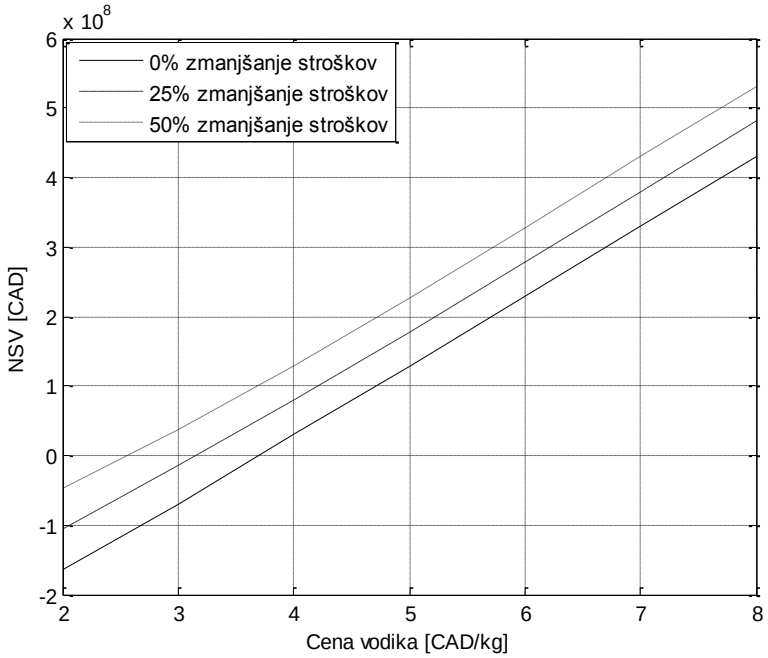

Sl. 7: NSV v odvisnosti od prodajnih cen vodika v scenariju z občasno omejenimi prenosnimi zmogljivostmi.

III.V Zaključki

Doktorat predstavlja novo metodologijo za ekonomsko vrednotenje različnih scenarijev uporabe vodika v elektroenergetskih sistemih z vetrnimi in jedrskimi elektrarnami; ta metodologija je uporabljena na realnem sistemu v Ontariu, Kanada.

Rezultati kažejo, da ob privzetih vrednostih parametrov samo za shranjevanje električne energije vodik ni ekonomsko sprejemljiv, še posebej če ga primerjamo z alternativami (npr. črpalnimi elektrarnami). Ta zaključek smo v doktoratu potrdili, tudi če so bili prodajani stranski produkti obratovanja vodikovega sistema, t.j. kisik in toplota. Izkazalo se je celo, da občutno znižanje investicijskih stroškov in občasne zamašitve v prenosnem sistemu ne privedejo do želenih nivojev donosnosti.

Vodikov sistem se je po drugi strani izkazal kot tehnično, okoljsko in ekonomsko sprejemljiv shranjevalnik energije v primeru ugodnih cen električne energije in ob možnosti prodaje vodika na trg z vodikom ob ugodnih cenah vodika. Te so seveda zelo odvisne od razvoja trga z vodikom, ki je zelo vezan na razvoj porabe vodika v potencialno razširjeni ekonomiji vodika. V slednji je največja poraba vodika predvidena v transportnem sektorju, pri čemer pa se bo moralo izkazati, da obstajajo zadostne tehnične in tudi ekonomske prednosti pred ekonomijo električne energije.

Vodik se lahko izkaže kot primeren medij v manjših nišnih aplikacijah, na primer kot prenosni energent na lokacijah, kjer električne energije zaradi različnih vzrokov ne moremo prenesti po klasični prenosnih sistemih, kot vir za zagotavljanje neprekinjene dobave električne energije, v porabniški elektroniki ali za pogon nekaterih vrst viličarjev.

III.VI Prispevki k znanosti

- Nova metodologija za modeliranje sistema sestavljenega iz vetrnih elektrarn, jedrskih elektrarn in vodikovega sistema, vključenega v elektroenergetski sistem.
- Nova metodologija za dvokoračno stohastično optimizacijo obratovanja vodikovega sistema.
- Natančna metodologija za ocena donosnosti uporabe vodika za shranjevanje električne energije v elektroenergetskih sistemih.
- Ocena donosnosti uporabe vodika za shranjevanje električne energije v elektroenergetskih sistemih z omejenimi prenosnimi zmogljivostmi (raba vodika kot alternativa izgradnji prenosnega omrežja).
- Ocena vpliva uporabe stranskih produktov, kot sta kisik in toplota, na donosnost vodika kot shranjevalnika električne energije.

IV NOMENCLATURE AND ABBREVIATIONS

IV.I Parameters

A: cross-sectional area of the wind-turbine rotor (m^2)
A_t: annuity of the debt in the year t (CAD)
a-g: parameters of the wind-power polynomial
C: wind-turbine power coefficient
cf_t: cash flow in year t (CAD)
c^H : hydrogen selling price (CAD/kg)
c^{HEAT} : heat selling price (CAD/MWh)
c^O : oxygen selling price (CAD/Nm^3)
cof_t: compound factor in year t
c_t : investment and reinvestment costs in year t (CAD)
d_a: density of air (kg/m^3)
df_t: discount factor in year t
d_t : depreciation in year t (CAD)
EBT_ACO_t: pretax profits after the carry-forward process in year t (CAD)
EBT_temp_t: temporary earnings before tax before the carry-forward process (CAD)
EBT_t: earnings before tax in year t (CAD)
eq: proportion of equity in the investment costs
$e_{t,k}$: costs of the equipment class k in year t (CAD)
F: Faraday constant (96,485 As/mol)
fr: finance rate
I: cell current (A)
ir: interest rate for the debt (%)
IRR: internal rate of return (%)
I_t: interests for taxation (CAD)
K: number of asset groups
M_r: relative molecular mass (2.016 g/mol)
n: number of electrons involved in water splitting
$\dot{n}_H$: molar production rate of hydrogen (mol/h)
n_k: lifetime of asset group k (years)
N_p : number of price scenarios
N_w : number of wind scenarios
μ_{ef} : electrical efficiency of stationary fuel cell (kg/MWh)
μ_{he} : hydrogen efficiency of electrolyzer (kg/MWh)
μ_{hf} : heat efficiency of stationary fuel cell (kg/MWh)
μ_{hc} : hydrogen efficiency of compressor (kg/MWh)
μ_I: current efficiency

μ_{oc}: oxygen efficiency of compressor (Nm^3/MWh)
μ_{oe}: oxygen efficiency of electrolyzer (Nm^3/MWh)
μ_U: voltaic efficiency of electrolyzer
om: operation and maintenance costs factor as percentage of equipment costs
o_t: operation and maintenance costs in year t (CAD)
p_1: gas pressure (bar)
P_t: principal of the debt taken to cover the investment costs (CAD)
PV: present value of a cash flow series (CAD)
PV_t: present value in year t (CAD)
$P_{\max}^{CH}$: maximum electrolyzer electricity consumption (MW)
$P_{\min}^{CH}$: minimum electrolyzer electricity consumption (MW)
$P_{\max}^{DIS}$: maximum stationary fuel-cell electricity production (MW)
$P_{\min}^{DIS}$: minimum stationary fuel-cell electricity production (MW)
$P_{\max}^{NET}$: transmission system capacity (if constant) (MW)
$P_{\max,i}^{NET}$: transmission system capacity in hour i (MW)
P_W^R: rated power of the wind turbine (MW)
r: discount rate
R: resistance of electric load (Ω)
R_T: yearly revenues of the hydrogen system (CAD)
ρ_H: density of hydrogen gas (0.08988 kg/Nm^3)
s: salvage value factor (%)
s_t: salvage value in yeat t (CAD)
T: number of time steps
ta_t: taxes in year t (CAD)
Tp: lifetime of the project (years)
tr: tax rate (%)
tr_t: transportation costs of the equipment in year t (CAD)
U_{an}: electrolyzer anode losses (V)
U_{cat}: electrolyzer catode losses (V)
U_{cell}: actual cell voltage (V)
U_{rev}: reversible cell voltage (V)
V_1: volume of the gas at pressure p_1 (m^3)
V_W: wind velocity (m/s)
V_W^{CO}: cut-out speed of the wind turbine (m/s)
V_W^R: rated speed of the wind turbine (m/s)
$V_{\max}^{STG}$: maximum storage level (kg)
$W_{1,2}$: theoretical work for isothermal compression (kWh)

IV.II Variables

$\alpha_{w,p,i}$: on/off status of stationary fuel cells for wind scenario *w* and price scenario *p* at hour *i*

$\hat{\alpha}_i$: actual on/off status of stationary fuel cells at hour *i*

$\beta_{w,p,i}$: on/off status of electrolyzers for wind scenario *w* and price scenario *p* at hour *i*

$\hat{\beta}_i$: actual on/off status of electrolyzers at hour *i*

C_B : costs for the hydrogen system operation (CAD)

C_{HYD} costs from hydrogen purchases due to hydrogen system operation (CAD)

P_C: total electrolyzer and oxygen compressor consumption (MW)

P_{CH}: hydrogen compressor consumption (MW)

$P_{w,p,i}^{CH}$: electricity consumed by electrolyzer for wind scenario *w* and price scenario *p* at hour *i* (MW)

$\hat{P}_i^{CH}$: actual electricity consumed by electrolyzer at hour *i* (MW)

P_{CO}: oxygen compressor consumption (MW)

$P_{w,p,i}^{DIS}$: fuel-cell electricity produced and sold for wind scenario *w* and price scenario *p* at hour *i* (MW)

$\hat{P}_i^{DIS}$: actual fuel-cell electricity produced and sold at hour *i* (MW)

P_E: electrolyzer consumption (MW)

P_F : fuel-cell electricity sales (MW)

P_G : utilized wind-nuclear power production (MW)

$P_{w,p,i}^{G}$: used wind-nuclear power for wind scenario *w* and price scenario p at hour *i* (MW)

$\hat{P}_i^{G}$: actual used wind-nuclear production at hour *i* (MW)

P_{GA} : available wind-nuclear power output (MW)

P_H : fuel-cell heat sales (MW)

$P_{w,p,i}^{HEAT}$: heat produced and sold for wind scenario *w* and price scenario *p* at hour *i* (MW)

$\hat{P}_i^{HEAT}$: actual heat produced and sold at hour *i* (MW)

P_M : power exchange with the market (MW)

P_N : nuclear power plant production (MW)

P_T : total compressor and electrolyzer consumption (MW)

P_W : wind power plant production (MW)

R_{ELEC} : revenues from electricity sales due to hydrogen system operation (CAD)

R_{HEAT} : revenues from oxygen sales due to hydrogen system operation (CAD)

R_{HYD} revenues from hydrogen sales due to hydrogen system operation (CAD)

$\hat{R}_i$: revenues at hour *i* (CAD)

R_{OXY} : revenues from oxygen sales due to hydrogen system operation (CAD)

R_S : revenues obtained from the hydrogen system operation (CAD)

$\hat{R}_i^{WH}$: Revenues without hydrogen system at hour *i* (CAD)

V_E : hydrogen production by electrolyzer (kg in one hour)

V_F : hydrogen consumption by fuel cells (kg in one hour)

V_H : hydrogen sales to the hydrogen market (kg in one hour)

$V_{w,p,i}^{H}$: hydrogen sold to the hydrogen market for wind scenario *w* and price scenario *p* at hour *i* (kg in one hour)

$\hat{V}_i^{H}$: actual hydrogen sold to the hydrogen market at hour *i* (kg in one hour)

V_O : oxygen sales to the oxygen market (Nm^3 in one hour)
$V_{w,p,i}^{O}$: oxygen produced and sold for wind scenario *w* and price scenario *p* at hour *i* (Nm^3 in one hour)
$\hat{V}_i^O$: actual oxygen produced and sold at hour *i* (Nm^3 in one hour)
V_i^{STG} : storage level at hour *i* (kg)
$\hat{V}_i^{STG}$: actual storage level at hour *i* (kg)
$\hat{V}_T^{STG}$: actual storage level in the final hour of the observed day (kg)
$\hat{V}_d^{STGEND}$: storage level in the last hour of the current day (kg)

IV.III Input data

$c_{p,i}^{M}$: market price forecast for price scenario *p* in hour *i* (CAD/MWh)
$\hat{c}_i^M$: actual market price in hour *i* (CAD/MWh)
$P_{w,i}^{GA}$: forecast for available wind and nuclear generation for wind scenario *w* in hour *i* (MW)
$\hat{P}_i^{GA}$: actual wind and nuclear generation in hour *i* (MW)
p_p : probability of price scenario *p*
p_w : probability of wind scenario *w*

IV.IV Abbreviations

AC	Alternating Current
AFC	Alkaline Fuel Cell
BCS	Base Case Scenario
CAD	Canadian Dollar
CANDU	CANadian Deuterium Uranium
CDCF	Cumulative Discounted Cash Flow
DC	Direct Current
DSPS	Dispatch Scheduling and Pricing Software
EEX	European Energy Exchange
EL	Electrolyzer
EXAA	Energy Exchange Austria
FABC	Flow Away from Bruce Complex
FC	Fuel Cells
FE	Forecast Error
FES	Fossil Energy Sources
GTO	Gate Turn Off
HHV	Higher Heating Value
HOEP	Hourly Ontario Electricity Price
IESO	Independent Electricity System Operator (system operator in Ontario, Canada)
IGBT	Insulated Gate Bipolar Transistor
IRR	Internal Rate of Return
LHV	Lower Heating Value

LWR	Light Water Reactor
MAE	Mean Absolute Error
MCFC	Molten Carbonate Fuel Cell
MILP	Mixed-Integer Linear Programming
MIRR	Modified Internal Rate of Return
MISLP	Mixed-Integer Stochastic Linear Programming
NFC	without Fuel Cells
NFE	without Forecast Error
NPP	Nuclear Power Plant
NPV	Net Present Value
O&M	Operation and Maintenance
PAFC	Phosphoric Acid Fuel Cell
PEM	Polymer Electrolyte Membrane
PMSG	Permanent-Magnet Synchronous Generator
PPI	Pressure Product Industries
RES	Renewable Energy Sources
ROE	Return on Equity
SMR	Steam Methane Reforming
SO	System Operator
SOFC	Solid Oxide Fuel Cell
USD	United-States Dollar
VAT	Value Added Tax
WRSG	Wound Rotor Synchronous Generator
WRIG	Wound Rotor Induction Generator

1 INTRODUCTION

1.1 Thesis motivation

Renewable energy resources have seen a rapid growth in the past several years due to increased environmental concerns, energy-security issues and the cost growth of fossil-energy sources; in this context, nuclear energy is seeing a renaissance too. The renewables, however, also present several new challenges for the system operators due to their specific operational requirements. Hydrogen as a storage option has therefore been foreseen as a possible solution by several authors [1]-[19]; it can, for example, be used to resolve some issues from the production intermittency of some renewable energy sources, e.g., wind farms. Hydrogen, on the other hand, is also envisaged to replace dwindling and emission-generating fossil-fuel-based energy sources in the future, especially in the transportation sector, in the concept of a hydrogen economy, where energy is stored and carried as hydrogen [1], [2].

The thesis motivation is thus an exact techno-economic evaluation of the different possible synergies between the so-called "electron economy" with significant renewable and nuclear installations and the "hydrogen economy". In this context, the electron economy is assumed to be beneficial from the efficiency viewpoint and the hydrogen economy from the energy-density and the possibility of storing large quantities of energy standpoints. Thus, the benefits from the following utilization potentials arising from hydrogen-system operations were studied:

- part of the electricity production can be stored as hydrogen during periods of low electricity prices and sold to the electricity market during high-price periods;
- the byproducts from the hydrogen-system operations might be marketed, resulting in additional profits that might improve the economics of the hydrogen system;
- in periods of insufficient line capacity to sell the whole electricity production to the market, the excess electricity may be stored as hydrogen and later sold to the hydrogen or electricity market, depending on transmission system parameters;
- hydrogen may be sold directly to a hydrogen market when the price of hydrogen is higher than the costs of producing it, and/or when profit is higher than selling it into the electricity market;
- hydrogen within the hub can be used as a storage mechanism to relieve some of the electricity grid's operational challenges associated with the variability of wind generation, in particular power dispatch, voltage and frequency control.

1.2 Literature review

A comprehensive set of technical literature is devoted to the use of hydrogen in power systems with renewable and nuclear power, a short review of which is presented in this chapter as an introduction to the thesis.

There is a growing concern about the negative environmental impacts associated with the use of fossil energy sources (FES), in particular those related to global warming. In this context, some of the main real emission-free and sustainable options for FES in electricity generation are nuclear and renewable energy sources (RES) [3]. Nuclear technology is already well developed and is a significant part of the energy mix in several jurisdictions around the world (e.g., France, Ontario). RES, on the other hand, are still at the development stage; however, some technologies, especially wind, are already playing a considerable part in the energy mix in several jurisdictions (e.g., Denmark, Germany).

Hydrogen integrated into electric power systems could be a possible solution to the electricity-storage problem, facilitating the use of intermittent renewable energy sources (RES) such as wind and solar, and reducing the CO_2 emissions and air pollution produced by power systems [4]. The authors in [5] present an economic viability study of hydrogen storage for different round-trip efficiencies, concluding that hydrogen storage is not economically competitive at the present state of technological development.

In a further study in [2], the technical and financial feasibility of hydrogen as an energy carrier in power systems is presented for a stand-alone application of RES in Australia; the results show that electricity produced by such a system is more expensive than the electricity for domestic customers connected to the grid (2.52 AUD/kWh compared to 0.13 AUD/kWh). It is further shown in [6] that hydrogen storage is not yet fully competitive compared to battery storage due to its low round-trip efficiency (about 37%, presented in the article), and high investment, operation and maintenance (O&M) costs. The two latter studies are only limited to the electricity storage capabilities of hydrogen and do not include other possible applications of hydrogen, within the context of a Hydrogen Economy, such as its possible use in the transportation sector.

There has also been some research done in the field of optimal generation scheduling with hydrogen electricity storage. In [7]-[10], the optimal operation of hydrogen storage together with intermittent RES on the European electricity markets is discussed. The results suggest that hydrogen storage with intermittent RES, such as wind, can considerably increase the income of the producer, and the byproducts of electrolysis and fuel-cell usage, such as oxygen and heat, might improve the hydrogen system’s economic performance. However, a comprehensive economic analysis considering the investment and operation and maintenance (O&M) costs of such a system is missing from this article.

With respect to transportation, there is still a lack of an energy carrier that would replace FES as an efficient and feasible storage option. In this context, the concept of a Hydrogen Economy, which is a hypothetical economy where energy is stored and carried as hydrogen

(H_2), has been proposed [1], [11]. Various Hydrogen Economy scenarios can be envisaged, using hydrogen in a number of different ways; a common feature of these scenarios is the use of hydrogen as an energy carrier for mobile applications (e.g., cars, trains, aircraft) as well as electricity generation.

Some authors argue that the Hydrogen Economy does not make sense because of the lower well-to-wheel efficiencies compared to the so called "electron economy", which is based on electricity as the main energy carrier [12]. However, this analysis is missing a consideration of the realistic bulk primary energy sources for hydrogen production (e.g., novel thermo-chemical cycles and high-temperature electrolysis [13], [14]), which may achieve hydrogen production efficiencies of 50%-60%, thus lowering the total costs and making large-scale hydrogen production economically feasible. These sources combined with large-scale hydrogen transportation (e.g., by hydrogen pipelines or shipping) should make hydrogen an efficient energy carrier that might replace liquid fossil fuels in the transportation sector in the future.

Furthermore, electricity-storage issues, such as the low range of electric vehicles compared to hydrogen-fueled vehicles due to the low energy density of batteries, limit the use of electricity as an energy carrier in the transportation sector [15]; battery-recharge times and lifetimes have to improve significantly for purely electrical systems to become more acceptable to the transportation market.

In [16], the economics of nuclear power for electrolytic hydrogen production in the context of the electricity market in Alberta, Canada, is analyzed. The results are compared with common steam-methane-reforming (SMR) hydrogen-production processes, with costs assumptions for the hydrogen subsystem being relatively low and without considering an adequate system operation optimization. Similar results from a wind-hydrogen system are presented in [17].

Using restructured electricity markets in the possible transition to a hydrogen economy, considering a number of potential strategies, is studied in [18]. The authors argue that the use of generation technologies to produce hydrogen via electrolysis is one possible option, given that it leverages capital that would otherwise be invested and has a potential option value. In addition, as off-peak electricity prices increase, the associated electricity demand decreases, providing additional generation capacity for the production of hydrogen. Another envisaged transition-period scenario is the small-scale production of hydrogen using the hydrolysis process together with the electric power systems presented in [19].

Several articles about the bidding for electricity from intermittent energy sources and considering the price forecasts in European electricity markets are available (e.g., [20], [21]); these articles use stochastic programming techniques to incorporate the stochastic variables

such as price and wind forecasts into the optimization process. In [20], the objective function is the minimization of imbalance costs due to the deviations of wind production from bids to the market. In [21], a similar methodology is used to incorporate electricity storage in the form of pumped-storage units in the optimization process in day-ahead European electricity markets, with a balancing market for the deviations of actual productions from the bids.

An in-depth analysis taking into account operational as well as economic parameters, analyzing several hydrogen usage options, is however missing in these contributions. To address several of the aforementioned shortcomings in the existing technical literature, the objective of this thesis is to examine, structure and concentrate the findings of these different scenarios in a single comprehensive study. This is done by the development of a detailed methodology for a techno-economic assessment of hydrogen systems, a realistic assessment of hydrogen-system parameters and performing several sensitivity analyses on the most important hydrogen-system parameters. This thesis combines the methodologies presented in [22]-[24], which are modified to allow for a detailed optimization and economic evaluation of the hydrogen system; furthermore, the developed methodology is applied to study new scenarios of hydrogen use with several sensitivity analyses, which were conducted to comprehensively analyze the impact of several parameters on hydrogen-system economics.

1.3 Thesis outline

The rest of the thesis is structured as follows. In chapter 2, the technology overview is presented together with its modelling. Chapter 3 provides a detailed description of the methodology for an economic evaluation of the different hydrogen-usage scenarios, which is applied to a realistic test system in Ontario, Canada, described in chapter 4. The results of different hydrogen-usage scenarios are presented in chapter 5. Finally, the concluding remarks and references are listed in chapters 6 and 7, respectively.

2 TECHNOLOGY OVERVIEW AND ITS MODELLING

In this chapter, the background of the technologies of the different hydrogen-system components considered in this thesis is described, accompanied by a definition of the models and the corresponding assumptions that were considered in the modelling process.

2.1 Hydrogen-system components

In the thesis hydrogen is assumed to be used to cope with the intermittent nature of RES production levels and transmission-system congestions. Moreover, hydrogen is also assumed to be sold to a prospective hydrogen market where it can be used especially for mobility applications (e.g. cars, trains, aircraft) as well as electricity generation. The sales of the byproducts (oxygen and heat) of the hydrogen-system operation are also assumed in some scenarios. Based on all this, a complex hydrogen-system setup is needed, which would allow for the described hydrogen-system operations. In this chapter, the models of different hydrogen-system components with the corresponding assumptions are presented.

2.1.1 Water electrolysis

Hydrogen can be produced from a variety of different sources, as depicted in Fig. 2.1, which shows the variety of hydrogen-production pathways and highlights the methods supported by existing electric utilities [25]. Those pathways are further evaluated in Tab. 2.1, where the conversion to hydrogen and specific emissions are listed for each primary energy source [26]; 70% hydrolysis efficiency is considered in these calculations. The prices for hydrogen production are also indicated in the table to assess the economic feasibility of the different energy carriers. One can conclude from the table that nuclear and wind sources are among the cheapest emission-free energy sources to be used for hydrogen production. The other importance of these two pathways for making hydrogen is that the fuel can be produced domestically, without a reliance on foreign sources.

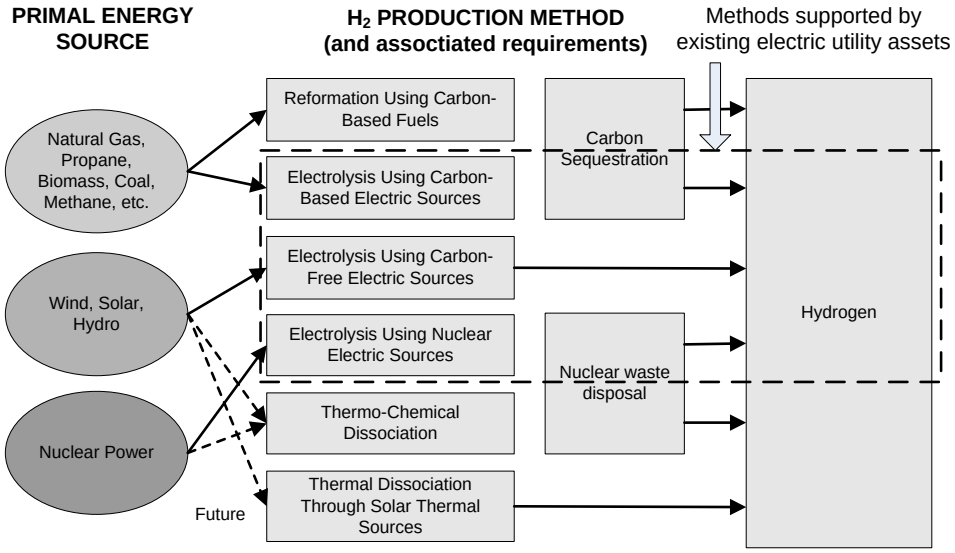

Fig. 2.1: Hydrogen-production pathways [26].

Tab. 2.1: Conversion efficiencies and CO_2 emissions of different primary energy sources for hydrogen production [26].

Conversion technology	Conversion efficiency	Hydrogen production price [USD/t H_2]	CO_2 emissions [kg CO_2/GJ]
Nuclear electrolysis	0.28	5197	0
Nuclear thermochemical	0.5	1270	0
Wind electrolysis	0.7	6081	0
Tidal electrolysis	0.7	5625	0
Solar PV electrolysis	0.105	14950	0
Solar biomass gasification	0.0024	5160	0
Solar photocatalysis	0.04	3447	0
Hydroelectric electrolysis	0.7	4725	0
Natural Gas reforming	0.76	982	55
Coal gasification	0.59	1621	110

Global hydrogen production in 2006 amounted to 444.7 billion cubic meters per year (40 billion kg/year) [25]. Currently, the main hydrogen-production technologies are the reforming of natural gas and the dissociation of hydrocarbons. A smaller amount of hydrogen is produced through water electrolysis. Reforming natural gas is cost effective, as shown in Tab. 2.1, and accounts for roughly 48% of the hydrogen currently produced in the world. The steam methane reforming (SMR) process is currently the least expensive natural-gas reforming technology for large-scale hydrogen production from natural gas (prices in the range of 1-5 USD/kg). However, this situation is expected to change in the future, both due to the limitations of fossil-fuel resources and due to CO_2 emissions. The only energy resource that ensures electricity for hydrogen production in a sustainable way is water electrolysis from renewables and nuclear power.

In the electrolysis process, water is split into hydrogen and oxygen in an electrolysis cell by the supply of direct current to the electrodes, as shown in Fig. 2.2.

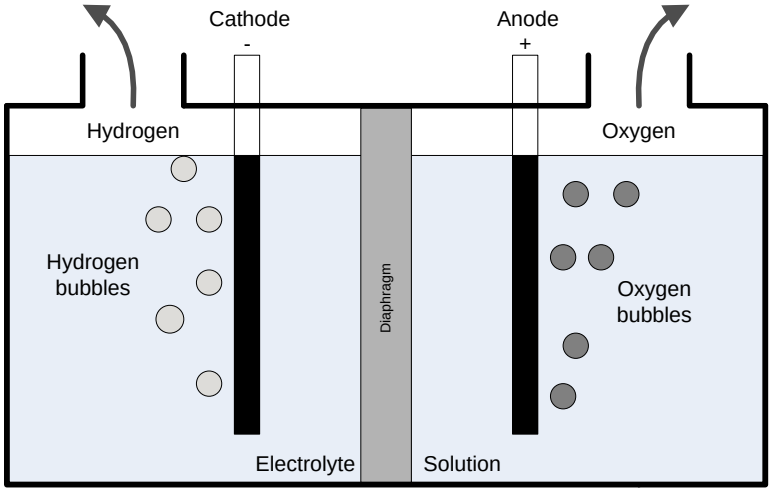

Fig. 2.2: Water electrolysis scheme.

Although the electrolysis process has been known since before the 19th century, only 0.5% of hydrogen production today comes from electrolysis. The net reaction for the splitting of water is [7]:

$$H_2O \rightarrow H_2 + \frac{1}{2}O_2 \tag{2.1}$$

The voltaic efficiency μ_U of the electrolysis process is defined as the relation between the reversible cell voltage U_{rev} and the actual cell voltage U_{cell}:

$$\mu_U = \frac{U_{rev}}{U_{cell}} \tag{2.2}$$

where U_{rev} is 1.23 V at room temperature and atmospheric pressure. An example of the how cell voltage depends on the operating conditions is presented in Fig. 2.3, which shows the polarization curve of an electrolysis cell.

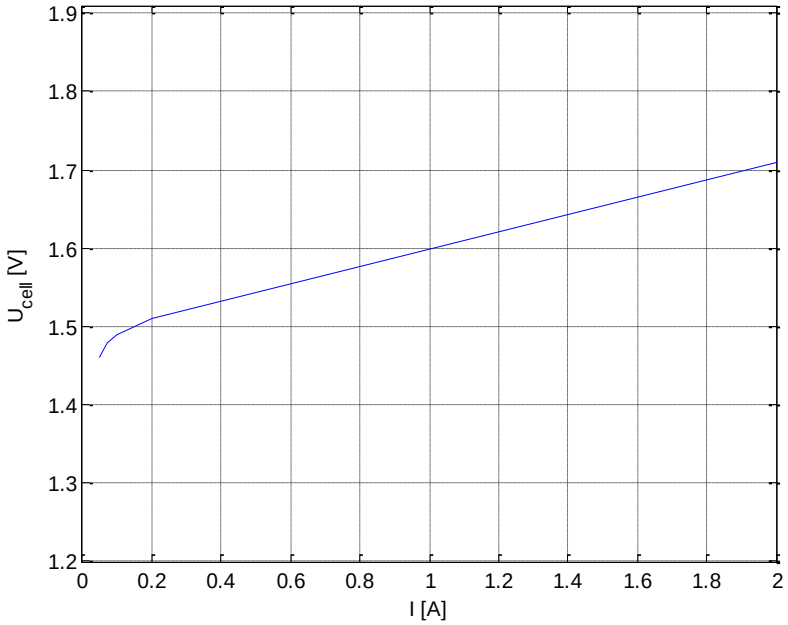

Fig. 2.3: Polarization curve of an electrolysis cell with a solid polymer electrolyte with an active cell area of 5 cm^2 [7].

The difference between U_{rev} and U_{cell} is due to irreversibilities, referred to as the overvoltage, overpotential or polarization. The overvoltage originates primarily from the electrical resistance (R) and the kinetic overvoltage at the electrodes:

$$U_{cell} = U_{rev} + U_{cat} + U_{an} + IR \tag{2.3}$$

where U_{cat} and U_{an} are the kinetic losses at the cathode and anode, respectively, I is the cell current and R is the resistance of the load. The kinetic overvoltage comprises an activation and concentration potential. The activation potential is the result of electronic barriers that have to be overcome prior to current and ion flow, and the concentration potential is due to gas transport losses, especially at high currents. According to Faraday's law, the amount of produced hydrogen is directly proportional to the cell current. The current efficiency of the electrolysis cell μ_I can be stated as:

$$\mu_I = \frac{n\mathrm{F} \cdot \dot{n}_H}{I} \tag{2.4}$$

In the above equation, F is the Faraday constant (96.485 As/mol), $\dot{n}_{\mathrm{H}}$ is the molar production rate of hydrogen and n is the number of electrons (n) involved in the reaction, which is 2 for water splitting. The current efficiency is close to 100% for electrolyzers with a proton-exchange membrane. Industrial electrolyzers consist of many cells, which are connected in series and/or parallel. Thus, as seen in Fig. 2.3, the voltaic efficiency can be improved by

installing more cells and operating the electrolyzer at low current densities. However, the efficiency gain must be leveled out against the increased investment cost.

Normally, the electrolyzer capacity V_E is expressed by the volumetric hydrogen-production rate (Nm^3/h):

$$V_E = \frac{3600}{1000} \cdot \frac{M_r}{\rho_H \cdot nF} \cdot \mu_l I \tag{2.5}$$

where M_r is the relative molecular mass and ρ_H is the density of hydrogen gas (0.08988 kg/Nm^3). In the thesis, the electrical efficiency of the electrolyzer is defined as the specific power consumption (kWh/Nm^3), where the unit Nm^3 refers to "Normal cubic meters" at 20 °C and 1.01 bars:

$$\mu_{he} = \frac{P_E}{V_E} = \frac{1}{3600} \cdot \frac{\rho_H \cdot nF \cdot U_{rev}}{\mu_l \cdot \mu_U \cdot M_r} \tag{2.6}$$

Here, μ_{he} is the electrolyzer hydrogen-to-electricity conversion efficiency. In Fig. 2.4, the hydrogen production rate and the efficiency are plotted as a function of power consumption by using the polarization curve in Fig. 2.3. The graphs are based on the assumptions that the current efficiency is 100% and that the maximum cell current is 2 A.

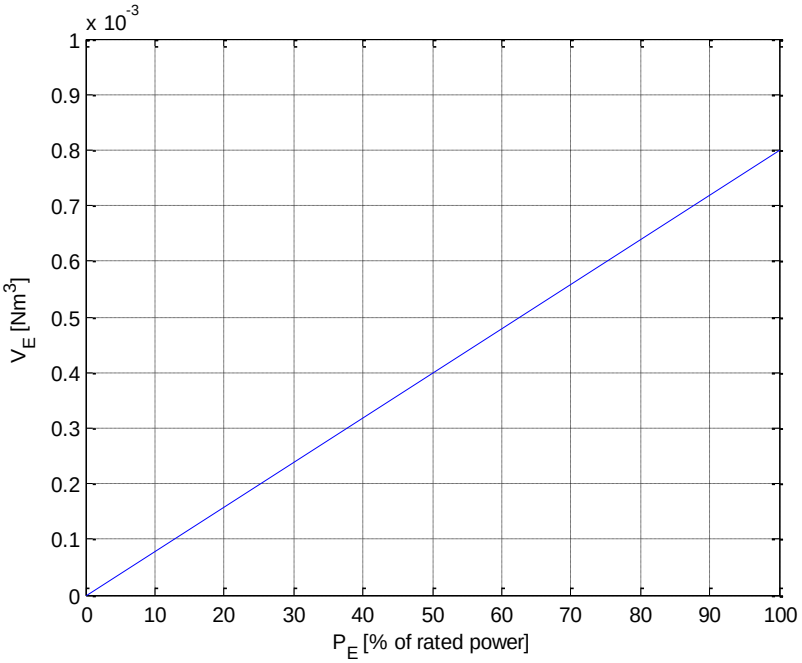

Fig. 2.4: Typical hydrogen-production rate and efficiency of an electrolyzer with respect to the power consumption [7].

2.1.1.1 Alkaline technology

There are several electrolyzer technologies for electrolysis hydrogen production, ranging from alkaline to proton-exchange solutions with various types of membranes. As the alkaline technology electrolyzers are assumed in the thesis, due to their simplicity and commercial availability, this technology will be described in detail.

The first type of water electrolysis utilized a tank design and an alkaline electrolyte [25]. These electrolyzers can be configured as uni-polar (tank) or bi-polar (filter press) designs. In the uni-polar design, which is presented in Fig. 2.5, there are a series of electrodes, anodes and cathodes that are alternatively suspended in a tank that is fuelled with a 20-30% solution of electrolyte (potassium hydroxide in pure water). In this design, each of the cells is connected in parallel and operated at DC with 1.9-2.5 V. The advantages to this design are that it is extremely simple to manufacture and repair. The disadvantage is that it usually operates at lower current densities and lower temperatures. The more recent uni-polar designs include electrolyzers that can operate at high-pressure outputs.

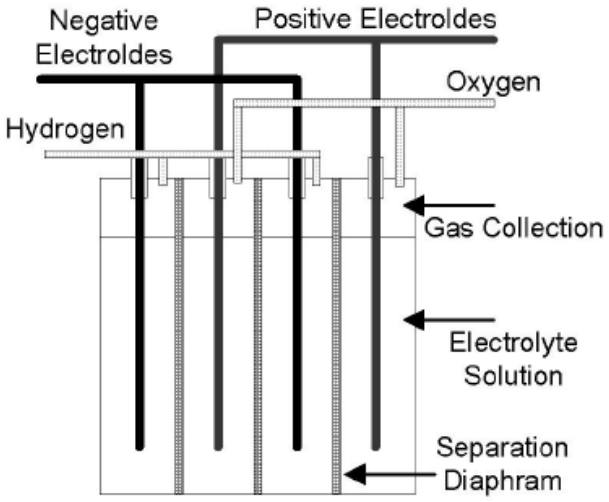

Fig. 2.5: The model of the uni-polar electrolyzer design [25].

The second type of electrolyzer construction is the bi-polar design, also called the filter-press design. It has alternating layers of electrodes and separation diaphragms that are clamped together [25]. The cells are connected in series and can result in higher stack voltages. Since the cells are relatively thin, the overall stack can be considerable smaller in size than the uni-polar design. The advantage of the bi-polar design is the reduced stack footprints and the higher current densities, as well as the ability to produce higher-pressure gas. The disadvantage is that they cannot be repaired without servicing the entire stack, although errors rarely occur. In the past, asbestos was used as a separation diaphragm, but manufacturers have replaced or are planning to replace this with new, polymer materials, such as Ryton.

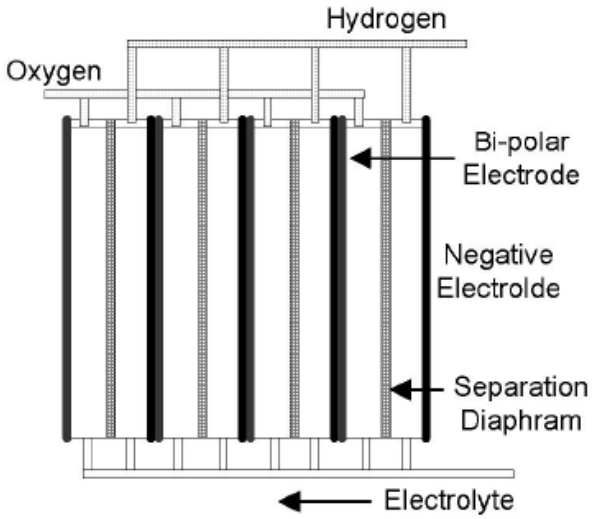

Fig. 2.6: The model of the bi-polar electrolyzer design [25].

Electrolysis plants with alkaline electrolytes are commercially available, both for large-scale and small-scale hydrogen production, and are therefore considered in this thesis. When the electrolyte is aqueous, usually with ~30% KOH by weight, the basic reactions are the following:

$$\text{Cathode: } 2H_2O_{(l)} + 2e^- \rightleftarrows H_{2(g)} + 2OH^- \tag{2.7}$$

$$\text{Anode: } 2OH^- \rightleftarrows \frac{1}{2}O_{2(g)} + H_2O_{(l)} + 2e^- \tag{2.8}$$

As one can see, the electrolysis cells also include separation diaphragms. These are intended to prevent the unhindered intermixing of the oxygen and hydrogen in the cell's chamber [27].

In addition to the electrolysis cells, an alkaline electrolysis plant consists of additional components, as follows [28]:

- direct-current supply,
- feed-water supply,
- electrolyte circulation,
- gas separation and purification,
- cooling,
- inert gas supply,
- process control,
- power supply to auxiliary equipment.

Traditionally, alkaline electrolyzers have been designed for constant hydrogen-production rates. In conjunction with wind power or electricity markets, on the other hand, the electrolyzer must be able to follow any sudden changes in the operating conditions due to a

variation in the wind or market prices. The electrochemical reactions are, however, fast enough to follow load changes within seconds. A 100 kW pressurized GHW-electrolyzer was reported to react to a jump between 20% and 100% in less than 3 seconds [29]. Most of the delay was due to non-optimized controller characteristics of the rectifier. Furthermore, laboratory tests of a pressurized 10 kW HYSOLAR electrolyzer showed that power fluctuations had no significant effect on the electrical stability [30].

Intermittent operation may cause impurities of hydrogen in the oxygen and vice versa [28]. The reason is that sudden changes in gas production affect the circulation balance of the electrolyte, and pressure differences between the anode side and the cathode side may arise. Consequently, the gas from one of the electrodes can diffuse through the diaphragm (gas separator) to the wrong side. Hydrogen in oxygen is a safety risk in terms of an explosion, while oxygen in hydrogen lowers the quality and thus the value of hydrogen. Moreover, fast power fluctuations can lead to incomplete separation of the gases from the electrolyte, so that hydrogen and oxygen are mixed in the electrolyte. It is important to ensure, as far as possible, equal pressure levels on the cathode side and on the anode side in order to prevent gas impurities. Pressurized electrolyzers use controlled expansion valves for this purpose

Another issue with wind-electrolyzer systems is how to operate the electrolyzer during periods of low wind speed. Since the alkaline electrolyte is very corrosive, the electrode will corrode if the production is stopped. The electrodes should be polarized as long as they are in contact with the electrolyte in order to prevent corrosion. For this, a polarization current must be provided from an external power source. For long periods with no hydrogen production, one can, alternatively, remove the electrolyte from the system. However, such shutdown procedures will increase the power consumption during start-up [7].

2.1.1.2 Electrolyzer modelling

The following assumptions are considered in the electrolyzer model:

- constant oxygen and hydrogen production efficiency;
- 100% availability;
- feed and cooling water that is technically suitable and does not require any treatment before going into the electrolysis process;
- no additional purification or drying systems are needed to achieve the desired level of hydrogen and oxygen purity;
- no dynamic behavior is considered and resulting production deviations are neglected.

As the electrolysis model is convolved with the compressor model, the exact methodology for the electrolysis modelling is described in the following chapter.

2.1.2 Hydrogen compression

Hydrogen can be stored as a compressed gas, as a cryogenic liquid, in solids (metal hydrides, carbon materials) and in liquid-hydrogen carriers (methanol, ammonia) [7]. Some of the hydrogen-storage and transportation pathways are depicted in the Fig. 2.7, where various hydrogen-transformation, storage and transportation technologies are considered, based on [12] and [27]. The thesis is focused on large-scale stationary storage systems, which makes compressed-gas storage the most relevant; thus these two technologies will be discussed in detail. Conventional methods of above-ground hydrogen storage range from small high-pressure gas cylinders (>200 bar) to large low-pressure 12-16 bar spherical gas containers. For the large-scale storage of hydrogen, underground storage is expected to be two orders of magnitude cheaper [27]. However, this option requires specific locations with, e.g., salt caverns or depleted natural-gas reservoirs, which limits the potential usage of this technology.

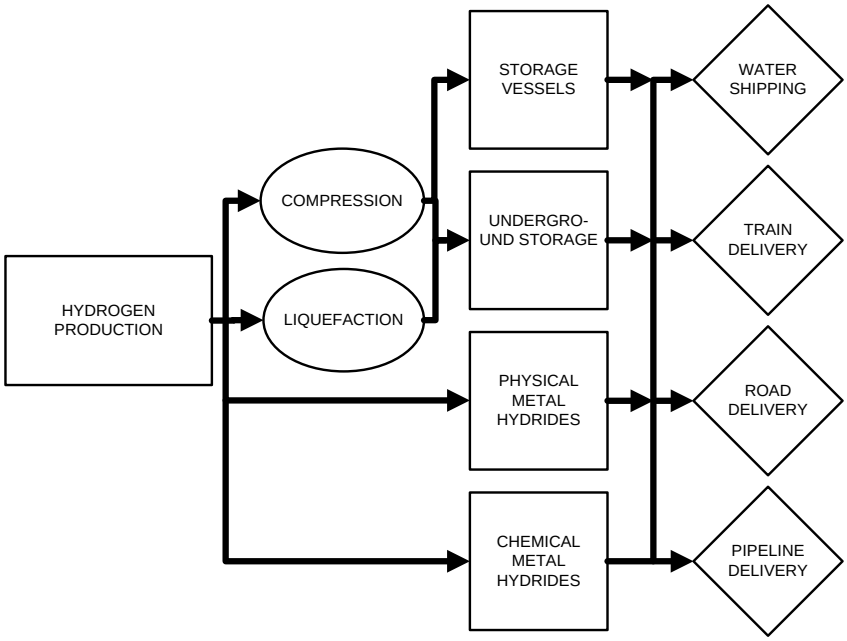

Fig. 2.7: Hydrogen-storage and transportation pathways.

Typically, hydrogen is compressed by the use of piston compressors or centrifugal compressors [7]. Several stages of compression are required because of the low density of the hydrogen. The theoretical work for the isothermal compression of an ideal gas from pressure p_1 to p_2 is given by:

$$W_{1,2} = p_1 \cdot V_1 \cdot \ln(p_2 / p_1) \tag{2.9}$$

where $W_{1,2}$ is the theoretical work for the thermal compressor and V_1 is the volume of the compressed gas. Because of the logarithmic relationship, the electricity consumption of the compressor is the highest in the low-pressure range. It is therefore interesting to consider

high-pressure electrolyzers, which can reduce or even eliminate the electricity consumption related to hydrogen compression.

For the adiabatic compression of diatomic hydrogen and five-atomic methane from atmospheric conditions to higher pressures, the energy consumed is shown in Fig. 2.8. Compared to methane, about nine times more energy per kg is required to compress hydrogen, and 15 times more (the ratio of molecular masses) than for air [12]. The energy consumption for the compression of hydrogen is substantial and has to be considered.

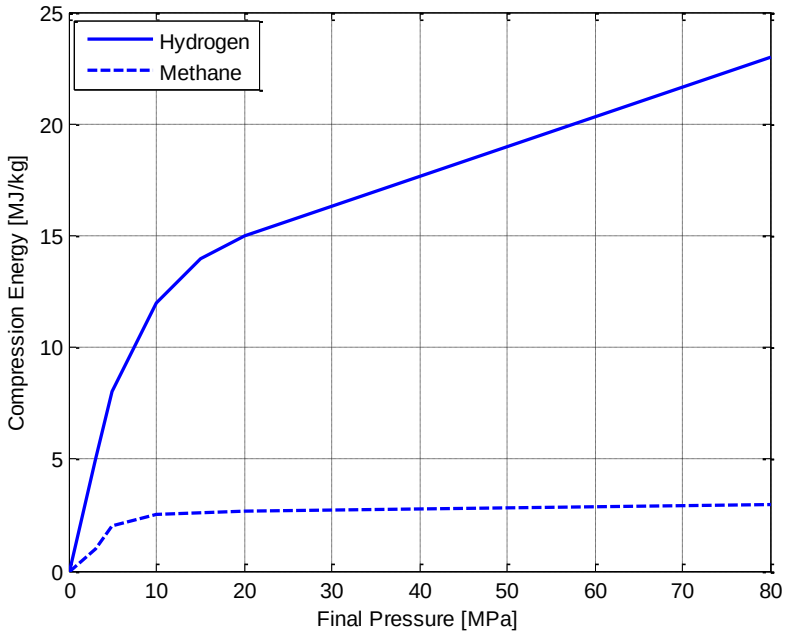

Fig. 2.8: Adiabatic compression work versus the final pressure for hydrogen and methane [12].

Multistage compressors with intercoolers operate somewhere between the isothermal and adiabatic limits. Compared with methane, hydrogen passes the compression heat faster to the cooler walls, thus bringing the process closer to isothermal. Data provided by a leading manufacturer of hydrogen compressors show that the energy required for a five-stage compression of 1000 kg of hydrogen per hour from ambient pressure to 20 MPa is about 7.2% of its HHV. Adiabatic, isothermal, and a multistage compression of hydrogen are compared in Fig. 2.9. For multistage compression to a final pressure of 20 MPa, about 8% of the HHV energy content of hydrogen is required. This analysis does not include any losses in the electrical power-supply system. At least 1.08 units of energy must be invested in compression to obtain 1 unit of hydrogen HHV at 20 MPa. The number becomes 1.12 for compression to 80 MPa for hydrogen transfer to the proposed 70 MPa standard vehicle tanks of automobiles. If mechanical and electrical losses are also considered, the total electricity needs for compression may reach 20% of the HHV hydrogen energy leaving the process.

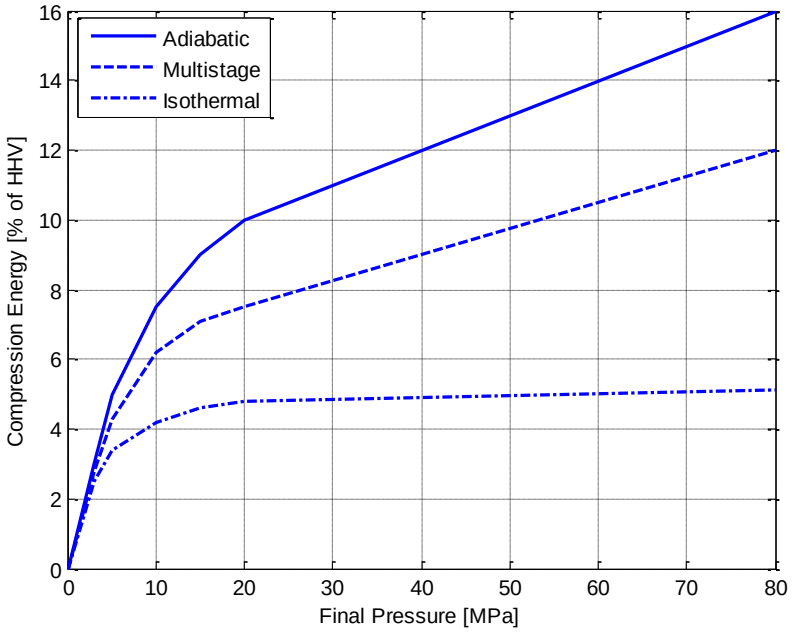

Fig. 2.9: Energy required for hydrogen compression [12].

2.1.2.1 Modelling of electrolyzers and compressors

Modelling assumptions of the compressors used in the thesis:

- constant compression efficiency;
- 100% availability;
- the hydrogen gas is technically suitable before going to the compression process;
- no dynamic behavior is considered and the resulting production deviations are neglected.

The compression model, which also considers the compression losses, is convolved with the electrolyzer model, as depicted in Fig. 2.10. One can see that the electrolyzer and compressor models are coupled as they are both electricity consumers. The oxygen and hydrogen flows are decupled, on the other hand, which enables a simplified modelling of the electrolyzer-compressor system.

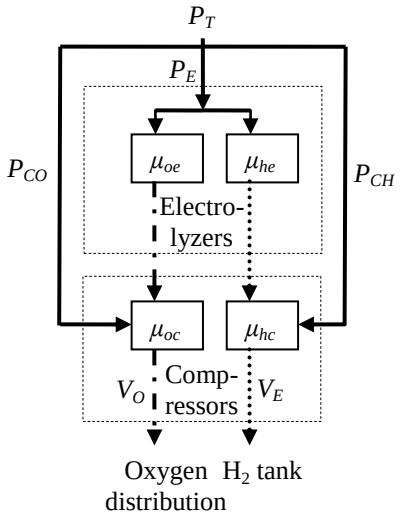

Fig. 2.10: Detailed electrolyzer model with hydrogen and oxygen compressors (- electricity flow, ·- oxygen flow, ·· hydrogen flow).

In the above figure, P_T is the total compressor and electrolyzer consumption, P_E is the electrolyzer consumption, P_{CH} is the hydrogen compressor consumption, P_{CO} is the oxygen compressor consumption, V_E is the hydrogen production by electrolyzer, V_O represents the oxygen sales to the oxygen market, μ_{he} is the hydrogen efficiency of the electrolyzer, μ_{oe} is the oxygen efficiency of the electrolyzer, μ_{hc} is the hydrogen efficiency of the compressor and μ_{oc} is the oxygen efficiency of the compressor. The electrolyzer consumption versus the hydrogen production for the described model can be calculated using the following equation:

$$P_E = \frac{1}{\mu_{he}} \cdot V_E \tag{2.10}$$

The compressor's electricity consumption for hydrogen compression can be calculated using the equation:

$$P_{CH} = \frac{1}{\mu_{hc}} \cdot V_E \tag{2.11}$$

In this process, hydrogen is assumed to be compressed to 25 MPa, which is the rated pressure of the storage tank. The system is also assumed to compress oxygen to the rated pressure of the storage tank. The power to compress the oxygen is calculated using the following equation:

$$P_{CO} = \frac{1}{\mu_{oc}} \cdot V_O \tag{2.12}$$

The oxygen production, as a function of the electricity consumed by the electrolyzer, can be described using equation (2.13).

$$V_O = \mu_{oe} \cdot P_E \tag{2.13}$$

The total electricity consumed by the electrolyser and the compressor can be calculated using the following equation:

$$P_T = P_E + P_{CH} + P_{CO} \tag{2.14}$$

By inserting equations (2.10)-(2.12) into (2.14), we obtain the total power consumption as a function of the hydrogen and oxygen production:

$$P_T = \frac{1}{\mu_{he}} \cdot V_E + \frac{1}{\mu_{hc}} \cdot V_E + \frac{1}{\mu_{oc}} \cdot V_O \tag{2.15}$$

As one can see, P_E can be calculated by the insertion of either equation (2.10) or (2.13). However, since we would like to obtain the power consumption as a function of hydrogen production only, we have chosen to use equation (2.10). Furthermore, we also have to replace the variable V_O. We will replace it by using equation (2.13):

$$P_T = \frac{1}{\mu_{he}} \cdot V_E + \frac{1}{\mu_{hc}} \cdot V_E + \frac{\mu_{oe}}{\mu_{oc}} \cdot P_E \tag{2.16}$$

As the total power consumption is still not solely a function of V_E we substitute P_E by the use of equation (2.10). This results in the following equation:

$$P_T = \frac{1}{\mu_{he}} \cdot V_E + \frac{1}{\mu_{hc}} \cdot V_E + \frac{\mu_{oc}}{\mu_{he} \cdot \mu_{oc}} \cdot V_E \tag{2.17}$$

The final equation that describes the hydrogen production of the coupled electrolizer and compressor as a function of the total electricity consumption is the following:

$$V_E = \frac{\mu_{he}}{\left(1 + \frac{\mu_{he}}{\mu_{hc}} + \frac{\mu_{oe}}{\mu_{oc}}\right)} \cdot P_T \tag{2.18}$$

To calculate the oxygen production as a function of the total electricity consumed, we have to substitute V_E in equation (2.15) with V_O. The first step is applying equation (2.10) to replace the V_E with P_E:

$$P_T = P_E + \frac{\mu_{he}}{\mu_{hc}} \cdot P_E + \frac{\mu_{oe}}{\mu_{oc}} \cdot P_E \tag{2.19}$$

The next step is replacing P_E with V_O by using equation (2.13). Thus, we obtain the following equation:

$$P_T = \frac{1}{\mu_{oe}} \cdot V_O + \frac{1}{\mu_{oc}} \cdot V_O + \frac{\mu_{he}}{\mu_{hc} \cdot \mu_{oe}} \cdot V_O \tag{2.20}$$

Finally, the equation of oxygen production with respect to the total electricity consumed by the coupled electrolyzer-compressor is the following:

$$V_O = \frac{\mu_{oe}}{\left(1 + \frac{\mu_{he}}{\mu_{hc}} + \frac{\mu_{oe}}{\mu_{oc}}\right)} \cdot P_T \tag{2.21}$$

The limitation of the electrolyzer's power consumption can be described by using the following equation:

$$P_E \leq P_E^{MAX} \tag{2.22}$$

where P_E^{MAX} is the installed power consumption capacity of the electrolyzer. For the complex electrolyzer model, P_E in the latter equation can be replaced by P_T. To be able to do so, we have to derive the total electricity consumption as a function of the electrolyzer consumption. For this purpose, we have to slightly reformulate equation (2.19), which gives us the following relation:

$$P_T = \left(1 + \frac{\mu_{he}}{\mu_{hc}} + \frac{\mu_{oe}}{\mu_{oc}}\right) \cdot P_E \tag{2.23}$$

Thus, we obtain the following constraint:

$$P_T \leq \left(1 + \frac{\mu_{he}}{\mu_{hc}} + \frac{\mu_{oe}}{\mu_{oc}}\right) \cdot P_E^{MAX} \tag{2.24}$$

The same equation development also yields the following formulation for the lower limit of the electricity consumption of the fuel-cell stack:

$$P_T \geq \left(1 + \frac{\mu_{he}}{\mu_{hc}} + \frac{\mu_{oe}}{\mu_{oc}}\right) \cdot P_E^{MIN} \tag{2.25}$$

2.1.3 Hydrogen storage

There are several technologies developed and also commercially available for hydrogen storage [31], [32]. In the thesis, the stationery, compressed-gas, storage-tank technology is assumed, which is the most straightforward technology.

Compressed-gas storage of hydrogen is the simplest storage solution where the only equipment required is a compressor and a pressure vessel [31]. The main problem with

compressed gas storage is the low storage density, which depends on the storage pressure, where higher storage pressures result in higher capital and operating costs. Low-pressure spherical tanks can hold as much as 1,300 kg of hydrogen at 1.2-1.6 MPa and high-pressure storage vessels have maximum operating pressures of 20-30 MPa. European countries tend to use low-pressure cylindrical tanks with a maximum operating pressure of 5 MPa and storage capacities of 115-400 kg of hydrogen. One concern with large storage vessels (especially the underground storage mentioned later) is the cushion gas that remains in the empty vessel at the end of the discharge cycle. In small containers this may not be a concern, but in larger containers this may represent a large quantity of gas.

2.1.3.1 Modelling of hydrogen storage

The following assumptions are considering when modelling the hydrogen-storage vessels:

- no boil-off of hydrogen gas;
- 100% availability;
- the hydrogen gas is technically suitable to be stored in the vessel.

According to the above assumptions, the hydrogen-storage levels can be calculated using the following:

$$V_i^{STG} = V_{i-1}^{STG} + V_E - V_F - V_H \tag{2.26}$$

where V_i^{STG} is the hydrogen-storage level in hour *i*, V_F is the hydrogen consumption of the fuel cells and V_H is the hydrogen sold directly to the hydrogen market. However, if the hydrogen cannot be sold directly to the hydrogen market, the latter variable is omitted. The limited storage capacity of the hydrogen storage tanks is modeled as a constraint in the hydrogen-system optimization model using the following equation:

$$0 \le V_i^{STG} \le V_{\max}^{STG} \tag{2.27}$$

Here, $V_{\max}^{STG}$ is the storage capacity of the storage tank. On the other hand, there are no oxygen-storage constraints considered in the model, as the oxygen produced is assumed to be readily prepared to be transported directly to the oxygen market.

2.1.4 Fuel cells

In a fuel cell powered by hydrogen, the reverse reaction of water electrolysis takes place:

$$\mathrm{H_2} + \frac{1}{2}\mathrm{O_2} \rightarrow \mathrm{H_2O} \tag{2.28}$$

The chemical energy of hydrogen is directly converted to electrical energy in the fuel cell; thus, a fuel cell can theoretically obtain a higher electrical efficiency than internal combustion engines, which are limited by the efficiency of the Carnot-cycle [7]. However, kinetic

overvoltages at the electrodes and electrical resistance cause relatively high losses in practical systems, as per the example case of a polarization curve shown in Fig. 2.11. For this particular cell, the cell voltage is about 50% of the reversible cell voltage when the current density is 850 mA/cm^2.

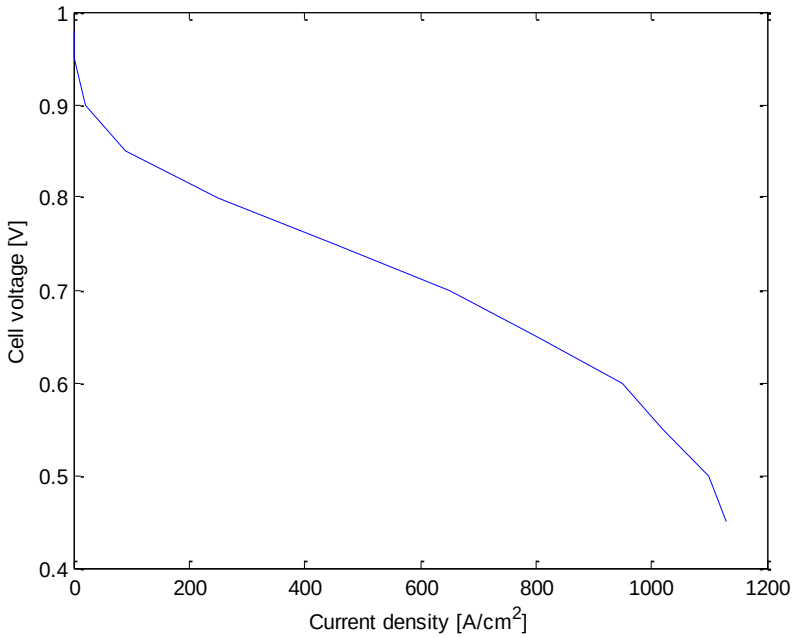

Fig. 2.11: Polarization curve of a fuel cell [7].

The electrolyte defines the key properties, particularly the operating temperature, of the fuel cell. Consequently, fuel cells are classified based on the types of electrolyte used, as described below [33]:

1. polymer Electrolyte Membrane (PEM);
2. alkaline Fuel Cell (AFC);
3. phosphoric Acid Fuel Cell (PAFC);
4. molten Carbonate Fuel Cell (MCFC);
5. solid Oxide Fuel Cell (SOFC).

These fuel cells operate at different temperatures and each is best suited to a particular application. The main features of the five types of fuel cells are summarized in Tab. 2.2.

Tab. 2.2: Comparison of five fuel-cell technologies [33].

Type	Electrolyte	Operating Temperature [°C]	Applications	Advantages
Polymer Electrolyte Membrane (PEM)	Solid organic polymer poly-perflourosulfonic acid	60–100	Electric utility, transportation, portable power	Solid electrolyte reduces corrosion, low temperature, quick start-up
Alkaline (AFC)	Aqueous solution of potassium hydroxide soaked in a matrix	90–100	Military, space	Cathode reaction faster in alkaline electrolyte; therefore high performance
Phosporic Acid (PAFC)	Liquid phosphoric acid soaked in a matrix	175–200	Electric utility, transportation, and heat	Up to 85% efficiency in cogeneration of electricity
Molten Carbonate (MCFC)	Liquid solution of lithium, sodium, and/or potassium carbonates soaked in a matrix	600–1000	Electric utility	Higher efficiency, fuel flexibility, inexpensive catalysts
Solid Oxide (SOFC)	Solid zirconium oxide to which a small amount of yttria is added	600–1000	Electric utility	Higher efficiency, fuel flexibility, inexpensive catalysts. Solid electrolyte advantages like PEM

In wind-hydrogen systems, low-temperature cells are considered as being the most interesting because of their operating flexibility regarding the startup and shutdown procedures, as well as intermittent operation [7]. However, if nuclear power plants are considered for hydrogen generation in periods without wind, higher-temperature and more efficient fuel cells can also be appropriate.

The power consumption of auxiliary equipment, such as an air blower and a deionized water pump, reduces the performance of a fuel-cell system. In Fig. 2.12, the net efficiency curve of a PEM fuel-cell system is plotted showing the deviations from the polarization curve in the low power range. This emphasizes not only the importance of the development of energy-efficient cells, but also the importance of an optimized plant design.

One way of achieving higher efficiencies is to make use of the heat produced in the stack, where the heat could be recuperated from the water-cooling system in the range of 50-100% of full power, as shown in [34]. The dynamic properties of this fuel-cell system have to enable the smooth operation of the system; here, a fast response is important, so that the fuel cells can adapt to sudden load changes.

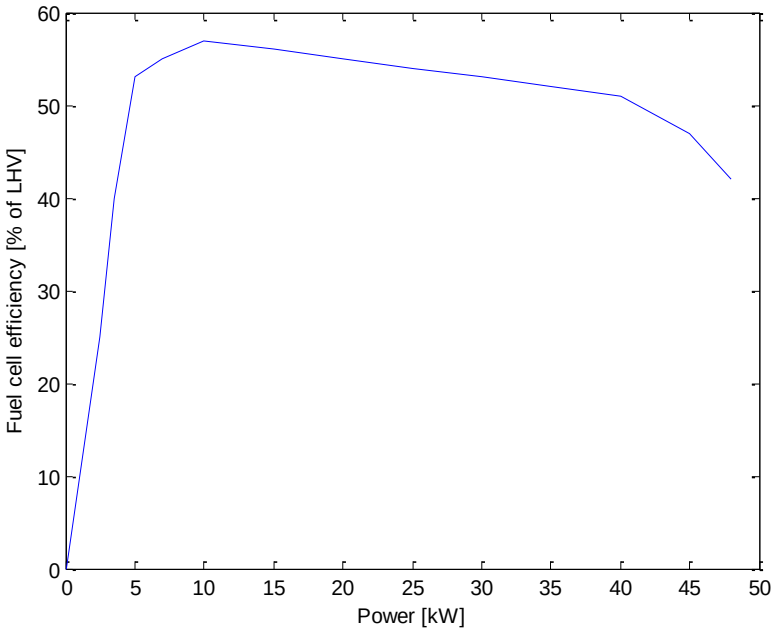

Fig. 2.12: Part-load characteristics of PEM fuel cell [7]. The efficiency is measured as a percentage of the lower heating value (LHV) of hydrogen.

2.1.4.1 Polymer Electrolyte Membrane (PEM)

The PEM cell (also referred to as a Proton Exchange Membrane cell) is one in a family of fuel cells that are in various stages of development [33] and are assumed in the thesis as in [35]. It is also being considered as an alternative power source for automotive applications for electric vehicles. The electrolyte in a PEM cell is a type of polymer and is usually referred to as a membrane, hence the name. Polymer electrolyte membranes are somewhat unusual electrolytes in that, in the presence of water, which the membrane readily absorbs, the negative ions are rigidly held within their structure. Only the positive (H) ions contained within the membrane are mobile and are then free to carry positive charges through the membrane in one direction only, from the anode to the cathode. At the same time, the organic nature of the polymer electrolyte membrane's structure makes it an electron insulator, forcing it to travel through the outside circuit, providing electric power to the load. Each of the two electrodes consists of porous carbon, to which very small platinum (Pt) particles are bonded. The electrodes are somewhat porous, so that the gases can diffuse through them to reach the catalyst. Moreover, as both platinum and carbon conduct electrons well, these electrons are able to move freely through the electrodes. The chemical reactions that take place inside a PEM fuel cell are presented in the following:

Anode:

$$2H_2 \rightarrow 4H^+ + 4e^- \tag{2.29}$$

Cathode:

$$O_2 + 4H^+ + 4e^- \rightarrow 2H_2O \quad (2.30)$$

Hydrogen gas diffuses through the polymer electrolyte until it encounters a Pt particle in the anode. The Pt catalyzes the dissociation of the hydrogen molecule into two hydrogen atoms (H) bonded to two neighboring Pt atoms. Only then can each H atom release an electron to form a hydrogen ion (H_+), which travels to the cathode through the electrolyte. At the same time, the free electron travels from the anode to the cathode through the outer circuit. At the cathode the oxygen molecule interacts with the hydrogen ion and the electron from the outside circuit to form water. The whole operation of a PEM fuel cell is presented in Fig. 2.13. The performance of the PEM fuel cell is limited primarily by the slow rate of the oxygen-reduction half-reaction at the cathode, which is 100 times slower than the hydrogen oxidation half-reaction at the anode.

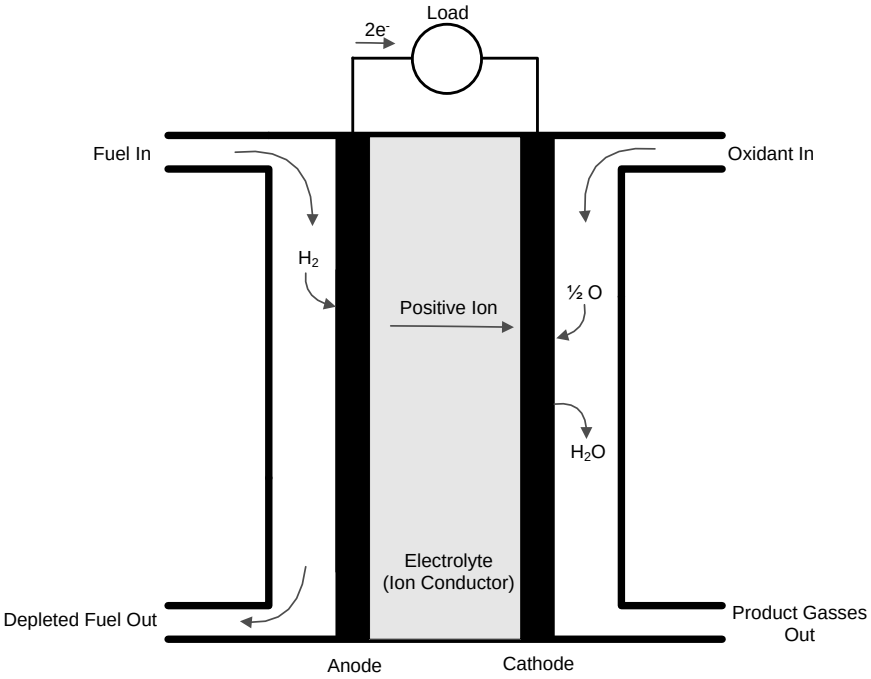

Fig. 2.13: Operational scheme of a PEM fuel cell [36].

2.1.4.2 Modelling of fuel cells

Some assumptions that will be considered in the thesis:

- no dynamics and other deviations from the dispatch instructions;
- a constant maximum efficiency.

The latter assumption can be easily justified by use of multiple fuel cells in the hydrogen system, thus assuming that fuel cells in operation will operate at full power. Like with the electrolyzer model, the fuel-cell model also assumes the decoupled production of electricity and the byproduct heat, as shown in Fig. 2.14.

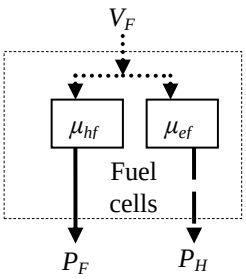

Fig. 2.14: Detailed stationary fuel-cell model (- electricity flow, --heat flow, ·· hydrogen flow).

Where P_F is the electricity produced by the fuel cells, V_F is the hydrogen consumed by the fuel cell, μ_{ef} is the hydrogen-to-electricity conversion efficiency, P_H is the heat produced by the conversion of hydrogen to electricity in the fuel cell and μ_{ef} is the efficiency of hydrogen-to-heat conversion process. The electricity produced by a fuel cell can be calculated using the next equation:

$$P_F = \frac{1}{\mu_{ef}} \cdot V_F \tag{2.31}$$

To calculate the heat production of the fuel-cell array, the following equation is added to the fuel-cell model:

$$P_H = \frac{1}{\mu_{hf}} \cdot V_F \tag{2.32}$$

Besides equations that describe the conversion of hydrogen to electricity and heat, we also have to consider the hydrogen-production capacity constraints. The maximum and minimum hydrogen consumptions are assumed to be functions of the electricity produced, as follows:

$$P_{\min}^{DIS} \le P_F \le P_{\max}^{DIS} \tag{2.33}$$

Here, $P_{\min}^{DIS}$ and $P_{\max}^{DIS}$ are the upper and lower bounds for the fuel-cell production, which are characteristic for certain types of fuel cells.

2.2 Electricity storage alternatives

There are many different electricity-storage alternatives that are competing with hydrogen storage. However, only a couple are meeting the tough criteria for a large-scale service introduction, which can be roughly divided in efficiencies and costs. Pumped-hydro is the technology that has seen the most wide-spread use. It has favorable efficiencies [37], but it is specific in terms of the required location, transmission system capacities and can be subject to local and environmental opposition, since it has considerable impacts on the surrounding environment. Alternatively, one might also assume battery storage as an efficient way of storing the electrical energy. However, large-scale installations of battery storage (e.g., for

storing 912 MWh of electricity) pose a significant environmental hazard because of the materials used in batteries and the large size of such a system due to the low energy density of batteries. Hydrogen, on the other hand, can be placed practically everywhere without any need for a specific terrain type. Furthermore, hydrogen has the potential to be applied as an energy carrier that can be directly sold to the hydrogen market (e.g., as a fuel in the automotive sector) without having to be converted back into electricity.

2.3 Wind power

Wind power is gaining significant attention nowadays due to possible CO_2-emission evasion and lowering the dependence on imported energy. Therefore, it is also foreseen as a source of energy in a Hydrogen Economy. The basic equation for the theoretical power in an air stream is [33]:

$$P_W = 0.5 \cdot d_a \cdot A \cdot V_W{}^3 \tag{2.34}$$

where P_W is the wind-turbine power production, d_a represents the density of air, A is the cross-sectional area of a wind-turbine rotor and V_W is the wind velocity. The actual power P extracted by a wind turbine, however, is of the same form as for water turbines:

$$P_W = C \cdot (0.5 \cdot d_a \cdot A \cdot V_W{}^3) \tag{2.35}$$

where C is the wind-turbine power coefficient. Modern designs of wind turbines for electricity generation operate with a power coefficient of about 0.4, with the major losses being caused by drag on the blades and the swirl imparted to the air flow by the preceding rotating blades. Any wind turbine will operate only between a minimum starting wind velocity value and its rated value. Typically, the ratio between the starting and rated velocity is between 2 and 3, although if the pitch of the blades can be altered at velocities greater than the rated velocity, the turbine should continue to operate at its rated output, the upper limit being set by design limitations. Depending on the location, the wind speed may be less than the starting velocity for 25% of the year when the turbine is shut down and the annual load factor, the ratio of energy produced to the energy that would be produced if run at maximum rated output over the whole year, is typically between 25% and 35%. A typical operating power characteristic is shown in Fig. 2.15.

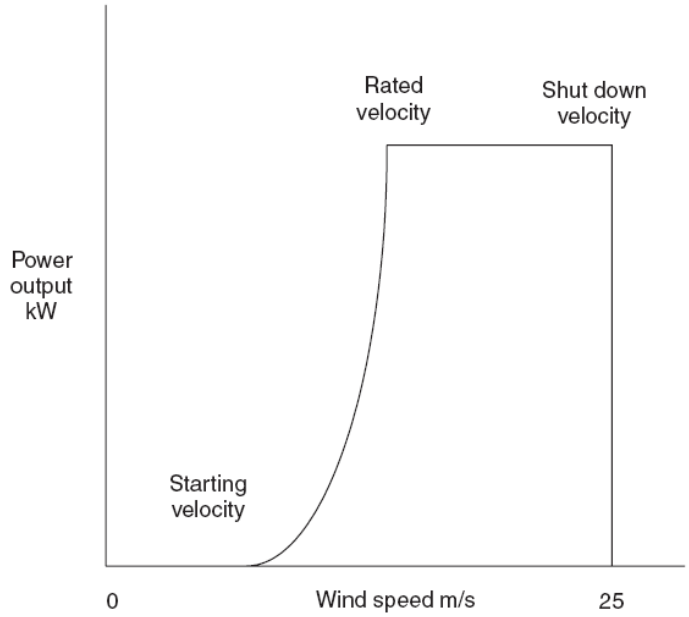

Fig. 2.15: Wind turbine's power characteristic [33].

In general, machines are designed to operate with a peak output in the range of 250-500 W/m^2; thus, 20 m machines have ratings of around 200 kW, 30 m machines around 300 kW and 50 m machines around 1 MW. The power limitation is accomplished either by using feathered blades in larger machines, with feathering along the whole blade length, or in smaller machines by taking advantage of the natural tendency of blades to stall as the angle of attack increases in high winds. Current commercial wind turbines tend to operate at a fixed speed with tip speeds of around 50-80 m/s for power generation and slower speeds for high-torque applications, such as pumping. The technical options available to the designers of wind turbines and the interaction of option choices in the determination of machine weight and cost are typically considered in wind-turbine design. Typical turbine-design characteristics are depicted in Fig. 2.16.

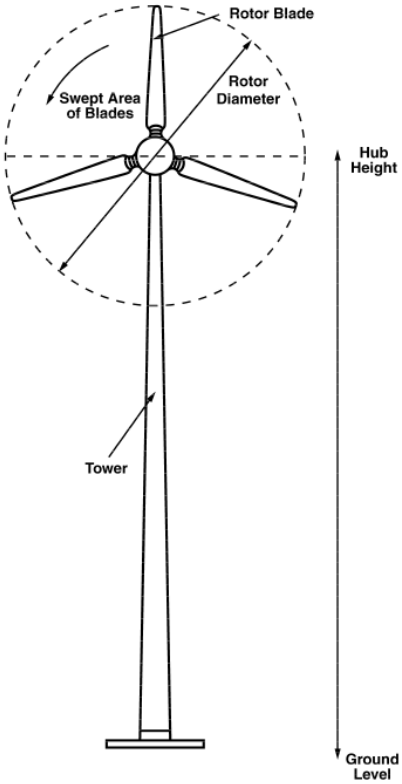

Fig. 2.16: Wind-turbine design and components [38].

The tower is put over strong, usually steel-reinforced concrete, foundations, which have to sustain large torques at high wind speeds. The turbine cupola is positioned on top of the tower using a yaw system for turning the cupola into the direction of the wind for achieving the optimal power coefficient. The generator and gearbox are positioned in the cupola, with the rotor hub mounted at its tip. The blades are fastened to the rotor hub via the blade-pitch mechanism, which is used to regulate the power and the speed of the wind turbine. The tower is also used to transmit the different measurement and control signals to the operators and to distribution companies, as well as to transfer the produced electricity to the grid.

2.3.1 State-of-the-art wind generators

The most commonly applied wind technologies, both in terms of their ability to control speed and the type of power control they use, are described in this chapter. According to the speed-control criterion, there are four different types of wind turbines that are dominant [39]:

1. fixed speed,
2. limited variable speed,
3. variable speed with a partial-scale frequency converter,
4. variable speed with a full-scale frequency converter.

These wind-turbine types can be further divided according to the mode of power (blade) control: stall, pitch, or active stall. These technologies are classified according to the speed

control and power control in Tab. 2.3, where the grey zones in the table indicate technologies that do not exist. The variable-speed technologies are used in practice only with the fast pitch control mechanism, due to its ability to reduce the power fast enough in case of emergencies, e.g. if the wind turbine is running at maximum speed and a strong gust occurs, the aerodynamic torque can get critically high and can result in a runaway if there is no fast shut-down option available.

Tab. 2.3: Wind turbine concepts [39].

Speed control		Power control		
		Stall	Pitch	Active stall
Fixed speed	Type A	Tape A0	Tape A1	Tape A2
Variable speed	Type B	Type B0	Tape B1	Tape B2
Variable speed with a partial-scale frequency converter	Type C	Tape C0	Tape C1	Tape C2
Variable speed with a full-scale frequency converter	Type D	Tape D0	Tape D1	Tape D2

A more detailed description of each mentioned wind technology can be found in [39] and [40] and the other available technical literature. As the wind generator in the wind farm considered in the thesis applies a gearless, variable speed, variable-pitch-control turbine with a direct-drive, synchronous, annular generator, this technology is fully described in this chapter.

The pitch-controlled wind turbine uses an electronic controller that checks the power output of the turbine several times per second; when the power output becomes too high, it sends an order to the blade pitch mechanism, which pitches (turns) the rotor blades slightly out of the wind [40]. Conversely, the blades are turned back into the wind whenever the wind drops again. The main advantages of this type of control are that in facilitates power controllability, controlled start-up and emergency stopping. However, even small variations in wind speed result in large variations in output power since the pitch-control mechanism is not fast enough to avoid such small power fluctuations; it is only possible to compensate slow wind variations.

A variable speed generator with a full-scale frequency converter utilizes a full variable-speed wind turbine and the direct connection of the generator to the grid using a full-scale frequency converter. The frequency converter is used for reactive-power compensation and smoothing

of the grid connection. The generator can be excited electrically, using a wound-rotor synchronous generator (WRSG) or wound-rotor induction generator (WRIG), or by permanent magnet using a permanent-magnet synchronous generator (PMSG). This concept is presented in detail in Fig. 2.17. Some full variable-speed wind turbines do not apply gearboxes (dotted in Fig. 2.17) in which case a direct-drive, multi-pole generator with a large diameter is used.

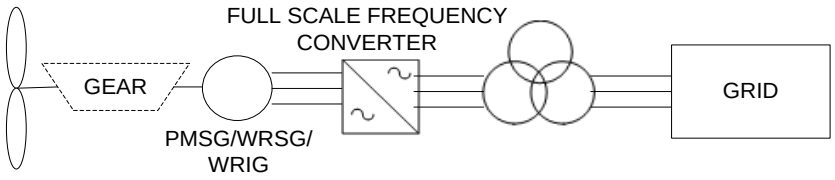

Fig. 2.17: The variable speed with full-scale frequency-converter design with PMSG/WRSG/WRIG [39].

In the thesis, the wind-turbine power curve (in MW) was modelled by a 6th-grade polynomial as follows:

$$P_W = \begin{cases} \left(a + b \cdot V_W + c \cdot {V_W}^2 - d \cdot {V_W}^3 - e \cdot {V_W}^4 - f \cdot {V_W}^5 - g \cdot {V_W}^6\right)/1000 \; if \; V_W < V_W^R \\ P_W^R \; if \; V_W \geq V_W^R \\ 0 \; if \; V_W \geq V_W^{CO} \end{cases} \tag{2.36}$$

In the above equation, the letters *a-g* represent the parameters of the wind-power polynomial, P_W^R is the rated power of the wind turbine, V_W^R is the rated speed of the wind turbine and V_W^{CO} is the cut-out speed of the wind turbine. The exact modelling of the wind turbine applied to the chosen wind-generation technology is presented in detail in chapter 4.4.

2.4 Nuclear power

Nuclear power has been present for electricity generation since the 1950s with a wide range of different technologies [41]. The common feature of all these technologies is that they produce thermal energy that can be converted into mechanical energy and finally, into electrical energy. In these reactors, the fission of heavy atomic nuclei, the most common of which is uranium-235, produces heat that is transferred to a fluid, which acts as a coolant. During the fission process, the bond energy is released and this first becomes noticeable as the kinetic energy of the fission products generated and that of the neutrons being released. Since these particles undergo intense deceleration in the solid nuclear fuel, the kinetic energy turns into heat energy. In the case of reactors designed to generate electricity, the heated fluid can be gas, water or a liquid metal. The heat stored by the fluid is then used either directly (in the case of a gas) or indirectly (in the case of water and liquid metals) to generate steam. The heated gas or the steam is then fed into a turbine, driving an alternator. This basic operation of a nuclear power plant is presented in Fig. 2.18.

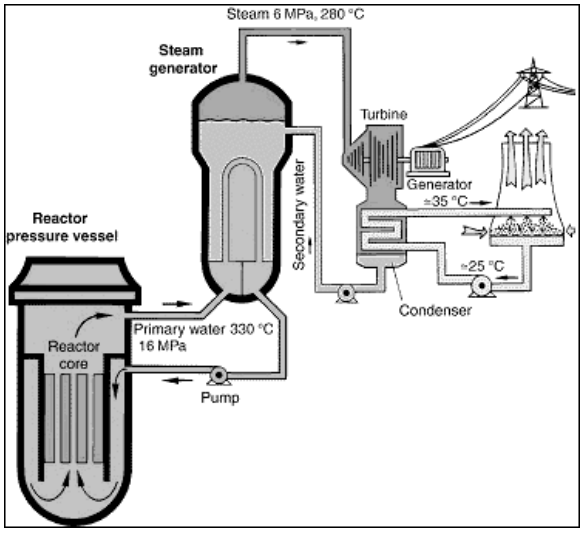

Fig. 2.18: The operational scheme of a pressurized-water reactor[42].

The main technologies in use today are the following:

1. Light-Water Reactors;
2. Heavy-Water Reactors;
3. Gas-Cooled Reactors;
4. Liquid-Metal-Cooled Reactors.

The majority of reactors in operation are light-water reactors (LWRs), but there is still a sizeable fraction of heavy-water reactors. Most of the nuclear power plants (NPPs) were built in the 1970s and 80s and a new cycle of investments in this technology is about to occur to replace the polluting, fossil-fueled power plants. Since the studied system in this thesis is assumed to be located in Ontario, Canada, with the operational Bruce Power Heavy Water CANDU reactor in the area, this technology is described in detail.

Pressurized heavy-water reactors are developed in a number of countries and use heavy water as a moderator and coolant, which enables the NPP to operate with enriched, or even with natural uranium. Traditional designs using light water as a moderator will absorb too many neutrons to allow a chain reaction to occur in natural uranium due to the low density of active nuclei. Heavy water absorbs fewer neutrons than light water, allowing a high neutron economy that can sustain a chain reaction even in an un-enriched fuel.

The Canadian-designed Canadian deuterium uranium (CANDU) reactors use natural uranium as a fuel, by employing heavy water as both a moderator and a coolant [41]. The first CANDU, NDP2-Rolpthon of just 23 MW, entered commercial operation in 1962 and a number of 2-, 3- and 4-unit plants evolved of a commercial power capacity, individual units

delivering power in the range of 500-800 MW. A schematic of the CANDU reactor is shown in Fig. 2.19, with the key of the figure explained below the figure.

The reactor consists of horizontal pressure tubes constructed with Zircaloy alloy. They pass through a large vessel (Calandria) filled with heavy water (deuterium oxide) at low pressure and temperature. Uranium oxide pellets are sealed in Zircaloy alloy cans, which are assembled in bundles or fuel assemblies. In a 500 MW plant, each bundle has about 28 elements. There are about 4860 bundles in total, with 12 or 13 such bundles in each pressure tube.

The heat generated is removed by the heavy water at about 9 MPa, a sufficiently high pressure to prevent boiling. The water circulates around the fuel elements and passes to a steam generator, a similar principle to the PWR and BWR concepts. However, the CANDU reactor is controlled by cadmium absorber rods. When fully inserted, these provide a shut-down margin. In addition, the reactor can be shut down by voiding the cold heavy water from the reactor core. Vertical steel “adjusting” rods are used to smooth out the sometimes uneven power distribution due to the use of different burnt-up fuel segments, even within one fuel channel.

As for the PWR, the CANDU primary system is located in a concrete containment building, of sufficient strength to accommodate a large coolant system break within its design basis. Modern CANDUs are connected by valves to a large vacuum building, where in the event of an accident these enable steam to pass from the affected containment to the vacuum building. The CANDU reactor has a low volumetric power density; about 10 times lower than a PWR, despite fuel ratings that are comparable with the PWR. It also has lower fuel costs because of the utilization of natural uranium. However, the need for considerable quantities of heavy water offset the lower costs of fuel.

The CANDU reactor does have a number of advantages, like on-load refueling, and hence a very high load factor. Since there is a large number of individual tubes, there is no need for a large pressure vessel. The main disadvantage is the large core required, compared with a PWR or BWR, to achieve a similar power output. Currently, various thermo-chemical cycles and high-temperature electrolysis for matching with the temperature capability of the new generations of CANDU reactor design are being evaluated by Atomic Energy of Canada Limited [13].

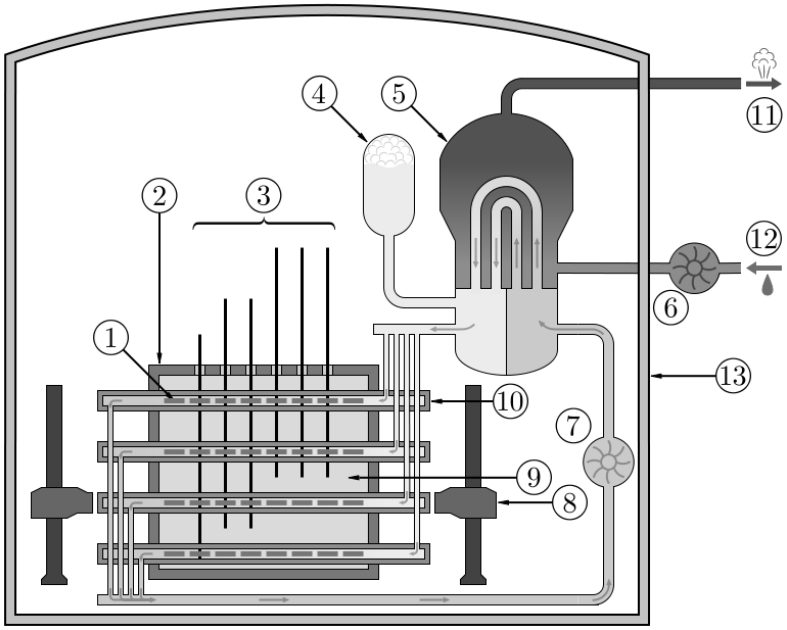

Fig. 2.19: The operational scheme of a CANDU, heavy-water reactor [43].

The numbers in Fig. 2.19 represent the following:

1. fuel bundle,
2. calandria (reactor core),
3. adjuster rods,
4. heavy-water pressure reservoir,
5. steam generator,
6. light-water pump,
7. heavy-water pump,
8. fuelling machines,
9. heavy-water moderator,
10. pressure tube,
11. steam going to the steam turbine,
12. cold water returning from the turbine,
13. containment building made of reinforced concrete.

Some studies propose the direct hydrogen production from CANDU reactors, which can result in higher efficiencies by utilization of the thermo-chemical cycle and high-temperature water splitting [13]. Efficiencies can be as high as 50-60%, instead of those lower than 30% assuming water electrolysis. However, a high hydrogen demand is needed to economically justify the building of such a purposely designed nuclear power plant from the economic viewpoint. Otherwise, large-scale production might cause a collapse of hydrogen prices in the shallow hydrogen markets.

2.4.1 Modelling of a nuclear power plant

The Bruce Power NPP's production (in MW) is described by the variable P_N. No ramp-up or ramp-down constraints were considered in the thesis due to the relatively small installed capacity of wind power plants compared to the installed capacity of the Bruce Power NPP. Since we already defined the production from both wind power plants and the Bruce Power NPP, the total available energy to be either sold to the electricity market, used by the hydrogen system, or shed, when no transmission capacities are available, is the following:

$$P_{GA} = P_N + P_W \tag{2.37}$$

Where P_N is the nuclear power plant production and P_{GA} is the available wind-nuclear power output. Thus the total hydrogen-system electricity consumption is limited by the above available electricity:

$$0 \le P_G \le P_{GA} \tag{2.38}$$

This additional equation is needed as the electricity produced by the power plants in the assumed energy hub may not be fully utilized during periods of insufficient transmission capacity. The nuclear power plant and the wind farm are assumed to be powered down in these periods to match the available transmission capacity.

2.5 Electrical integration

The nuclear-wind-hydrogen energy hub consists of various components with a variety of characteristics, which have to be properly integrated to allow for the effective operation of the system. As electrolyzers and fuel cells are DC-current devices, a DC/AC conversion is required in order to connect them to the bulk AC grid. Moreover, a wind turbine normally drives a three-phase AC generator, which means that AC/DC conversion is necessary to connect the wind power plant to an electrolyzer. In addition to controlling the active power flow, power converters could also be designed to provide reactive-power support. The thyristor-based converters require the AC-grid and are thus not suitable for stand-alone operation [7]. Another type of power converters is based on semiconductor power devices known as "controllable switches" like Gate-Turn-Off (GTO)-thyristors and Insulated Gate Bipolar Transistors (IGBT) and can be controlled independently of the grid.

The electrical integration concept of wind-nuclear-hydrogen system depends on geographical location and the suitability of the nearby grid [7]. If the wind-hydrogen system is considered to be connected to a strong grid, simple and low-cost solutions are preferred, such as the one presented in Fig. 2.20. In this case, different components are connected individually to the local AC grid. If, on the other hand, the wind-nuclear-hydrogen system is assumed to be connected to a weak or isolated grid, the ability to provide reactive power support and the ability to improve power quality, such as reducing flickering and harmonic currents, may be

crucial. In this case, an alternative where the components are connected to the grid by a common DC-link, as shown in Fig. 2.21, might be preferred.

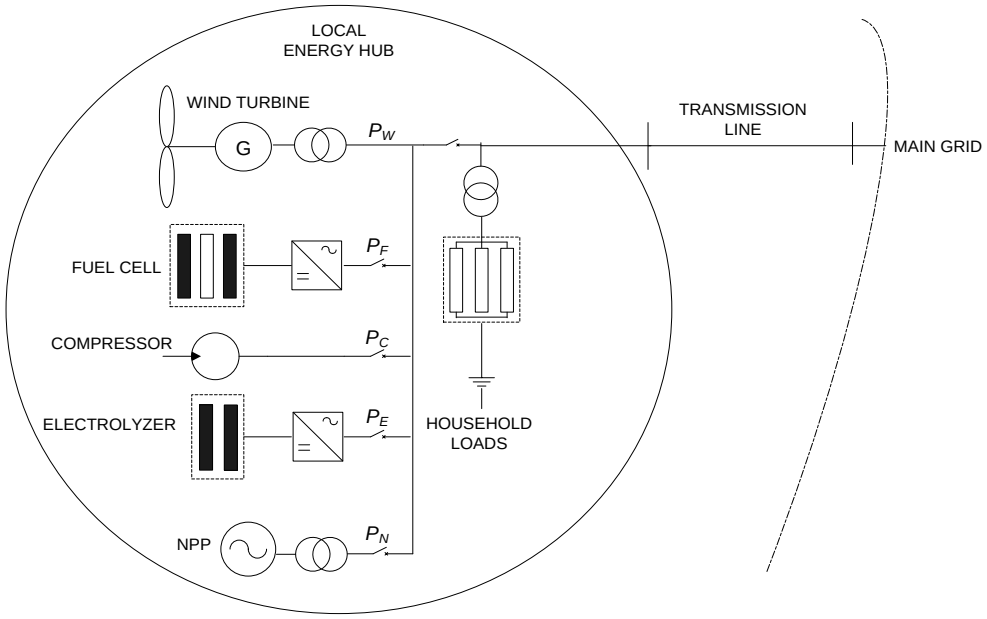

Fig. 2.20: Wind-nuclear-hydrogen system with integration through an AC-link, partly based on [7].

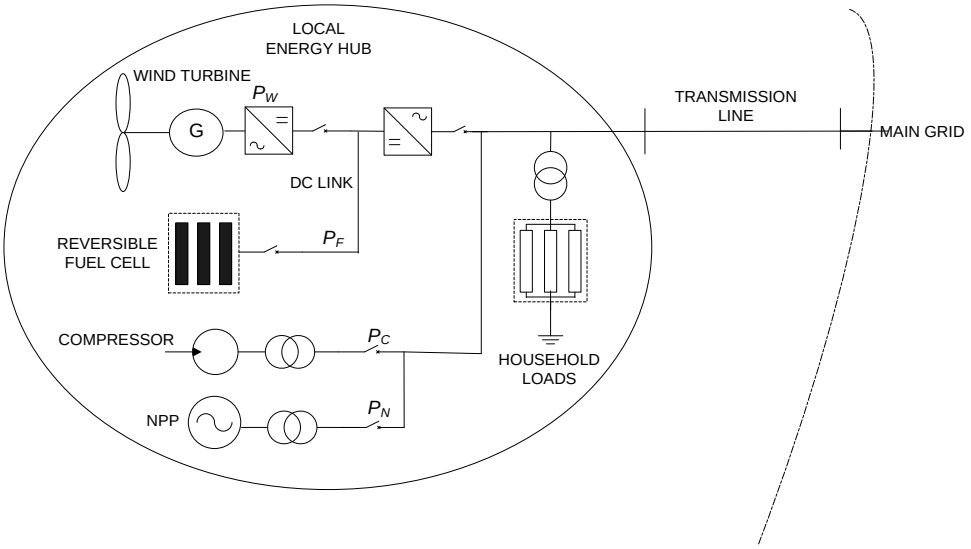

Fig. 2.21: Wind-nuclear-hydrogen system connected through a common DC link on the wind-hydrogen side, partly based on [7].

There can also be other integration scenarios considering a combination of dc and ac links and with other components, such as photovoltaic facilities, hydro power, industrial demand, etc.

Due to an existing strong grid in the area, we have focused on the wind-nuclear-hydrogen integration presented in Fig. 2.20, with the exact integration scheme shown individually for each studied scenario. The electricity production and consumption from the energy hub is

limited by the capacity of the transmission system. This operational constraint considering the wind-nuclear-hydrogen energy hub is described in the following equation:

$$-P_{\max}^{NET} \le P_G + P_F - P_E - P_C \le P_{\max}^{NET} \tag{2.39}$$

where $P_{\max}^{NET}$ is the capacity of the transmission system and P_C is the total consumption of the oxygen and hydrogen compressors.

3 METHODOLOGY

The methodology for the optimal operation and the economic evaluation developed for this thesis is described in detail in this chapter. As the case-study hydrogen system is assumed to be located in Ontario, Canada, the dispatch-optimization model is based on the structure of this market and is developed on the basis of state-of-the-art dispatch-optimization procedures presented in [20] and [21].

A two-level approach is used for the dispatch optimization: (a) dispatch levels are first obtained one-day ahead, based on a stochastic optimization model, and (b) the system's real-time operation is then simulated based on real-time data, so that financial parameters, such as energy sold, energy purchased, income, etc., can be calculated based on the real-time operation results. Thus, the system operation and market bidding, for the system depicted in Fig. 3.1, are optimized on the basis of a mixed-integer stochastic linear programming (MISLP) model. In this model, wind production and electricity prices are the stochastic input parameters. This procedure yields daily profits, which are then aggregated for a year and used as an input in the second stage of the economic evaluation procedure, where financial indices (e.g., the internal rate of return) are calculated on the basis of constant profits throughout the system's lifetime.

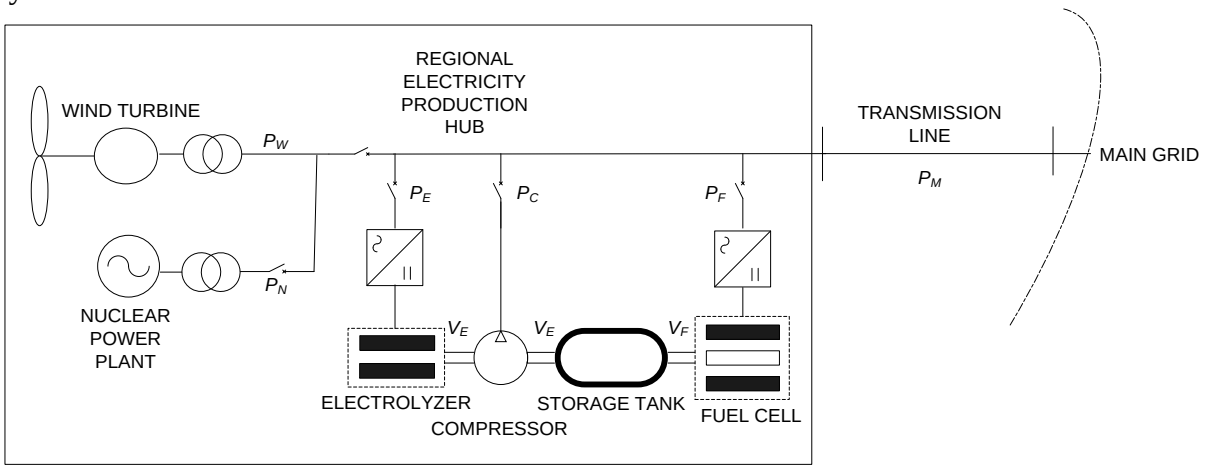

Fig. 3.1: Structure of a "regional energy hub" including hydrogen as the energy storage and energy carrier. The notation used is detailed in Chapter IV.

The flowchart of the complete system operation evaluation procedure and the bidding processes used for the studies presented here is shown in Fig. 3.2.

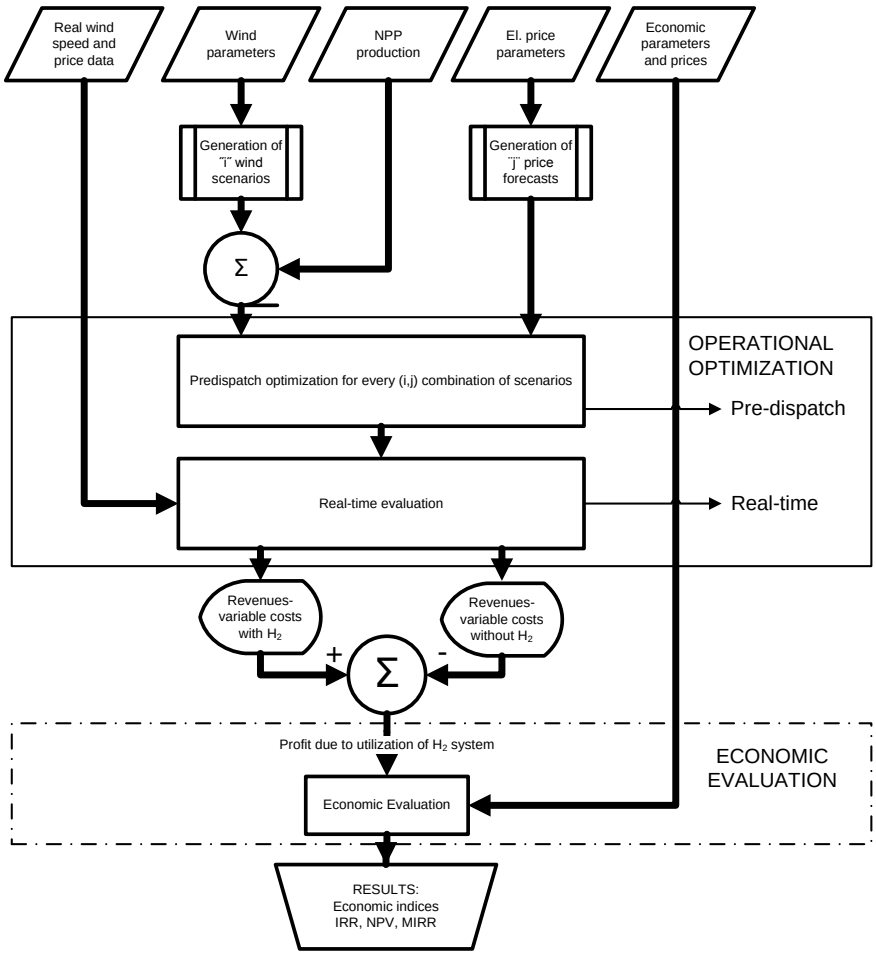

Fig. 3.2: System-evaluation procedure.

This economic evaluation procedure is used throughout the thesis with the general methodology described in Chapters 3.1-3.4, which is modified in Chapters 4.7-4.10 to consider the specifics of each studied scenario of hydrogen use in the power system. Parts of the general methodology that are not changed in the scenarios remain the same as those described in the general methodology.

3.1 Pre-dispatch

The following optimization model for obtaining one-day-ahead dispatch levels considers that the only variable that links operating hours and days together is the storage content; hence, the storage-content variable is fixed in this model, making it time dependent but not scenario dependent, as can be seen from the definition of the storage-content variable. The pre-dispatch optimization procedure was developed on the basis of the hydrogen-system component models described in Chapter 2. The following objective function is designed to maximize the profits by considering all the possible wind-speed and price-forecast scenarios:

$$\max \quad \sum_{w=1}^{Nw} p_w \cdot \sum_{p=1}^{Np} p_s \cdot \sum_{i=1}^{T} c_{p,i}^{M} (P_{w,p,i}^{G} + P_{w,p,i}^{DIS} - P_{w,p,i}^{CH}) \tag{3.1}$$

Here, p_w is the probability of wind scenario *w*, p_s is the probability of price scenario *s*, *Nw* is the number of wind scenarios, *Np* is the number of price scenarios, $c^M_{p,i}$ is the electricity-market price forecast for hour *i* and price-forecast scenario *p*, $P^G_{w,p,i}$ is the used wind-nuclear power in the wind scenario *w*, price scenario *p* in hour *i*, $P^{DIS}_{w,p,i}$ is the fuel-cell electricity production in the wind scenario *w*, price scenario *p* in hour *i* and $P^{CH}_{w,p,i}$ is the electrolyzer consumption in the wind scenario *w*, price scenario *p* in hour *i*. This objective function is followed by constraints depicting the operational characteristics of the hydrogen-system components. The electricity production and consumption limitations of the nuclear-wind-hydrogen system are based on equation (3.2):

$$-P^{NET}_{\max} \le P^G_{w,p,i} + P^{DIS}_{w,p,i} - P^{CH}_{w,p,i} \le P^{NET}_{\max} \tag{3.2}$$

where $P^{NET}_{\max}$ is the maximum capacity of the transmission system connected to the Bruce region. In equation (3.3), the power produced by the wind-nuclear facilities is limited to the available power from these facilities. This equation is based on (2.38) and is needed during periods when the production of electricity is limited due to a lack of transmission capacities.

$$0 \le P^G_{w,p,i} \le P^{GA}_{w,i} \tag{3.3}$$

In the above equation, $P^{GA}_{w,i}$ refers to the available power production from wind-nuclear power plants for wind-forecast scenario *w* in hour *i*. Based on (2.26), the hydrogen-storage state of charge for two consecutive hours is described by the following equation:

$$V^{STG}_i = V^{STG}_{i-1} + \frac{\mu_{he} \cdot \mu_{hc}}{\mu_{he} + \mu_{hc}} \cdot P^{CH}_{w,p,i} - \mu_{ef} P^{DIS}_{w,p,i} \tag{3.4}$$

Where V^{STG}_i is the state of charge of the hydrogen storage in hour *i*, μ_{he} is the electricity-to-hydrogen conversion efficiency of the electrolyzer, μ_{hc} is the compressor efficiency, which is expressed as the power consumption of the compressor when compressing one kilogram of hydrogen, and μ_{ef} is the hydrogen-to-electricity conversion efficiency of fuel cells. The initial storage level is given by equation (3.5):

$$V^{STG}_0 = \hat{V}^{STGEND}_{d-1} \tag{3.5}$$

Here, $\hat{V}^{STGEND}_{d-1}$ represents the actual storage state of charge in the last hour of the previous day. The maximum and minimum power constraints of the fuel cells, based on (2.33), are described in the following equation:

$$\alpha_{w,p,i} \cdot P^{DIS}_{\min} \le P^{DIS}_{w,p,i} \le \alpha_{w,p,i} \cdot P^{DIS}_{\max} \tag{3.6}$$

where $\alpha_{w,p,i}$ is the binary variable representing the on/off status of the fuel-cell stack in wind scenario *w*, price scenario *p* in hour *i*; $P^{DIS}_{\min}$ is the minimal power of the stationary fuel cells and

$P_{\max}^{DIS}$ is the maximum output power of the fuel-cell stack that corresponds to the installed capacity of the fuel-cell rack. The same constraint for the electrolyzer-compressor block is described in equation (3.7), which is derived from equations (2.24) and (2.25).

$$\beta_{w,p,i} \cdot \left(1+\frac{\mu_{he}}{\mu_{hc}}\right) \cdot P_{\min}^{CH} \le P_{w,p,i}^{CH} \le \beta_{w,p,i} \cdot \left(1+\frac{\mu_{he}}{\mu_{hc}}\right) \cdot P_{\max}^{CH} \tag{3.7}$$

Here, $\beta_{w,p,i}$ is the on/off state of the electrolyzer in wind scenario *w*, price scenario *p* in hour *i*, $P_{\min}^{CH}$ is the minimum power of the electrolyzer facility and $P_{\max}^{CH}$ is the maximum power of the electrolyser stack. Finally, the hydrogen state of charge is limited by the capacity of the hydrogen-storage tank as follows:

$$0 \le V_i^{STG} \le V_{\max}^{STG} \tag{3.8}$$

This equation is based on (2.27) with the variable $V_{\max}^{STG}$ depicting the capacity of the hydrogen-storage tank. The variables $c_{p,i}^{M}$ and $P_{w,i}^{GA}$ are stochastic, and $\alpha_{w,p,i}$ and $\beta_{w,p,i}$ are binary variables, making the above model a mixed-integer stochastic linear programming (MISLP) model. The optimization model is solved for a forecasting horizon of one day, with hourly resolution, since a longer horizon would not improve the overall performance of the system due to the increased forecasting error of the electricity prices and wind speeds [44], which would limit the ability to properly assess the optimal operation of the system. On the other hand, a shorter pre-dispatch optimization horizon would mean only an increased number of local optimums, without having the ability to make use of all the wind power and price fluctuations. Two consecutive days are linked via the hydrogen-storage content at the end of the first period.

3.2 Real-time Dispatch

A simple real-time operating strategy that follows the scheduled hydrogen-storage levels obtained from the solution of the MILSP problem (1)-(9) is used. The optimization is made on an hourly basis. The constraints are similar to those described in the pre-dispatch optimization model. Thus, the real-time dispatch problem is modeled as a mixed-integer linear programming (MILP) optimization problem with the following objective function:

$$\max \quad \hat{c}_i^M (\hat{P}_i^G + \hat{P}_i^{DIS} - \hat{P}_i^{CH}) \tag{3.9}$$

The network constraints are depicted in the following equation:

$$-P_{\max}^{NET} \le \hat{P}_i^G + \hat{P}_w^{DIS} - \hat{P}_i^{CH} \le P_{\max}^{NET} \tag{3.10}$$

where $\hat{P}_i^G$, $\hat{P}_w^{DIS}$ and $\hat{P}_i^{CH}$ are the real-time values for the used power from the wind-nuclear facilities, electrolyzer and fuel cell stacks in hour *i*, respectively. The actually available power from the wind-nuclear power plants is depicted in equation (3.11).

$$0 \le \hat{P}_i^G \le \hat{P}_i^{GA} \tag{3.11}$$

Here, $\hat{P}_i^{GA}$ is the actually available power production by the wind and nuclear power plant in hour i. The hydrogen-storage state of charge for two consecutive hours is given in (3.12).

$$\hat{V}_i^{STG} = \hat{V}_{i-1}^{STG} + \frac{\mu_{he} \cdot \mu_{hc}}{\mu_{he} + \mu_{hc}} \cdot \hat{P}_i^{CH} - \mu_{ef} \hat{P}_w^{DIS} \tag{3.12}$$

In the above equation, $\hat{V}_i^{STG}$ is the actual value for the storage level in hour *i*. The equation (3.13) is used for the hydrogen system to follow the optimal levels obtained in the pre-dispatch optimization procedure:

$$\hat{V}_1^{STG} = V_i^{STG} \tag{3.13}$$

The fuel cell, electrolyzer and compressor power limitations are described in equations (3.14) and (3.15).

$$\hat{\alpha}_i \cdot P_{\min}^{DIS} \le \hat{P}_i^{DIS} \le \hat{\alpha}_i \cdot P_{\max}^{DIS} \tag{3.14}$$

$$\hat{\beta}_i \cdot \left(1 + \frac{\mu_{he}}{\mu_{hc}}\right) \cdot P_{\min}^{CH} \le \hat{P}_i^{CH} \le \hat{\beta}_i \cdot \left(1 + \frac{\mu_{he}}{\mu_{hc}}\right) \cdot P_{\max}^{CH} \tag{3.15}$$

Where $\hat{\alpha}_i$ and $\hat{\beta}_i$ describe the actual fuel-cell and electrolyzer on/off state in hour *i*. The hydrogen-storage level is limited by (3.16) and the final value of the storage level is saved as the initial hydrogen-storage level for the subsequent pre-dispatch optimization in equation (3.17).

$$0 \le \hat{V}_i^{STG} \le V_{\max}^{STG} \tag{3.16}$$

$$\hat{V}_d^{STGEND} = \hat{V}_T^{STG} \tag{3.17}$$

Observe that the real-time optimization model is very similar to the pre-dispatch model (3.1)-(3.8); however, in this case, there are no stochastic parameters and the optimization model corresponds to only one hour, which is solved on an hourly basis for 24 h.

3.3 Calculation of profits obtained from hydrogen-system operation

The income or profit obtained from the hydrogen subsystem is the difference between the total income of the wind-nuclear system with hydrogen and without hydrogen, where the income with the hydrogen system is calculated using:

$$\hat{R}_i = \hat{c}_i^M (\hat{P}_i^G + \hat{P}_i^{DIS} - \hat{P}_i^{CH}) \tag{3.18}$$

Where $\hat{R}_i$ is the income with the hydrogen system in hour i. The income without the hydrogen system in hour i is specified by $\hat{R}_i^{WH}$ and is calculated using the following equation:

$$\hat{R}_i^{WH} = \hat{c}_i^M \cdot \min(P_{\max}^{NET}, \hat{P}_i^G) \tag{3.19}$$

The input into the economic analysis is the profit obtained due to the utilization of the hydrogen system, which is the difference between equations (3.18) and (3.19).

3.4 Financial Evaluation of the projects

The financial evaluation of the projects is a study that determines the performance and return (profitability) with respect to expenditures of the current wealth and other resources in the expectation of generating future benefits, whether in the form of profits, cost savings or social benefits [45]. For an investment to be worthwhile, the future benefits expected, in whatever form, should compare sufficiently favorably with the prior expenditures of resources needed to achieve them. Thus, the costs and benefits of a project must be evaluated in a manner that gives a prospective investor the information about the financial feasibility and profitability of the project.

Cash Flow is firstly generated by representing the difference between the costs and benefits of the project, resulting in net benefits [46]. The negative values of net benefits are mainly due to construction or refurbishment of the equipment in the project's life time. The positive values, on the other hand, are the profits created by the project and should outbalance the costs for the project to become financially acceptable.

The ***Financial Costs*** of the project can be divided into three major groups [46]:

- **Investment costs:** are further divided into the initial investment, replacement and salvage costs. Initial costs refer to those costs involved in construction and commissioning, including land, civil works, equipment and installation, Replacement costs refer to the costs of equipment and installations procured during the operating phase of the project, to maintain its original productive capacity. The salvage value refers to the value of the investment items (equipment, land, etc.) at the end of the project's useful life.
- **Operating costs:** are a combination of fixed and variable costs. Fixed costs are incurred whatever the level of production, like salaries, costs of management, and part

of the maintenance costs. Variable costs depend upon the level of production and include those items like fuel and energy, water, lubricants, and part of the maintenance cost.

- **Working capital:** refers to the physical stock needed to allow continuous production (spare parts, fuel, raw materials). The stock has to be built up at the commissioning phase and before the beginning of the commercial operation. For power plants and network projects, there is usually one component of working capital, which is the initial stock of material necessary for commercial operation.

On the other hand, the ***Financial Benefits*** are brought about by selling the project's product. These benefits are usually equal to the amount of production multiplied by the estimated base price.

The financial evaluation is usually part of a broader analysis in the pre-investment stage of a project called the pre-feasibility or feasibility study. The feasibility study provides all the data and details necessary to take a decision to invest in the project. It defines and critically examines the results of the studies undertaken in the pre-feasibility stage: demand, technical, financial, economic and environmental. The result of the feasibility stage is a project where all the background features have been well defined: the size and location of the facilities, technical details, fuels, network features, and the environmental impact and how to deal with it, the timing of the project, and the implementation schedule. The financial part of the feasibility study will cover the required investment and its sources, the expected financial and economic costs and the returns. The financial evaluation in this thesis is assumed to be of the pre-feasibility type, since it does not cover a specific investment but generally addresses the suitability of hydrogen technology for storage purposes. Thus, several assumptions are made in the financial evaluation:

- some costs are neglected or are assumed to be part of other costs, e.g., investment costs include the transportation costs, O&M costs include labor costs and working capital;
- the revenues are calculated for a single year and then extrapolated for the rest of the project.

The description of financial costs and financial benefits is evaluated in the cash-flow calculation, which is described in one of the following chapters.

3.4.1 Income statement

An Income Statement, also called a Profit and Loss Statement, is a financial statement for companies that indicates how much revenue (money received from the sales of products and services before expenses are taken out, also known as the "top line") is transformed into net income (the result after all the revenues and expenses have been accounted for, also known as the "bottom line"). The purpose of the income statement is to show managers and investors

whether the company made or lost money during the period being reported. It is also generated to show the projections of net profits of a potential evaluated project. As one will observe later on in the thesis, the results of the calculation of the Income Statement will be used in the following chapter, describing a cash-flow analysis of a project. The Income Statement described here is modified to reflect the structure of the studied system and the optimization models. Thus, the following assumptions are made:

- the revenues and costs of goods sold are combined in a single variable;
- depreciation is not included in the costs of goods sold, but is considered separately.

3.4.1.1 Revenues and Costs of Goods Sold (Variable Costs)

As per the above assumption, the difference of the revenues and the costs of goods sold (i.e., variable costs) are assumed to be an input to the economic evaluation model and are calculated for a typical year using the optimization procedures described in the previous chapter. Furthermore, the difference is taken to be constant throughout the project's lifetime. It is calculated as a sum of hourly revenues, which are the difference between the profits with hydrogen and without the hydrogen system, using the following equation:

$$R_T = \sum_{i=1}^{8760} \hat{R}_i - \hat{R}_i^{WH} \tag{3.20}$$

Here, r is the yearly revenue obtained from the operation of the hydrogen system. The variable costs for electricity purchases are already considered in the above equation.

3.4.1.2 Investment costs

The initial investment and reinvestment costs are calculated separately for each year of the project. For the year t, they are calculated as the sum of the equipment and the equipment-installation costs:

$$c_t = \sum_{k \in K} e_{t,k} + \sum_{k \in K} tr_{t,k} \tag{3.21}$$

Here, c_t are the investment or reinvestment costs in the year t, $e_{t,k}$ are the investment or reinvestment costs for asset class k for year t and $tr_{t,k}$ are the transportation costs for year t for asset class k. The variable K represents all the different asset classes considered in the project, where asset classes refer to different system components that are needed in the investment, e.g., electrolyzers, fuel cells. In the equation, the reinvestment costs represent the cost for the replacement of worn-down assets after their lifetime. It should be mentioned here, that investment costs are not considered as a taxable cost in the formation of the income statement but only as money outflow in the generation of cash-flow projections.

3.4.1.3 Financing

One of the goals in the project's planning is also a proper planning of the financing of investments. Management must therefore identify the "optimum mix" of financing - the capital structure that results in the maximum value [47]. The sources of financing generically comprise some combination of debt and equity. Financing a project through debt results in a liability that must be serviced and hence there are cash-flow implications regardless of the project's success. Equity financing is less risky in the sense of cash-flow commitments, but it results in a dilution of ownership and earnings. In the thesis, the financing is assumed to be twofold: with equity and with a bank loan. For the loan, the project planner has to pay certain interest to the bank in addition to repaying the principal. Here, the principal can be calculated using the equation below:

$$P_t = \sum_{k \in K} (1 - eq) \cdot e_{t,k} / n_k \tag{3.22}$$

where P_t is the principal in year t, eq is the proportion of equity in the investment, $e_{t,k}$ are the initial or the replacement costs for asset group k in year t and n_k is the lifetime of asset group k. The term annuity is used in finance theory to refer to any terminating stream of fixed payments over a specified period of time [47]. This usage is most commonly seen in the financing of projects, usually in connection with the valuation of the stream of payments of bank loans, taking into account the time value of money concepts such as interest rate and future value. The annuity is calculated using the following equation:

$$A_t = \sum_{k \in K} (1 - eq) \cdot e_{t,k} \cdot \frac{ir \cdot (1 + ir)^{n_k}}{(1 + ir)^{n_k} - 1} \tag{3.23}$$

where A_t is the annuity in year t, ir is the interest rate of the bank loan. The difference between the annuity and the principal is the interest for taxation (designated with I_t), which can be calculated using the next equation:

$$I_t = A_t - P_t \tag{3.24}$$

Interests are used for the calculation of the Income Statement; the annuity, on the other hand, is only used for the generation of cash-flow projections, which is described in Chapter 3.4.2.

3.4.1.4 Depreciation (Amortization)

The depreciation (amortization) method used in the thesis is straight-line depreciation, which is the simplest and most often used technique in which the company estimates the "salvage value" of the asset after the length of time over which it will be used to generate revenues (useful life), and will recognize a portion of that original cost in equal increments over that amount of time. The depreciation is thus calculated using the following equation:

$$d_t = \sum_{k \in K} \frac{e_{0,k} \cdot (1-s)}{n_k} \tag{3.25}$$

where d_t is the depreciation in year t, $e_{0,k}$ are the investment or replacement costs in the investment or replacement year of asset group k and s is the proportion of asset costs that can be salvaged at the end of the lifetime of the asset. With the inclusion of the salvage value of the assets in the equation, the difference between the initial investment value of the assets and the salvage (scrap) value of the assets is considered.

3.4.1.5 Salvage value

Furthermore, the salvage value of the assets is considered as revenues at the end of the project's lifetime. It can be included in the income statement in the following form:

$$s_t = \sum_{k \in K} e_{0,k} \cdot s \tag{3.26}$$

where s_t is the salvage value in year t. In the Income Statement projections in the thesis, it is assumed that the project's salvage value is obtained one year after the closure of the project. Thus, an additional year is considered in the Income Statement sheet, as it will be shown in the simple showcase in the Chapter 3.4.5.

3.4.1.6 Operation and maintenance costs

The operation and maintenance costs are assumed to be constant throughout the project's lifetime and are taken as the percentage costs of the different asset groups. Therefore, they can be calculated using the following:

$$o_t = \sum_{k \in K} e_k \cdot om_k \tag{3.27}$$

Here, o_t is referred to as the operation and maintenance costs in year t and om_k as the operation and maintenance factor for the asset class k.

3.4.1.7 Taxes

The result of the income statement are the projections of pretax profits (also referred to as Earnings Before Tax, EBT), corporate taxes and profits after tax. Typically, the negative profits are considered in the project's pretax profits in the following years of the project as tax shields. It is assumed in the thesis, that negative profits can be carried forward indefinitely. Thus, we have to firstly calculate the pretax profits before the carry-forward process, which can be done using the following equation:

$$EBT\_temp_t = R_T + s_t - d_t - I_t - o_t \tag{3.28}$$

where EBT_temp_t is the pretax profit before the carry-forward process. Following that, the next equation is used to calculate the pretax profits after the carry-on of negative profits:

$$EBT\_ACO_t = \begin{cases} EBT\_temp_t + EBT\_ACO_{t-1} & if\ \ EBT\_ACO_{t-1} < 0 \\ EBT\_temp_t & if\ \ EBT\_ACO_{t-1} \geq 0 \end{cases} \tag{3.29}$$

And finally, negative pretax profits after the carry-on process are set to zero using:

$$EBT_t = \begin{cases} EBT\_ACO_t & if\ \ EBT\_ACO_t \geq 0 \\ 0 & if\ \ EBT\_ACO_t < 0 \end{cases} \tag{3.30}$$

Here, EBT_t are the earnings before tax after the carry-on process. Finally, the taxes can be calculated using the following equation:

$$ta_t = EBT_t \cdot tr \tag{3.31}$$

Here, ta_t is assumed to be the tax for year t and tr is assumed to be the corporate tax rate. As one can see in the methodology described so far, the Value Added Tax (VAT) is not considered anywhere in the generation of the income statement as the outgoing VAT for purchased goods during the lifetime of the projects is compensated with the income VAT from the revenues obtained by the selling of goods. The time difference between the incoming and outgoing VAT is assumed not to have any impact on project's profitability.

3.4.2 Cash-Flow Projections

Cash flow is a term that refers to the amount of cash being received and spent by a business during a defined period of time, sometimes tied to a specific project. The cash-flow calculation is the basis for the calculation of economic indices, such as net present value and internal rate of return, which will be described later on in this chapter. A measurement of the cash flow in the thesis is used to evaluate the state or performance of an investment on a yearly basis where the initial investment is considered to be in year 0. Note, that the depreciation is included implicitly in the calculation of the taxes rather than directly in the cash-flow calculation below. The cash flow in year t (depicted with variable cf_t) is generated by merging all the revenues and costs into a single money flow using the following equation:

$$cf_t = R_T + s_t - A_t - c_t - o_t - ta_t \tag{3.32}$$

A graphical representation of a simple cash flow is illustrated in Fig. 3.4 using a cash-flow diagram. The cash flow in the initial investment year is assumed to be 15000 CAD and 1000 CAD later on in every year of the system's operation. The salvage value of the assets in the last year of the project increases the cash flow to 1500 CAD. The negative cash flow in year 0, which is designated as an investment year, is without any incomes due to initial

investments in this year. Later flows are positive due to project's revenues being higher than the costs.

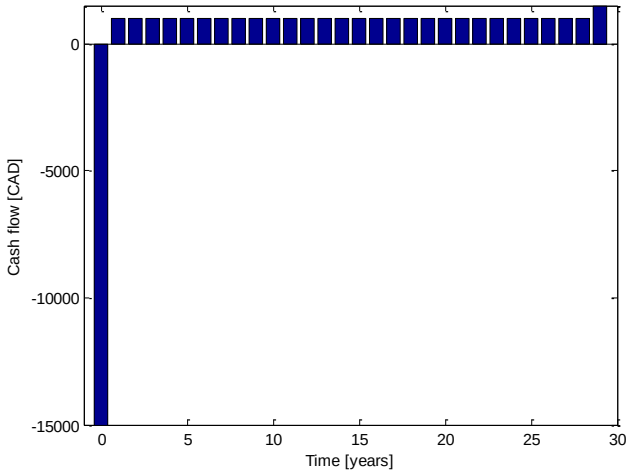

Fig. 3.3: Graphical representation of a simple cash flow

More common and more meaningful is the representation of the cash flow in a cumulative way, referred to also as the cumulative cash flow, which is the cumulative sum of successive cash flows representing the sum of the past cash flows in a specific point in time. A graphical representation of the cumulative cash flow from the cash flow in Fig. 3.3 is presented in Fig. 3.4.

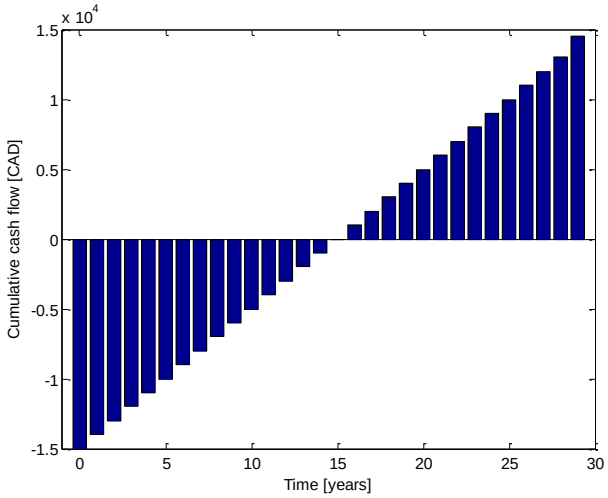

Fig. 3.4: Cumulative cash flow of the cash flow presented in Fig. 3.3.

As one can see from the figure, the cumulative cash flow is negative due to the initial investment in year zero, but becomes positive through the project's lifetime due to the addition of yearly positive cash flows.

3.4.3 The present-value concept

Generally, financial flows (cash flows) from projects do not occur during the project evaluation [47], [48]. They occur after a year or a couple of years and cannot be readily added since the value of 1 Canadian dollar (CAD) today is different from 1 CAD next year and very different from same amount of money in 20 years' time. The reasons for this are the following:

- future incomes are eroded by inflation; therefore, the purchasing power of a CAD today is higher than a CAD in a year's time;
- the existence of risk and income or expenditure that occurs today, is a sure amount. Future income or expenditure may vary from anticipated values;
- the need for a return; by undertaking investment and foregoing expenditures today, an investor expects to be rewarded by a return in the future.

Even if the inflation rate is neglected in the evaluation of time-worth of money, to an investor 1 CAD is worth more today than tomorrow simply because he can earn a real income, that is, a return higher than inflation. Therefore, an important factor to recognize in the project evaluation is the time value of money. Hence, before dealing with the cash flows occurring at different times, these have to be adjusted to the value of the money at a specific date, which is normally called the base date or base year.

Present valuing or discounting is central to the financial and economic evaluation process. Since most of the project costs, as well as the benefits, occur in the future, it is essential that these should be discounted to their present value (worth) to enable a proper evaluation. Present valuing will be carried out through discounting the next period's financial outlay (cf_{n+1}) to its present value through multiplying it by a **discount factor**. The discount factor is a function of the discount rate *dr,* which is a reward that an investor wants for accepting a delayed payment. It is also referred to as the rate of return or opportunity cost of capital, so that:

$$PV_t = df_t \cdot cf_t \tag{3.33}$$

where PV_t is the present value of the cash flow cf_t calculated using the discount factor df_t. The discount factor is also called the **present-value factor** and is defined as how much a CAD in the future is worth today. Therefore, if the discount rate is 10% annually, the discount factor is 0.909, and 110 CAD materializing next year is worth 100 CAD today. Thus, the discount factor is calculated using the following equation:

$$df_t = \frac{1}{(1+r)^t} \tag{3.34}$$

where r is referred to the discount factor. The combination of the latter two equations gives the complete formula for the calculation of the present value of a future cash flow:

$$PV_t = \frac{1}{(1+r)^t} \cdot cf_t \tag{3.35}$$

According to that equation, a cash flow of 1000 CAD occurring in year five of the project represents 620.96 CAD today, considering a 10% discount factor. After thirty years the present value of the 1000 CAD would be 57.31 CAD. In Fig. 3.5, the present value of 1000 CAD is described during a 30 years' period, illustrating the impact of the discount rate on the value of money.

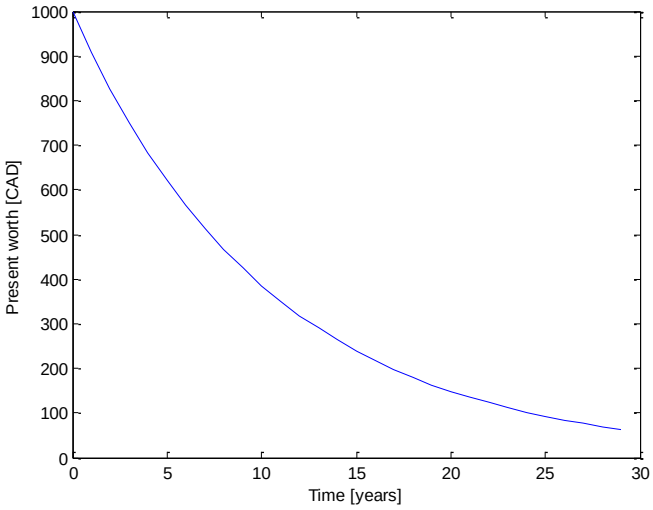

Fig. 3.5: The present worth of 1000 CAD in thirty years assuming a 10% discount rate

Similarly, the worth of money can also be discounted to a point of time in the future or to the present time from the past. This can be done using a compound factor, which is the reciprocal of the discount factor:

$$cof_t = (1+r)^t \tag{3.36}$$

where cof_t is the compound factor. For example, a 1000 CAD cash flow that occurred a year from now, has a present value of 1100 CAD, assuming a 10% discount rate.

3.4.3.1 Discounted Cash Flow

The cash flows presented in Chapter 3.4.1 are better represented in terms of discounted cash flows using the process of net present valuing presented in the above chapter [47]. Hence, each year's cash flow can be discounted to the present value by dividing it by the discount factor for the particular year. Therefore, the extended streams of cash flows cf_0 .. cf_t occurring at years $0..t$ have a present value of:

$$PV = cf_0 + \frac{1}{(1+r)^1} \cdot cf_1 + \ldots + \frac{1}{(1+r)^t} \cdot cf_t = \sum_{Tp} \frac{cf_t}{(1+r)^t} \tag{3.37}$$

The difference between the nominal and the discounted cumulative cash flows is shown in Fig. 3.6, using the data from the cash flow depicted in Fig. 3.3. One can see that, contrary to the cumulative net cash flow, the cumulative discounted cash flow does not exceed the zero margin line, meaning that the project is not profitable at the end of its lifetime.

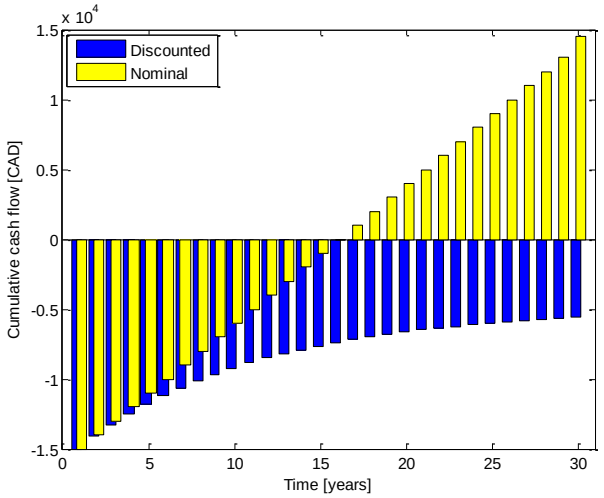

Fig. 3.6: The nominal and discounted cash flows assuming a 10% discount rate

3.4.3.2 Discount rate

The discount rate is one of the most important factors that impact on the financial feasibility of the project [47]-[49]. It greatly impacts the economics of the projects of a company and the process of decision making; particularly in capital-intensive projects like those in the electricity-supply industry. It governs the least-cost solution and affects the estimation of the net returns from the project. Thus, the discount rate has to be selected carefully, to avoid any wrong investment decisions with financial consequences that might occur if it is selected too high or too low; a high discount rate will favor a low capital cost with a higher operational cost project alternatives and a low discount rate will tend to weigh the decision in favor of the high capital cost and low operational cost alternatives. The NPV for different discount rates, assuming the cash flow from Fig. 3.3, is presented in Fig. 3.7, to demonstrate the impact of different discount factors on project's net present value.

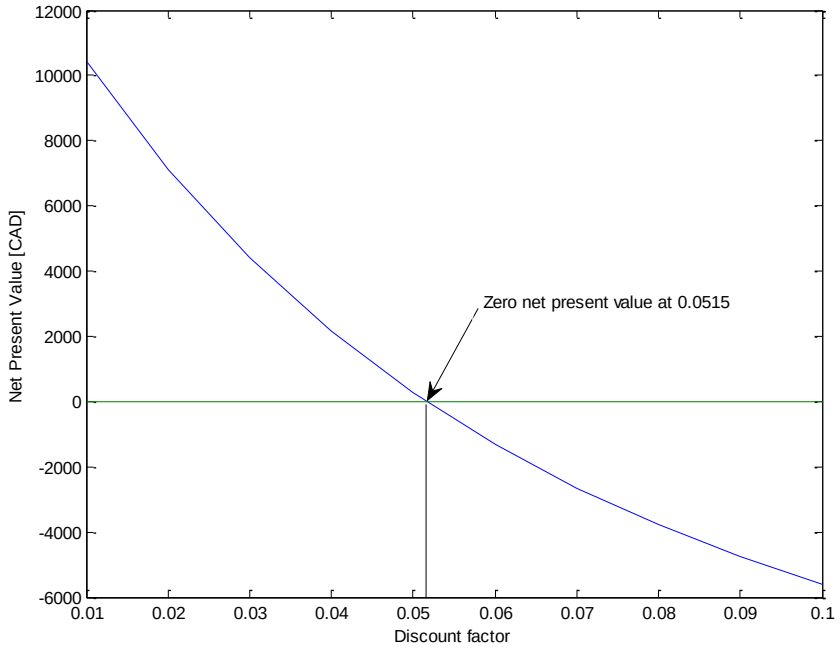

Fig. 3.7: The impact of discount factor on the net present value of a project.

The discount rate is the opportunity cost of capital (as a percentage of the value of the capital). The opportunity cost of capital is the return on the investments forgone elsewhere by committing capital to the project under consideration. It is also referred to as the marginal productivity of capital, i.e., the rate of return that would have been obtained by the least acceptable project. In the investment decisions, the opportunity cost of capital is the cut-off rate, below which it is not worthwhile to invest in the project.

The discount rate connotes the investor's indifference to the timing of the return. If it is equal to 10% the investor is indifferent to whether he receives 1 CAD today or 1.1 CAD a year from today. This indifference is the basis for engineering economics. To serve this purpose, the nominal discount rate should be at least equal to a value which, after tax, would compensate the investor for the three objectives mentioned in Chapter 3.4.3. The value of the nominal discount rate is correspondingly a function of the mentioned factors. Inflation can be ignored if the cash flow is presented in the base-year value of money.

Setting a correct companies discount rate is a complex task and involves the evaluation of several impact factors that are subject to different risks. A detailed description of the different methodologies for the calculation of the discount rate is given in [47].

3.4.4 Financial Indices

There are several financial indices that are commonly used among analysts to assess the economic viability of a certain project [45]-[49]. They range from the simple, e.g., simple

payback time, to the more complex, e.g., modified internal rate of return, indices, all considering different economic parameters in a different manner. In this thesis, the most commonly used Net Present Value (NPV) and Modified Internal Rate of Return (MIRR) indices are used, where the latter is derived from the well-known Internal Rate of Return (IRR) index.

3.4.4.1 Net Present Value

During the lifetime of a project there will be two financial streams: one is the costs stream (which includes all capital, operation, maintenance and other costs) and the other is the revenues stream [47]. These two streams must contain all the costs and benefits for the same estimated life frame of a project. The costs stream, being outward-flowing cash, is regarded as negative. Discounting the difference between the two streams (the cash flow) will provide the net present value (NPV) of the project. A detailed simple case of an NPV calculation is given in Tab. 3.1, which utilizes a discount rate of 10%. Notice that the last revenue is due to the salvage value of the assets in that year.

Tab. 3.1: Net Present Value calculation

YEAR	COST	REVENUE	BENEFITS	DISCOUNT FACTOR	DISCOUNTED BENEFITS
-1	40	-	-40	1.100	-44.00
0	110	40	-70	1.000	-70.00
1	10	40	30	0.909	27.27
2	10	40	30	0.826	24.79
3	10	40	30	0.751	22.54
4	-	70	70	0.683	47.81
					NPV: 8.41

All values are considered to occur at the same point in time during one year; most commonly the middle of the year is chosen. Usually, projects are undertaken because they have a positive net present value; that is, their rate of return is higher than the discount rate, which is the opportunity cost of capital. The calculation of the net present value is the most important aspect in the project evaluation and its positive estimation, at the designated discount rate, is essential before undertaking a project.

3.4.4.2 Internal Rate of Return

The Internal Rate of Return (IRR) is a very popular and commonly used index for an economic evaluation of prospective projects, besides the NPV index [47]. The IRR is the discount rate that equates the two streams of costs and benefits, i.e., it is the discount rate where the NPV index is equal to zero. This is clearly shown in Fig. 3.7, where the NPV is zero at a discount factor of 0.0515, which is equal to an IRR of 5.15%. The internal rate of return can be calculated using the following equation:

$$\sum_{Tp} \frac{cf_t}{(1+IRR)^t} = 0 \tag{3.38}$$

If the IRR is equal to or above the opportunity cost of capital (discount rate) in private projects or the social discount rate (as set by the government) in public projects, then the project is deemed to be a worthwhile undertaking. How the discount rate is calculated is described in detail in the previous chapter.

The internal rate of return has some deficiencies that have to be taken into account when evaluating projects using this index. The IRR makes no assumptions about the reinvestment of the positive cash flow from a project. As a result, the IRR should not be used to compare projects of different duration and with a different overall pattern of cash flows.

Furthermore, the IRR is inappropriate for use with projects that start with an initial positive cash inflow (or in some projects with large negative cash flows at the end), for example, where a customer makes a deposit before a specific machine is built, resulting in a single positive cash flow followed by a series of negative cash flows (+ - - - -). In this case, the usual IRR decision rule needs to be reversed.

If there are multiple sign changes in the series of cash flows, e.g. (- + - + -), there may be multiple IRRs for a single project, so that the IRR decision rule may be impossible to implement. Examples of this type of project are strip mines and nuclear power plants, where there is usually a large cash outflow at the end of the project.

A further critical shortcoming of the IRR method is that it is commonly misunderstood to convey the actual annual profitability of an investment. However, this is not the case, because intermediate cash flows are almost never reinvested at the project's IRR; and, therefore, the actual rate of return (like the one that would have been yielded by stocks or bank deposits) is almost certainly lower. Accordingly, a measure called the **Modified Internal Rate of Return** (MIRR) is used, which has an assumed reinvestment rate, usually equal to the project's cost of capital and is described in the next chapter.

Despite a strong academic preference for the NPV, surveys indicate that the IRR is preferred among executives over the NPV in the industry, because of the easier understanding of the IRR and the easier comparison of investments of different sizes in terms of percentage rates of return rather than by dollars of NPV. However, the NPV is the more accurate reflection of value to the business and is a better choice when comparing mutually exclusive projects.

3.4.4.3 Modified Internal Rate of Return

The Modified Internal Rate of Return (MIRR) is a modification of the IRR. The MIRR basically provides the same information about the economic feasibility of a project, but assuming one more impact factor. Rather than ignoring the investment rate of the positive cash flow, the MIRR makes an explicit assumption about the rate of return of the investment

of those flows [47], [48]. The negative cash flows are also treated differently compared to the IRR; they are discounted to the first year of the project using the finance rate.

The modified internal rate of return assumes all positive cash flows are re-invested at the reinvestment rate (usually the company's discount rate) to the terminal year of the project. All negative cash flows are discounted and included in the initial investment outlay. The MIRR can be calculated using the following equation:

$$MIRR = \left(\frac{NPV(positive\,cash\ flows, r) \cdot (1+r)^{Tp-1}}{NPV(negative\,cash\ flows,\ fr)} \right)^{\frac{1}{Tp-1}} - 1 \tag{3.39}$$

Generally, the MIRR is a successful successor to the IRR since it solves the main problems of the IRR method such as reinvesting of the cash flow and multiple sign changes in the cash flow. As we assumed the projects to be financed by a variety of different sources, we are calculating returns on equity (ROE) and the NPV of equity rather than the return on the whole investment or the Net present value of the whole investment.

3.4.5 Simple case study

A simple case study is presented here to illustrate the complete economic evaluation procedure described so far in the Financial Evaluation chapter. The cash flow is taken in real values in the economic evaluation with the appurtenant discount rate. The initial investment is assumed to be 50 for asset class A with a lifetime of 3 years and equal costs are assumed for asset class B with a lifetime of 6 years. The project is assumed to be financed in 20% by equity and 80% by debt with a 7% debt interest rate. Both the discount rate as well as the reinvestment rate are assumed to be 10 % in this evaluation and the finance rate is taken to be 7%. Since taxes are implicitly included in the cash flow, no additional modification of the discount rate is needed. The depreciation method is straight-line depreciation and the salvage value of the assets is 5% of the initial investment value. The operation and maintenance costs are assumed to be 3% of the initial investment per year and the costs for goods sold (variable costs) are 10% a year. The yearly profits are assumed to be constant throughout the project's lifetime and amount to 40 monetary units. The corporate tax rate is assumed to be 25%. The economic evaluation methodology from equations (3.20)-(3.32) and (3.37)-(3.39) is used to calculate the economic indices. The results of the income-statement calculations resulting taxes are listed in Tab. 3.2.

Tab. 3.2: Income statement of the simple case.

YEAR	0	1	2	3	4	5	6	7
INVESTMENT	20	0	0	10	0	0	0	0
DEPRECIATION	0	23.75	23.75	23.75	23.75	23.75	23.75	0
PRINCIPAL	0	20	20	20	20	20	20	0
ANNUITY	0	23.63	23.63	23.63	23.63	23.63	23.63	0
INTERESTS	0	3.63	3.63	3.63	3.63	3.63	3,63	0
SALVAGE VAL.	0	0	0	0	2.5	0	0	5
REVENUES	0	40	40	40	40	40	40	0
VAR. COSTS*	0	10	10	10	10	10	10	0
O&M COSTS	0	3	3	3	3	3	3	0
EBD_TEMP	0	-0.38	-0.38	-0.38	2.12	-0.38	-0.38	5
EBD_ACO	0	-0.38	-0.76	-1.14	0.96	-0.38	-0.76	4.23
EBD	0	0	0	0	0.96	0	0	4.23
TAXES	0	0	0	0	0.24	0	0	1.06

*Variable costs or costs of goods sold

As one can see from the Income statement, the taxes are negative in some years. This is not realistic, but given the assumption that the negative pre-tax profits make tax shields in later years, this result makes more sense. The cash flow projections are listed in Tab. 3.3.

Tab. 3.3: Cash-flow projection of the simple case.

YEAR	0	1	2	3	4	5	6	7
INVESTMENT	20	0	0	10	0	0	0	0
ANNUITY	0	23.63	23.63	23.63	23.63	23,63	23,63	0
SALVAGE VAL.	0	0	0	0	2.5	0	0	5
REVENUES	0	40	40	40	40	40	40	0
VAR. COSTS	0	10	10	10	10	10	10	0
O&M COSTS	0	3	3	3	3	3	3	0
TAXES	0	0	0	0	0.24	0	0	1.06
NCF*	-20	3.37	3.37	-6.63	5.63	3,36	3,36	3.94
DF**	1	0.90	0.82	0.75	0.68	0,62	0,56	0.51
DCF***	-20	3.06	2.78	-4.98	3.84	2,09	1,90	2.02
CDCF****	-20	-16.93	-14.15	-19.14	-15.30	-13.21	-11.31	-9.29
						NPV -9.29	IRR Neg.	MIRR 2.68

*Net Cash Flow
**Discount Factor
***Discounted Cash Flow
****Cumulative Discounted Cash Flow

One can see the difference between the IRR (negative) and the MIRR (2.68%) indices, which results from different reinvestment rates of the positive cash flow. The profits are reinvested at the project's IRR when calculating the IRR; they are reinvested at the reinvestment rate, on the other hand, when the MIRR is calculated. As the results suggest, the project is not worthwhile undertaking due to negative NPV and due to insufficient IRR and MIRR, which are both below the desired 10% margin. The cumulative discounted cash flow from the example is further illustrated in Fig. 3.8.

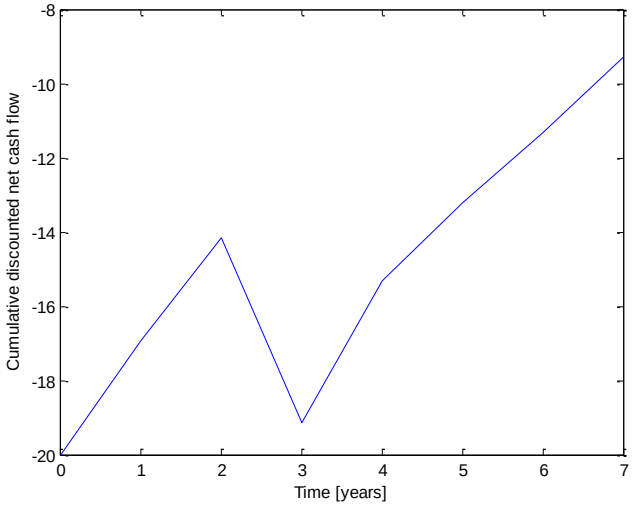

Fig. 3.8: Cumulative Discounted Net Cash Flow from the example in Tab. 3.3.

3.5 Software packages and optimization algorithms used in the thesis

The operational optimization and the economic evaluation models were programmed in two commercially available programming languages: Matlab [50] and AMPL [51]. The first was used for the data definition, the economic model and the data evaluation and the second for the optimization model development. The CPLEX package [52] was used with the AMPL modelling language for solving the optimization problems.

3.5.1 Optimization problem description and algorithms used by the solver

The operational optimization problem was simplified resulting in a linear model. The On-Off modelling of electrolyzers and fuel cells makes the problem mixed-integer and the inclusion of probabilistic variables, e.g., multiple wind-speed forecasts and multiple price forecasts with different probabilities, make this model a stochastic one. The stochastic nature of the model does not require special solvers and can be solved by typical mixed-integer linear programming routines. The AMPL with CPLEX optimization software is suitable for solving described problems and is commercially available. It is capable of solving linear and quadratic problems as well as integer, binary and mixed-integer problems.

The Simplex and Interior point algorithms with some sub-versions are used for linear programming problems by CPLEX together with the branch & cut approach for problems that contain integer variables.

3.5.1.1 Linear programming

For problems with linear constraints, CPLEX employs either a simplex method or a barrier method to solve the problem. Four distinct methods of optimization are incorporated into the CPLEX package [52]:

- A primal simplex algorithm that first finds a solution feasible in the constraints (Phase I), then iterates toward optimality (Phase II).
- A dual simplex algorithm that first finds a solution satisfying the optimality conditions (Phase I), then iterates toward feasibility (Phase II).
- A network primal simplex algorithm that uses logic and data structures tailored to the class of pure network linear programs.
- A primal-dual barrier (or interior-point) algorithm that simultaneously iterates toward feasibility and optimality, optionally followed by a primal or dual crossover routine that produces a basic optimal solution (see below).

CPLEX automatically chooses one of these algorithms where the default algorithm is the dual simplex algorithm. However, there is also an option to override the chosen method by the user. For problems with quadratic constraints, only the barrier method is used and there is no crossover algorithm. As there were no problems with convergence and time needed to solve the problems, the default dual simplex algorithm was used to solve the problems in this thesis.

Every linear program has an equivalent "opposite" linear program; the original is referred to as the primal LP, and the equivalent as the dual. For each variable and each constraint in the primal there is a corresponding constraint and variable, respectively, in the dual. Thus, when the number of constraints is much larger than the number of variables in the primal, the dual has a much smaller basis matrix, and CPLEX may be able to solve it more efficiently. The primal and dual directives instruct CPLEX to set up the primal or the dual formulation, respectively. The dual-threshold directive makes a choice: the dual LP if the number of constraints exceeds the number of variables by more than the predefined margin, and the primal LP otherwise.

The simplex algorithm maintains a subset of basic variables (or, a basis) equal in size to the number of constraints. A basic solution is obtained by solving for the basic variables, when the remaining nonbasic variables are fixed at appropriate bounds. Each iteration of the algorithm picks a new basic variable from among the nonbasic ones, steps to a new basic solution, and drops some basic variable at a bound. The coefficients of the variables form a constraint matrix, and the coefficients of the basic variables form a nonsingular square submatrix called the basis matrix. During each iteration, the simplex algorithm must solve certain linear systems involving the basis matrix. For this purpose, CPLEX maintains a factorization of the basis matrix, which is updated during most iterations, and is occasionally recomputed. The sparsity of a matrix is the proportion of its elements that are not zero. The constraint matrix, basis matrix and factorization are said to be relatively sparse or dense according to their proportion of nonzeros. Most linear programs of practical interest have many zeros in all the relevant matrices, and the larger ones tend also to be the sparser. Refer to [53] and [54] for more information about these algorithms.

3.5.1.2 Mixed-integer programming

The mixed-integer optimization algorithm maintains a hierarchy of related linear programming subproblems, referred to as the search tree, which is usually visualized as branching downward:

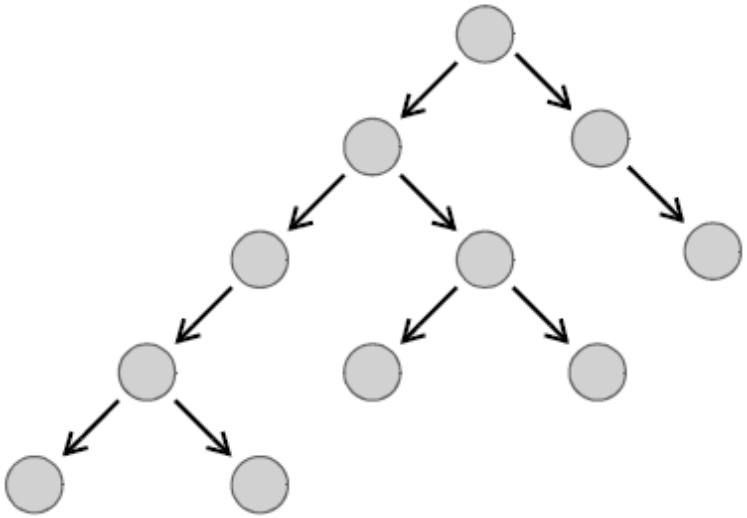

Fig. 3.9: CPLEX Mixed-Integer Algorithm: the Search Tree.

There is a subproblem at each node of the tree, and each node is explored by solving the associated subproblem. The algorithm starts with just a top (or root) node, whose associated subproblem is the relaxation of the integer program - the LP that results when all the integrality restrictions are dropped. If this relaxation happened to have an integer solution, then it would provide an optimal solution to the integer program. Normally, however, the optimum for the relaxation has some fractional-valued integer variables. Additional constraints, called cutting planes, are added to the subproblem. These cutting planes tighten the feasible region. Also, heuristic algorithms for finding integer solutions are applied, using the information from the solution of the subproblem. A fractional variable is then chosen for branching, and two new subproblems are generated, each with more restrictive bounds for the branching variable. For example, if the branching variable is binary (0 or 1), one subproblem will have the variable fixed at zero, the other node will have it fixed at one. In the search tree, the two new subproblems are represented by two new nodes connected to the root. Most likely, each of these subproblems also has fractional-valued integer variables, in which case the branching process must be repeated; successive branchings produce the tree structure shown above. If there are more than a few integer variables, the branching process has the potential to create more nodes than any computer can hold. There are two key circumstances, however, in which branching from a particular node can be discontinued:

- *The node's subproblem has no fractional-valued integer variables.* It thus provides a feasible solution to the original integer program. If this solution yields a better

objective value than any other feasible solution found so far, it becomes the incumbent, and is saved for future comparison.

- *The node's subproblem has no feasible solution, or has an optimum that is worse than a certain cut-off value.* Since any subproblems under this node would be more restricted, they would also be either infeasible or have an optimum value worse than the cut-off.

Thus, none of these subproblems need to be considered. In these cases the node is said to be fathomed. Because subproblems become more restricted with each branching, the likelihood of fathoming a node becomes greater as the algorithm gets deeper into the tree. So long as nodes are not created by branching much faster than they are inactivated by fathoming, the tree can be kept to a reasonable size. When no active nodes are left, CPLEX is finished, and it reports the final incumbent solution back to AMPL. If the cut-off value has been set throughout the algorithm to the objective value of the current incumbent CPLEX's default strategy, then the reported solution is declared optimal. Other cut-off options, described below, cannot provide a provably optimal solution, but may allow the algorithm to finish much faster. CPLEX's memory requirement for solving linear subproblems is about the same as its requirement for linear programs discussed in the previous chapter. In the branch & cut algorithm, however, each active node of the tree requires additional memory. The total memory that CPLEX needs to prove optimality for an integer program can thus be much larger and less predictable than for a linear program of comparable size. Because a single integer program generates many LP subproblems, even small instances can be very computationally intensive and require significant amounts of memory.

4 CASE STUDY

The methodology for the evaluation of various hydrogen-usage schemes developed in the thesis is applied to a test system, which is assumed to be located in Bruce County in Ontario, Canada. This location was chosen because of Bruce Power's NPP currently operating in the region, together with a growing wind capacity in the region, e.g., the Huron Wind's and Ripley wind farms.

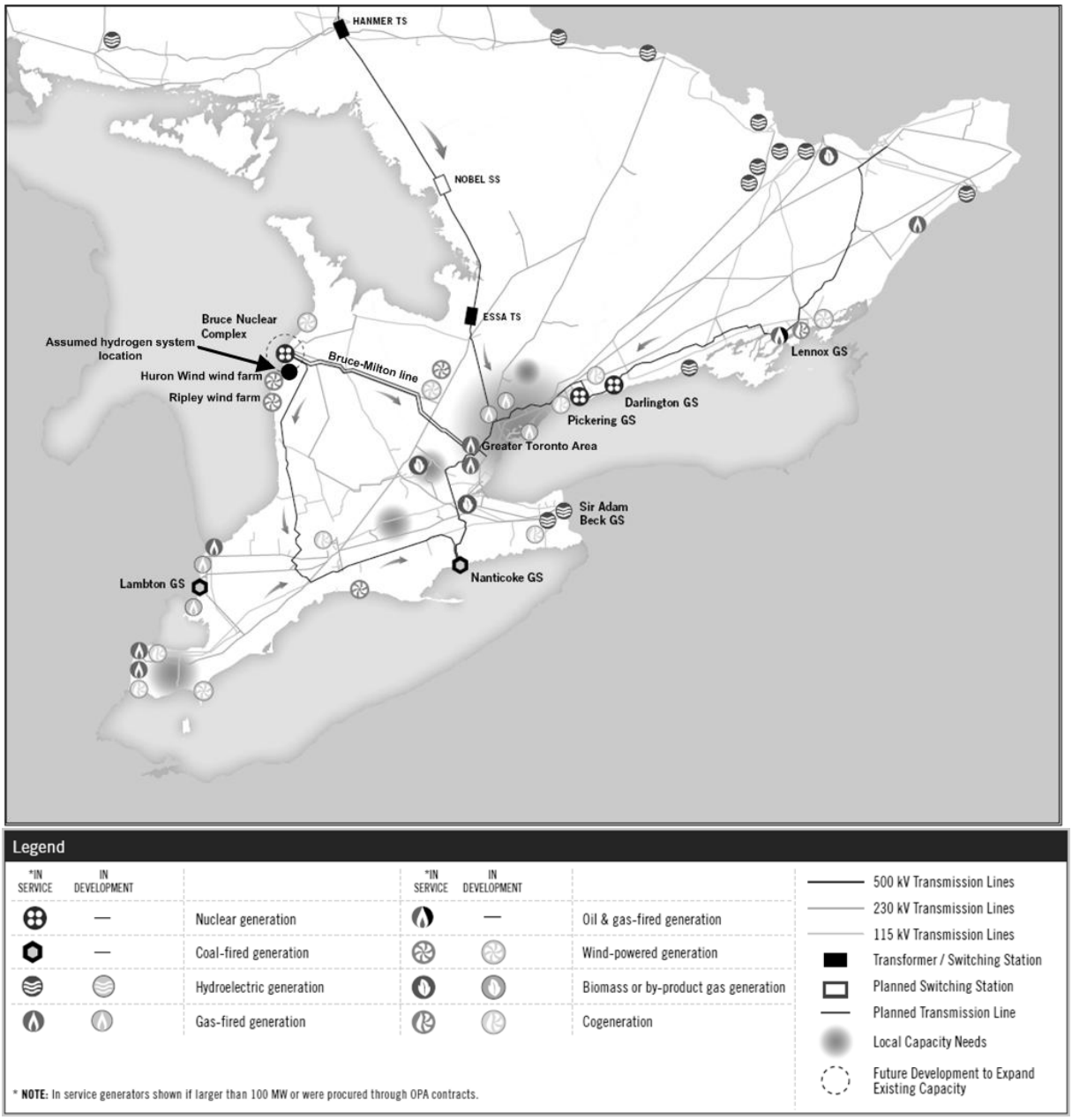

Fig. 4.1: Map of the southern Ontario power system with the location of the assumed wind-nuclear-hydrogen system [56].

4.1 Hydrogen-system location and transmission system description

The Ontario power system together with the location of the studied hydrogen system, wind farms and Bruce nuclear power plant is presented in the Fig. 4.1. Because the thesis utilizes a multiple-energy-carrier optimization, the concept of "energy hubs" is used, as proposed in [10] and [57]. An energy hub is an interface between energy loads (e.g., electricity, hydrogen, heat, compressed air) and primary energy sources and carriers (e.g., wind power, nuclear power, coal power), and can be studied as the comprehensive node of an integrated energy system with different inputs and outputs and various converters, such as transformers, micro-turbines, electrolyzers and fuel cells, and storage devices for gas, heat and hydrogen. In the thesis the energy hub will consist of nuclear and wind power as the primary energy sources and the electricity, hydrogen and heat as the transporting energy carriers. Oxygen, which is the byproduct of the water electrolysis, is also considered as goods that can be traded to a corresponding market.

4.1.1 Scenario with constant transmission system capacity

As one can see from the figure, the Bruce Station is connected to the Greater Toronto Area via a double 500 kV line and a 230 kV line with a total capacity of 5000 MW. This transmission system also connects the assumed hydrogen system located to the north and the Bruce power plant. These parameters are considered in all the hydrogen-usage scenarios, except the scenario considering use of hydrogen for transmission-congestion alleviation described in 4.10.

4.1.2 Scenario with variable transmission-system capacity

In the scenario described in chapter 4.10, the transmission capacity is assumed to be variable. Therefore, the IESO, Ontario's system operator, provided the Ontario's Flow Away from Bruce Complex (FABC) data, which are used as a measure of the power transferred out of the Bruce Power complex to the rest of the Ontario grid. The 2006 data set includes the hourly transmission system operating limits set by the IESO (Ontario's system operator), which are considered to be the network constraints $P_{MAX,i}^{NET}$ in this paper, and the actual power-transfer levels, which are assumed to correspond to the electricity production of the Bruce Power complex. To obtain the total production from the Bruce area, the Ripley wind-farm production levels were added to the actual power transfer obtained from the dataset. The hourly FABC line-capacity levels together with the sum of the hourly wind and nuclear power productions and the corresponding differences are depicted in Fig. 4.2.

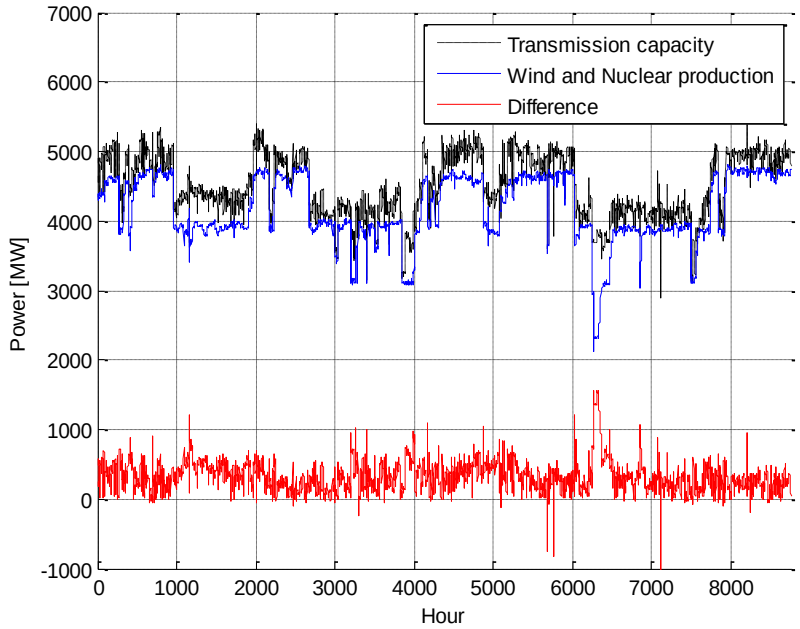

Fig. 4.2: Available transmission capacity from the Bruce region, sum of wind and nuclear power production and the difference.

Negative numbers represent the lack of transmission capacities. In these hours, the hydrogen system is utilized to consume the extra electricity that would otherwise be wasted; this electricity is thus assumed to be sold at zero price. The sum of the energy that cannot be transferred is 6529 MWh, and if we assume we can sell this energy at an average price of 46.38 CAD/MWh with additional oxygen and heat sales, the maximum additional profit of this scenario with respect to the profit obtained in scenario 5.2.1.3, adds up to around 220,000 CAD. The actual additional profits are expected to be lower since the hydrogen system is operated differently with line capacity constraints than the scenario without these constraints.

4.2 Electricity Market structure in Ontario, Canada

The model for optimal operation of the hydrogen system in this thesis was developed considering the rules of the Ontario electricity market [58]-[60]. The Ontario physical market is jointly optimized for energy and operating reserves, where three operating reserve classes are considered [58]:

- minute synchronized operating reserve (also called the 10 minute spinning or the 10S),
- minute non-synchronized operating reserve (also called the 10 minute non-spinning or the 10N),
- 30 minutes non-synchronized operating reserve (the 30R).

Only dispatchable generators are authorized to offer the 10S, while dispatchable generators, loads and boundary entities can participate in the market for the 10N and 30R operating reserves. The physical market is optimized to maximize the market's "Economic Gain",

which is conceptually the same as the social welfare and represents the difference between the value of the electricity produced and the costs of producing that electricity.

The market-optimization program, referred to as the Dispatch Scheduling and Pricing Software (DSPS), is used to calculate the pre-dispatch and real-time electricity prices and dispatch orders. It consists of a DC-based security-constrained optimal power flow block and an AC-power-flow-based contingency analysis tool. A separate AC power flow is run to calculate the transmission losses, which are incorporated into the power-balance requirements constraint using the appropriate penalty factors, and reactive power dispatch and voltage profiles.

The DSPS is run in two time-frames, i.e., the pre-dispatch and real-time (dispatch), and in two modes, i.e., the unconstrained and constrained. The pre-dispatch run is used to provide the market participants with the projected schedules and prices for advisory purposes in advance, while the final schedules and prices for financial settlement are determined in the real-time run. This timeline of the DSPS operation was the basis for the development of the pre-dispatch and real-time methodologies for hydrogen-system dispatch optimization in the thesis. In the unconstrained algorithm, the Economic Gain is optimized on the basis of supply and demand bids, but most of the physical power-system constraints are neglected, except for some of the operational constraints, such as the intertie energy trading limits and ramping constraints. In the constrained algorithm, however, the system security limits together with a representation of the Ontario transmission network model are considered.

According to the above-described market model and the rules described in [58]-[60], the following assumptions for the operations of the assumed hydrogen system are considered:

- The hydrogen-system operator is a price taker, i.e., he does not influence the market prices with his operations. This is a reasonable assumption, given the relatively small scale of the hydrogen facility.
- The electricity production and consumption bids from the hydrogen system are assumed to be the same as the minimum bid allowed at the Ontario electricity market, which is -2000 CAD/MWh. This ensures that the hydrogen system is always dispatched. The NPP production is added to the wind-power production, and the aggregated production is used as an input to the model.
- The NPP production is greater than the maximum electrolyzer demand; thus, there is always enough electricity to feed the electrolyzer.
- For real-time operation, the wind farm is considered as an intermittent generator according to [59]. Intermittent generators supply the Independent Electricity System Operator (IESO) with production forecasts, but are not obliged to actually deliver the forecasted power, and do not have to follow the IESO's dispatch instructions. These

types of generators may not register for the provision of any physical service, other than energy and reactive support and voltage control services.

- Qualifying large-scale wind-energy generation projects are also eligible for a Wind Power Production Incentive [61], which is basically a feed-in tariff to encourage potential wind-power investors. An initial incentive payment of 12 CAD/MWh of production, gradually declining to 8 CAD/MWh, is available for the first ten years of production.

4.2.1 Electricity price forecasts

A simple electricity-price forecasting model was developed, assuming a normal distribution of electricity-price forecasts around the actual electricity prices. Therefore, the price forecasts were generated by adding an error to the actual hourly Ontario electricity price (HOEP), using random numbers generated on the basis of a normal distribution with a mean value μ=0 CAD and a standard deviation σ=13.8 CAD; the maximum relative error is limited to 30% of the HOEP, which is chosen so that similar mean absolute errors (MAE) of the forecast models reported in [58] are obtained. The yearly HOEP for 2006 are used for this study; thus, the mean HOEP is 46.38 CAD/MWh [62]. A sample of four price forecasts generated with the above methodology with the corresponding real price is presented in Fig. 4.3.

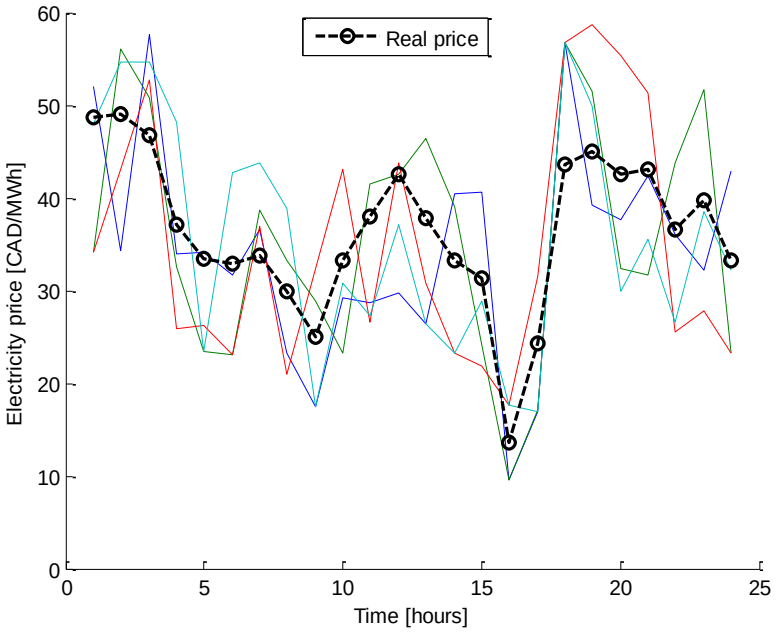

Fig. 4.3: Sample of electricity price forecasts including the real price.

As these prices are highly volatile compared to other markets [63], price developments in other markets will be investigated in the sensitivity analyses of the analysed scenarios of the use of hydrogen technologies. To represent the stochastic price behaviour in the thesis, 30 price scenarios are generated for each optimization period, which is considered to be 24 h with hourly resolution.

4.3 Assumed hydrogen-system parameters

This chapter offers a description of the technologies assumed for the case-study hydrogen system. This also includes the list of parameters needed by the model presented in Chapter 3.

4.3.1 Electrolyzers

The Hydrogenics Corporation Hystat-A Hydrogen plants are assumed for the electrolytic hydrogen production in the thesis [64]. The primary component of the HySTAT-A Generator Module is the IMET-1000 cell stack. The cell stack consists of circular electrolysis cells containing electrode pairs and an advanced alkaline inorganic ion-exchange type membrane. They use alkaline technology, where a variable hydrogen production from 25–100% capacity is possible, allowing for quick automatic response. The availability of this product is expected to be higher than 98%, according to the producer's data. Other detailed data are available in [64].

The hydrogen-storage system is dimensioned to have the same consumption capacity as the production capacity of the wind farm (76 MW); thus, the hydrogen production capacity amounts to 1424 kg/h and the oxygen production capacity of 7919.49 Nm^3/h. The corresponding technical and financial data are listed in Tab. 4.1. Since the prices are confidential, a price of 1437.45 CAD/kW (1370 USD/kW) is used here, chosen from the prices reported in [3] and [65], assuming a large-scale economy and medium-sized units. A hydrogen efficiency of 4.8 kWh/Nm^3 or 18.73 kg/MWh was considered according to [64]; this figure represents the amount of hydrogen produced by 1 MWh of electricity, and results in an efficiency of 62.5%, including rectifier and auxiliaries, and considering the energy value of 1 kg of hydrogen to be equal to 33.33 kWh [12]. The oxygen production efficiency is assumed to be 104.16 Nm^3/MWh.

Tab. 4.1: Hydrogen System Parameters.

PARAMETER	ELECTROLYZER	COMPRESSOR	STORAGE	FUEL CELL
Number	264	2	28	322
Price (CAD per module)	413,985	2'560,121	881,353	65,000
Lifetime (years)	10	20	20	20
Max. capacity	0.288 (MW/module)	1661 (kg/h per module-Hydrogen) 9250 (Nm^3/h per module Oxygen)	1240 (kg/module at 41.36MPa)	0.065 (MW/module)
Min. capacity (MW/module)	0.072	—	—	0.065
Hydrogen efficiency (kg/MWh)	18.73	449	—	68.09925
Oxygen efficiency (Nm^3/MWh)	104.16	2500	—	—
Thermal efficiency (kg/MWh)	—	—	—	76.92

4.3.2 Hydrogen compression

The compressor array in the thesis will be composed of Pressure Products Industries (PPI) 3-stage metal-diaphragm compressors. Generally, diaphragm compressors can be used for cylinder filling, hydrogen technology or the transfer of high-purity or dangerous gases under pressure without contamination or leakage [66]. A variety of head-closure designs, power-frames, accessories, and materials of construction are available to match a diaphragm compressor to process the parameter needs and the most appropriate design for the hydrogen

compression process is assumed in the thesis. The metal-diaphragm group of the diaphragm compressor isolates the process gas from the hydraulic fluid and all the lubricated parts to ensure purity. A design scheme of a diaphragm compressor is presented in Fig. 4.4.

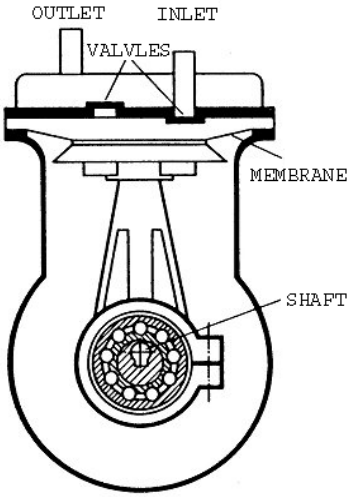

Fig. 4.4: The design scheme of a diaphragm compressor.

Detailed characteristics of the PPI Diaphragm Compressors can be found in [66]. A single 3700 kW compressor is chosen for the hydrogen compression of the maximum hydrogen production of 1424 kg/h to 410 bar, which is the storage pressure of the storage tanks. All the compressor parameters are listed in Tab. 4.1. The hydrogen-compression efficiency is assumed to be 449 kg/MWh (5 Nm^3/kWh), as in [9]; thus, the total capacity of the compressor is 1661 kg/h (18474 Nm^3/h) of hydrogen, costing 2'560,121 CAD (2'440,000 USD). The technical and financial parameters (except the efficiencies) are taken from [31].

Since the oxygen efficiency of the compressors used here is 2.5 Nm^3/kWh [9], the same 3700 kW compressor with a capacity of 9250 Nm^3/h is used to compress the maximum hourly electrolyzer oxygen production of 7919.49 Nm^3/h. An additional compressor for the oxygen compression is only considered in scenarios with the utilization of oxygen. Note that it is assumed here that all the hydrogen is compressed to the highest tank pressure, which is not realistic, since some of the hydrogen is actually compressed to a much lower pressure, depending on the current storage levels of the hydrogen tank at any given time. This variation in the amount of energy required to actually fill the tanks is a further refinement of this analysis for future work.

4.3.3 Hydrogen storage

CP Industries hydrogen-storage pressure vessels with the following characteristics are used in the thesis:

- dimensions: outside diameter: 610 mm, wall diameter 29.30 mm, length 6096 mm;
- maximum pressure: 27.6 MPa;
- water volume 1306 l;

- hydrogen capacity 23.3 kg H_2 at 24.8 MPa.

The auxiliary equipment that comes with the storage vessels consists of vessel CRN, O.D. neck threads, ultrasonic 5% inspection, 3/4" NGT outlet plugs, 6.89 MPa leak test and a coat of primer.

The hydrogen storage is dimensioned to be capable of storing 12 consecutive hours of hydrogen production, according to the assumption that the system's operation will be optimized in 24-hour time intervals and that peak price is reached in the afternoon. Thus, at least 17093 kg of hydrogen-storage capacity is needed. In total, 14 hydrogen-storage units mentioned in [31] were assumed in the thesis, with a capacity of 1240 kg of hydrogen each; this results in a total capacity of 17360 kg of hydrogen, with a price of 840,000 USD (881,353 CAD) per tank. The storage parameters are listed in Tab. 4.1. The oxygen storage, in the scenarios considering oxygen utilization, is assumed to be the same as the hydrogen storage, which means that 28 vessels are used for storing both hydrogen and oxygen.

4.3.4 Fuel cells

The stationery fuel-cell array is assumed to consist of Hydrogenics' HyPM 500 series power-module fuel cells, which use the Proton Exchange Membrane technology [67]. The fuel cells are assumed to be equipped with HyPM DC Power Solutions DC power conditioning, thus no extra power converters are needed for the AC/DC electricity transformation. The Fuel Cell Power Pack is assumed to be integrated with a small hydrogen buffer tank as well as with the thermal management and built-in diagnostics and controls.

According to the producer's data, the fuel-cell power pack is capable of a rapid dynamic response and a peak operating efficiency of 55%. Furthermore, unlimited start-stop cycles are assumed in the thesis, although the producer states a maximum of 6,000 turn-on/shut-down sequences and an accumulated operating lifetime of more than 1000 hours.

The producers provides for a wide range of fuel cells, with different installed peak powers, to be included in the power module. In the thesis only those of 65 kW peak power are assumed to be used in a scalable architecture, where the number of fuel cells depends on the size of the hydrogen system considered.

It is assumed that the Fuel cell ISX racks are integrated with outdoor hydrogen storage and indoor radiator connected with outdoor heat dissipation (chilled water or radiator) or with a district heating system, dependent on the studied scenario. The heat dissipation accounts for less than 15 kW of heat at full load with one module. The fuel needed is 99.99% dry gaseous hydrogen, which is assumed to be provided in a technically suitable form from the hydrogen-

storage vessels. The cold start-up time of the fuel cells is 20 seconds, according to the producer's data and is assumed to be zero in the thesis.

The stationary fuel-cell array was designed to have the same hydrogen-consumption capacity as is the hydrogen output from the electrolyzers. Hydrogenics HyPM 500 series proton-exchange-membrane (PEM) stationary fuel cells are assumed here, with the technical parameters taken from [67], except for the thermal efficiency, which was obtained from [9]. A moderate 1000 USD/kW price is assumed in this paper, based on [3], [65] and [68], due to the probable large-scale production of stationary fuel cells with the corresponding economies of scale in the next 20 years, and due to the large-scale application in the discussed system setup. The combined heat and power efficiency of the stationary fuel cell is 83%, according to the fuel-cell parameters listed in Tab. 4.1.

4.4 Assumed wind-power-plant parameters

The wind potential in the Bruce area is considerable, attracting many investors, and several wind projects were undertaken thus far. The Suncor's Ripley wind project is chosen for the thesis, since its location is close to the Bruce nuclear power plant. The location is important from the grid viewpoint since the energy hub is assumed to be both constraint and unconstrained, depending on the considered scenario.

The Ripley Wind Farm is the first power development in Ontario Canada from Suncor Energy Products Inc. and Acciona Energy. The wind-power project is located on the eastern shores of Lake Huron in Huron-Kinloss Township, approximately 220 kilometres west of Toronto. The Ripley wind-farm project consists of 38 Enercon E-82 2 MW wind turbines with a total installed capacity of 76 MW [69]. The Enercon E-82 wind turbine, with an advanced rotor blade design and tower versions up to 138m hub height, offers good performance in the 2 MW category. The rated power of the turbine is 2,000 kW, with a rotor diameter of 82 m and hub heights between 70 m and 138 m [70]. The concept of the turbine is gearless with a variable speed and pitch control. The rotor is of the upwind type with active pitch control and a clockwise direction of rotation. It uses 3 blades made of fiberglass with a total swept area of 5281 m^2. The blade-pitch system is used for the pitch control with one independent pitching system per rotor blade, also including the emergency supply. The rotational speed is variable, ranging between 6 and 19.5 rpm.

Yearly wind-speed data were obtained for the project of Suncor and Acciona from the town of Ripley with wind-speed measurements at 43 m, 50 m and 60 m. The latter measurements were taken as the assumed hub heights of this type of wind-power plants are typically between 70 m and 138 m. The Weibull distribution of the wind speeds for the mentioned area is given in Fig. 4.5.

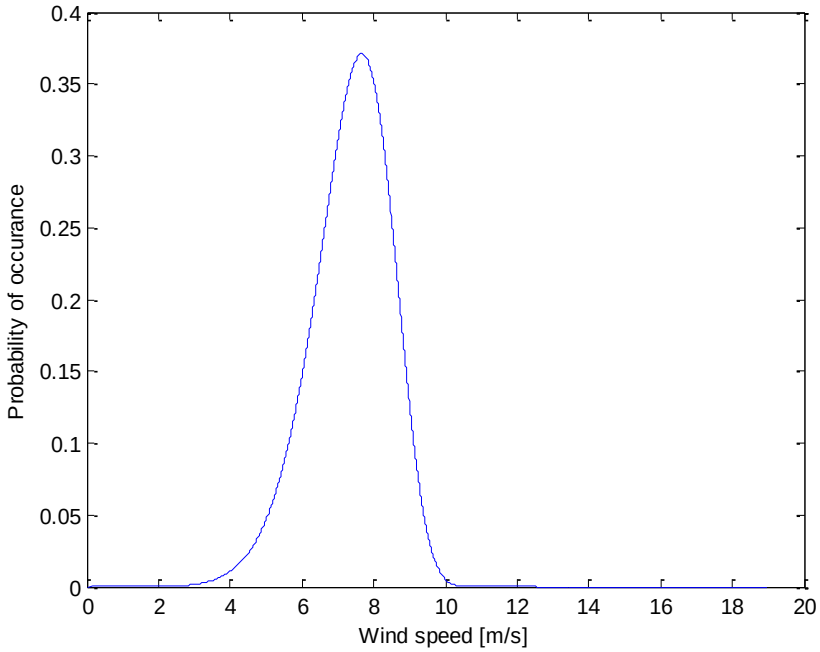

Fig. 4.5: The Weibull distribution of the 2006 wind speeds in the Ripley wind-farm area.

The Enercon E82 wind-turbine power curve was obtained using the data from the producer's manual [70], which were applied to equation (2.36) using a least-square curve-fitting process. The resulting power curve (in MW) for the Enercon E82 wind turbine is thus calculated using the following equation:

$$P_W = \begin{cases} \left(4.32 \cdot V_W + 1.87 \cdot {V_W}^2 - 0.31 \cdot {V_W}^3 - 0.03 \cdot {V_W}^4 - 0.01 \cdot {V_W}^5 - 0.01 \cdot {V_W}^6\right)/1000 \\ 2.05 \; if \; V_W \geq 13 \\ 0 \; if \; V_W \geq 28 \end{cases} \tag{4.1}$$

The graphical representation of the above equation with the corresponding rated and cut-out wind speeds is presented in Fig. 4.6.

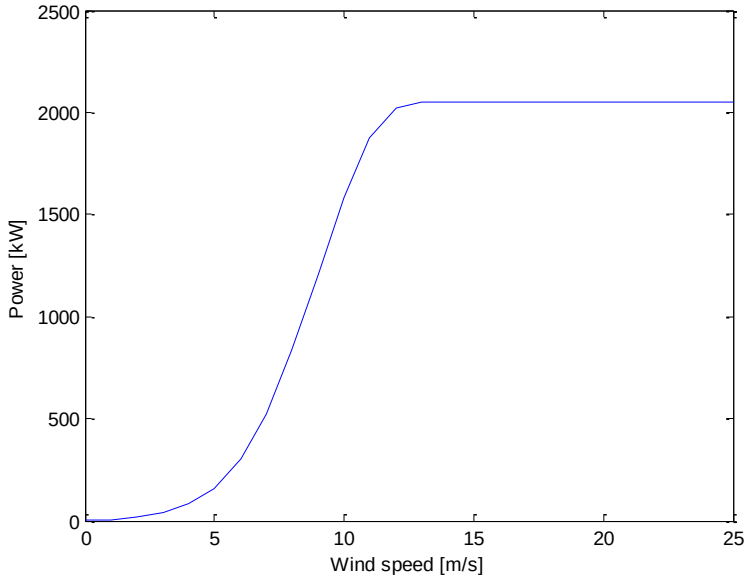

Fig. 4.6: The calculated Enercon E82 Power Curve.

Based on the 2006 wind speeds and the Power curve of the Enercon E82 Turbine we estimated the production of the Ripley wind farm for the year 2006. We assumed this production pattern to be constant throughout the analysed project's lifetime.

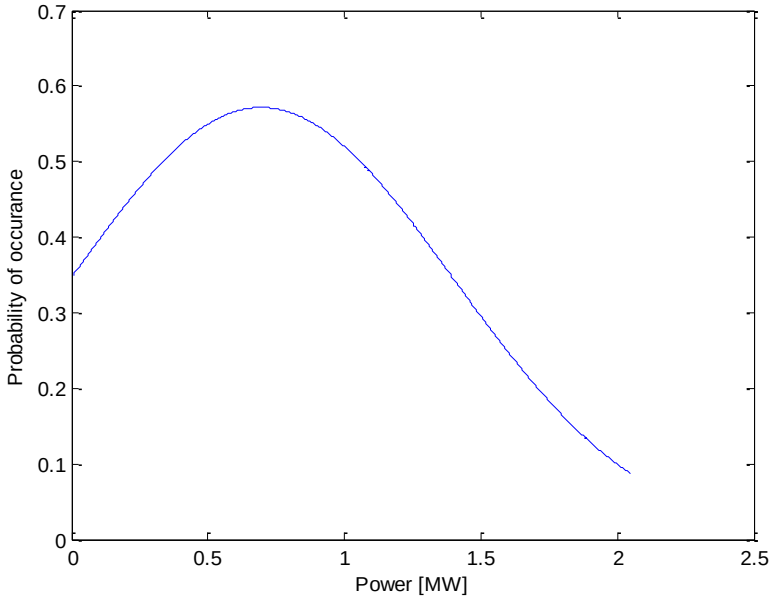

Fig. 4.7: The distribution of the 2006 power production of the Ripley wind farm.

From some initial studies, it was observed that the number of wind scenarios did not impact on the operation of the system, due to sufficient capacity of the Bruce-Milton line (5000 MW) and the fact that the energy production from Bruce Power's NPP is sufficient to run the electrolyzers; hence, only one wind scenario is considered here in the optimization procedure.

Even in the case of insufficient line capacity, wind forecasts will not impact the system profitability due to the observed low fuel-cell utilization. This assumption is further justified on the basis of the results presented and discussed in Chapter 5.

4.5 Assumed nuclear-power-plant parameters

Bruce Power is Canada's first privately owned nuclear generating company, and the source of more than 20% of Ontario's electricity [71]. It is located approximately 250 km northwest of Toronto and currently operates six reactors, with an installed capacity of 4820 MW. In May 2001, Bruce Power became the licensed operator of the Bruce A and Bruce B nuclear generating stations, acquiring the sites from the defunct Ontario Hydro. Both Bruce A and Bruce B are equipped with eight CANDU nuclear reactors (four in each building). The initial four reactors were commissioned at Bruce A between 1977 and 1979, while the Bruce B reactors were added between 1984 and 1987. Six of those units are currently operational and combined they produce more than 4,700 megawatts of electricity. Bruce Power is also in the process of restarting the remaining two units at Bruce A, which will provide another 1,500 megawatts of emission-free electricity in 2010-2011. This expansion is not considered to impact on the operation and revenues of the hydrogen system in the scenarios described in Chapters 4.7 and 4.9 due to probable transmission-line expansions; however, the issue of transmission congestion is considered in the scenarios described in Chapters 4.9 and 4.10.

Because Bruce Power is privately owned, the actual production profile and income data are confidential. In 2004, Bruce Power produced 33.6 TWh of electricity [71], which gives them a capacity factor of 82%, equal to 3952.4 MW of constant electricity production. It is assumed that 3000 MW of constant electricity is sold to the IESO on a bilateral contract, and the remaining 952.4 MW capacity is bid into the electricity market or may be converted to hydrogen.

In scenario described in chapter 4.9, where hydrogen storage is considered as an alternative to the transmission expansion, the line capacity is assumed to remain unchanged. The refurbished Bruce power plant, on the other hand, is foreseen to increase its capacity by 1500 MWh, resulting in a total capacity of 6320 MW. Any other potential generation developments in the area are not considered. With the same capacity factor used in the base case scenario, this capacity expansion would result in 5207 MW of constant electricity production by the NPP. This results in a permanent production overflow of 207 MW, which have to be either shed or converted to hydrogen and sold to the hydrogen market.

4.6 Assumed economic parameters

Any investment or O&M costs associated with wind and nuclear units are disregarded in the economic analysis, since these units are already operational, regardless of whether the hydrogen-storage option is considered. All location-specific parameters are considered to be

those for Ontario; thus, the chosen currency is Canadian dollars (CAD), which is converted from US dollars (USD) at a rate of 1 USD per 1.04923 CAD. The profit calculation is carried out for one year, which is then used in the economic evaluations. The project's lifetime is assumed to be 22 years, where the first year is the construction year without any profit gains and the last year is the deconstruction year, with revenues obtained from the salvage value of the assets sold after the project's end.

In the thesis, the financial support from the government in the form of a standard offer program, which is mainly applied for wind projects, is assumed for the hydrogen projects [61]. The standard offer program offers governmental guaranties for loans that are taken for project financing. Thus the interest rate for the loan for the project is assumed to be 7.5%, which is lower than the standard rates ranging typically between 8% and 9% in the year 2008, according to an energy-investments expert. It is further assumed that governmental guaranties enable the project to be financed with 75% of the total investment costs in debt, which happens both in the project's initial year as well as in other years, when part of the equipment needs to be replaced/refurbished. The profits are calculated for one operational year of the hydrogen subsystem and are then assumed to be constant for the whole lifetime of the project. Straight-line amortization is considered throughout the thesis. As the negative cash flows in the MIRR calculation are assumed to be solely equity, the finance rate is assumed to be equal to the discount rate. The discount rate used in the calculations of the NPV and as a threshold for the evaluation of the IRR and MIRR is assumed to be 8%, as per typical values ranging from 5% to 10% [72]. The corporate tax rate levied by Canada on the corporate profits for 2009 is assumed to be 33% [73]. A provincial tax incentive is assumed, because of the production of hydrogen from RES; thus the lower 16.5% tax rate that is used for small business is chosen [61]. The uniformed salvage value of the equipment at the end of its lifetime is assumed to be 10% of the investment costs [32]. The operation and maintenance costs are assumed to be 2% per year of initial investment [32].

4.6.1 Hydrogen, Oxygen and Heat market prices

The hydrogen selling price is taken as the bulk hydrogen price produced from natural gas in 2020 [68]. The bulk pre-tax price of hydrogen for different natural-gas prices is reported in [74], where at the expected price for gas in 2020, the hydrogen production price is assumed to be 2.74 USD/kg. With carbon and sales taxes included [68], the selling wholesale hydrogen price becomes 4.35 CAD/kg, which is a conservative price, since it only covers the production costs. Note that, since 1 kg of hydrogen yields about the same energy as 1 gallon (3.8 l) of gasoline [12], a car running on a 50%-efficiency fuel cell would cost less to operate (0.035 CAD/km) then a 20%-efficiency combustion engine (0.072 CAD/km), assuming a gasoline price of 0.95 CAD/l (3.44 USD/gal) and fuel consumption of 13.2 km/l (27 mpg) [16]. The hydrogen price is assumed to remain constant without any elasticity if an increase in supply occurs. This can be assumed for small-scale hydrogen-production stations or considering an

increase in demand for hydrogen due to the development of the hydrogen economy resulting in a higher hydrogen demand.

The volumetric price of oxygen is assumed to be 0.15 CAD/Nm^3 (0.11 CAD/kg for an oxygen density of 1.429 kg/Nm^3), based on information provided by oxygen producers. This price includes compression and piping to the end consumer, assuming constant demand with maximum fluctuations of 10% in the average yearly demand. Since this process will generate a large amount of oxygen, the oxygen is assumed here to be utilized as a waste dissolvent, or potentially for the oxy-fuel combustion process or some other industrial applications.

The heat price is assumed to be equal to the gas-heating price without the distribution, storage and dispensing costs. Thus, the price of gas was 8.77 CAD/MBtu (29.93 CAD/MWh) in the Waterloo region as of August 2007; if a 90% heat-utilization efficiency from the gas is assumed, heat prices would be 33.24 CAD/MWh. The temperature of the water from the PEM stationary fuel cells is assumed to be high enough for district water heating.

All the mentioned prices are assumed to be time-independent, in contrast to the electricity prices, which are assumed to change from hour to hour. This assumption is reasonable, taking into account constant-price contracts for all three commodities suggested by experts in energy markets.

4.7 Basic scenario: use of hydrogen as an electricity-storage medium

The purpose of this scenario of hydrogen usage is to assess whether it is feasible to invest in a hydrogen-storage system for storing electricity and using the price differences in a intraday spot electricity market in Ontario. No line congestions are assumed in this scenario and neither is the utilization of by-products such as oxygen and heat. Two different scenarios are studied:

1. Scenario without the option of selling hydrogen directly to the hydrogen market
2. Scenario with the option of selling hydrogen directly to the hydrogen market

4.7.1 Scenario without the option of selling hydrogen to the hydrogen market

Firstly, the scenario without the option of sales of the produced hydrogen directly to the hydrogen market is studied. The proposed system consists of a nuclear power plant (NPP) and a wind farm selling electricity to the Ontario electricity market, which is a realistic scenario being currently faced by the Bruce Power company and Ripley wind farm. The system includes hydrogen-storage and distribution facilities according to the model depicted in Fig. 3.1. The pre-dispatch, real-time dispatch, revenue calculation and economic evaluation models (3.1)-(3.8), (3.9)-(3.17), (3.18)-(3.19) and (3.20)-(3.39), respectively, are used for the economic evaluation of this scenario.

4.7.2 Scenario with the option of sales of hydrogen to the hydrogen market

In the previous scenario only profits from market-price fluctuations were considered for the hydrogen system to become economically feasible. In this chapter, however, additional profits that can be made from direct hydrogen sales to a prospective hydrogen market (e.g., fuel-cell electricity market, mobility market, industrial market) are also foreseen to improve the economics of the hydrogen system. The scheme of the analyzed hydrogen system with the option of hydrogen sales to the hydrogen market is depicted in Fig. 4.8.

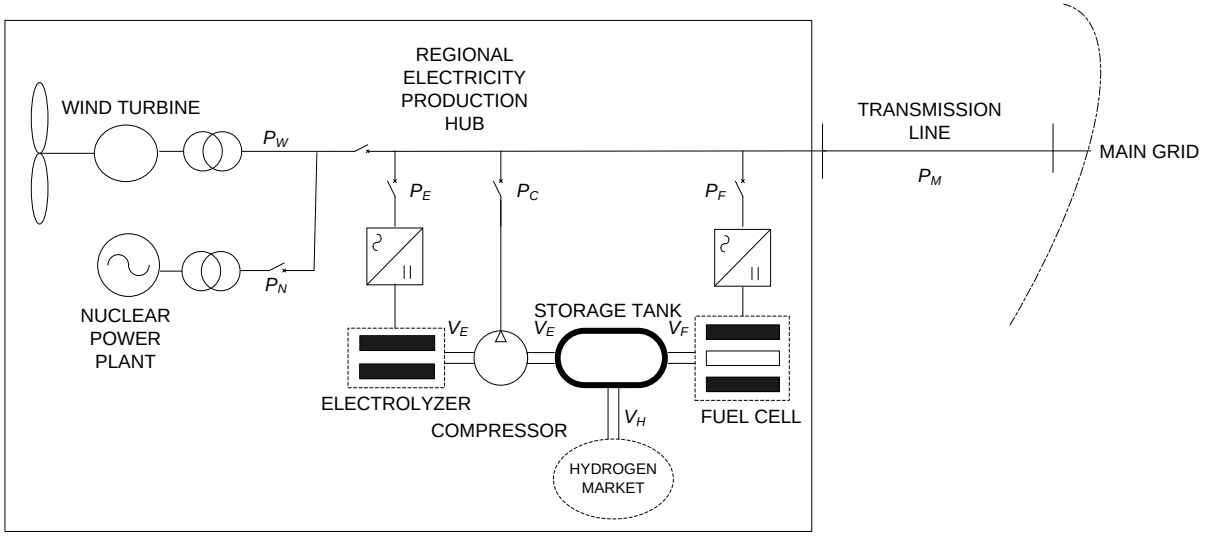

Fig. 4.8: Structure of a "regional energy hub" including hydrogen for energy storage and as an energy carrier. The notation used is detailed in Chapter IV .

In the above figure, P_M corresponds to the electricity exchange with the power market.

4.7.2.1 Pre-dispatch

The system operation and market bidding for the system depicted in Fig. 4.8 was developed on the basis of the pre-dispatch, real-time dispatch, revenue calculation and economic evaluation models described in Chapters 3.1-3.4. However, the models have to be modified to allow for hydrogen sales. Thus, in the pre-dispatch model (3.1)-(3.8), the objective function (3.1) is modified to account for hydrogen sales as follows:

$$\max \quad \sum_{w=1}^{Nw} p_w \cdot \sum_{p=1}^{Np} p_s \cdot \sum_{i=1}^{T} c_{p,i}^{M} (P_{w,p,i}^{G} + P_{w,p,i}^{DIS} - P_{w,p,i}^{CH}) + c^{H} V_{w,p,i}^{H} \tag{4.2}$$

Where $V_{w,p,i}^{H}$ depicts the hydrogen sales in the wind-production forecast scenario *i*, price forecast scenario *p* in hour *i*. Additionally, the hydrogen-storage balance in equation (3.4) is influenced by hydrogen sales to the hydrogen market according to the following equation:

$$V_i^{STG} = V_{i-1}^{STG} + \frac{\mu_{he} \cdot \mu_{hc}}{\mu_{he} + \mu_{hc}} \cdot P_{w,p,i}^{CH} - \mu_{ef} P_{w,p,i}^{DIS} - V_{w,p,i}^{H} \tag{4.3}$$

4.7.2.2 Real-time Dispatch

Like with the pre-dispatch model, the objective function and the hydrogen-storage balance functions are changed from equations (3.9) and (3.12), respectively, to equations (4.4) and (4.5).

$$\max \quad (\hat{c}_i^M (\hat{P}_i^G + \hat{P}_i^{DIS} - \hat{P}_i^{CH}) + c^H \hat{V}_i^H) \tag{4.4}$$

$$\hat{V}_i^{STG} = \hat{V}_{i-1}^{STG} + \frac{\mu_{hc} \cdot \mu_{he}}{\mu_{hc} + \mu_{he}} \cdot \hat{P}_i^{CH} - \mu_{ef} \hat{P}_w^{DIS} - \hat{V}_i^H \tag{4.5}$$

4.7.2.3 Economic evaluation

In the profit calculation, the additional profits from the hydrogen calculation have to be considered. Thus, equation (3.18) has to be substituted with the following equation:

$$\hat{R}_i = (\hat{c}_i^M (\hat{P}_i^G + \hat{P}_i^{DIS} - \hat{P}_i^{CH}) + c^H \hat{V}_i^H) \tag{4.6}$$

4.8 Scenario with the utilization of oxygen and heat

In this scenario, the feasibility of the hydrogen system studied in Chapter 4.7 is analyzed, also considering the sales of oxygen, which is the byproduct of electrolysis, and heat, the byproduct of the electricity generation in fuel cells. According to this, the hydrogen system is expected to become more profitable and thus more interesting for potential investment decisions. The expected revenue sources are as follows:

- the use of price differences in a intraday spot electricity market in Ontario;
- the additional profits made by the sales of byproducts (oxygen and heat);

No line congestions are assumed in this chapter. As in the previous chapter, the following two scenarios are investigated:

1. scenario without the option of hydrogen sales to the hydrogen market;
2. scenario with the option of hydrogen sales to the hydrogen market

4.8.1 Scenario without the option of hydrogen sales to the hydrogen market

The hydrogen system without the option of hydrogen sales directly to the hydrogen market is studied first. The system is properly defined in 4.7.1 and modified here to also encompass the possible oxygen and heat sales, as depicted in Fig. 4.9.

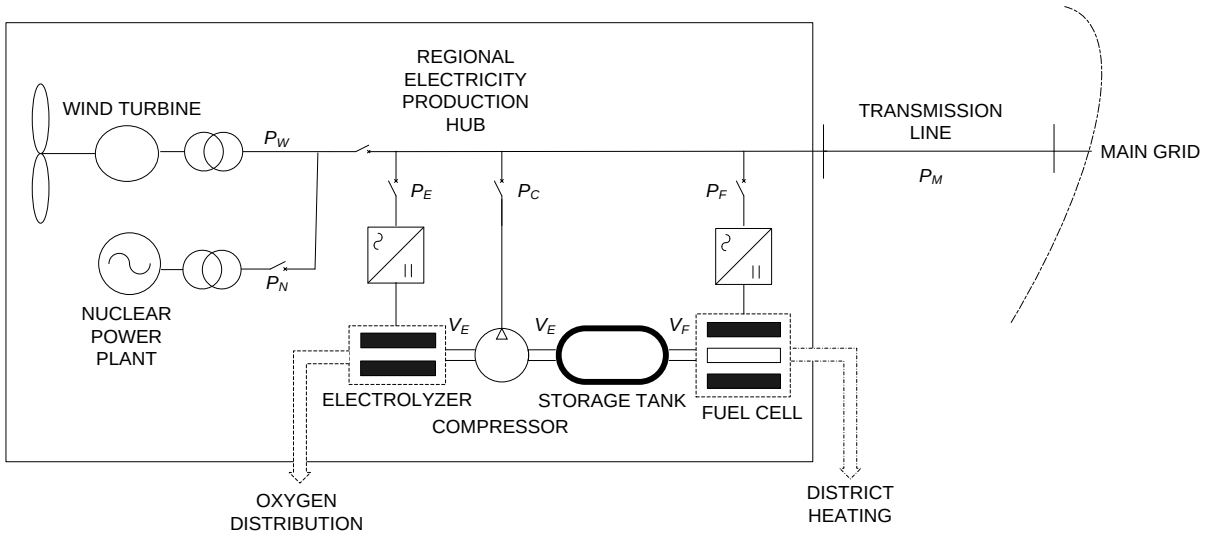

Fig. 4.9: Structure of a "regional energy hub" including hydrogen as an energy storage and an energy carrier with the option of oxygen and heat sales.

According to the above structure of the hydrogen system, an additional compressor is used for the oxygen compressor and additional storage tanks are used for the oxygen storage. The oxygen and heat consideration also reflects in a modification to the operational optimization procedures.

4.8.1.1 Pre-dispatch

To optimize the one-day-ahead operation of the system, the model (3.1)-(3.8) has to be modified to include the oxygen and heat sales. Thus, the following objective function, based on (3.1), is used:

$$\max \quad \sum_{w=1}^{Nw} p_w \cdot \sum_{p=1}^{Np} p_s \cdot \sum_{i=1}^{T} (c_{p,i}^{M} (P_{w,p,i}^{G} + P_{w,p,i}^{DIS} - P_{w,p,i}^{CH}) + c^{O} V_{w,p,i}^{OSELL} + c^{HEAT} P_{w,p,i}^{HEATSELL}) \tag{4.7}$$

Here, c^{O} is the oxygen selling price, $V_{w,p,i}^{OSELL}$ is the oxygen production in wind scenario *w*, price scenario *p* in hour *i*, c^{HEAT} is the heat selling price and $P_{w,p,i}^{HEATSELL}$ is the heat sold in wind scenario *w*, price scenario *p* in hour *i*. The hydrogen-storage level equation (3.4) has to be modified to also consider the compressor losses for the oxygen compression:

$$V_i^{STG} = V_{i-1}^{STG} + \mu_{he} \cdot \frac{1}{\left(1 + \frac{\mu_{oe}}{\mu_{oc}} + \frac{\mu_{he}}{\mu_{hc}}\right)} \cdot P_{w,p,i}^{CH} - \mu_{ef} P_{w,p,i}^{DIS} \tag{4.8}$$

where μ_{oe} and μ_{oc} are the oxygen-production and oxygen-compression efficiencies. The oxygen-compression losses have to be considered in the maximum and minimum electrolyzer powers from equation (3.7) as well:

$$\beta_{w,p,i} \cdot \left(1+\frac{\mu_{oe}}{\mu_{oc}}+\frac{\mu_{he}}{\mu_{hc}}\right) \cdot P_{\min}^{CH} \le P_{w,p,i}^{CH} \le \beta_{w,p,i} \cdot \left(1+\frac{\mu_{oe}}{\mu_{oc}}+\frac{\mu_{he}}{\mu_{hc}}\right) \cdot P_{\max}^{CH} \tag{4.9}$$

Since the profits from the oxygen and heat sales are expected to considerably improve the economics of the hydrogen system, they are calculated by (4.10) and (4.11), respectively.

$$V_{w,p,i}^{O} = \mu_{oe} \cdot \frac{1}{\left(1+\frac{\mu_{oe}}{\mu_{oc}}+\frac{\mu_{he}}{\mu_{hc}}\right)} \cdot P_{w,p,i}^{CH} \tag{4.10}$$

$$P_{w,p,i}^{HEAT} = \frac{\mu_{ef}}{\mu_{hf}} \cdot P_{w,p,i}^{DIS} \tag{4.11}$$

where $V_{w,p,i}^{O}$ and $P_{w,p,i}^{HEAT}$ are the oxygen and heat productions in wind scenario *w*, price scenario *p* in hour *i*. Equations (4.10) and (4.11) are based on (2.21) and (2.32), respectively.

4.8.1.2 Real-time dispatch

This chapter presents the real-time version of the pre-dispatch model, which follows the scheduled hydrogen storage obtained from the solution of the MISLP problem described in 4.8.1.1. As in the pre-dispatch model, the objective function from equation (3.9) is modified to consider oxygen and heat sales as follows:

$$\max \quad (\hat{c}_i^M (\hat{P}_i^G + \hat{P}_i^{DIS} - \hat{P}_i^{CH}) + c^O \hat{V}_i^O + c^{HEAT} \hat{P}_i^{HEAT}) \tag{4.12}$$

In the above equation, $\hat{V}_i^O$ represents the actual oxygen production and $\hat{P}_i^{HEAT}$ depicts the actual heat production of the hydrogen system in the hour *i*. The oxygen-compressor efficiency is added to equation (3.12) resulting in the following equation for the calculation of the hydrogen-storage state of charge:

$$\hat{V}_i^{STG} = \hat{V}_{i-1}^{STG} + \mu_{he} \cdot \frac{1}{\left(1+\frac{\mu_{oe}}{\mu_{oc}}+\frac{\mu_{he}}{\mu_{hc}}\right)} \cdot \hat{P}_i^{CH} - \mu_{ef} \hat{P}_w^{DIS} \tag{4.13}$$

The oxygen-compression efficiency also has to be considered in equation (3.15), which limits the electrolyzer's operational range. The resulting equation is presented here:

$$\hat{\beta}_i \cdot \left(1+\frac{\mu_{oe}}{\mu_{oc}}+\frac{\mu_{he}}{\mu_{hc}}\right) \cdot P_{\min}^{CH} \le \hat{P}_i^{CH} \le \hat{\beta}_i \cdot \left(1+\frac{\mu_{oe}}{\mu_{oc}}+\frac{\mu_{he}}{\mu_{hc}}\right) \cdot P_{\max}^{CH} \tag{4.14}$$

As in the pre-dispatch procedure, equations (4.15) and (4.16) are added to calculate the actual profits from the oxygen and heat sales, respectively.

$$\hat{V}_i^O = \mu_{oe} \cdot \frac{1}{\left(1 + \frac{\mu_{oe}}{\mu_{oc}} + \frac{\mu_{he}}{\mu_{hc}}\right)} \cdot \hat{P}_i^{CH} \tag{4.15}$$

$$\hat{P}_i^{HEAT} = \frac{\mu_{ef}}{\mu_{hf}} \hat{P}_i^{DIS} \tag{4.16}$$

In the above equations, $\hat{V}_i^O$ is referred to as the actual oxygen production in hour *i* and $\hat{P}_i^{HEAT}$ as the actual heat production in hour *i*.

4.8.1.3 Economic Evaluation

The income with the hydrogen system, which is calculated in (3.18), in this scenario should be modified to consider oxygen and heat sales as follows:

$$\hat{R}_i = (\hat{c}_i^M (\hat{P}_i^G + \hat{P}_i^{DIS} - \hat{P}_i^{CH}) + c^O \hat{V}_i^O + c^{HEAT} P_{w,p,i}^{HEAT}) \tag{4.17}$$

The income without the hydrogen-storage system is calculated using equation (3.19). Based on these profits, the methodology described in 3.4 is applied to calculate the economic indices.

4.8.2 Scenario with the option of hydrogen sales to the hydrogen market

Chapter 4.8 has so far only considered the profits obtained from market-price fluctuations considering also heat and oxygen sales. This chapter extends this assumption, also considering possible additional profits that can be made from direct hydrogen sales to a prospective hydrogen market that would improve the economics of the hydrogen system. The scheme of the proposed system is depicted in Fig. 4.10.

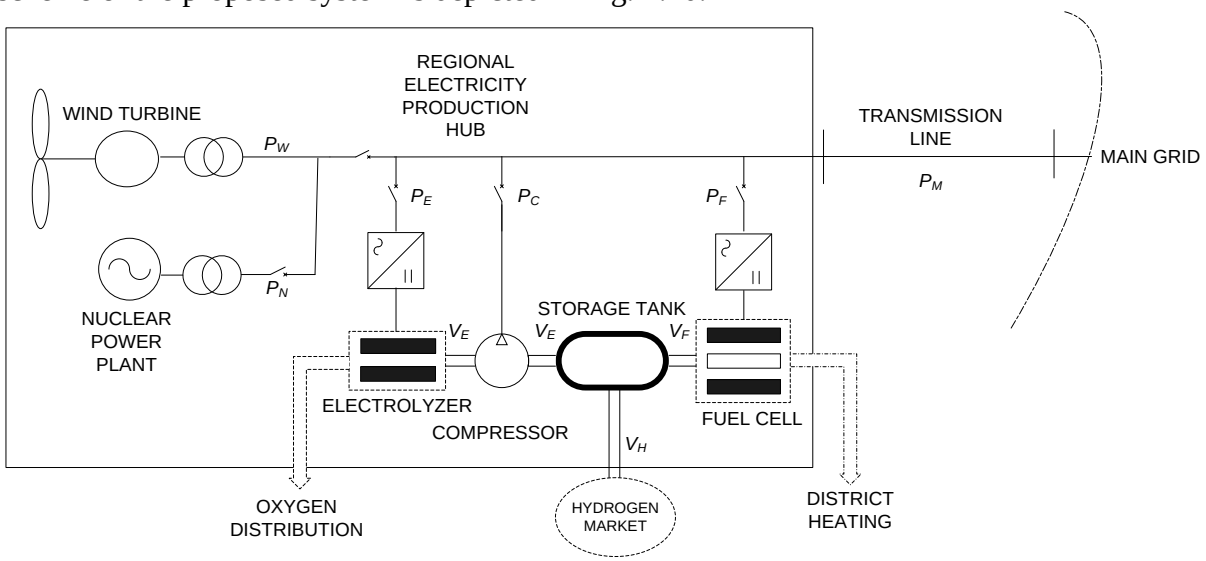

Fig. 4.10: Structure of a "regional energy hub" including hydrogen as energy storage and as an energy carrier and oxygen and heat sales.

The economic evaluation procedure used in this chapter is depicted in Fig. 3.2 and properly described in 4.7.1.

4.8.2.1 Pre-dispatch

The optimization model for obtaining the one-day-ahead dispatch levels is a combination of the models presented in Chapters 4.7.2.1 and 4.8.1.1. Thus, the objective function (4.7) is expanded to also consider the hydrogen sales as follows:

$$\max \quad \sum_{w=1}^{Nw} p_w \cdot \sum_{p=1}^{Np} p_s \cdot \sum_{i=1}^{T} (c_{p,i}^{M}(P_{w,p,i}^{G} + P_{w,p,i}^{DIS} - P_{w,p,i}^{CH}) + c^{H} V_{w,p,i}^{H} + c^{O} V_{w,p,i}^{O} + c^{HEAT} P_{w,p,i}^{HEAT}) \qquad (4.18)$$

The hydrogen-storage charge level function is also modified to consider hydrogen sales as shown in equation (4.8).

$$V_i^{STG} = V_{i-1}^{STG} + \mu_{he} \cdot \frac{1}{\left(1 + \frac{\mu_{oe}}{\mu_{oc}} + \frac{\mu_{he}}{\mu_{hc}}\right)} \cdot P_{w,p,i}^{CH} - \mu_{ef} P_{w,p,i}^{DIS} - V_{w,p,i}^{H} \qquad (4.19)$$

4.8.2.2 Real-time dispatch

The objective and hydrogen-storage level functions (4.12) and (4.13) from the previous scenario in Chapter 4.8.1.2 are modified to consider hydrogen sales to the hydrogen market as in equations (4.20) and (4.21), respectively.

$$\max \quad (\hat{c}_i^{M}(\hat{P}_i^{G} + \hat{P}_i^{DIS} - \hat{P}_i^{CH}) + \hat{c}^{H} \hat{V}_i^{H} + c^{O} \hat{V}_i^{O} + c^{HEAT} \hat{P}_i^{HEAT}) \qquad (4.20)$$

$$\hat{V}_i^{STG} = \hat{V}_{i-1}^{STG} + \mu_{he} \cdot \frac{1}{\left(1 + \frac{\mu_{oe}}{\mu_{oc}} + \frac{\mu_{he}}{\mu_{hc}}\right)} \cdot \hat{P}_i^{CH} - \mu_{ef} \hat{P}_w^{DIS} - \hat{V}_i^{H} \qquad (4.21)$$

4.8.2.3 Economic Analysis

The economic evaluation model used in this chapter is similar to the one described in Chapter 4.8.1.3 with an additional consideration of hydrogen sales:

$$\hat{R}_i = (\hat{c}_i^{M}(\hat{P}_i^{G} + \hat{P}_i^{DIS} - \hat{P}_i^{CH}) + c^{O} \hat{V}_i^{O} + c^{HEAT} P_{w,p,i}^{HEAT} + c^{H} \hat{V}_i^{H}) \qquad (4.22)$$

4.9 Hydrogen storage as an alternative to transmission expansion

In addition to the scenarios in Chapters 4.7 and 4.8, where no transmission network restrictions were considered, a scenario studying a hydrogen system's economic performance by permanent limited transmission system capacity is presented here. This scenario addresses realistic possible delays in the planned transmission expansion in the Bruce area, which would not follow-up the planned new generation capacities [55] and thus result in permanent transmission system congestions. Therefore, the possibility that the energy produced by Bruce

Power and wind generators is not going to be entirely transferable to end-users is investigated. This niche application scenario considers that the generation capacities are already available; thus, no additional investment costs are considered in the economic analysis model. Assuming that the investor in the hydrogen system is the owner of the local electricity generation facilities, one can observe that the cost for the electricity, which would otherwise be shed, is zero. The scheme of the scenario studied in this chapter is depicted in Fig. 4.11.

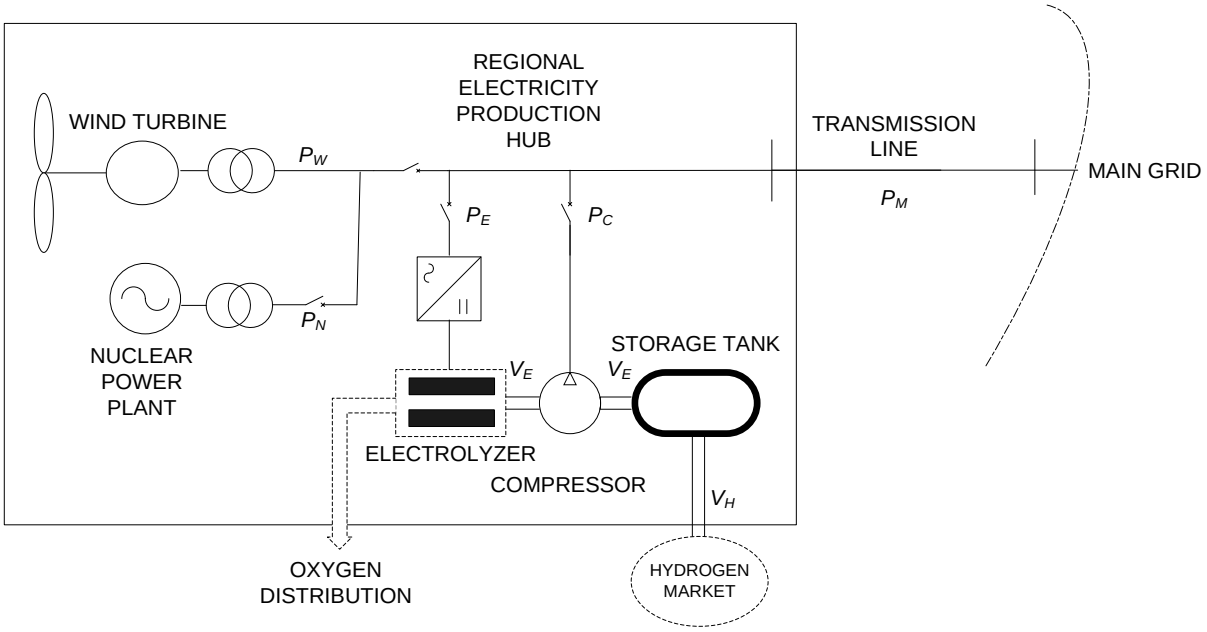

Fig. 4.11: Structure of a "regional energy hub" including hydrogen as energy storage for the hydrogen as an alternative to a transmission expansion scenario.

4.9.1 Operation modelling

For this scenario, a simple methodology for pre-dispatch and dispatch optimization of the hydrogen system can be used, since hydrogen is always sold to the market at a constant price without any consideration of fuel cells. This can be done by a modification of the equations in the pre-dispatch and real time models presented so far, or simply by setting either the price of the hydrogen and the electricity selling price to zero or setting both fuel-cell efficiencies to zero. The latter is proposed in the thesis without the need to change the models in Chapter 4.8.2. Thus, the parameters μ_{ef} and μ_{hf} were set to zero in this scenario.

4.10 Hydrogen storage for transmission-congestion alleviation

In Chapter 4.9, a permanent transmission system congestion was assumed, which means that new capacities, either as hydrogen or electricity, are needed to transfer the produced energy to the load centres. In this chapter, on the other hand, a scenario with a periodically congested transmission system is studied. Thus, a transmission system capacity forecast is added to the hydrogen-system optimization model to maximize the profits considering intermittent transmission system congestions. The overall scheme of the energy-production hub with

wind, nuclear and hydrogen facilities remains the same as in Chapter 4.8.1; thus it is depicted in Fig. 4.9.

4.10.1 Scenario without the option of hydrogen sales

As in the previous scenarios of hydrogen use, the hydrogen system is evaluated separately with and without the option of hydrogen sales directly to the market. In this chapter the latter option is considered.

4.10.1.1 Pre-dispatch

This scenario is generally similar to the one presented in Chapter 4.8.1.1. To optimize the one-day-ahead operation of the system, however, the following network-capacity constraint is used instead of the one described by equation (3.2):

$$-P_{\max,i}^{NET} \le P_{w,p,i}^{G} + P_{w,p,i}^{DIS} - P_{w,p,i}^{CH} \le P_{\max,i}^{NET} \tag{4.23}$$

where $P_{\max,i}^{NET}$ is the forecasted network capacity in the Bruce region in hour *i*; in contrast to $P_{\max}^{NET}$, which describes the constant network capacity.

4.10.1.2 Real-time dispatch

Like with the pre-dispatch methodology, the real-time model has to be adapted to consider variable transmission system capacity levels. Thus, the model presented in 4.8.1.2 is modified with the following equation:

$$-P_{\max,i}^{NET} \le \hat{P}_{i}^{G} + \hat{P}_{w}^{DIS} - \hat{P}_{i}^{CH} \le P_{\max,i}^{NET} \tag{4.24}$$

Observe that equation (4.24) is modified equation (3.10).

4.10.1.3 Economic Evaluation

The income or profit obtained from the hydrogen-storage system can be calculated using the methodology described in 4.8.1.3 and the economic indices are calculated using the model presented in 3.4.

4.10.2 Scenario with the option of hydrogen sales

In addition to the scenario without the option of hydrogen sales directly to the hydrogen market described in 4.10.1, the scenario that considers this option is presented in this chapter. In this scenario, the models described in chapters 4.8.2.1 and 4.8.2.2 are modified with the corresponding transmission system capacity constraints (4.23) and (4.24). All the other modelling remains the same as in scenario 4.8.

5 RESULTS

The results of the methodology for the scenarios of hydrogen use presented in Chapters 4.7-4.10, which was applied to the system setup presented in Chapter 4, are presented in this chapter. This chapter thus consists of the following studied scenarios:

- the use of hydrogen for hydrogen storage without the utilization of by-products;
- the use of hydrogen as a hydrogen-storage medium with the utilization of oxygen and heat;
- the use of hydrogen as an alternative to grid expansion;
- the use of hydrogen for transmission-congestion alleviation.

5.1 Basic scenario: use of hydrogen as an electricity-storage medium

In the first scenario, hydrogen is assumed to be used solely for hydrogen storage without any grid constraints and additional profits from oxygen and heat sales.

5.1.1 Scenario without the option of selling hydrogen to the hydrogen market

The results of the methodology described in 4.7.1 are provided in this chapter, which does not include the option of selling hydrogen directly to the hydrogen market. Firstly, some pre-dispatch and real-time dispatch figures are provided to clarify the calculation procedure for the dispatch-optimization methodology. Then, the results for the base-case scenario are provided with sensitivity analyses studying the effect of key parameter changes on the economics of the hydrogen system.

5.1.1.1 Pre-dispatch and real-time dispatch

A simple calculation shows that, based on a round-trip efficiency of the hydrogen system (60% electrolyzer and compressor and 44% fuel cells) of 26.4% for the studied scenario, the selling electricity price should be at least 3.78 times higher than the buying price in the chosen optimization horizon for the hydrogen system to cover the losses and to make a profit. If the difference in electricity prices rarely reaches these levels, the fuel-cell utilization might be very low. To further demonstrate how the pre-dispatch procedure is applied (the real-time dispatch procedure works in a similar way), a simple test-case scenario is firstly presented, where the results of a day with a high hydrogen-system utilization level are shown with a time horizon of 24 h and with a single price-forecast scenario. The results of solving the optimization models (3.1)-(3.8) for day 97, which is a typical day when the hydrogen system is utilized, can be depicted from Fig. 5.1 and Fig. 5.2. One can see that the electricity is stored as hydrogen in the morning at low electricity prices and supplied back to the grid at daily peak prices in afternoon; the profit made in this case due to the hydrogen-subsystem utilization is 217 CAD. It should be highlighted, that for the studied scenario, the utilization of the hydrogen system and the resulting profits are mainly dependent upon the following two

factors: electricity prices and their profiles, and the efficiencies of the hydrogen system's components. The investments and other costs are not a factor in optimum dispatch scheduling.

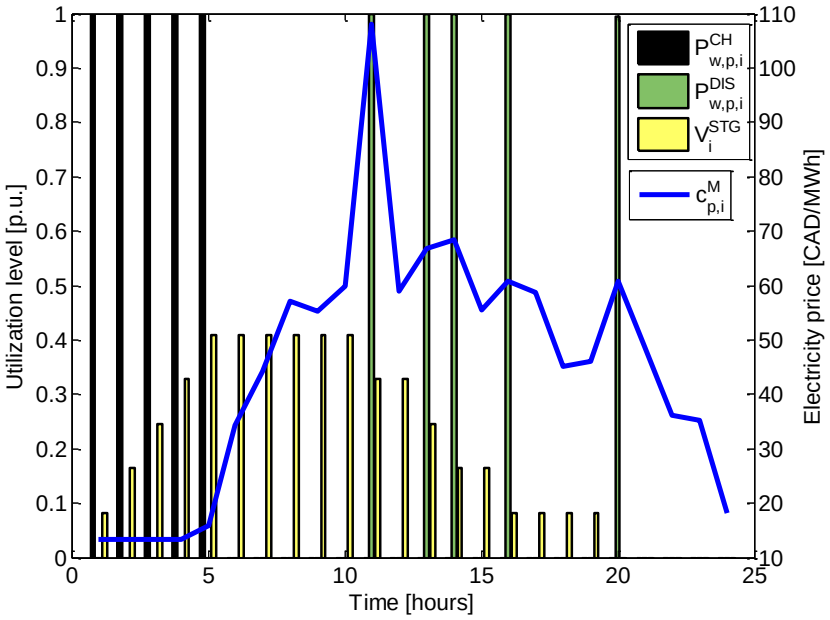

Fig. 5.1:Electrolyzer, fuel cell and storage operation with respect to the electricity price for a typical day (Day 97).

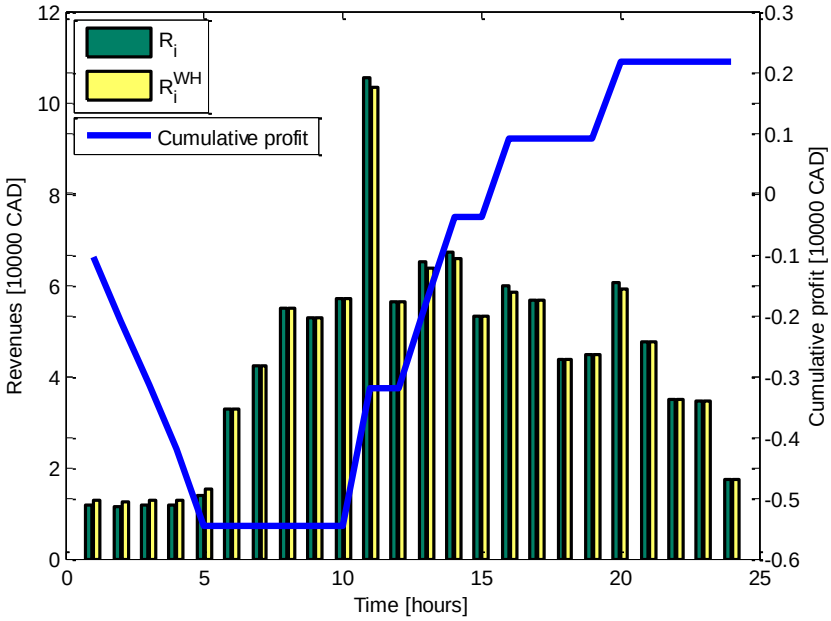

Fig. 5.2: The revenues with and without the hydrogen system and the resulting cumulative profit for the analyzed day (Day 97).

5.1.1.2 Base-Case Scenario

The results of the base-case scenario, where the parameters listed in Chapter 4 were used, are presented in Tab. 5.1. The results are given for the scenario with a forecasting error (With FE) and without a forecasting error (Without FE) to present the impact of the forecasting on the

economics of the whole system. Notice that the investment costs in the table refer to the total investment costs and that only 25% of them are assumed to be paid in equity with the remaining part covered by debt.

Tab. 5.1: Results of use of hydrogen as an electricity storage medium.

FACTOR	With FE	Without FE
Profit [CAD/year]	160,744	162,153
Investment costs [CAD]	145’121,103	145’121,103
O/M costs [CAD/year]	2’902,422	2’902,422
Utilization FC [%]	2.9	2.8
Utilization EL [%]	2.9	2.8
NPV [CAD]	-214’845,944	-214’817,468
MIRR [%]	Neg.	Neg.

The results show that for the assumed scenario, the profits that are obtained from the utilization of the hydrogen system do not cover the O&M, let alone the investment costs (specific installation costs amount to almost 8000 CAD/kW, normalized on the fuel-cell electricity production capacity, compared to 1000-1500 CAD/kW for pumped hydro storage), which is expected as the electricity prices do not vary enough to allow for a higher utilization of the hydrogen system. Hence, only 256 full-load operating hours are achieved annually, which gives the hydrogen system a utilization factor of 2.9%. The economics of the hydrogen system can only improve by an improvement in the efficiency of the components, higher price volatility in the electricity market or by much lower investment costs. The cumulative discounted cash-flow and net-cash-flow projections for this scenario are presented in Fig. 5.3. One can observe the accumulation of negative cash flows throughout the project’s lifetime, yielding a considerable net present loss in the project’s terminal year. The change in the cash flow in year 10 is due to a replacement of the electrolyzers due to their relatively short lifetime. The positive jump in the last year is due to the profits obtained from the salvage value of the hydrogen components after their decommissioning.

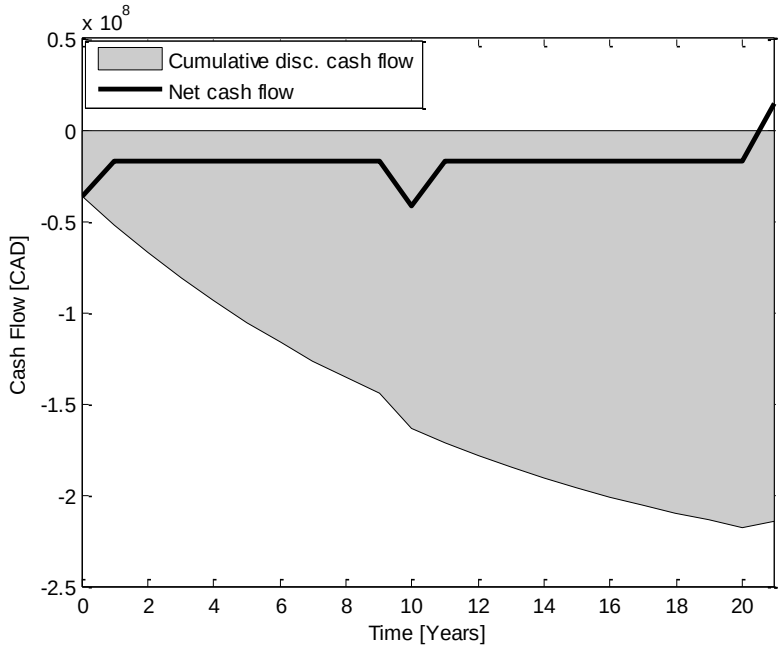

Fig. 5.3: Net cash flow and the cumulative discounted net cash flow for the use of hydrogen as an electricity-storage medium.

The differences between the scenario with the forecasting error (With FE) and the scenario without the forecasting error (Without FE) can also be seen from Tab. 5.1. The annual profits obtained without the forecasting error are less than 2000 CAD higher than the profits with the forecasting error, which does not change the economic efficiency of the hydrogen system. One can also see that the number of operating hours is ideally lower than in the scenario with the forecasting error. This implies that the forecasting error reduces the profits in some operational hours of the hydrogen system, where the actual prices deviate considerably from the forecasts, which is to be expected.

5.1.1.3 Sensitivity Analyses

Sensitivity analyses are performed to account for possible technology advances and price changes in the future. They therefore help the investor to determine the potential risks from any market changes that influence the investment economics. Through these studies, possible technology advances or price reductions are evaluated, showing the impact on the economics of the hydrogen system. The sensitivities with respect to the following parameters were studied:

- electrolyzer hydrogen and fuel-cell electrical efficiencies;
- investment costs reductions;
- prices on a variety of electricity markets in various periods.

As the results of previous analyses show no considerable dependency on price-forecast errors, these were not considered in the studies presented here.

The possible technical advances of the electrolyzers and fuel cells were investigated with electrolyzer hydrogen efficiencies varying from 60% to 90% with a step of 10%, simultaneously with the fuel-cell efficiencies, changing from 45% to 60% with a step of 5%. Thus, sensitivity step 0 represents the combination of 60% electrolyzer efficiency and 45% fuel-cell efficiency, sensitivity step 1 the combination 65%/50%, etc. In Fig. 5.4, the profits and equivalent full-load operating hours are depicted with respect to the efficiency deviations, showing that the utilization and profits obtained rise considerably with the improvement of efficiencies. The maximum annual profits thus amount to about 900,000 CAD.

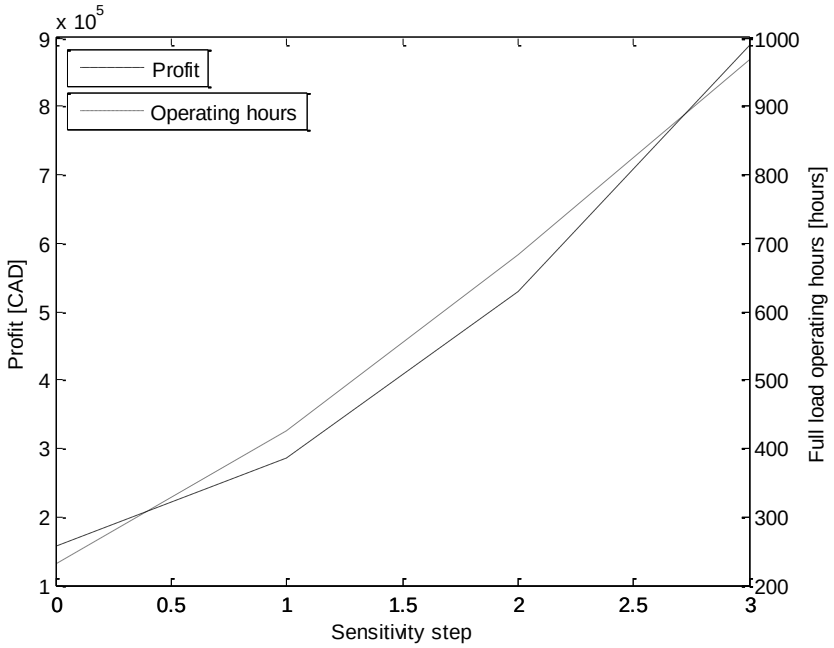

Fig. 5.4: Profit and the number of equivalent operating hours with respect to the efficiency step of the fuel cells and electrolyzers.

Fig. 5.5 represents the net present value for the various efficiency levels, taking into account the profits from Fig. 5.4 and the investment costs from Tab. 5.1; furthermore, the investment costs were scaled down to 50% to also represent the possible future price deviation due to the large-scale production of hydrogen-system components. The results in Fig. 5.5 show that no sufficient NPV changes are expected for the hydrogen system despite a 50% investment cost reduction and 90% electrolyzer and 60% fuel-cell efficiencies. This is mainly because the profits between 150,000 CAD and 900,000 CAD simply cannot bear the investment costs of 72'560,551 CAD to 145'121,103 CAD. When comparing the results in Fig. 5.5 to those in Tab. 5.1, one should only consider the electrolyzer efficiencies, as the fuel-cell efficiency can be disregarded due to low utilization of fuel cells. Thus, the electrolyzer efficiency of 62.5% assumed in the base case scenario basically corresponds to the sensitivity step 0.5 in the Fig. 5.5. The NPV in both cases equals -214'845,944 CAD.

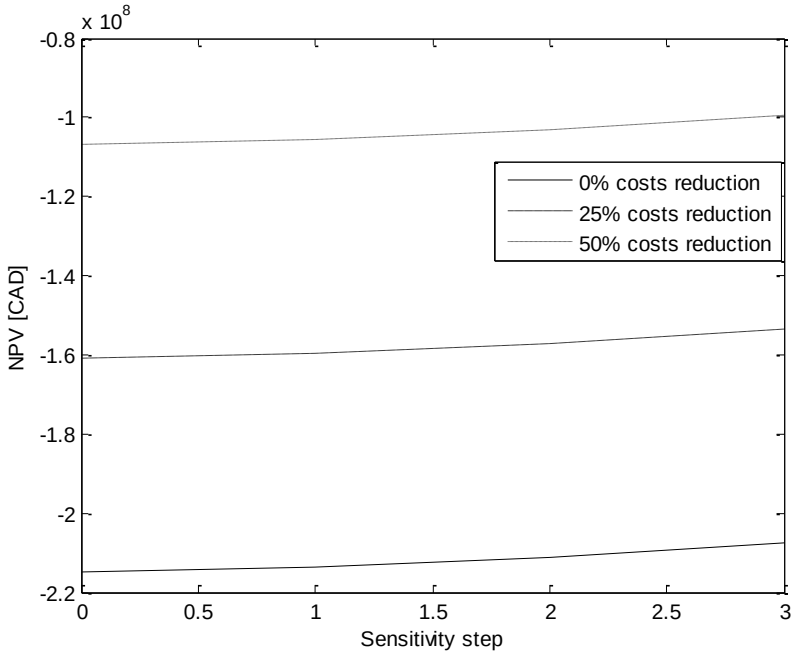

Fig. 5.5: NPV with respect to the efficiency step of the fuel cells and electrolyzers for different investment-cost reduction scenarios.

Some further calculations have shown that yearly profits of around 12'000,000 CAD are needed for the investment in the hydrogen system to become economically feasible, which is more than 75 times the profits calculated in Chapter 5.1.1.2.

As the operation of the hydrogen system is highly electricity-market-price dependent, we analyzed the economics with respect to different electricity markets in different periods. Thus, the following market-price datasets were considered:

- Hourly Ontario Market Price (HOEP) for the year 2006
- Hourly Ontario Market Price (HOEP) for the year 2007
- Hourly Ontario Market Price (HOEP) for the year 2008
- European Energy Exchange (EEX) spot-market single-hour prices for the year 2007
- European Energy Exchange (EEX) spot-market single-hour prices for the year 2008
- Energy Exchange Austria (EXAA) spot-market single-hour prices for the year 2007
- Energy Exchange Austria (EXAA) spot-market single-hour prices for the year 2008

The results of these analyses are presented in Tab. 5.2 where EUR was converted to CAD at a rate of 1.5734 CAD per 1 EUR. Interestingly, the results show that the profits and economics of the hydrogen system do not directly depend upon the average market prices and the corresponding standard price deviation but from the exact price profiles (e.g., HOEP 2008 provides better profits compared to EEX 2008, despite a lower average price and standard deviation).

Tab. 5.2: Profits and NPVs for different periods and electricity markets.

Electricity Price Dataset	Average Price [CAD]	Standard Deviation [CAD]	Profit [CAD]	NPV [CAD]
HOEP 2006	46.38	23.98	162,153	-214'817,468
HOEP 2007	47.81	24.66	211,385	-214'334,101
HOEP 2008	48.84	29.77	819,738	-208'361,208
EEX 2007	59.77	47.76	553,132	-210'978,787
EEX 2008	103.65	44.98	429,649	-212'191,161
EXAA 2007	61.31	47.03	454,524	-211'946,928
EXAA 2008	104.14	44.34	227,361	-214'177,254

5.1.2 Scenario with the option of hydrogen sales to the hydrogen market

In this chapter, additional profits of the hydrogen system from hydrogen sales directly to the hydrogen market are considered as per the methodology described in Chapter 4.7.2.

5.1.2.1 Simple Test Scenario

To demonstrate the pre-dispatch and real-time procedures with the option of hydrogen sales, a simple test-case scenario is presented first. Thus, the models described in Chapters 4.7.2.1 and 4.7.2.2 were used, with a time horizon of 4 h and with two price-forecast scenarios. The results of solving the optimization models presented in chapter 4.8.2 are shown in Tab. 5.3 and Tab. 5.4.

Tab. 5.3: The Pre-Dispatch Results for the Simple Test Case

p	i	$P_{w,i}^{GA}$	$c_{p,i}^{M}$	$P_{w,p,i}^{G}$	$P_{w,p,i}^{CH}$	$P_{w,p,i}^{DIS}$	$V_{w,p,i}^{H}$	V_{i}^{STG}
1	1	1016.38	42.76	1016.38	79.20	0	1423.99	0
1	2	1009.32	34.37	1009.32	79.20	0	1423.99	0
1	3	1010.72	48.42	1010.72	79.20	0	1423.99	0
1	4	1004.09	40.99	1004.09	79.20	0	1423.99	0
2	1	1016.38	39.18	1016.38	79.20	0	1423.99	0
2	2	1009.32	60.94	1009.32	79.20	0	1423.99	0
2	3	1010.72	60.71	1010.72	79.20	0	1423.99	0
2	4	1004.09	25.92	1004.09	79.20	0	1423.99	0

Tab. 5.4: The Real-Time Results for the Simple Test Case

i	$\hat{P}_{i}^{GA}$	$\hat{c}_{i}^{M}$	$\hat{P}_{i}^{G}$	$\hat{P}_{i}^{CH}$	$\hat{P}_{i}^{DIS}$	$\hat{V}_{i}^{H}$	$\hat{V}_{i}^{STG}$	$\hat{R}_{i}$	$\hat{R}_{i}^{WH}$
1	1016.38	48.73	1016.38	79.20	0	1423.99	0	51,863.43	49,528.65
2	1009.32	49.10	1009.32	79.20	0	1423.99	0	51,863.46	49,557.98
3	1010.72	46.70	1010.72	79.20	0	1423.99	0	49,696.39	47,200.82
4	1004.09	37.03	1004.09	79.20	0	1423.99	0	40,443.09	37,181.63
							Total	193,866.39	183,469.09
								Profit	10,397.29

The profit obtained in this case from the hydrogen-system utilization is 10,397.29 CAD. It should be highlighted that in this scenario, the utilization and the resulting profits of the hydrogen system are dependent mainly on then following three factors: (a) electricity prices and electricity-price profiles, (b) the efficiencies of the components, and (c) the hydrogen selling price. The investment and other costs are not a factor in this case. One can easily

calculate that if there are no price-forecast errors, the hydrogen selling price is 4.35 CAD/kg, the efficiency of the electrolyzer is 18.73 kg/MWh (60%) and the efficiency of the compressor is 449 kg/MWh the electrolyzer would be utilized when the prices of electricity drop below 78.21 CAD/MWh. This is consistent with the results obtained in Tab. 5.3, where one can see that $P_{w,p,i}^{CH}$ is always positive since the $c_{p,i}^{M}$ values are always below the threshold of 78.21 CAD/MWh. Similarly, the fuel cell would be utilized when the price of electricity exceeds 296.24 CAD/MWh, for a hydrogen selling price of 4.35 CAD/kg and an efficiency of 68.10 kg/MWh. Since the price of electricity rarely reaches these levels, the fuel-cell utilization is very low, as shown in Tab. 5.3 and Tab. 5.4 ($P_{w,p,i}^{DIS}$, $\hat{P}_{i}^{DIS}$). Notice that an increase in the hydrogen selling prices decreases the utilization and profitability of the electricity-generating stationary fuel cells, whereas an increase of the efficiency of the fuel cells increases them.

5.1.2.2 Base-Case Scenario

The base-case scenario (BCS) is the most probable scenario in practice, and is further divided into four sub-scenarios based on the inclusion of price forecasts and stationary fuel cells. The investment evaluation results obtained excluding fuel cells (NFC) and including them (FC), with (FE) and without (NFE) forecast errors are presented in Tab. 5.5. The investment costs presented in the table are the total investment costs and not the investment in equity, which amounts to 25% of the total investment costs. Neither forced outages of the electrolyzers nor the scheduled maintenance outages were considered in the operational and economic evaluation. Observe that the hydrogen system with stationary fuel cells is not profitable, due to much higher investment costs, almost equal profits and the low utilization of the fuel cells; this clearly reflects in much lower values for the NPV and MIRR compared to the scenario without fuel cells.

Tab. 5.5: Results for BCS Considering FC and FE

FACTOR	FC/FE	NFC/FE	FC/NFE	NFC/NFE
Profit [CAD/year]	23’337,511	23’322,516	23’337,546	23’322,516
Utilization FC [%]	0.03	/	0.05	/
Utilization EL [%]	92.18	92.18	92.19	92.18
Investment costs [CAD]	145’121,103	124’191,103	145’121,103	124’191,103
O/M costs [CAD/year]	2’902,422	2’483,822	2’902,422	2’483,822
NPV [CAD]	5’848,016	26’411,385	5’848,303	26’411,385
MIRR [%]	8.62	10.67	8.62	10.67

On the other hand, the electrolyzer utilization is shown to be considerably higher, at about 92.18%, which provides enough profits from electricity-to-hydrogen conversion to exceed the profitability margin. The forecasting error is shown to have only a limited impact on the profitability of the hydrogen system with fuel cells due to low efficiency of the fuel-cell power modules and the relatively high hydrogen selling prices compared to the electricity prices. In the scenario without fuel cells, no differences in the hydrogen-system economics were observed with and without the consideration of price forecast errors, since the electricity converted to hydrogen is always sold at a constant price irrespective of electricity price

forecasts, which is not the case in the scenario with the fuel cells. Thus, the hydrogen is produced and sold when the prices of electricity fall below the aforementioned 78.3 CAD/MWh, almost regardless of the results of the pre-dispatch phase. Fig. 5.6 shows the cumulative discounted net cash flows (CDCF) with and without fuel cells, and without price forecast errors.

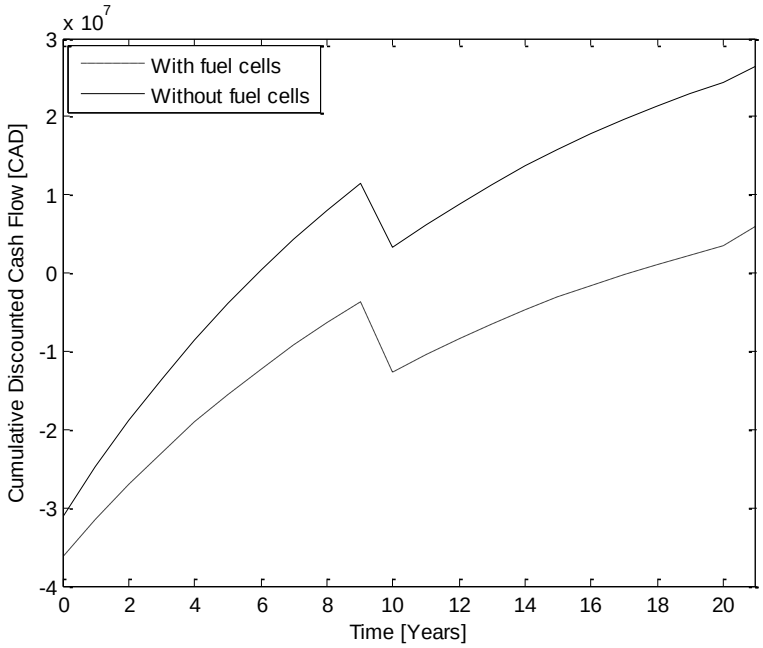

Fig. 5.6: Cumulative discounted net cash flow of use of hydrogen as an electricity-storage medium with the option of hydrogen sales.

It is evident from the figure that the hydrogen subsystem with stationary fuel cells results in a much lower NPV (the final value of the CDCF) compared to the scenario without them. Observe the considerable change of cash flows in year 10; this is due to the replacement of the electrolyzers at full costs in that year. In the last year of the project, the effect of salvage values is clearly visible. It should be highlighted that because the system is mainly utilized for hydrogen production instead of electricity storage, due to low fuel-cell utilization, the electricity price profile and wind forecasts do not have any significant impact on the system profitability. For different hydrogen and electricity prices and efficiencies, these forecasts may have a more significant effect on the system economics. The comparison of the scenarios with and without direct sales to the hydrogen market shows that a prospective hydrogen market might prove economical for large-scale hydrogen production from electricity; on the other hand, the hydrogen is not expected to be utilized for the sole purpose of electricity storage due to its low efficiencies and high costs.

5.1.2.3 Sensitivity Analysis

The sensitivity analysis is based on the BCS and concentrates on studying the following main issues:

- the effect of the efficiency of the electrolyzers and the fuel-cell power modules;

- the effect of the hydrogen selling price.

The impacts of equipment prices, price forecasting errors and the exclusion of fuel cells are also considered in all these studies.

In this paragraph, the efficiencies of the fuel cells were assumed to vary from 45% to 60% for the fuel-cell power modules in parallel with the 60% to 90% efficiency variation of the electrolyzer subsystem. The results obtained indicate the utilization of stationery fuel-cell power modules to be near zero for all the studied efficiency ranges; this is due to the low efficiency of the fuel cells and the low electricity market prices. Based on this, the profit, electrolyzer utilization and the internal rates of return depend solely on the electrolyzer's efficiency and not on the fuel-cell efficiency. In Fig. 5.7, the profit and the number of full-load electrolyzer operating hours are shown with respect to the electrolyzer efficiencies. The results show an almost linear dependency of profit with respect to efficiencies. The electrolyzer utilization, on the other hand, is shown to saturate and converges to the maximum number of 8760 hours. The price and wind-forecast errors do not have any considerable impact on the profitability and utilization of stationary fuel cells and electrolyzers, as well as on the internal rates of returns, similar to what was reported in the previous chapter.

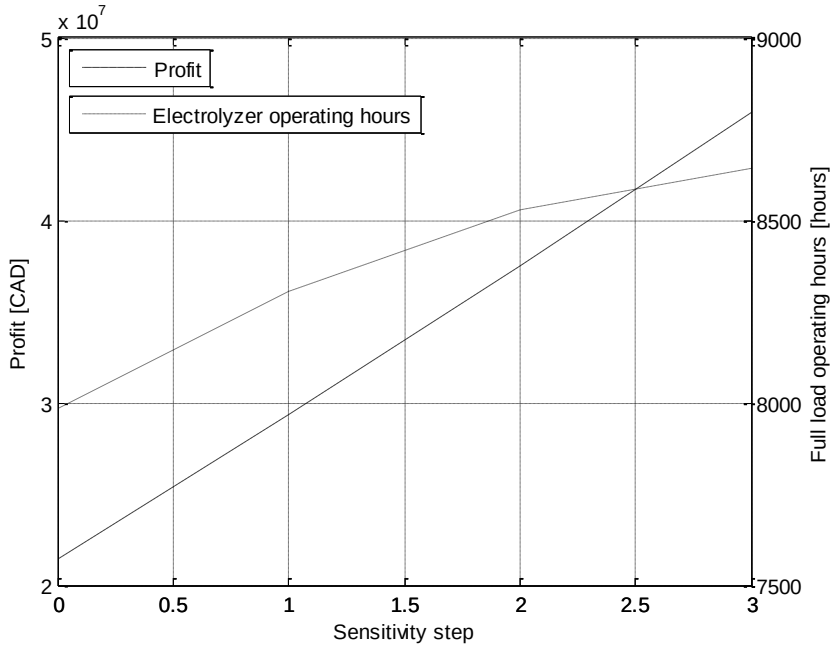

Fig. 5.7: Profit and number of electrolyzer operating hours with respect to electrolyzer efficiency.

The NPV of the project with respect to electrolyzer efficiencies is depicted in Fig. 5.8. Different equipment price reductions are considered here, which strongly impact on the profitability of the hydrogen subsystem; the higher the reduction, the higher the profitability of the hydrogen subsystem. The efficiencies of the electrolyzers should be about 63% (18.90 kg/MWh) if there are no investment-cost reductions available. For other investment-cost

reduction scenarios, the hydrogen system is also attractive to potential investors at electrolyzer efficiencies below 60%.

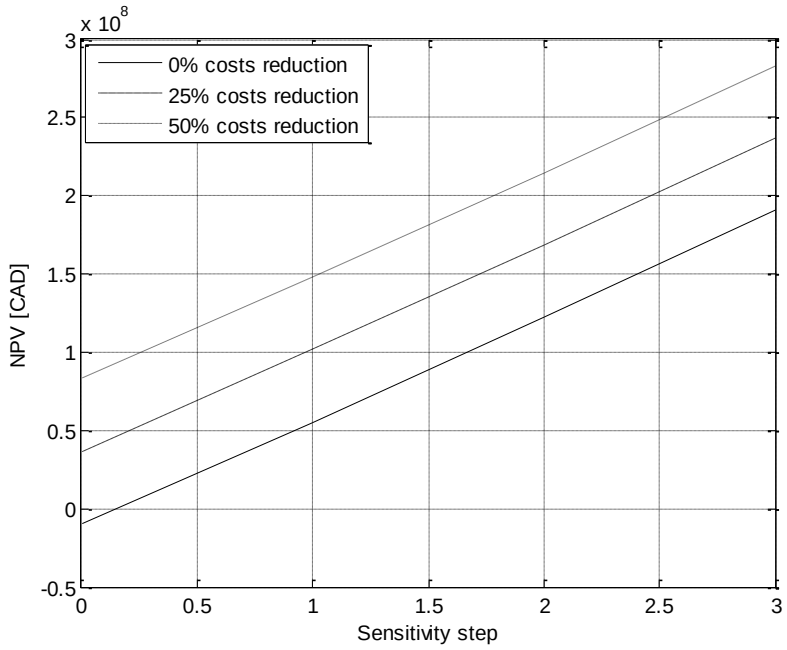

Fig. 5.8: NPV with fuel cells for various electrolyzer efficiencies and equipment price reductions.

As is shown in the base-case scenario, the fuel cells are seldom utilized; hence the sensitivity analysis of the hydrogen system without fuel cells on the efficiency variations was carried out with the results depicted in Fig. 5.9. As expected, this figure shows the higher economic benefits of the hydrogen system compared to Fig. 5.8, with the NPV difference of about 2×10^7 CAD.

The second part of the sensitivity analysis was devoted to studying the impacts of hydrogen selling prices on the economics of the hydrogen system, assuming a hydrogen price range of 2 CAD/kg to 8 CAD/kg. Again, a very limited impact of the price and wind-forecast errors on the profitability of the system was observed. The effect on the profit and utilization of the electrolyzer versus the hydrogen selling price is illustrated in Fig. 5.10. The results again show a negligible fuel-cell utilization due to unfavorable fuel-cell efficiencies and electricity and hydrogen prices. Thus, only the electrolyzer utilization is presented in the figure. Observe that the utilization of the electrolyzers is close to 100% for prices above 6 CAD/kg. The profit is almost linearly dependent on hydrogen prices, with an approximate slope of 10’000,000 CAD per each CAD/kg hydrogen selling-price increase.

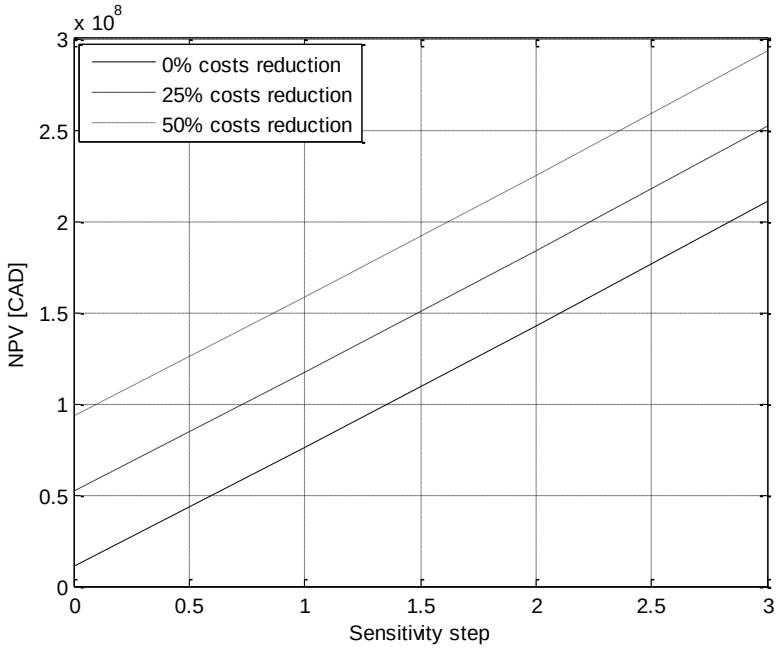

Fig. 5.9: NPV without fuel cells for various electrolyzer efficiencies and equipment price reductions.

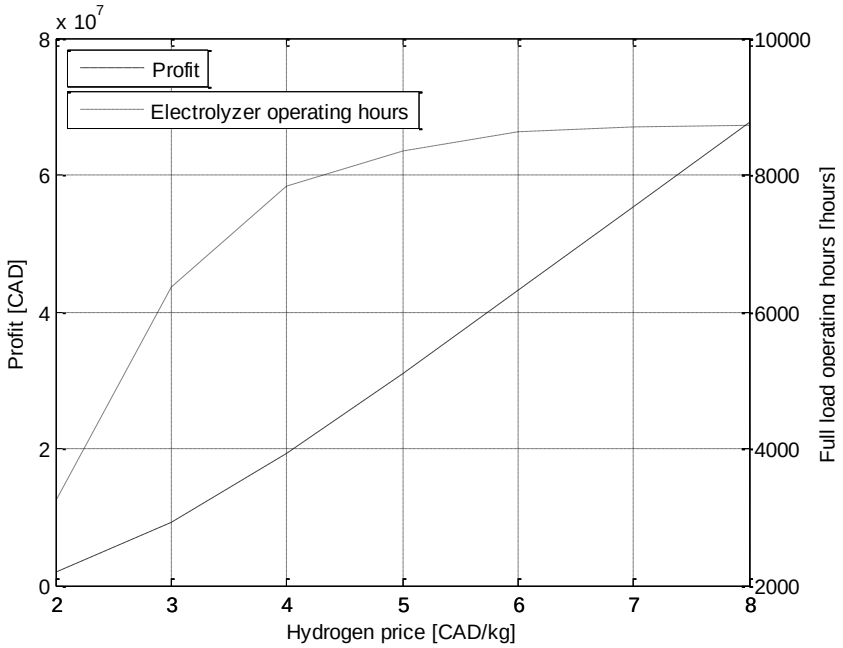

Fig. 5.10: Profit and number of electrolyzer operating hours with respect to hydrogen selling prices.

The impact of the hydrogen selling prices on the profitability of the subsystem with respect to equipment price costs is depicted in Fig. 5.11. These results show that the NPV of the hydrogen subsystem increases considerably as hydrogen prices increase. The complete subsystem becomes economically viable at hydrogen prices above 4.3 CAD/kg in the base-case scenario; at lower equipment prices the system becomes profitable at hydrogen prices of 3.8 CAD/kg and 3.2 CAD/kg for 25% and 50% investment cost reductions, respectively.

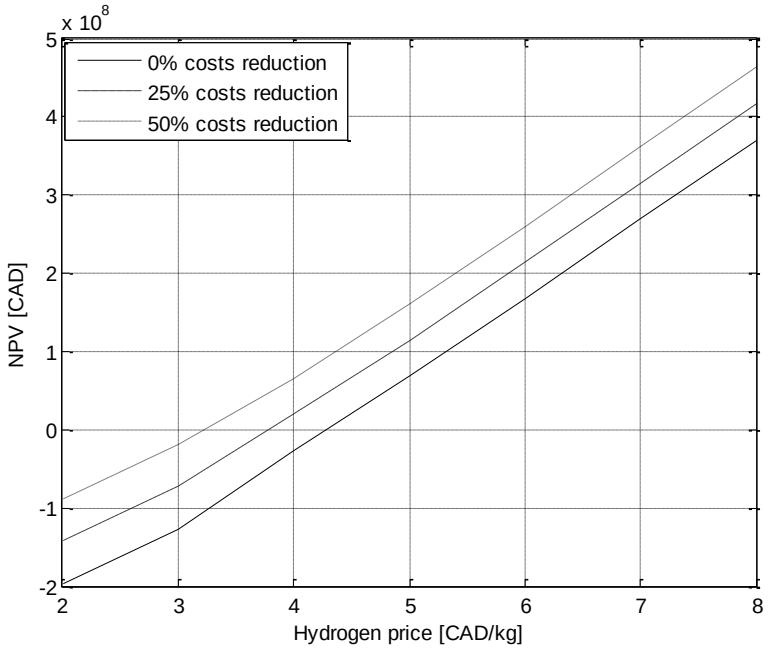

Fig. 5.11:NPV with fuel cells with respect to various hydrogen selling prices.

Again, the sensitivity analysis was carried out without any consideration of the fuel cells. The economic viability of hydrogen for this scenario is presented in Fig. 5.12 and shows that the NPV curve is shifted upwards by about 10^7 CAD. The required minimum hydrogen selling price can therefore be lower than the scenario with fuel cells.

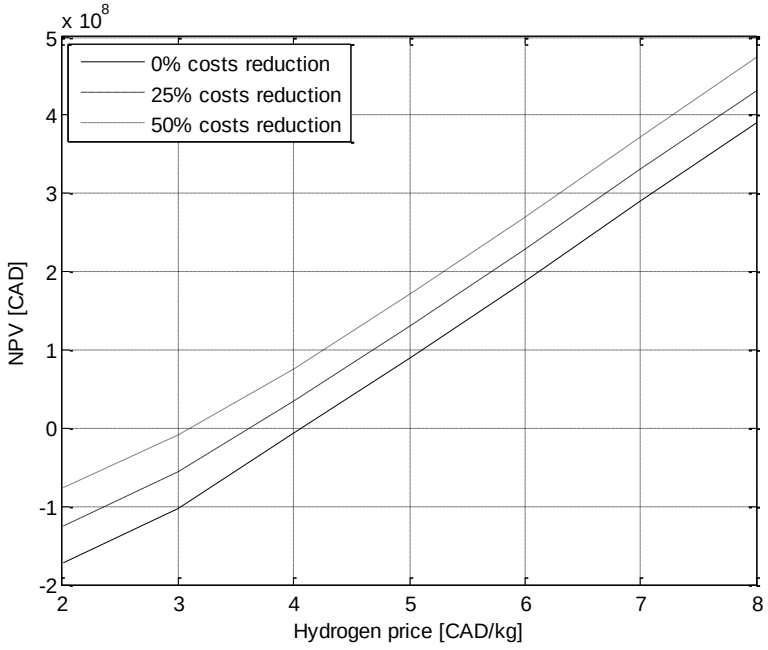

Fig. 5.12: NPV without fuel cells with respect to hydrogen selling prices.

5.2 Scenario with the utilization of oxygen and heat

In this scenario of use of hydrogen in power systems with the additional profits from oxygen and heat utilization are considered as described in the methodology in Chapter 4.8.

5.2.1 Scenario without the option of selling hydrogen to the hydrogen market

Firstly, the sub-scenario without the option of hydrogen sales is considered, where the model presented in Chapter 4.8.1 is used.

5.2.1.1 Required conditions for the hydrogen-system operation

Firstly, the required conditions for the hydrogen system to be utilized are analyzed. The basic condition that should apply is that profits from the sales of electricity should be greater than the costs when buying the electricity; this can be written as follows:

$$R_S > C_B \tag{5.1}$$

where R_S are the revenues obtained and C_B are the costs for the bought electricity. This equation can be expanded with a breakdown of the revenues as per the following equation:

$$R_{OXY} + R_{HEAT} + R_{ELEC} > C_B \tag{5.2}$$

where one can observe that the revenues consist of oxygen sales R_{OXY}, heat sales R_{HEAT} and electricity sales R_{ELEC}. The costs are incurred by electricity purchases. The individual revenue components and costs for the purchased electricity can be calculated with the following four equations:

$$R_{OXY} = \frac{1}{\left(1+\frac{\mu_{oe}}{\mu_{oc}}+\frac{\mu_{he}}{\mu_{hc}}\right)} \cdot \mu_{oe} \cdot c^{O} \cdot \hat{P}_i^{CH} \tag{5.3}$$

$$R_{ELEC} = \frac{1}{\left(1+\frac{\mu_{oe}}{\mu_{oc}}+\frac{\mu_{he}}{\mu_{hc}}\right)} \frac{\mu_{he}}{\mu_{ef}} c_{p,j}^{M} \cdot \hat{P}_i^{CH} \tag{5.4}$$

$$R_{HEAT} = \frac{1}{\left(1+\frac{\mu_{oe}}{\mu_{oc}}+\frac{\mu_{he}}{\mu_{hc}}\right)} \frac{\mu_{he}}{\mu_{hf}} c^{HEAT} \cdot \hat{P}_i^{CH} \tag{5.5}$$

$$C_B = c_{p,i}^{M} \cdot \hat{P}_i^{CH} \tag{5.6}$$

All the parameters are properly defined in Chapter IV. By putting equations (5.3)-(5.6) in (5.2), one can easily show that the utilization of the hydrogen-storage system becomes profitable only when the following condition is satisfied:

$$\frac{1}{\left(1+\frac{\mu_{oe}}{\mu_{oc}}+\frac{\mu_{he}}{\mu_{hc}}\right)}\cdot\left((\mu_{oe}\cdot c^{O}+\frac{\mu_{he}}{\mu_{ef}}c^{M}_{p,j}+\frac{\mu_{he}}{\mu_{hf}}c^{HEAT}\right)>c^{M}_{p,i}\quad \text{for } i<j \tag{5.7}$$

Note that this is a necessary, but not a sufficient condition, since the system has to be capable of storing the required energy, i.e., it has to have enough storage and production capacity. If we insert the parameters of the case-study system defined in Chapter 4, the following equation is obtained:

$$0.92\cdot(23.71+0.28\cdot c^{M}_{p,j})>c^{M}_{p,i}\quad \text{for } i<j \tag{5.8}$$

which can be reformulated as follows:

$$c^{M}_{p,j}>3.88\cdot c^{M}_{p,i}-84.68\quad \text{for } i<j \tag{5.9}$$

The characteristics of (5.9) are depicted in Fig. 5.13, which represents the threshold above which the system makes a profit by storing electricity as hydrogen.

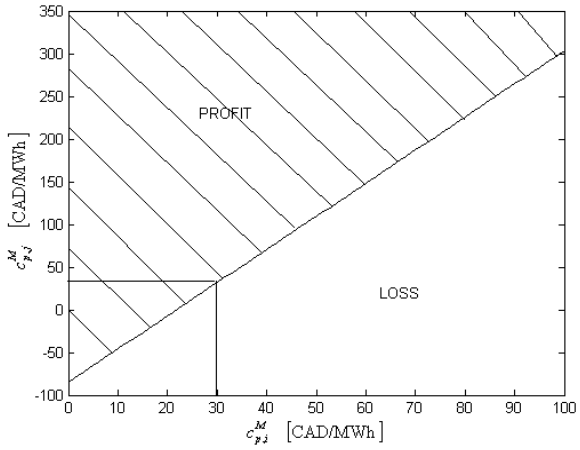

Fig. 5.13: Price threshold for the hydrogen-storage system utilization.

In the above figure, the point at which the forecasted electricity prices are $c^{M}_{p,i}=c^{M}_{p,j}=29.4\,\text{MWh}$ is shown. To the right of this point, one has to sell electricity to the system at higher prices than it was bought earlier, to make a profit; on the other hand, to the left of that point, one can sell electricity to the system at lower prices than it was bought earlier, and still make a profit. This is possible due to the additional profits from oxygen and heat sales; if these byproducts are not sold, the breakeven point for the utilization of the hydrogen storage system will be defined by the following:

$$c_{p,i}^{M} < \frac{1}{\left(1+\frac{\mu_{he}}{\mu_{hc}}\right)} \frac{\mu_{he}}{\mu_{ef}} c_{p,j}^{M} \quad \text{for } i < j \tag{5.10}$$

which, for our system setup, results in:

$$c_{p,j}^{M} > 3.79 \cdot c_{p,i}^{M} \quad \text{for } i < j \tag{5.11}$$

This equation shows that electricity should be sold at about 3.8 times the price at which it was bought earlier to make a profit.

5.2.1.2 Pre-dispatch and Dispatch

The pre-dispatch model described in 4.8.1.1 and the real-time dispatch model described in 4.8.1.2 were solved for one year of operation of the system described previously. The real-time dispatch results obtained for the same day (Day 97) as in 5.1.1.1 are presented in Fig. 5.14, where the electrolyzer and fuel cell together with the hydrogen-storage operations are depicted. All the variables are referred to with respect to their maximum values and are hence presented in p.u. Observe that oxygen and heat are being produced and sold to the market in periods of electrolyzer and fuel-cell operation. One can see that the hydrogen system is both consuming and producing electricity in hour 24 in the Fig. 5.14, which can be justified by Fig. 5.13, where it is shown that the hydrogen can be produced even at electricity selling prices lower than 0 CAD/MWh if the buying price is lower than 20 CAD/MWh; this is due to the additional revenues from oxygen and heat.

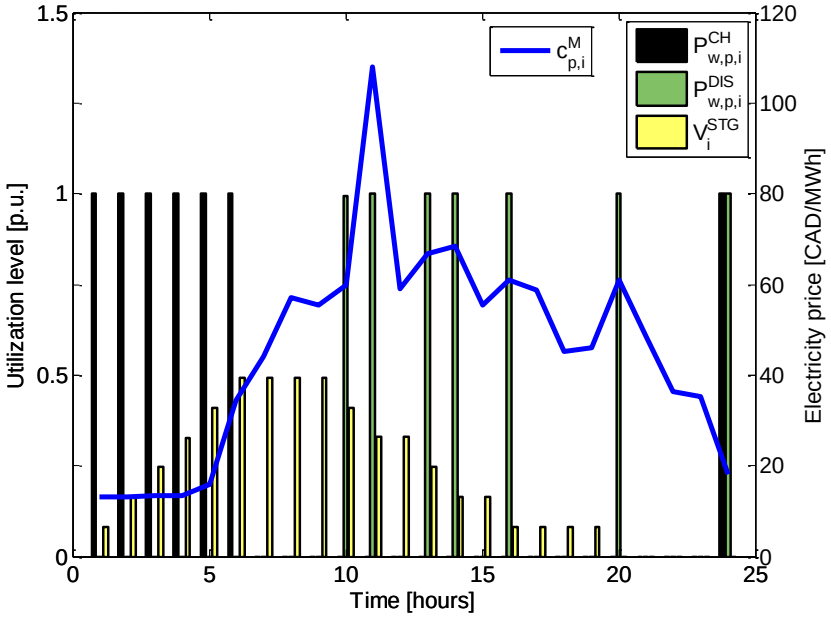

Fig. 5.14: Electrolyzer and fuel-cell operation and the actual electricity prices for a typical day (Day 97).

The results in Fig. 5.14 further show that the hydrogen is produced during the early hours of the day, corresponding to low electricity prices, and sold to the market when the prices are higher. The similarities with the results from Fig. 5.1 can be observed in the hydrogen-system operations; however, due to additional profits from the oxygen and heat sales, the system is utilized more frequently in the current scenario. This is further confirmed by the observation of profits earned in the observed day, which amount to 1,188 CAD in Fig. 5.15 compared to 217 CAD earned by Fig. 5.2.

Fig. 5.15 further presents the revenues with and without the hydrogen-storage system together with the resulting cumulative profit, which is a cumulative sum of the differences between the revenues with and without the hydrogen storage system. Observe that the cumulative profit is negative during the early hours of system operation, since the electricity is being bought and stored in this period, and becomes positive when the electricity is sold back to the grid; the cumulative profit during the last hour of operation in this figure is the total profit made by the hydrogen system in the observed day.

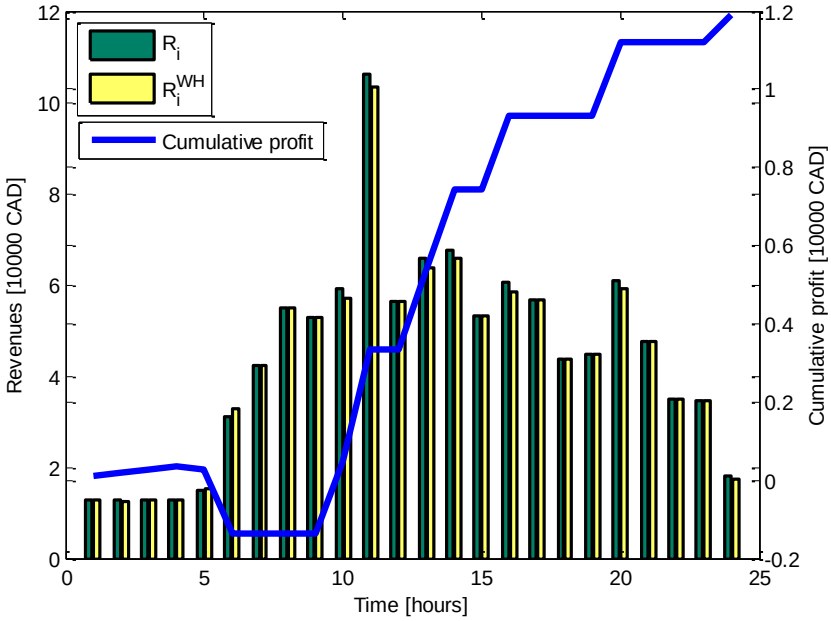

Fig. 5.15: The revenues with and without the hydrogen-storage system and the resulting cumulative profit for a typical day (Day 97).

5.2.1.3 Base-Case Scenario

As in Chapter 5.1.1.2, two possible scenarios are discussed here: the scenario with a forecasting error (With FE) and the scenario without a forecasting error (Without NFE). The results of these two scenarios are presented in Tab. 5.6. Observe that the profits from the hydrogen-system operations are considerably (more than 10 times) higher than the results of the scenario without oxygen and heat utilization in Tab. 5.1. This is mainly due to the heat and oxygen sales, which considerably increase the hydrogen-system utilization. On the other

hand, a considerable investment and O&M costs increase (about 10%) can be observed due to the additional investment in the storage tanks and the compressor for oxygen utilization. The end effect of both the revenues and costs increase is a NPV that still shows the hydrogen system not to be viable for a prospective investor as the profits again do not cover the O&M costs, let alone the investment.

Observe also that the utilization of stationary fuel cells (FC) is slightly lower than the electrolyzers (EL), due to higher installed hydrogen-consumption capacity of the stationary fuel cells compared to the hydrogen production capacity of the electrolyzers. The impact of electricity-price forecasting on the results is also evident; thus, without forecasting errors, the profit and NPV values increase somewhat, but do not have any considerable impacts on the overall hydrogen-system economics.

Tab. 5.6: Economic parameters of the hydrogen system with oxygen and heat sales.

FACTOR	With FE	Without FE
Profit [CAD/year]	1’919,194	1’958,731
Investment costs [CAD]	160’020,166	160’020,166
O/M costs [CAD/year]	3’200,403	3’200,403
Utilization FC [%]	25.24	26.80
Utilization EL [%]	25.22	26.82
NPV [CAD]	-214’682,774	-214’294,598
MIRR [%]	Neg.	Neg.

The nominal and discounted cumulative cash flows (CCF) of the scenario with forecasting errors are presented in Fig. 5.16. The cash flows are negative and then get lower, as the profits do not even cover the O&M costs. The utilization of the heat and oxygen does not change the cash flow in comparison with the cash flow from the scenario without heat and oxygen utilization in Fig. 5.3.

5.2.1.4 Sensitivity Analyses

Several sensitivity analyses were carried out for this scenario with respect to the following parameters:

- the electrolyzer hydrogen and fuel-cell electrical efficiencies;
- the investment costs reductions;
- the prices on a variety of electricity markets in various periods.

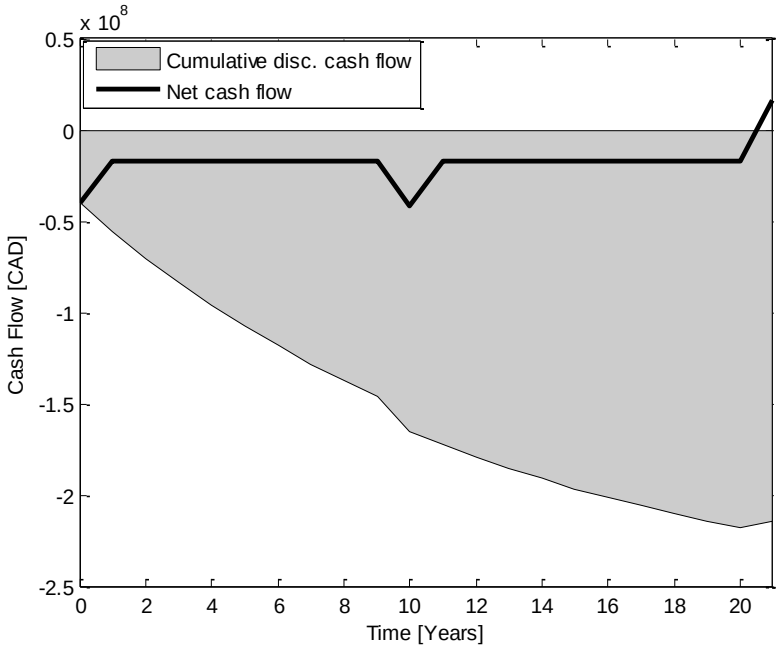

Fig. 5.16: The nominal and discounted cumulative cash flows for the scenario with a forecasting error.

Due to the negligible impact of price-forecast errors, these were not considered in the studies presented here. Firstly, possible technical advances of the electrolyzers and fuel cells are investigated with electrolyzer hydrogen efficiencies varying from 60% to 90% with a step of 10%, simultaneously with fuel-cell efficiencies, changing from 45% to 60% with a step of 5%. In Fig. 5.17, the profits and equivalent full-load operating hours are depicted with respect to the efficiency deviations, showing that the utilization and profits obtained rise considerably with the improvement of the efficiencies. The maximum annual profits thus amount to about 5'250,000 CAD with 3700 equivalent full-load operating hours. These profits are about 7-10 times higher compared to the profits from the scenario without heat and oxygen utilization.

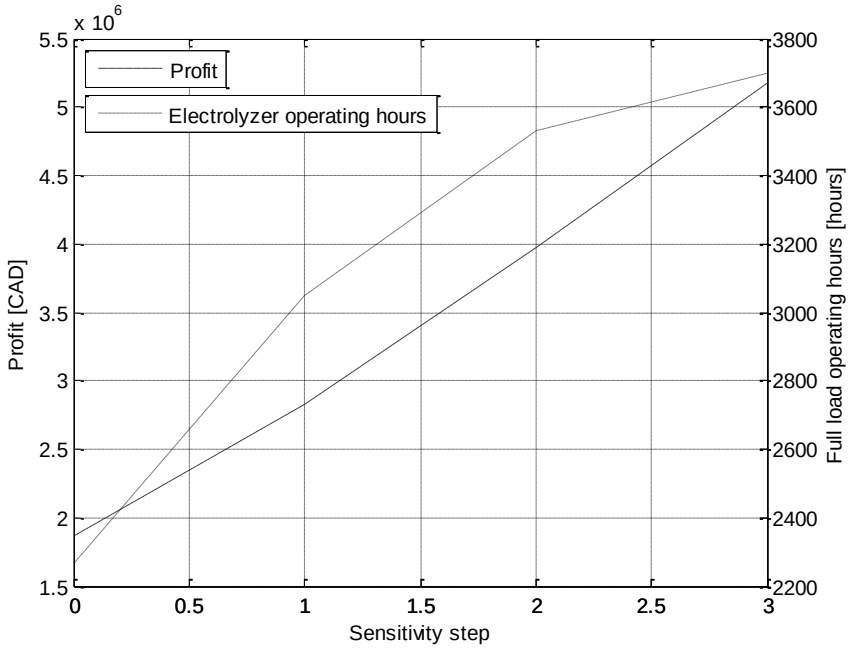

Fig. 5.17: Profit and the number of equivalent operating hours with respect to the efficiency step of the fuel cells and electrolyzers.

Despite higher profits, the hydrogen system still does not provide enough revenues to cover the investment and other costs, as shown in Fig. 5.18, even at an investment-cost reduction of 50% and the highest assumed electrolyzer and fuel-cell efficiencies. However, the economics of this scenario is somewhat improved compared to the scenario without the oxygen and heat utilization.

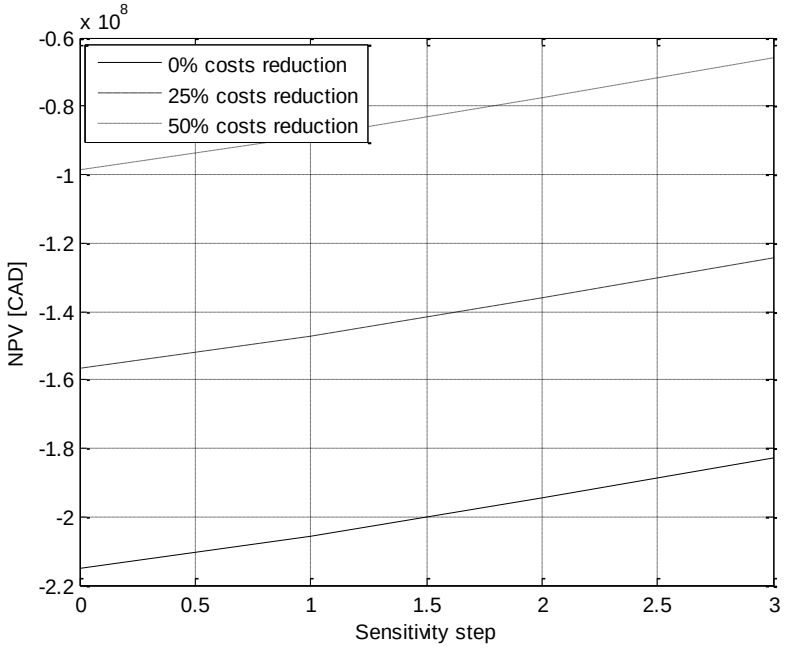

Fig. 5.18: NPV with respect to the efficiency step of the fuel cells and electrolyzers for different investment-cost reduction scenarios.

The NPV index with respect to several oxygen-price scenarios is depicted in Fig. 5.19. It once more shows that in spite of oxygen and heat utilization and despite the most favorable assumed oxygen prices at the lowest investment costs, a hydrogen system used solely for electricity storage is not profitable.

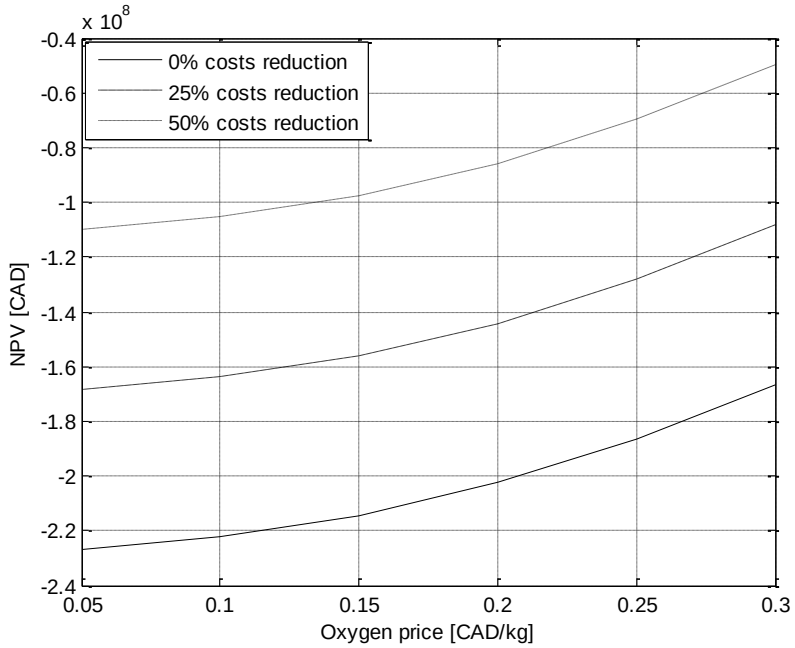

Fig. 5.19: NPV with respect to oxygen-price variations for different investment-cost reduction scenarios.

Some further sensitivity analyses were carried out to assess the impacts of prices in different periods and electricity markets defined in Chapter 5.1.1.3. The results of these studies are presented in Tab. 5.7 and again show some improvements in profits with respect to different electricity-price datasets. However, a comparison with the results in Tab. 5.2 shows that these profits are insufficient for the hydrogen system to become economically feasible.

Tab. 5.7: Profits and NPVs for different periods and electricity markets.

Electricity Price Dataset	Average Price [CAD]	Standard Deviation [CAD]	Profit [CAD]	NPV [CAD]
HOEP 2006	46.38	23.98	1'958,731	-214'294,598
HOEP 2007	47.81	24.66	2'504,836	-208'932,863
HOEP 2008	48.84	29.77	3'306,005	-201'066,864
EEX 2007	59.77	47.76	2'640,528	-207'600,614
EEX 2008	103.65	44.98	1'318,110	-220'584,304
EXAA 2007	61.31	47.03	2'581,907	-208'176,160
EXAA 2008	104.14	44.34	1'106,862	-222'658,370

5.2.2 Scenario with the option of selling hydrogen to the hydrogen market

The second sub-scenario also considers hydrogen sales directly to the hydrogen market and thus considers the model defined in Chapter 4.8.2.

5.2.2.1 Pre-dispatch and Actual Dispatch

The pre-dispatch and dispatch models described in Chapters 4.8.2.1 and 4.8.2.2, respectively, were solved for one year, followed by the economic evaluation model run. The pre-dispatch and real-time model results obtained for a typical day are presented in Tab. 5.8 and Tab. 5.9, where the electrolyzer and hydrogen-storage operations are depicted together with electricity prices and levels of hydrogen, oxygen and heat sales. These results show constant hydrogen production throughout the day due to the relatively low electricity prices; hydrogen is simultaneously sold to the market. Note that this is only one optimal system dispatch solution; due to the assumed lossless hydrogen storage, profits would be the same if hydrogen is firstly stored and then sold to the market.

Tab. 5.8: The Pre-Dispatch Results for the Simple Test Case

p	i	$P_{w,i}^{GA}$	$c_{p,i}^{M}$	$P_{w,p,i}^{G}$	$P_{w,p,i}^{CH}$	$P_{w,p,i}^{DIS}$	$V_{w,p,i}^{H}$	V_{i}^{O}	P_{i}^{HEAT}	V_{i}^{STG}
1	1	1016.38	51.89	1016.38	82.37	0	0	7919.49	0	1423.99
1	2	1009.32	57.88	1009.32	82.37	0	2847.98	7919.49	0	0
1	3	1010.72	52.70	1010.72	82.37	0	1423.99	7919.49	0	0
1	4	1004.09	37.66	1004.09	82.37	0	1423.99	7919.49	0	0
2	1	1016.38	34.11	1016.38	82.37	0	0	7919.49	0	1423.99
2	2	1009.32	60.32	1009.32	82.37	0	2847.98	7919.49	0	0
2	3	1010.72	60.71	1010.72	82.37	0	1423.99	7919.49	0	0
2	4	1004.09	48.13	1004.09	82.37	0	1423.99	7919.49	0	0

Tab. 5.9: The Real-Time Results for the Simple Test Case

i	$\hat{P}_{i}^{GA}$	$\hat{c}_{i}^{M}$	$\hat{P}_{i}^{G}$	$\hat{P}_{i}^{CH}$	$\hat{P}_{i}^{DIS}$	$\hat{V}_{i}^{H}$	$\hat{V}_{i}^{O}$	$\hat{P}_{i}^{HEAT}$	$\hat{V}_{i}^{STG}$	$\hat{R}_{i}$	$\hat{R}_{i}^{WH}$
1	1016.38	48.73	1016.38	82.37	0	0	7919.49	0	1423.99	46702.62	49528.65
2	1009.32	49.10	1009.32	82.37	0	2847.98	7919.49	0	0	59090.22	49557.98
3	1010.72	46.70	1010.72	82.37	0	1423.99	7919.49	0	0	50736.38	47200.82
4	1004.09	37.03	1004.09	82.37	0	1423.99	7919.49	0	0	41513.71	37181.63
									Total	198042.94	183469.09
										Profit	14573.84

The actual revenues with and without the hydrogen-storage system are shown in Tab. 5.9, together with the resulting profit, which is the sum of the differences between the revenues with and without the hydrogen-storage system. Observe that the profit is negative for the first hour of system operation, since the electricity is being bought and stored as hydrogen in this period; however, profit becomes positive in the second hour when the hydrogen is sold to the market. One can readily show that the electrolyzer is utilized when one of these two conditions is fulfilled:

- electricity buying costs are lower than the incomes from electricity, oxygen and heat sales according to (5.7); this condition is based on the electricity-to-electricity conversion route;

- electricity buying costs are lower than the hydrogen and oxygen incomes, which are based on the electricity-to-hydrogen conversion route.

The latter condition can be derived as follows. The basic condition that hydrogen and oxygen sales should provide revenues higher than the electricity costs can be formulated as:

$$R_{OXY} + R_{HYD} > C_B \tag{5.12}$$

where R_{HYD} is referred to as the revenues from hydrogen sales. The above equation can be expanded with the respective equations depicting the electricity-to-hydrogen and electricity-to-oxygen efficiencies as in the following equation:

$$\frac{\mu_{oe} \cdot c^{O}}{\left(1+\frac{\mu_{oe}}{\mu_{oc}}+\frac{\mu_{he}}{\mu_{hc}}\right)} \cdot \hat{P}_i^{CH} + \frac{\mu_{he} \cdot c^{HYD}}{\left(1+\frac{\mu_{oe}}{\mu_{oc}}+\frac{\mu_{he}}{\mu_{hc}}\right)} \cdot \hat{P}_i^{CH} > c_{p,i}^{M} \cdot \hat{P}_i^{CH} \quad \text{for } i < j \tag{5.13}$$

Lastly, the above equation can be reduced as follows:

$$c_{p,i}^{M} < \frac{\mu_{oe} \cdot c^{O} + \mu_{he} \cdot c^{HYD}}{\left(1+\frac{\mu_{oe}}{\mu_{oc}}+\frac{\mu_{he}}{\mu_{hc}}\right)} \quad \text{for } i < j \tag{5.14}$$

According to (5.14), hydrogen is bought at prices for electricity lower than 89.62 CAD/MWh, based on hydrogen and oxygen prices and the electrolyzer and compressor efficiencies defined in Chapter 4. Fuel cells, on the other hand, are again utilized depending on two conditions:

- electricity buying costs are lower than the incomes from electricity, oxygen and heat sales according to (5.7); this is the same condition as for electrolyzers and describes the electricity-to-electricity conversion route;
- hydrogen costs are lower than electricity and heat revenues according to the hydrogen-to-electricity conversion route.

The latter is based on the following condition:

$$R_{HEAT} + R_{ELEC} > C_{HYD} \tag{5.15}$$

Expanding equation (5.15) with the corresponding efficiencies and prices we obtain the following equation describing the second condition for the fuel-cell utilization:

$$c^{HYD} \cdot \mu_{ef} \cdot \hat{P}_i^{DIS} < c^{HEAT} \cdot \frac{\mu_{ef}}{\mu_{hf}} \cdot \hat{P}_i^{DIS} + c_{p,i}^{M} \cdot \hat{P}_i^{DIS} \tag{5.16}$$

The above can be reduced as follows:

$$c_{p,i}^{M} > c^{HYD} \cdot \mu_{ef} - c^{HEAT} \cdot \frac{\mu_{ef}}{\mu_{hf}} \tag{5.17}$$

According to (5.17) one can calculate that the minimum electricity price, if the fuel cells are to be utilized, is 266.80 CAD/MWh for the assumed fuel-cell electrical and heat efficiencies and based on the given prices of heat and hydrogen; this is consistent with the simulation results, which indicate that the fuel cells are seldom utilized (only when electricity prices are high).

5.2.2.2 Base-Case Scenario

The results for the BCS are presented in Tab. 5.10 and show the profitability of a hydrogen-storage system for all four sub-scenarios. The MIRR is shown to be about 3-4% higher compared to the scenario without oxygen and heat utilization presented in Tab. 5.5, which makes the option of using oxygen and heat more economically attractive. The low utilization of stationary fuel cells and the higher profitability of the hydrogen system without stationary fuel cells suggest that fuel cells are redundant, despite the additional heat utilization; the same can be observed in the scenario without oxygen and heat use. Thus, the hydrogen system is mainly utilized for hydrogen-production purposes rather than electricity storage in both cases. It can be further concluded from Tab. 5.10, that the price-forecast error does not have any considerable impact on the system economics; however, for different hydrogen and electricity prices and efficiencies, these forecasts might have a more significant effect.

Tab. 5.10: Results for BCS Considering FC and FE

FACTOR	FC/FE	NFC/FE	FC/NFE	NFC/NFE
Profit [CAD/year]	32’013,388	31’994,948	32’013,389	31’994,948
Utilization FC [%]	0.057	/	0.057	/
Utilization EL [%]	95.40	95.40	95.40	95.40
Investment costs [CAD]	160’020,166	139’090,166	160’020,166	139’090,166
O/M costs [CAD/year]	3’200,403	2’781,803	3’200,403	2’781,803
NPV [CAD]	62’248,598	82’783,723	62’248,607	82’783,723
MIRR [%]	12.48	13.91	12.48	13.91

The nominal cash flow and discounted cumulative cash flow of the scenario without fuel cells with a forecasting error are presented in Fig. 5.20. The change in the cash flow in year 10 is due to the replacement of the electrolyzers because of their relatively short lifetime.

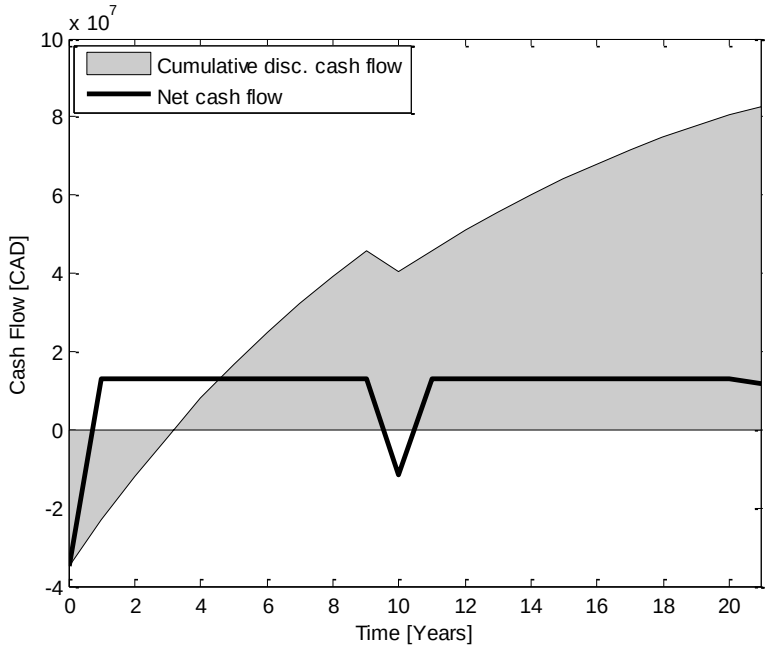

Fig. 5.20: Nominal cash flow and discounted cumulative cash flow for the scenario without stationary fuel cells.

5.2.2.3 Sensitivity Analyses

The sensitivities with respect to the following parameters were studied in the current chapter:

- the electrolyzer hydrogen and fuel-cell electrical efficiencies;
- the hydrogen selling prices;
- the oxygen selling prices;
- the investment costs reduction.

The impact of equipment prices was studied considering fuel cells as part of the system, which is a conservative assumption, since the results from the BCS suggest that the profitability is higher when fuel cells are disregarded. The results of the previous analyses show no considerable dependency on the price-forecast errors; hence, these errors were not considered in the studies presented here.

Firstly, possible technical advances of electrolyzers and fuel cells are investigated, where electrolyzer hydrogen efficiencies are varied from 60% to 90%, simultaneously with fuel-cell efficiencies, changing from 45% to 60%. The utilization of fuel cells on the hydrogen system's economics is negligible according to the results. In Fig. 5.21, the profit and the number of full-load electrolyzer operating hours are presented with respect to electrolyzer and fuel-cell efficiencies. The results show a strong and almost linear dependency of profit with respect to efficiencies.

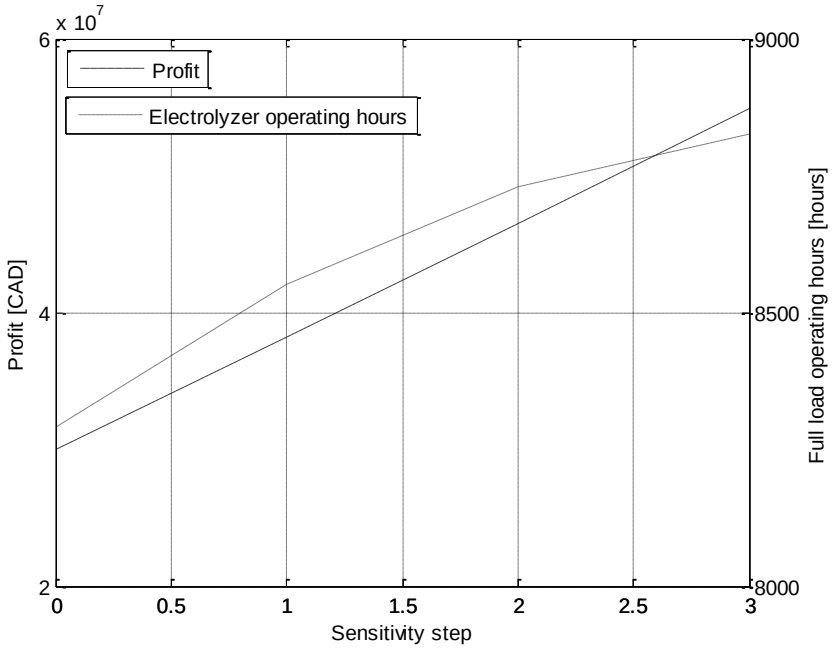

Fig. 5.21: Profit and electrolyzer utilization with respect to the increase of the electrolyzer and fuel-cell efficiency.

One can see in Fig. 5.22 that the profits obtained from the utilization of the hydrogen system suffice for the system to be profitable enough for the whole range of electrolyzer hydrogen efficiencies.

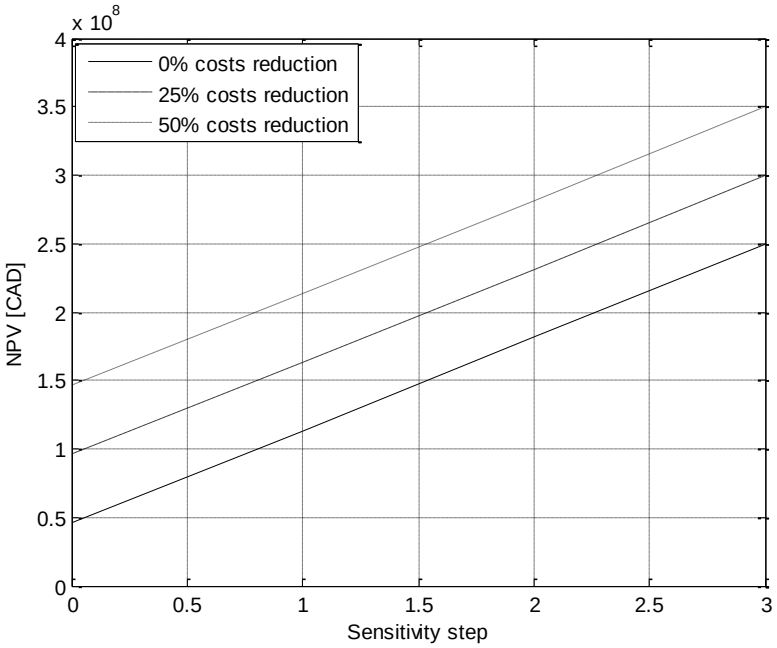

Fig. 5.22: NPV with respect to the increase of the electrolyzer and fuel-cell efficiency.

Since hydrogen prices may vary in the future, depending on the developments of hydrogen markets and in general on the hydrogen economy, the impact of different hydrogen selling prices are investigated in this chapter; these prices are assumed to vary from 2 to 8 CAD/kg. The actual level of these prices is dependent on the consumption levels of the developing hydrogen economy. If no major technical breakthroughs in hydrogen-economy technologies (e.g., hydrogen cars) occur, the hydrogen market might be shallow and would not sustain large-scale hydrogen production and thus high hydrogen prices. If, on the other hand, hydrogen consumption increases due to possible technical as well as economic superiority of hydrogen technologies, hydrogen prices are expected to reach favorable levels.

The utilization rates and profits with respect to different hydrogen selling prices are shown in Fig. 5.23. Again, an almost linear dependency of profit with regards to hydrogen selling price can be observed with the electrolyzer utilization reaching almost 100% at hydrogen prices above 6 CAD/MWh.

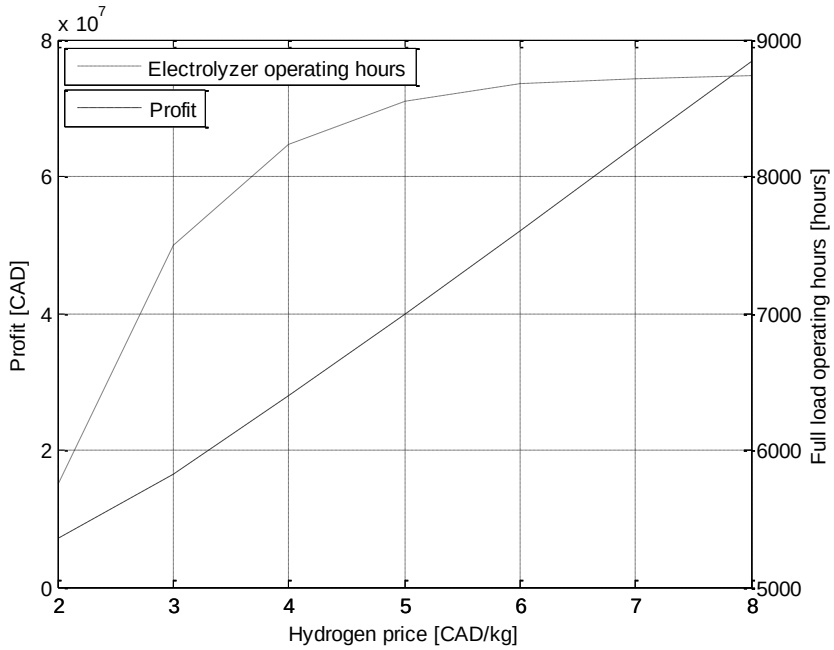

Fig. 5.23: Profit and electrolyzer utilization with respect to hydrogen selling prices.

The corresponding NPV indices are presented in Fig. 5.24 for different equipment cost reductions. Notice that the NPV should be above a 0 CAD threshold for the hydrogen system to be economically viable. This happens at hydrogen prices of 3.7 CAD/MWh, 3.2 CAD/MWh and 2.6 CAD/MWh for 0%, 25% and 50% equipment-cost reductions, respectively. A comparison of these results and the results of the sensitivity analyses without oxygen and heat sales show that the hydrogen price can be about 0.6 CAD/kg lower if heat and oxygen are also utilized and sold to the respective markets at assumed prices.

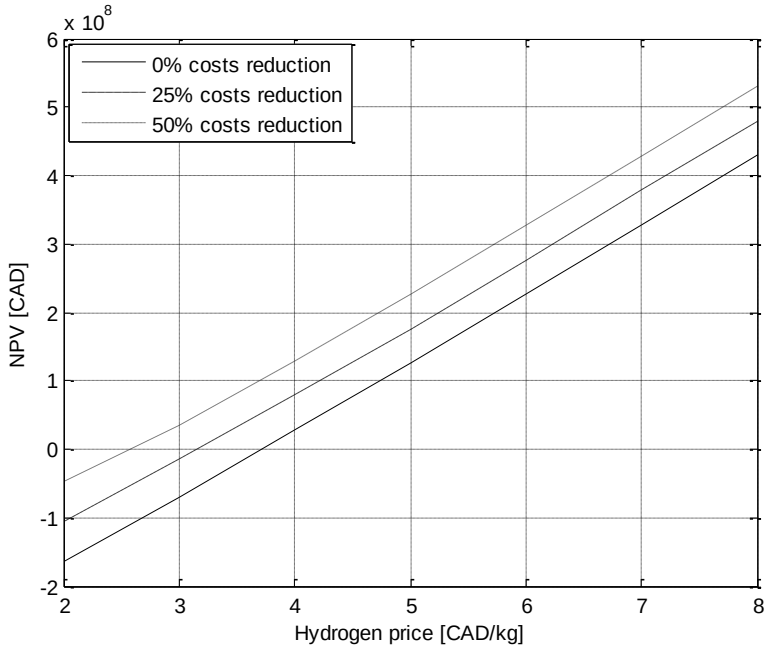

Fig. 5.24: NPV with respect to hydrogen selling prices.

Oxygen prices are also subject to market forces and cannot be predicted in a reliable manner; thus, the impact of oxygen prices varying from 0.05 to 0.3 CAD/Nm^3 is investigated here. The resulting profits and electrolyzer utilizations are presented in Fig. 5.25, and the corresponding NPV factors in Fig. 5.26.

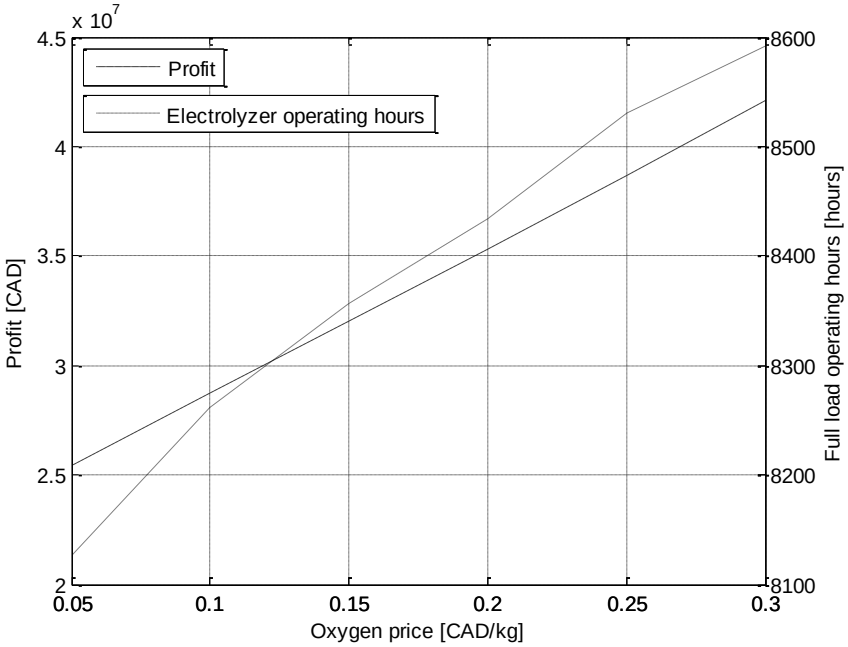

Fig. 5.25: Profit and electrolyzer utilization with respect to oxygen selling prices.

One can observe from Fig. 5.25 that the profits are strongly correlated with the oxygen selling price; however, the correlation with the hydrogen price is even stronger; this can be explained

by a simple calculation, which shows that 14.42 CAD from oxygen sales and 75.20 CAD from hydrogen sales is earned for each MWh that is consumed by the electrolyzers. Observe from Fig. 5.26 that the system is economically acceptable for all oxygen prices, since the NPV is always above the 0 CAD threshold. However, the correlation between the economics of the hydrogen system and oxygen prices remain substantial and oxygen should be thus considered in any new hydrogen-system investment.

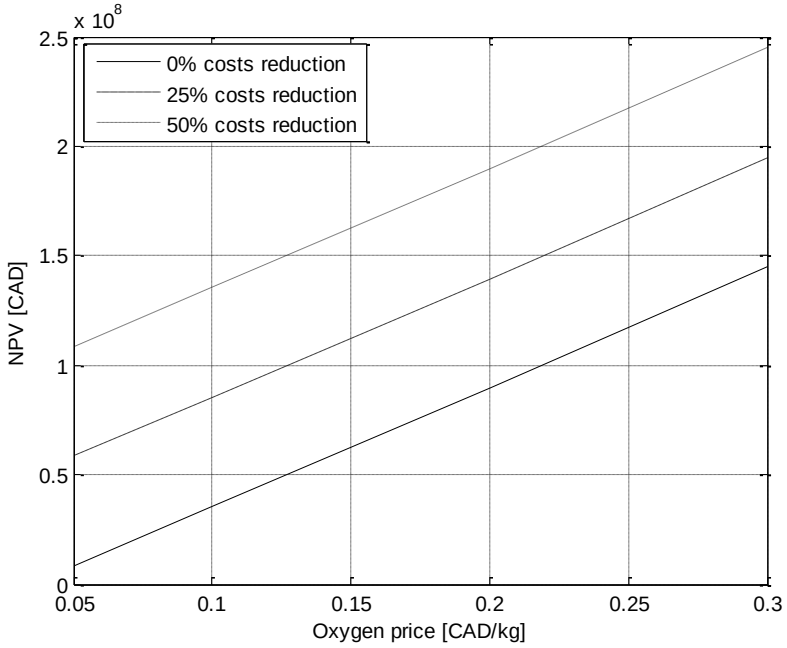

Fig. 5.26: NPV with respect to oxygen selling prices.

5.3 Hydrogen storage as an alternative to transmission expansion

In this scenario, Bruce power's nuclear power plant's reactor B is assumed to be refurbished, giving the power plant a constant production of 5207 MW as described in Chapter 4.5. With an assumed transmission system capacity of 5000 MW, a production surplus of 207 MW is assumed to be available from the nuclear power plant. With the addition of 76 MW from the Ripley wind farm, the installed capacity of the hydrogen subsystem is assumed to be 283 MW to account for the potential lack of transmission capacity. The suitable hydrogen subsystem for storing this amount of excess electricity is therefore modified and is assumed to consist of 907 electrolyzers with a maximum electricity consumption of 261.22 MW and a total hydrogen production capacity of 4892 kg/h and oxygen production capacity of 27209 Nm^3/h; the hydrogen and oxygen compressor stack is assumed to consume the rest of the 21.78 MW of electricity; it consists of three compressors for hydrogen compression and an additional three compressors for oxygen compression. The operational optimization model described in Chapter 4.9 is used in this chapter.

5.3.1 Base-Case Scenario

The results for the congestion scenario studies are shown in Tab. 5.11. They show very high profits due to the utilization of free electricity, which would otherwise be lost due to a lack of transmission capacities. Hence, the overall profitability of the nuclear-wind-hydrogen system is higher than in scenarios without line congestions where the electricity price for hydrogen production was equal to the electricity market price. As there is no forecasting, since the operation of the hydrogen system is solely real-time price dependent, the forecast errors do not have any impacts on the system's operation and profits.

Tab. 5.11: Results for Base Case Scenario.

FACTOR	NFE
Profit [CAD/year]	202'565,891
Utilization FC [%]	99.14
Utilization EL [%]	/
Investment costs [CAD]	475'455,009
O/M costs [CAD/year]	9'509,100
NPV [CAD]	1'046'296,770
MIRR [%]	20.40

5.3.2 Sensitivity Analysis

Some sensitivity analyses were carried out in this chapter to account for possible technology advances and price changes; the impact of the following parameters was analysed:

- the electrolyzer hydrogen efficiencies;
- the hydrogen prices;
- the oxygen prices;
- the investment costs reductions.

As in previous studies depicting the impacts of efficiency changes due to hydrogen-system components' development, the efficiency of the electrolyzers was varied from 60% to 90% in this chapter too. The results of these analyses are presented in Fig. 5.27. As expected, the profits and economic indices show a big market potential for this niche application of a hydrogen system, due to the utilization of free electricity. The possible price reductions are shown to improve the economics even further.

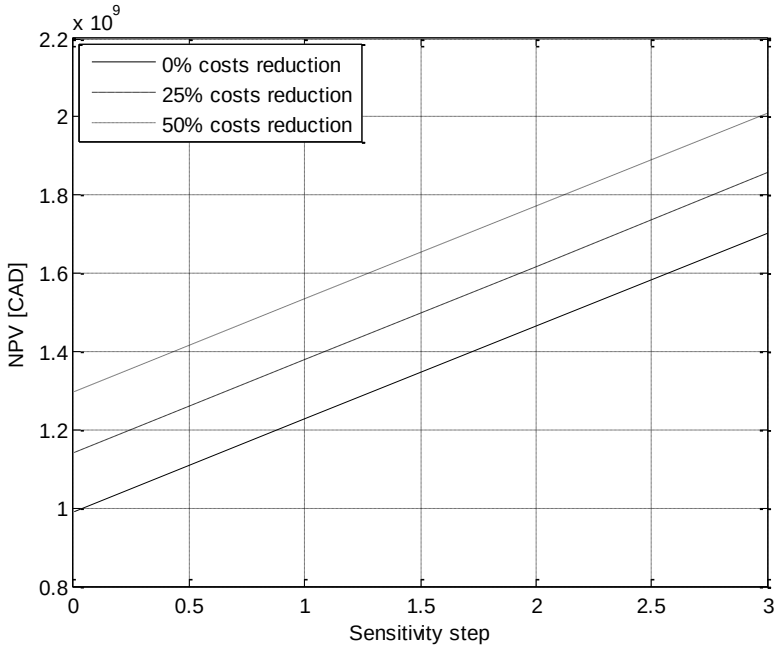

Fig. 5.27: NPV with respect to different electrolyzer hydrogen efficiencies.

The impact of possible future hydrogen-price fluctuations on the hydrogen system's economic performance was also assessed in this chapter. As before, the hydrogen prices were shifted between 2 CAD/kg and 8 CAD/kg, resulting in the NPV values presented in Fig. 5.28. The results show that free electricity also makes the hydrogen system profitable at very low hydrogen prices. Any further equipment price reductions would additionally improve the overall economics of the hydrogen system.

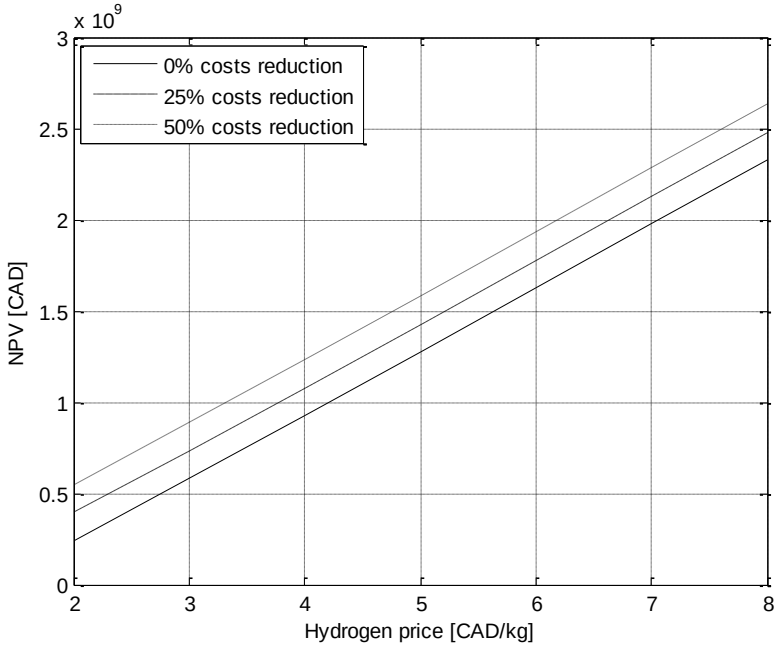

Fig. 5.28: NPV with respect to hydrogen selling prices.

Lastly, the hydrogen system's economics was tested against different oxygen prices. As in Chapter 5.2.2.3, the oxygen prices were altered between 0.05 to 0.3 CAD/Nm^3. The results presented in Fig. 5.29 show that cheap electricity again contributes to the economics of the system to the extent that the hydrogen system is economically acceptable for all the different oxygen prices.

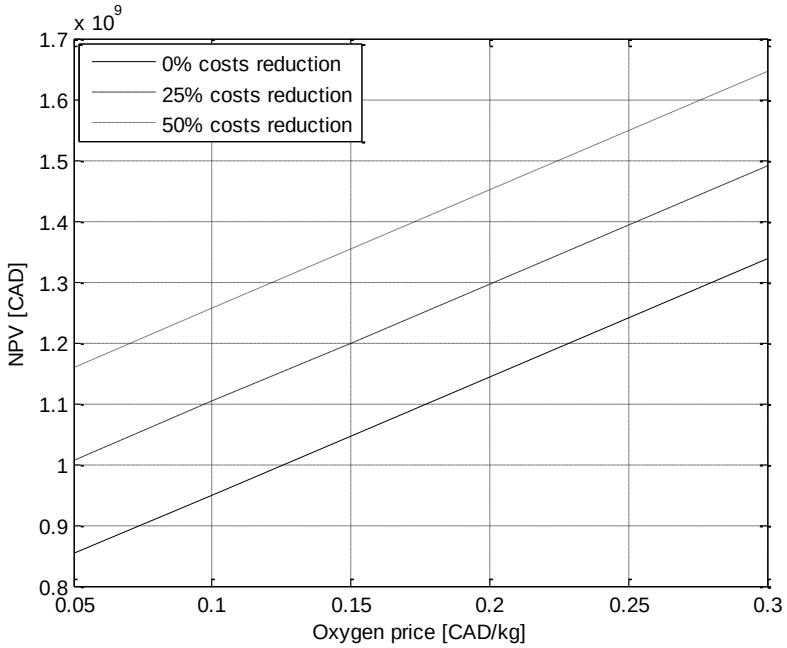

Fig. 5.29: NPV with respect to oxygen selling prices.

5.4 Hydrogen storage for transmission-congestion alleviation

In this chapter, the scenario considering the use of hydrogen storage for transmission-congestion alleviation is presented where the congestions are assumed to occur only periodically, as described in Chapter 4.10.

5.4.1 Scenario without the option of hydrogen sales

The required conditions for the hydrogen-system operation are basically the same as those described 5.2.1.1, where one should further consider the transmission capacity constraints. The results of the pre-dispatch and the real-time dispatch methodologies presented in Chapter 4.10.1 for a typical day with the constrained transmission capacity presented in Fig. 5.30 are depicted in Fig. 5.31 and Fig. 5.32.

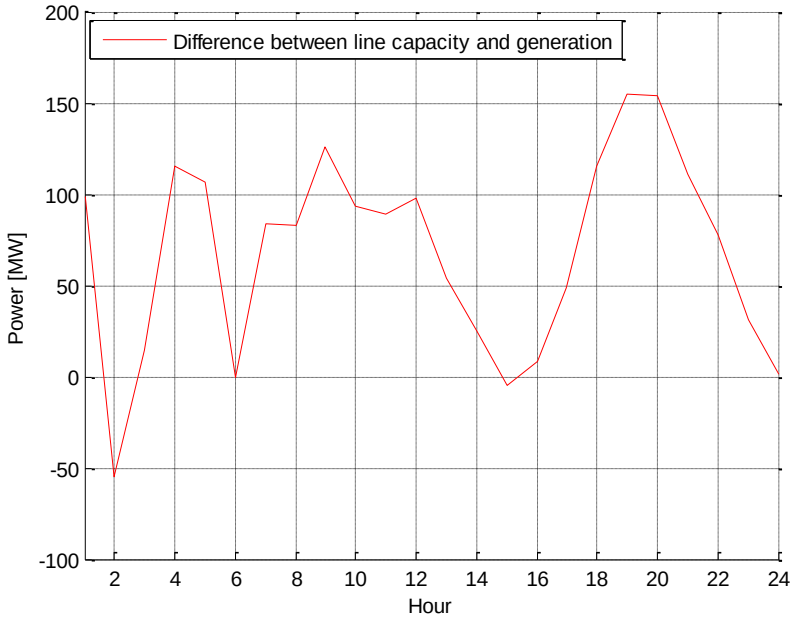

Fig. 5.30: Difference between transmission capacity and wind and nuclear generation in the Bruce area for a typical day (day 28).

As one can see from Fig. 5.31, the hydrogen system is operated in constrained hours 2, 6 and 15. The electricity consumption of the electrolyzers in hours 2 and 15 is limited to the energy that cannot be transmitted to consumers; this amounts to 54.9 MW and 4.9 MW for hours 2 and 15, respectively. The price difference between hours 6 and 19, on the other hand, is sufficient for the full-load operation of the electrolyzers and fuel cells.

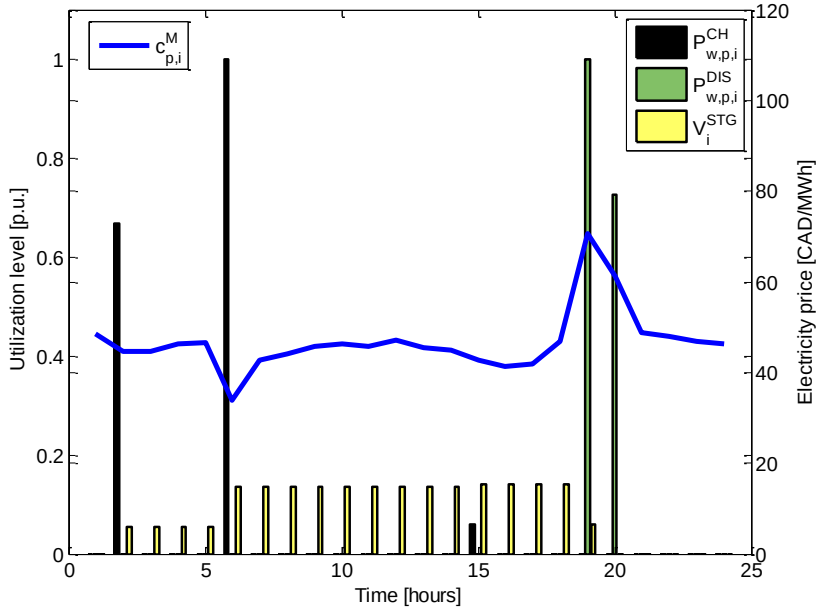

Fig. 5.31: Electrolyzer and fuel-cell operation and actual electricity prices for a typical transmission constrained day (day 28).

Observe from Fig. 5.32 that the operation of the hydrogen system on day 28 yields profits of about 2800 CAD, utilizing the price differences and the 60.20 MWh of electricity that would otherwise be wasted due to lack of transmission capacities.

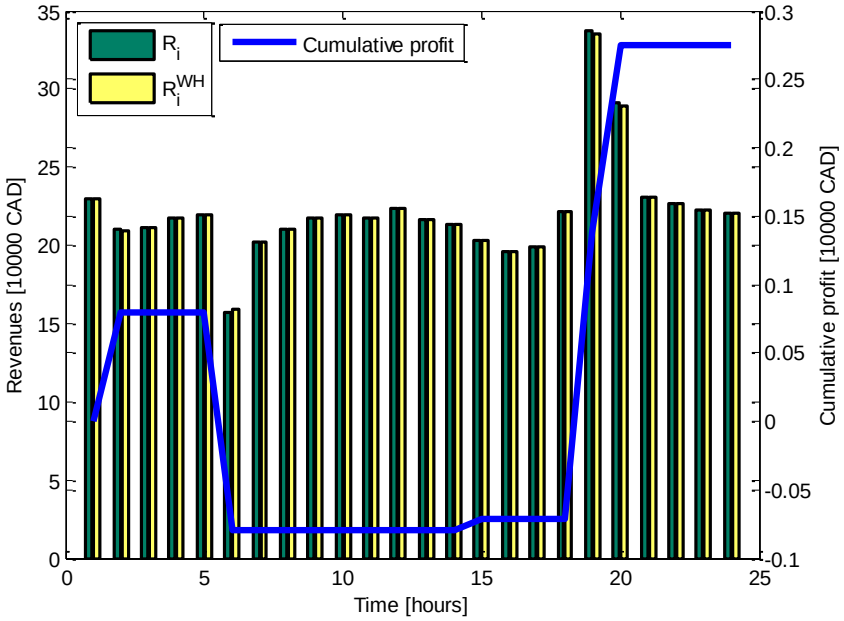

Fig. 5.32: The revenues with and without the hydrogen-storage system and the resulting cumulative profit for a typical capacity constrained day (day 28).

5.4.1.1 Base-Case Scenario

As in other chapters, the scenarios with and without forecasting errors are going to be studied in this chapter. The results of the optimization models presented in Chapters 4.10.1.1 and 4.10.1.2 and the economic evaluation model in 3.4 are presented in Tab. 5.6. Observe that annual additional profits of 87,925 CAD are obtained with respect to scenario 5.2.1.3 with only a slight improvement in the fuel-cell and electrolyzer utilization. However, this profit improvement is not sufficient to make the economics of the hydrogen system interesting for potential investors. One of the reasons is that the line is not congested frequently enough to provide sufficient free electricity for the hydrogen system to reach the economic margin. The impact of increased wind-generation capacity in the Bruce area, which would lead to further line congestions, on the hydrogen system economics is studied in the following chapter. One can also observe a considerable difference in profits and the utilization of the hydrogen system between the scenarios with and without a forecasting error. These differences, however, would not lead to different investment decisions in both scenarios. The cash flows for this base-case scenario are similar to those presented in Fig. 5.16.

Tab. 5.12: Economic parameters of hydrogen system with oxygen and heat sales.

FACTOR	With FE	Without FE
Profit [CAD/year]	1’998,013	2’046,656
Investment costs [CAD]	160’020,166	160’020,166
O/M costs [CAD/year]	3’200,403	3’200,403
Utilization FC [%]	25.26	26.95
Utilization EL [%]	25.28	26.98
NPV [CAD]	-213’908,923	-213’431,339
MIRR [%]	Neg.	Neg.

5.4.1.2 Sensitivity analyses

The economics with respect to the changes of several parameters is investigated in this chapter. The analyses were carried out to consider the following parameter deviations:

- the electrolyzer hydrogen and fuel-cell electrical efficiencies;
- the oxygen prices;
- the wind-generation capacity increase in the Bruce region;
- the investment costs reductions;
- the prices on a variety of electricity markets in various periods.

Forecasting errors were not considered in these analyses as they were shown not to influence the investment decisions. Firstly, the impact of possible future efficiency developments of the hydrogen system’s components with respect to hydrogen-system economics was assessed by a calculation of the respective NPV levels. The results obtained from these studies are depicted in Fig. 5.33. One can see that although the NPV increases rapidly with the efficiency improvements it still does not reach the desired zero margin, even at a 50% investment-cost discount.

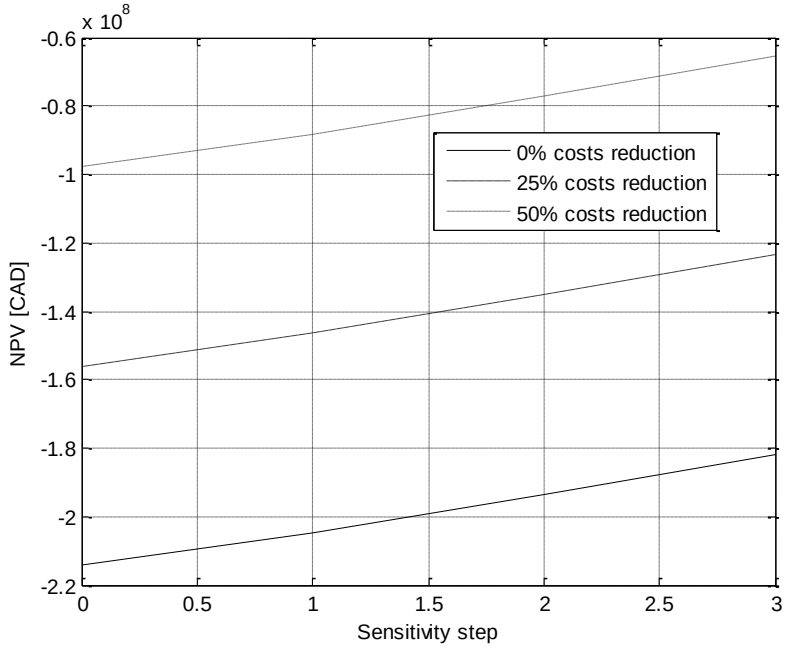

Fig. 5.33: NPV with respect to the efficiency step of the fuel cells and electrolyzers for different investment-cost reduction scenarios.

Furthermore, the economic behaviour of the hydrogen system with regard to several oxygen price levels was investigated by a calculation of the respective NPV indices, which was carried out for three different investment-cost reduction scenarios. The results of these studies are presented in Fig. 5.34 and show that the oxygen sales at all the different price levels do not provide sufficient profits for the hydrogen system to become economically feasible. One can interpret this also as the low sensitivity of the hydrogen-system economics to the different oxygen price levels.

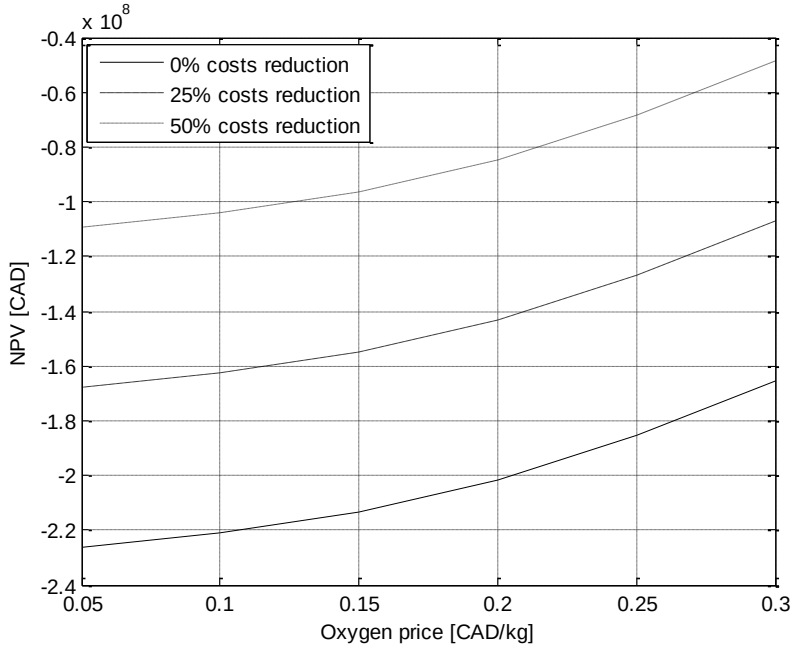

Fig. 5.34: NPV with respect to oxygen selling prices.

As several new wind projects with an additional capacity of almost 1000 MW are expected to be completed in the forthcoming years in Ontario [55], this might put additional strain on the transmission system and thus several congestions can emerge if the transmission system is not going to be refurbished or upgraded. As the profits and economics of the hydrogen system strongly depend on the frequency of the occurrence of congestions and congestion levels, this scenario might therefore present a new opportunity for the hydrogen system, which might become economically feasible if all the mentioned assumptions are fulfilled. Thus, the wind capacity is expanded for the factors between 1 and 10, i.e., 76 MW to 760 MW of installed capacity, and the corresponding NPV are calculated for the hydrogen system, which is assumed to have the constant capacity assumed so far. The results of these studies are thus depicted in Fig. 5.35; they show considerable improvements in the economics of the hydrogen system due to the increase in the line congestion frequency and severity. However, these additional profits are not sufficient for the hydrogen system to become viable, even at highest investment cost discounts and congestion levels.

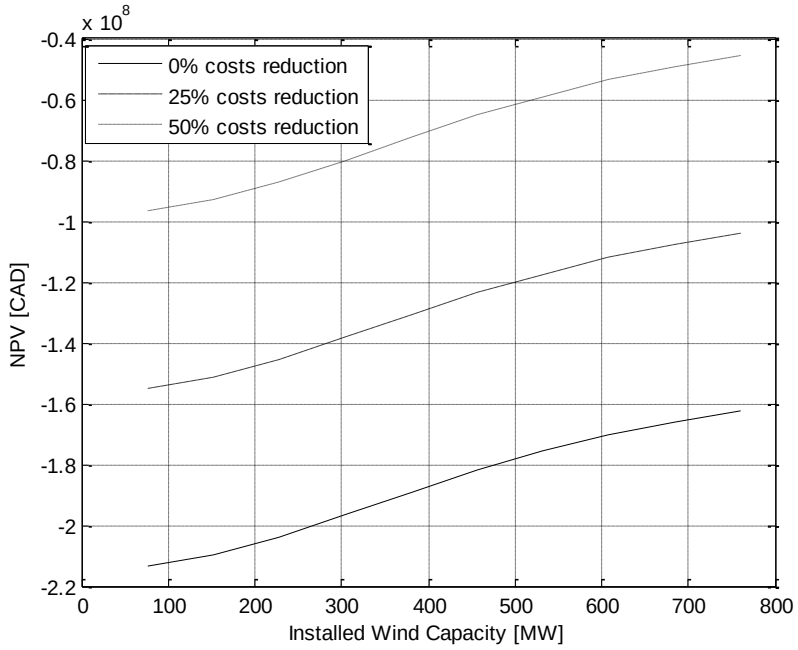

Fig. 5.35: NPV with respect to the increase of the installed wind capacity.

5.4.2 Scenario with the option of hydrogen sales

The required conditions for the hydrogen-system operation are equal to those in Chapter 5.2.1.1 modified by additional transmission capacity constraints. The typical results of the pre-dispatch and real-time dispatch phases, calculated with models described in Chapter 4.10.2, are depicted in Tab. 5.13 and Tab. 5.14. As one can see, the price differences are not sufficient for fuel cells to be utilized; this is an overall observation leading again to extremely low fuel-cell utilization levels, as will be presented in the next chapter.

Tab. 5.13: The Pre-Dispatch Results for the Simple Test Case

p	i	$c^{M}_{p,i}$	$P^{GA}_{w,i}$	$P^{NET}_{\max,i}$	$P^{G}_{w,p,i}$	$P^{CH}_{w,p,i}$	$P^{DIS}_{w,p,i}$	$V^{H}_{w,p,i}$	V^{STG}_{i}
1	1	42,82	4746,50	4844.87	4746,50	82,37	0	0	1423,99
1	2	41,19	4742,64	4687.71	4742,64	82,37	0	0	2847,98
1	3	46,32	4724,08	4738.65	4724,08	82,37	0	0	4271,97
1	4	32,39	4697,70	4813.01	4697,70	82,37	0	5695,97	0
2	1	33,88	4746,50	4844.87	4746,50	82,37	0	0	1423,99
2	2	31,26	4742,64	4687.71	4742,64	82,37	0	0	2847,98
2	3	58,07	4724,08	4738.65	4724,08	82,37	0	0	4271,97
2	4	52,66	4697,70	4813.01	4697,70	82,37	0	5695,97	0

Notice that the network capacity in the second operational hour is insufficient to transmit the produced electricity. Thus, the hydrogen system converts the surplus electricity into hydrogen, which is sold in hour 4 to the hydrogen market. The hydrogen system is fully utilized in hour 3 due to favorable electricity prices. The profits obtained in these 4 hours due to the utilization of the hydrogen system amount to 16823.76 CAD.

Tab. 5.14: The Real-Time Results for the Simple Test Case

i	$\hat{P}_i^{GA}$	$\hat{c}_i^M$	$\hat{P}_i^G$	$\hat{P}_i^{CH}$	$\hat{P}_i^{DIS}$	$\hat{V}_i^H$	$\hat{V}_i^{STG}$	$\hat{R}_i$	$\hat{R}_i^{WH}$
1	4746.50	48.41	4844.87	82.37	0	0	1423.99	226978.56	229778.23
2	4742.64	44.67	4687.71	82.37	0	0	2847.98	209362.12	209400.39
3	4724.08	44.67	4738.65	82.37	0	0	4271.97	208533.05	211024.65
4	4697.70	46.28	4813.01	82.37	0	5695.97	0	239562.84	217409.55
							Total	884436.57	867612.83
								Profit	16823.75

5.4.2.1 Base-Case Scenario

The basic, most realistic scenario is the base-case scenario, which considers the hydrogen-system model described in 4.10.2. As the hydrogen system is now expected to be used mostly for hydrogen production, scenarios with and without fuel cells are considered.

Tab. 5.15: Results for BCS Considering FC and FE

FACTOR	FC/FE	NFC/FE	FC/NFE	NFC/NFE
Profit [CAD/year]	32’150,372	32’131,931	32’150,372	32’131,931
Utilization FC [%]	0.057	/	0.057	/
Utilization EL [%]	95.42	95.42	95.42	95.42
Investment costs [CAD]	160’020,166	139’090,166	160’020,166	139’090,166
O/M costs [CAD/year]	3’200,403	2’781,803	3’200,403	2’781,803
NPV [CAD]	63’371,611	83’906,727	63’371,611	83’906,727
MIRR [%]	12.54	13.96	12.54	13.96

Once more a limited dependency of the NPV with regards to the forecasting error can be observed. Also, the hydrogen system is again shown to be utilized solely for hydrogen production due to specific oxygen, hydrogen, heat and electricity price relations. The profits are shown to increase only slightly (by about 150,000 CAD) in comparison with the results of the scenario without line congestions listed in Tab. 5.10. These profit changes slightly improve the overall economics of the hydrogen system. Considerable improvements, however, can be expected in the case of more frequent line congestions, which is going to be considered in the sensitivity analyses chapter. The differences in the discounted cumulative cash flows are depicted in Fig. 5.36; they once more confirm the redundancy of fuel cells in the hydrogen system.

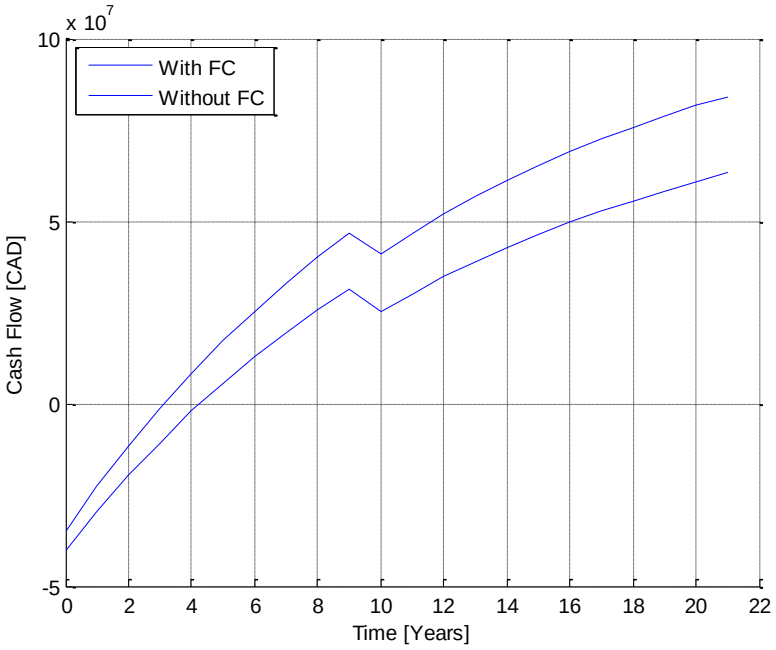

Fig. 5.36: Discounted cumulative cash flows for scenarios with and without stationary fuel cells.

5.4.2.2 Sensitivity Analyses

The assessment of correlations between the economics and the following parameters was carried out in this chapter:

- the electrolyzer hydrogen and fuel-cell electrical efficiencies;
- the hydrogen selling prices;
- the oxygen selling prices;
- the wind capacity;
- the investment costs reduction.

A conservative scenario for the hydrogen-system setup is considered, assuming fuel cells to be a part of the hydrogen system. Based on some of the above results, the forecasting error was not considered in the analysis.

The dependency of the hydrogen system's economics, i.e., the NPV, with respect to various fuel-cell and electrolyzer efficiencies was considered first with a simultaneous electrolyzer and fuel-cell efficiency variation, described in the previous sensitivity analysis chapters. The results obtained in Fig. 5.37 show a considerable correlation of the economics, efficiencies and cost discounts; however, these correlations are not strong enough to jeopardize the economic feasibility of the hydrogen system.

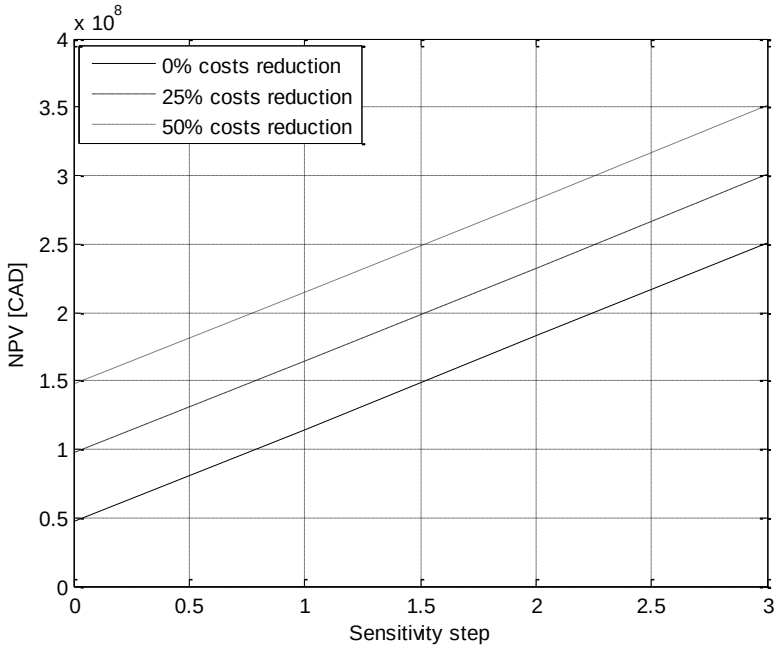

Fig. 5.37: NPV with respect to the increase of the electrolyzer and fuel-cell efficiency.

On the other hand, the hydrogen price sensitivity analysis shows a very strong dependency of the NPV on hydrogen prices. Thus, only prices of hydrogen above 2.5 CAD/kg, 3.2 CAD/kg 3.7 CAD/kg, for investment costs reductions of 0%, 25% and 50%, respectively, ensure the profitability of the hydrogen system. This profitability, however, rapidly improves with hydrogen prices above these marginal levels.

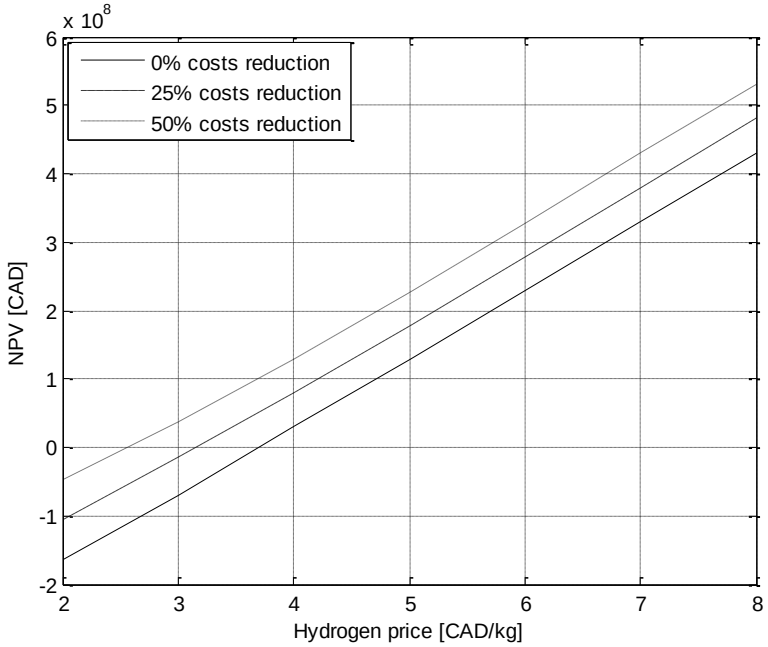

Fig. 5.38: NPV with respect to hydrogen selling prices.

In Fig. 5.39, the oxygen price is shown not to be the key parameter in the economics of the hydrogen system although the dependency of the NPV upon oxygen prices is considerable. This can be concluded since the NPV does not get below the zero margin for the studied oxygen price range and costs discounts. Observe also that the NPVs in these scenarios are shifted slightly upwards if compared with the results of the scenario without line congestions depicted in Fig. 5.26.

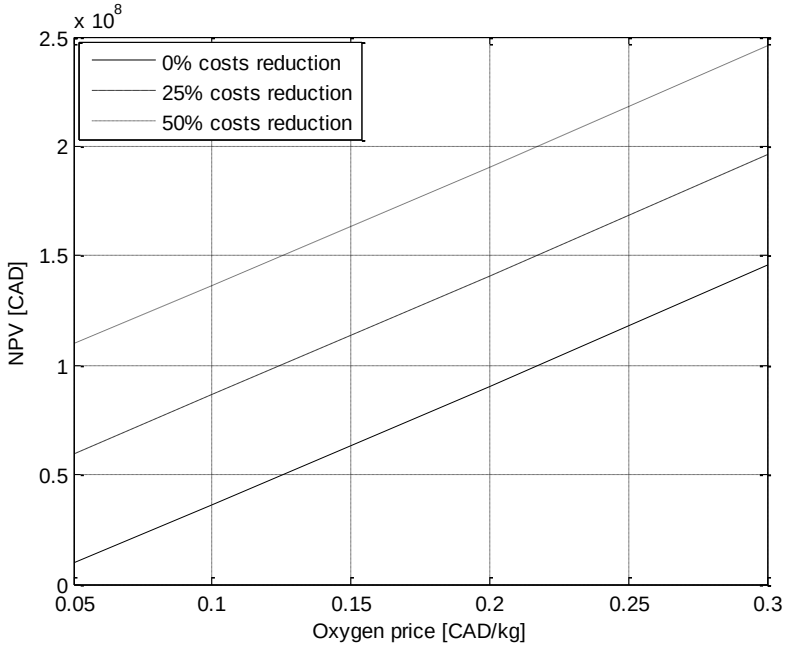

Fig. 5.39: NPV with respect to oxygen selling prices.

The economic potential of the hydrogen system, in the context of possible wind-generation developments described in 5.4.1.2, is depicted in Fig. 5.40. As expected, the hydrogen sales improve the profits of the hydrogen system to an economically acceptable level and the additional profits from free energy in the congestion periods further improve the already satisfactory economics. Any further investment cost reductions would only improve the economics of the hydrogen system.

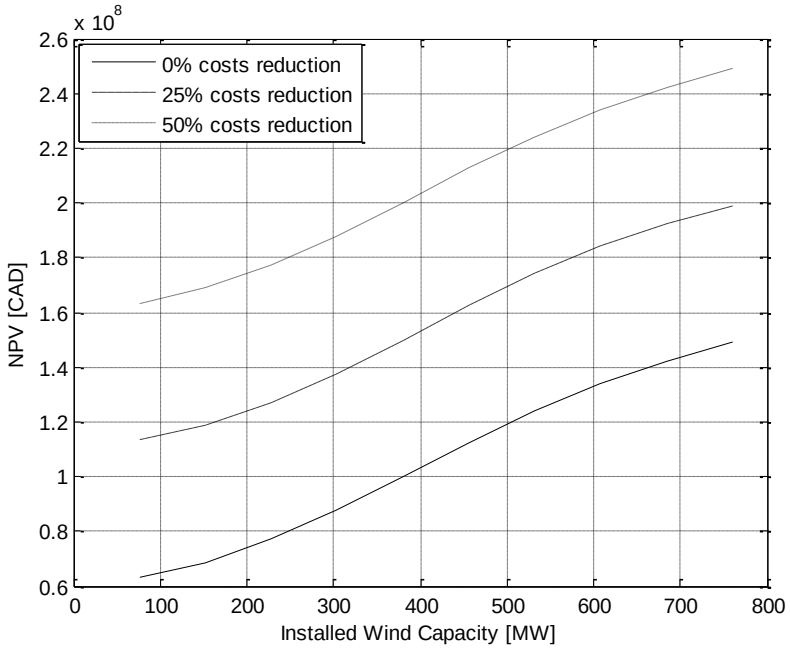

Fig. 5.40: NPV with respect to an increase of the installed wind capacity.

6 CONCLUSIONS

In the thesis, various techno-economic feasibility studies of a variety of hydrogen-utilization scenarios were carried out in the context of a Hydrogen Economy. Furthermore, these studies assumed an energy hub consisting of a wind-farm and a nuclear power plant. To assess the feasibility of the mentioned scenarios, a novel methodology has been developed, taking into account all the key technical as well as economic factors. This methodology was modified to consider the characteristics of each of the studied hydrogen-usage scenarios and was used to study the feasibility of a realistic wind-nuclear-hydrogen system located in Ontario, Canada.

In Chapter 4.7, a scenario considering a hydrogen system only as an electricity storage medium was evaluated, without any line congestions and the sales of any other byproducts from the hydrogen system's operation. The results for this scenario show that for the given realistic assumptions, hydrogen is presently not a viable option for electricity storage. This is mainly due to the low efficiencies of the hydrogen-storage system at the present state of technology development (around 25–30% compared to 70–80% efficiencies of pumped hydro storage) and investment costs (about 8000 CAD/kW of installed fuel-cell power compared to around 1000–1500 CAD/kW of pumped hydro storage). It is also shown that price- and wind-forecasting errors do not play a major role in the feasibility studies presented. Some sensitivity studies further show that the hydrogen system will not become economically feasible even at considerable price reductions and efficiency improvements as these do not considerably impact the overall hydrogen system's economics. The sensitivities with respect to electricity prices in different electricity markets in different periods show similar disadvantageous results.

The hydrogen system is shown to be profitable, however, if a hydrogen demand, i.e., sales to a prospective hydrogen market (e.g., for transportation applications), is considered; in that case, one can conclude from the studies presented in Chapter 4.7.2, that it might be viable to produce hydrogen from electricity and invest in hydrogen-production equipment in an existing mixed wind-nuclear energy hub at favorable hydrogen prices. These prices, however, are strongly correlated with the hydrogen demand levels and thus the technical and economical development of technologies that constitute the hydrogen economy. In this context, some sensitivity analyses confirm that the hydrogen system is most profitable if used solely for hydrogen production. These further show a strong positive correlation of the NPV index with respect to hydrogen prices, electrolyzer efficiencies and equipment price reductions. The economics of the hydrogen system is shown to depend heavily upon hydrogen prices; these determine whether the profits are sufficient for the investment to be economically feasible.

The impact of the utilization of oxygen and heat, which are the byproducts of the hydrogen system's operations, on the hydrogen system's economics is studied in Chapter 4.8. The results show that a hydrogen system for the sole purpose of electricity storage is not economically viable, despite additional profits obtained from oxygen and heat sales. The sensitivity analyses carried out to assess the correlation between variations of different parameters and economic indices show considerable improvements in profitability of the hydrogen system; however, these are shown to be insufficient for the hydrogen system to become economically acceptable.

The results of the economic assessment of a hydrogen system, making profits from oxygen, hydrogen and heat sales, are depicted in 4.8.2. They show economic feasibility with high rates of return and considerably higher profitability when heat and oxygen are utilized and the hydrogen can be sold directly to the hydrogen market, in comparison with the scenario 4.7.2, were the oxygen and heat are not anticipated to be utilized. The results further show, similar to those in 4.7.2, that stationary fuel cells for this system are not justifiable; thus, the hydrogen system is mainly used for the production of hydrogen and oxygen rather than electricity storage. Different parameter variations such as efficiencies, oxygen price and investment costs are shown not to threaten the overall economic viability of the hydrogen system; the only exception is the hydrogen price, which is of critical importance for the hydrogen system's economics.

A developed hydrogen economy facilitating a hydrogen market for a large-scale hydrogen production with different transportation options may be an alternative for grid expansion as presented in Chapter 4.9, especially in locations where the transmission system expansion is not an option due to environmental, local or other reasons. As the electricity is assumed to be supplied by an already operational local power producer, who would otherwise be forced to shed the surplus electricity due to insufficient transmission capacity, the hydrogen system economics is shown to be highly profitable. The sensitivity analyses show positive results, not only for oxygen and efficiency variations but also for assumed hydrogen price deviations.

Chapter 4.10 analyses the scenario with limited intermittent congestions in the transmission grid, which is a possible scenario for the Bruce region, as opposed to the scenario with constant congestion in Chapter 4.9. Without the direct sales of hydrogen to a prospective hydrogen market, this scenario shows that also increased profits due to free electricity in periods of line congestions do not suffice for an economically viable hydrogen-system utilization. Furthermore, some sensitivity analyses show that the economics of the hydrogen system is not achieved even for a considerable oxygen price increase and investment costs decrease. As it was expected that the planned increase of wind capacity in the Bruce area would increase the congestion frequency and thus the profitability of the hydrogen system, this scenario was also studied in the sensitivity analyses. The profit increase, however, proved

to be insufficient to make the hydrogen system economically viable, although the economics improved considerably.

If a hydrogen sales option is added to the intermittent congestion scenario in 4.10.1, the profitability of the hydrogen system is shown to increase beyond the economically acceptable margin, according to the results presented in chapter 4.10.2. Sporadic congestions, in this scenario, force the surplus electricity production to be converted to hydrogen and sold to the hydrogen market or sold to the electricity market during later hours with adequate transmission capacities. This scenario is shown to be the most profitable scenario as the hydrogen system is making a profit from hydrogen, oxygen, heat and electricity sales, with free electricity supplied during periods of transmission congestion. The hydrogen price, however, is still shown to be of critical importance for the hydrogen system's economics in the sensitivity analysis chapter.

6.1 Overall conclusions

A novel methodology for the economic evaluation of various hydrogen applications in power systems is presented in this thesis, which was applied to several realistic scenarios in the Bruce area in Ontario, Canada.

One can conclude from the results that hydrogen is not feasible for the sole purpose of storing electrical energy, especially not against other alternative storage options (e.g., pumped storage). This statement holds even if byproducts such as oxygen and heat are utilized, efficiencies are considerably improved, investment costs drop or if the transmission system is frequently congested.

The hydrogen system, on the other hand, is shown to be technically, environmentally and economically a very good hydrogen production option, which however heavily depends on stable and high hydrogen prices that can be only expected if a large-scale hydrogen economy (especially its transportation sector) is to emerge in the future. The key role in this hydrogen-economy development is going to be played by the advances in battery technology in the context of the so called "electron economy", which is seen as the main competitor of the hydrogen economy – especially in the mobility sector.

Hydrogen can also be successful at small-scale levels for special niche applications such as in providing back-up power for buildings, battery packs for consumer electronics devices, and fuel for fork-lift trucks.

6.2 Directions for future work

In future research there is a need to focus on the application of the proposed models and the analysis methodology for other possible system configurations and issues. For instance, an optimal sizing methodology might provide investment levels in which a hydrogen system might improve its overall economics. Furthermore, the hydrogen system is also technically capable of operations in the ancillary services market, e.g., the spinning reserve, where additional profits might considerably improve the economics of the hydrogen system. There are also further niche applications that have to be studied, such as distant off-shore wave and wind farms, where the hydrogen might be produced at a better economic efficiency than electricity due to the high electricity-transmission costs.

6.3 Scientific contributions

- Novel methodology for modeling of a power system, consisting of a wind farm, nuclear power plant and hydrogen system, connected to a bulk electric power system.
- Novel methodology for a two-stage stochastic dispatch optimization of a hydrogen system.
- Exact methodology for the economic evaluation of the use of hydrogen as an electricity storage medium in electric power systems.
- Economic evaluation of the use of hydrogen as an electricity storage medium in electric power systems with limited transmission capacities, i.e. the use of hydrogen as an alternative to the grid expansion.
- Evaluation of the impact of utilization of byproducts of hydrogen system operation, i.e. oxygen and heat, on the hydrogen system economics.

7 REFERENCES

[1] National Research Council and National Academy of Engineering, "The Hydrogen Economy: Opportunities, Costs, Barriers and R&D needs", The national Academies press, Washington, 2004.

[2] B. D. Shakyaa, Lu Aye, P. Musgrave, "Technical feasibility and financial analysis of hybrid wind–photovoltaic system with hydrogen storage for Cooma", International Journal of Hydrogen Energy, Vol. 30, pp. 9-20, 2005.

[3] A. I. Miller, R. B. Duffy, "Integrating large-scale co-generation of hydrogen and electricity from wind and nuclear sources (NUWIND ©)", IEEE EIC Climate Change Technology, pp. 1-9, May 2006.

[4] E. Troncoso, M. Newborough, "Implementation and control of electrolysers to achieve high penetrations of renewable power", International Journal of Hydrogen Energy, Vol. 32, pp. 2253-2268, 2007.

[5] I. Segura, A. Perez-Navarro, C. Sanchez, F. Ibanez, J. Paya, E. Bernal, "Technical requirements for economical viability of electricity generation in stabilized wind parks", International Journal of Hydrogen Energy, Vol. 32, pp. 3811-3819, 2007.

[6] D. B. Nelson, M. H. Nehrir, C. Wang, "Unit Sizing of Stand-Alone Hybrid Wind/PV/Fuel Cell Power Generation Systems", IEEE PES General meeting, Vol. 3, pp. 2116-2122, June 2005.

[7] M. Korpas, "Distributed energy systems with wind power and Energy Storage", PhD thesis, Trondheim 2004.

[8] M. Korpas, A. T. Holen, "Operation Planning of Hydrogen Storage Connected to Wind Power Operating in a Power Market", IEEE Transactions on Energy Conversion, Vol. 21, No. 3, 2006.

[9] M. Korpas, R. Hildrum, A. T. Holen, "Optimal Operation of Hydrogen Storage for Energy Sources with stochastic Input", IEEE Bologna PowerTech Conference, Bologna, Italy, June 23-26, 2003.

[10] A. Hajimiragha, C. Canizares, M. Fowler, M. Geidl, G. Andersson, "Optimal Energy Flow of Integrated Energy Systems with Hydrogen Economy Considerations", Bulk Power System Dynamics and Control – VII, Charleston, South Carolina, USA, August 19-24, 2007.

[11] G. Marban, T. Valdes-Solis, "Towards the hydrogen economy?", International Journal of Hydrogen Energy, Vol. 32, pp. 1625–37, 2007.

[12] U. Bossel, "Does a Hydrogen Economy Make Sense", Proceedings of the IEEE, Vol. 94, Issue 10, 2006.

[13] R. R. Sadhankar, J. Li, H. Li, D. K. Ryland, S. Suppiah, "Future Hydrogen Production Using Nuclear Reactors", IEEE EIC Climate Change Technology, pp. 1-9, 2006.

[14] C. W. Forsberg, "Hydrogen, nuclear energy, and the advanced high-temperature reactor", International Journal of Hydrogen Energy, Vol. 28, pp. 1073 – 1081, 2003.

[15] A. F. Burke, "Batteries and Ultracapacitors for Electric, Hybrid, and Fuel Cell Vehicles", Proceeding of the IEEE, Vol. 95, No. 4, 2007.

[16] A. Miller, R. Duffey, "Sustainable and economic hydrogen cogeneration from nuclear energy in competitive power markets", Energy, Vol. 30, pp. 2690-2702, 2005.

[17] D. Prischich, A. J. Ruddell, "Experience in the design, sizing, economics, and implementation of autonomous wind powered hydrogen production systems", International Journal on Hydrogen Energy 25, 2000.

[18] F. A. Felder, A. Hajos, "Using Restructured Electricity Markets in the Hydrogen Transition: The PJM Case", Proceedings of the IEEE, Vol. 94, No. 10, October 2006.

[19] P. H. Floch, S. Gabriel, C. Mansilla, F. Werkhoff, "On the production of hydrogen via alkaline electrolysis during offpeak periods", International Journal of Hydrogen Energy, Vol. 32, pp. 4641–4647, 2007.

[20] J. Matevosyan, L. Soder, "Minimization of Imbalance Cost Trading Wind Power on the Short-Term Power Market", IEEE Trans. on Power Syst., Vol. 21, No. 3, August, 2006.

[21] J. Gonzales, R. Moraga, L. Matres, A. Mateos, "Stochastic joint optimization of wind generation and pumped-storage units in an electricity market". [Online] Available: .<http://www.upcomillas.es/catedras/crm/descargas/proyectos_y_tesis/PFC/Energias%20limpias%20y%20renovables/ART%20LuzMatres%20-%20JGarcia%20y%20RMoraga.pdf>.

[22] G. Taljan, C. Cañizares, M. Fowler, G. Verbič, "The Feasibility of Hydrogen Storage for Mixed Wind-Nuclear Power Plants", IEEE Transactions on Power Systems, vol. 23, no. 3, august 2008.

[23] G. Taljan, M. Fowler, C. Cañizares, G. Verbič, "Hydrogen storage for mixed wind–nuclear power plants in the context of a Hydrogen Economy", International Journal of Hydrogen Energy, vol. 33, pp. 4463– 4475, 2008.

[24] G. Taljan, M. Fowler, C. Cañizares, G. Verbič, "Study of mixed wind-nuclear-hydrogen power plants", North American Power Symposium, Calgary, Canada, 2008.

[25] B. Kroposki, J. Levene, K. Harrison, F. Novachek, "Electrolysis: Opportunities for Electric Power Utilities in a Hydrogen Economy", 38th North American Power Symposium, 2006.

[26] B. C. R. Ewan, R. W. K. Allen, "A figure of merit assessment of the routes to hydrogen", International Journal of Hydrogen Energy, Vol. 30, pp. 809 – 819, 2005.

[27] R. H. Jones, G. J. Thomas, "Materials for the Hydrogen Economy", CRC Press, USA, 2007.

[28] W. Schnurnberger, W. Seeger, H. Steeb, "Selected hydrogen production systems", Hydrogen as an energy carrier: Technologies, systems, economy, Springer Verlag, Berlin, Germany, 1988.

[29] C. A. Schug, "Operational characteristics of high-pressure, high-efficiency water-hydrogen-electrolysis", International Journal of Hydrogen Energy, Vol. 23, 1998.

[30] A. G. Dutton, J. A. M. Bleijs, H. Dienhart, M. Falchetta, W. Hug, D. Prischich, A. J. Ruddell, "Experience in the design, sizing, economics, and implementation of autonomous

wind-powered hydrogen production systems", International Journal of Hydrogen Energy, Vol. 25, pp. 705-722, 2000.

[31] W. A. Amos, "Costs of Storing and Transporting Hydrogen", NREL, November, 1998.

[32] J. B. Taylor, J. E. Alderson, K. M. Kalyanam, A. B. Lyle, L.A. Phillips, "A Technical and Economic Assessment of Methods for the Storage of Large Quantities of Hydrogen", International Journal of Hydrogen Energy, Vol. 11, No. 1, pp. 5-22, 1986.

[33] L. L. Grigsby, "The Electric Power Engineering Handbook", Boca Raton, CRC Press LLC, 2001.

[34] J. Hamelin, K. Agbossou, A. Laperrière, F. Laurencelle, T. K. Bose, "Dynamic behavior of a PEM fuel cell stack for stationary applications", International Journal of Hydrogen Energy, Vol. 26, pp. 625-629, 2001.

[35] M. Fowler, "Renewable Energy Generation Facility Design Report", University of Waterloo, 2006.

[36] EG&G Services, "Fuel Cell Handbook", Fifth edition, October 2000.

[37] E. Spahić, G. Balzner, B. Hellmich, W. Munch, "Wind Energy Storages - Possibilities", IEEE Power Tech, Lausanne, pp. 615-620, 2007.

[38] S. Clarke, "Electricity generation using small wind turbines at your home or farm", Ontario Ministry of Agriculture, September 2003. [Online]. Available: http://www.npp.ca/images/OntarioWindFactSheet.pdf

[39] T. Ackerman, "Wind Power in Power Systems", John Wiley & Sons, England, 2005.

[40] M. R. Patel, "Wind and Solar Power Systems", CRC Press, 1999.

[41] J. Lillington, "The future of Nuclear Power", Elsevier, 2004.

[42] European Nuclear Society, "Pressurized water reactor". [Online]. Available: http://images.google.si/imgres?imgurl=http://www.euronuclear.org/info/encyclopedia/images/pressurized.gif&imgrefurl=http://www.euronuclear.org/info/encyclopedia/p/pressurized-water-reactor.htm&usg=WEotQ2kL0Rae6f3U2qoxeSBC--U=&h=339&w=373&sz=16&hl=sl&start=2&um=1&tbnid=kip7cSlurIJttM:&tbnh=111&tbnw=122&prev=/images%3Fq%3Dpressurized%2Bwater%2Breactor%26hl%3Dsl%26rls%3Dcom.microsoft:sl%26rlz%3D1I7GGLD_sl%26sa%3DN%26um%3D1

[43] Wikipedia, "CANDU reactor", [Online]. Available: http://en.wikipedia.org/wiki/CANDU_reactor

[44] L. Soder, "Simulation of Wind Speed Forecast Errors for Operation Planning of Multi-Area Power Systems", 8th International Conference on Probabilistic Methods Applied to Power Systems, Iowa State University, Ames, Iowa, September 12-l6, 2004.

[45] D. Allen, "Economic evaluation of projects", Institution of chemical engineers, Third edition, 1991.

[46] H. Khatib, "Economic Evaluation of Projects in the Electricity Supply Industry", IEE Power & Energy Series 44, The institution of electrical engineers, London, UK, 2003.

[47] S. T. Myers, R. A. Brealey, "Principles of Corporate Finance", Irwin McGraw-Hill, 2000.

[48] F. J. Stermole, "Economic Evaluation and Investment Decision Methods", Investment Evaluations Corporation, 1984.

[49] International Energy Agency, "Guidelines for the economic analysis of renewable energy technology applications", Paris, 1991.

[50] MATLAB, "Matlab Online Manuals". [Online]. Available: http://www-ccs.ucsd.edu/matlab/fulldocset.html

[51] R. Fourer, D. M. Gay, B. W. Kernighan, "AMPL: A Modeling Language for Mathematical Programming", Duxbury Press, 2 edition, November, 2002.

[52] ILOG, "ILOG AMPL CPLEX System Version 10.0 User's Guide", January, 2006.

[53] R. Bronson, G. Naadimuthu, "Schaum's outline of theory and problems of operations research", Schaums outline series, Second Eddition, 1997.

[54] E. Castillo, A. J. Coneho, P. Pedregal, R. Garcia, N. Alguacil, "Building and Solving Mathematical Programmin Models in Engineering and Science", A Wiley-Interscience Series of Texts, Monographs and Tracts, 2002.

[55] Ontario Clean Air Alliance, "A new Bruce transmission line: Does it make sense for Ontario?", Air Quality Issues Fact Seet #23, 2007. [Online]. Available: http://www.cleanairalliance.org/resource/fs23.pdf

[56] IESO, "Ontario Reliability Outlook 2007", Vol. 2, Issue 2, 2007.

[57] M. Geidl, G. Andersson, "Operational and Structural Optimization of Multi-Carrier Energy Systems", European Transactions on Electrical Power, Vol. 16, Issue 5, Pages 463 – 477, September, 2006.

[58] H. Zareipour, "Price Forecasting and Optimal Operation of Wholesale Customers in a Competitive Electricity Market", PhD thesis, 2006.

[59] Independent Electricity System Operator (IESO), "Market Manual 9: Day-Ahead Commitment Process Operations and Settlement", Issue 4.0, March 2007.

[60] Independent Market Operator (now IESO), "Market Manual 4: Market Operations Part 4.0: Market Operations Overview", Issue 9.0, June 2004.

[61] Renewable Energy Development in Ontario (REDO), "General information for potential developers", 2005.

[62] IESO, "Hourly Ontario Energy Price (HOEP)", [Online]. Available: http://www.ieso.ca/imoweb/marketdata/marketData.asp

[63] H. Zareipour, K. Bhattacharya, C. A. Cañizares, "Electricity Market Price Volatility: The Case of Ontario", Accepted to Energy Policy, April, 2007.

[64] Hydrogenics Corporation, "Hystat-A Hydrogen plants brochure". [Online]. Available: http://hydrogenics.com/onsite/pdf/Hydrogen_Plants_web.pdf

[65] J. X. Weinert, T. E. Lipman, "An Assessment of the Near-Term Costs of Hydrogen Refueling Stations and Station Components", Institute of transportation studies, University of California, Davis, 2006.

[66] Pressure product industries, "Fuel cell station compressor -brochure". [Online]. Available: http://www.pressureproductsindustries.com/pdfs/PPI_HP340_fuelcell.pdf

[67] Hydrogenics Corporation, "HyPM 500 series power module fuel cell brochure".

[68] F. Doty, "A Realistic Look at Hydrogen Price Projections", Doty Scientific, Inc. Columbia, 2004. [Online]. Available: http://www.dotynmr.com/PDF/Doty_H2Price.pdf

[69] Suncor, "Ripley Wind Power Project", [Online]. Available: http://www.suncor.com/default.aspx?ID=1091.

[70] Enercon, "Product Overwiev", 2007. [Online]. Available: http://www.enercon.de/www/en/broschueren.nsf/vwwebAnzeige/15686F537B20CA13C125719400261D37/$FILE/ENERCON_Product_Overview_Eng.pdf

[71] Bruce Power, "2004 year review", 2004. [Online]. Available: http://www.brucepower.com/uc/GetDocument.aspx?docid=952.

[72] G. Houston, T. Hird, N. Tully, "International comparison of utilities' regulated post tax rates of return in North America, the UK and Australia", National Economic Research Associates-NERA, March 2001.

[73] Canadian Revenue Agency, "Corporation tax rates", 2009. [Online]. Available: http://www.cra-arc.gc.ca/tx/bsnss/tpcs/crprtns/rts-eng.html

[74] International Energy Agency, "World energy outlook 2006", 2006.